From Anionic Polymerization in Continuous Flow to Macromolecular Architectures and Stimuli-Responsive Surfaces

Dissertation zur Erlangung des Grades

eines „Doktor rerum naturalium (Dr. rer. nat.)“ der Fachbereiche:

08 – Physik, Mathematik und Informatik

09 – Chemie, Phamarzie und Geowissenschaften

10 – Biologie

Universitätsmedizin

der Johannes Gutenberg-Universität

Christoph Tonhauser

Max Planck Graduate Center

mit der Johannes Gutenberg-Universität Mainz

Max Planck Graduate Center
mit der Johannes Gutenberg-Universität Mainz

The thesis was carried out from September 2009 until Mai 2012 in the group of Professor Holger Frey at the Institute of Organic Chemistry (Subject: Macromolecular Chemistry), Johannes Gutenberg-University Mainz.

Day of oral examination: July 05th 2012

I hereby declare that I wrote the dissertation submitted without any unauthorized external assistance and used only sources acknowledged in the work. All textual passages which are appropriated verbatim or paraphrased from published and unpublished texts as well as all information obtained from oral sources are duly indicated and listed in accordance with bibliographical rules. In carrying out this research, I complied with the rules of standard scientific practice as formulated in the statutes of Johannes Gutenberg-University Mainz to insure standard scientific practice.

_____

Christoph Tonhauser

Meinen Eltern

Persönlichkeiten werden nicht durch schöne Reden geformt, sondern durch Arbeit und eigene Leistung.

(Albert Einstein)

Table of Content

Motivation and Objectives

Since the initial reports on carbanionic polymerization in the seminal works of Michael Szwarc (*Nature* **1956**, *178*, 1168), the anionic polymerization technique has remained an important and powerful method to prepare well-defined polymer-based macromolecules with low polydispersities and precisely defined molecular weights. Despite the significant progress in controlled radical polymerization in the last decade, anionic polymerization remains the method of choice, when well-defined macromolecules with *in-chain* and *chain-end* functionalities are desired. Deliberate chain termination represents an additional powerful feature of anionic polymerization techniques. The facile addition of an electrophilic end-capping reagent terminates the 'living' polymerization and affords end-functional polymers with a high degree of functionalization. Often full functionalization of the chain ends is possible. The corresponding precursors can be employed for the preparation of complex macromolecular architectures, e.g., tailored in-chain functionalized block co-polymers with defined position of the functionality. Established procedures for end-functionalization in carbanionic polymer synthesis employ universal termination reagents, like diphenylethylene (DPE) or chlorosilane derivatives. An additional valuable class of end-capping reagents are epoxide derivatives, which have been utilized to a smaller extent. Particularly the introduction of various functionalities in proximity to the emerging hydroxyl group at the chain terminus represents a surprisingly neglected area. This facile procedure affording end-functional polymers with high functionalization efficiency and chemical versatility shows promising potential for application in the synthesis of complex macromolecular architectures and stimuli-responsive materials

Micro reaction technology currently represents a fast growing area of research. The implementation of organic reactions in microflow setups is already established. The continuous flow helps to reduce the time- and energy-consuming optimization process of reaction parameters and oftentimes increased yield and quality of products as well as chemical selectivity of the reactions can be obtained. Especially the micro reaction technology in polymer science is extremely advantageous to obtain a facile and rapid access to well-known as well as novel polymeric materials. In particular, highly exothermic

polymerizations like living carbanionic polymerization of vinyl monomers can benefit from the continuous flow process due to efficient mixing of monomer and initiator, which leads to an excellent heat dissipation and a superior reaction control at convenient temperatures.

The objectives of this thesis can be summarized as follows:

(i) Investigation and development of a continuous flow synthesis procedure affording end-functional polymers by anionic polymerization and subsequent termination in one reaction step and on a multigram scale. This methodology can be used as rapid and cost-efficient polymer screening. Furthermore, the implementation of not only a single hydroxyl but multiple orthogonal functionalities at the chain terminus can be achieved by utilizing individually designed, functional epoxide-based end-capping reagents.

(ii) In an additional step, the respective polymers can be used as macroinitiators to prepare in-chain functionalized block copolymers and star polymers bearing intriguing novel structural and material properties. Therefore, the second objective of this thesis is the utilization of end-functional polymers as precursors for the synthesis of amphiphilic complex and in some cases unprecedented macromolecular architectures, such as miktoarm star polymers based on poly(vinyl pyridine), poly(vinyl ferrocene) and PEO.

(iii) Based on these structures, the third goal of this thesis is a detailed investigation of the preparation of stimuli-responsive ultrathin polymer films, using amphiphilic junction point-reactive block copolymers. The single functionality at the block interface can be employed as anchor group for the covalent attachment on surfaces. Furthermore, the change of surface properties will be studied by applying different external stimuli.

(iv) An additional topic related to the oxyanionic polymerizations carried out in the context of this thesis is the investigation of viscoelastic properties of different hyperbranched polyethers, inspired by the recent and intense research activities in the field of biomedical applications of multi-functional hyperbranched materials.

Graphical Abstract

Chapter 1: Introduction

Chapter 1.1: Micro Flow Technology in Polymer Synthesis

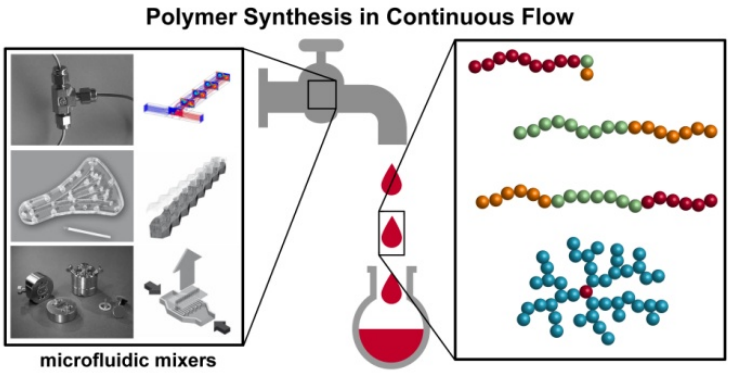

Chapter 1.2: A Road Less Traveled to Functional Polymers: Epoxide Termination in Living Carbanionic Polymer Synthesis

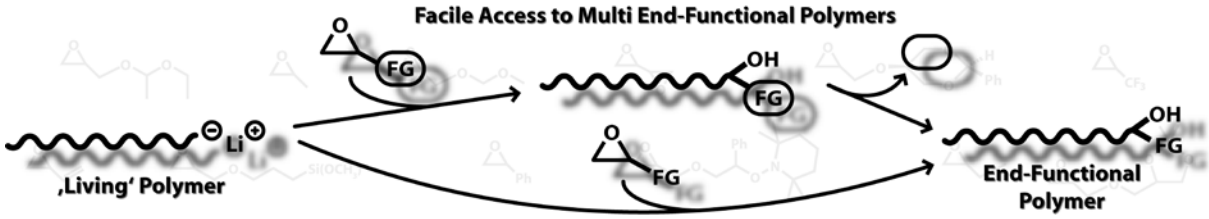

Chapter 2: Continuous Flow End-Functionalization

Chapter 2.1: Multihydroxyl-Functional Polystyrenes in Continuous Flow

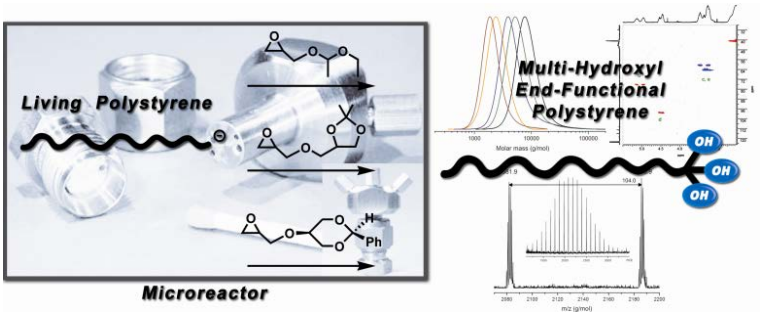

Chapter 3: Macromolecular Architectures

Chapter 3.1: Introducing an Amine Functionality at the Block Junction of Amphiphilic Block Copolymers by Anionic Polymerization Strategies

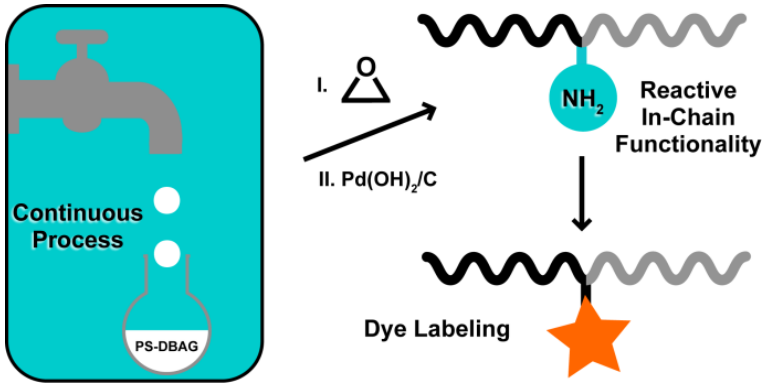

Chapter 3.2: Water-Soluble Poly(vinyl ferrocene)-*b*-Poly(ethylene oxide) Diblock and Miktoarm Star Polymers

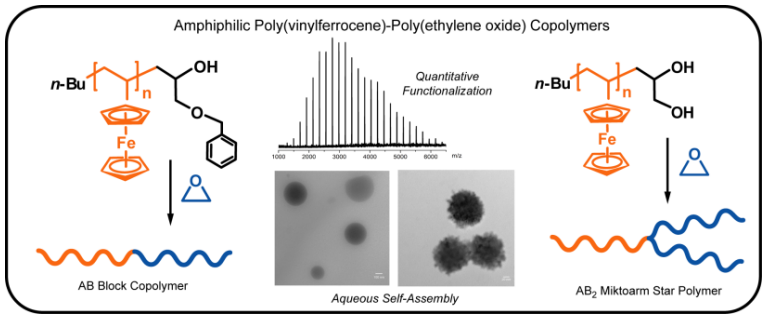

Chapter 3.3: A Combined DPE/Epoxide Termination Strategy for Hydroxyl End-functional Poly(2-vinylpyridine) and Amphiphilic AB_2-Miktoarm Stars*

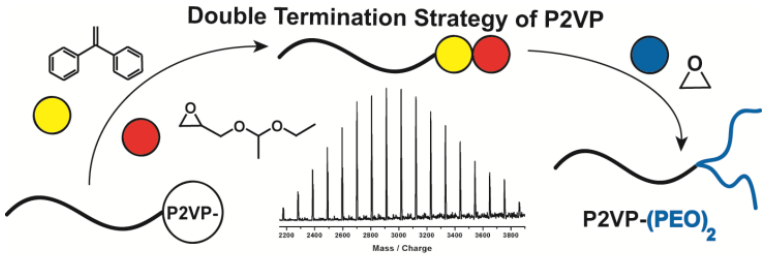

Chapter 4: Stimuli-Responsive Polymer Films

Chapter 4.1: Stimuli-Responsive Y-Shaped Polymer Brushes Based on Junction-Point Reactive Block Copolymers

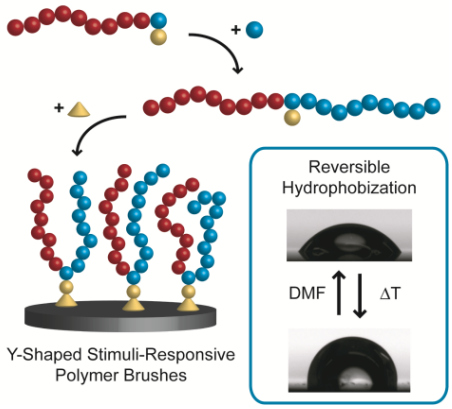

Chapter 5: Viscoelastic Properties of Hyperbranched Polyethers

Chapter 5.1: Entanglement Transition in Hyperbranched Polyether-Polyols

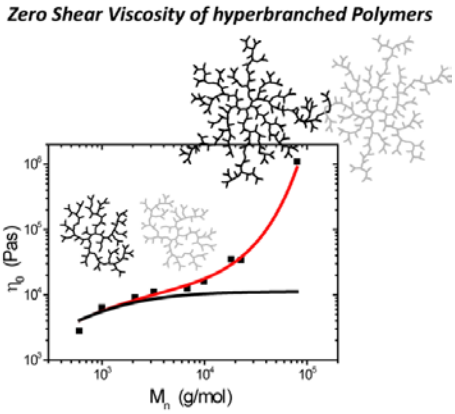

Chapter 5.2: Effect of Hydrogen Bonds on Entanglement Behavior and Thermorheological Properties of Hyperbranched Polyglycerol Melts

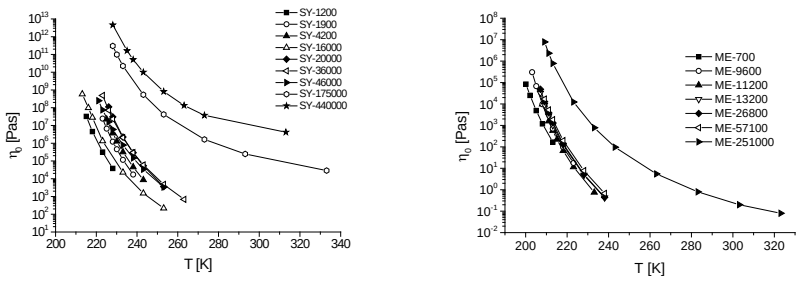

Abstract

Within this thesis, a novel access to functional materials was developed, employing both conventional and continuous flow synthetic strategies. Anionic polymerization techniques were utilized for the preparation of conventional as well as complex macromolecular architectures. ***Chapter 1*** represents the introduction of this thesis.

Chapter 1.1 deals with micro reaction technology in polymer synthesis and reviews novel synthetic strategies and reactor designs of this valuable synthesis platform. Recent developments in ionic as well as (controlled) radical polymerization have greatly enhanced the strategies for tailoring of polymer properties. This is highlighted in this comprehensive *Macromolecules Perspectives* article. Benefits and limitations of these strategies are compared to conventional laboratory setups. For instance, the continuous flow pathways to complex macromolecular architectures (e.g., dendrimers or hyperbranched polymers) represent reduced experimental effort and facile access to polymeric materials with architectural variation and structural design. Upon the general description of various polymer syntheses, future challenges and potential applications, mainly enabled by the efficient heat and mass transfer, are discussed.

In ***Chapter 1.2***, a review article highlights the epoxide termination in living carbanionic polymer synthesis. This termination process still is “a road less traveled” to functional polymers, which offer tremendous potential for both academia and industry. The review deals with the fascinating possibilities arising from the employment of common and individually designed epoxide derivatives for the synthesis of end-functional polymers. Applications in continuous flow synthesis and as precursors for the formation of complex macromolecular architectures are summarized and future perspectives are discussed.

Chapter 2 deals with the continuous flow synthesis of end-functional polymers using epoxide derivatives as termination reagents. A first successful approach to multihydroxyl-functional poly(styrene)s in continuous flow is presented in ***Chapter 2.1***. This newly developed polymerization-termination sequence enables the quantitative functionalization of living poly(styrene) (PS) using specifically designed acetal-protected glycidyl ethers (ethoxy ethyl glycidyl ether (EEGE), 1,2-isopropylidene glyceryl glycidyl ether (IGG), and trans-2-phenyl-

1,3-dioxane glycidyl ether (PDGE)). Molecular-weight distributions remained narrow ($M_w/M_n \leq 1.2$) and variation of flow rate ratios led to control over molecular weight (1 800-9 000 g mol^{-1}). Because of the hermetically sealed microstructured reactor, end-functionalization was quantitative and could be confirmed by MALDI-ToF MS. Upon acidic hydrolysis, the end-capped poly(styrene) releases multiple hydroxyl groups at the chain end. The presented approach can be extended to a large variety of monomers that are polymerizable by carbanionic polymerization.

Chapter 3 represents one application of a thus prepared end-functionalized polymer. Here, the polymers were employed as macroinitiators for further polymerization to generate simple and complex macromolecular architectures. By using only one terminal functionality as initiator group, block copolymers could be synthesized. Furthermore, in-chain functionalities between the two polymer blocks could be introduced by terminating the living polymer chain with functional epoxide derivatives (Chapter 3.1). The possibilities offered by the utilization of two identical groups as initiator species with respect to the generation of AB_2 miktoarm star polymers are further explored in Chapter 3.2 and Chapter 3.3.

The preparation of a series of amphiphilic block copolymers (M_n = 8 000-28 000 g mol^{-1}, M_w/M_n = 1.06-1.20) with a single amino in-chain functionality by anionic polymerization techniques is presented in ***Chapter 3.1***. Living poly(styrene) was quantitatively end-functionalized with *N,N*-dibenzyl amino glycidol in a continuous flow as well as a conventional set-up. The polymerization of the ethylene oxide (EO) segment was initiated by the terminal hydroxyl groups and the subsequent complete release of the amine functionality was confirmed by ^{13}C NMR. The reactivity of the amine group was investigated by addressing a fluorescein active ester. ***Chapter 3.2*** covers the synthesis of water-soluble diblock and miktoarm star polymers consisting of poly(vinylferrocene) (PVFc) and poly(ethylene oxide) (PEO) blocks. Monohydroxyl end-functionalized PVFc was generated by end-capping of the living carbanionic PVFc with benzyl glycidyl ether (BGE) and subsequent hydrogenolysis leading to the dihydroxyl PVFc species. Well-defined polymers (M_n = 1 000-3 600 g mol^{-1}, $M_w/M_n \leq 1.1$) with quantitative end-capping and release of the protecting group were obtained (MALDI-ToF MS). The respective end-functionalized PVFcs were utilized as macroinitators for the anionic ring-opening polymerization (AROP) of EO to afford block copolymers and AB_2 miktoarm star polymers in the range of 10 000-50 000 g mol^{-1}. The

morphology in aqueous solution was studied by transmission electron microscopy and showed formation of micelles and multicompartment micellar structures. ***Chapter 3.3*** demonstrates a two-step termination strategy of living poly(2-vinylpyridine) (P2VP) with consecutive use of DPE and EEGE as end-capping reagents. Quantitative end-functionalization was confirmed by MALDI-ToF MS. After removal of the acetal protecting group by acidic hydrolysis, the dihydroxyl end-functionalized P2VP was utilized as macroinitiator for the AROP of EO to afford well-defined AB_2 miktoarm star polymers (P2VP-PEO_2). A remarkable part of this project was carried out in close collaboration with Adrian Natalello (diploma thesis 2011).

Chapter 4 demonstrates an intriguing example for a successful application of the previously introduced synthetic concept. The preparation of junction point-reactive block copolymers (JPR-BC) was established and stimuli-responsive polymer films could be obtained. The manuscript in ***Chapter 4.1*** describes a general strategy for the synthesis of the JPR-BC with the subsequent covalent attachment on silicon surfaces. In this contribution, allyl glycidyl ether (AGE) was utilized as end-capping reagent to obtain quantitative AGE-functionalized PS (confirmed by MALDI-ToF MS). Analogous to Chapter 3, the polymer was employed as macroinitiator for the AROP of EO to obtain amphiphilic block copolymers with different block ratios (M_n = 6 000-24 000 g mol^{-1}) and a single functionality at the block junction. For the chemical grafting to silicon surfaces triethoxy silane as anchor group was introduced via hydrosilylation. The JPR-BCs were grafted onto silicon surfaces under basic conditions and Y-shaped polymer brush films were obtained. The ultrathin films (1-3 nm) were analyzed by X-ray reflectivity (XRR), scanning force microscopy (SFM), and contact angle measurements, confirming the covalent attachment via the reactive junction point. The surface wetting shows reversible stimuli-responsive behavior upon application of external stimuli (e.g., temperature or solvent) as observed by contact angle measurements.

Chapter 5 presents detailed rheological investigations of an additional type of macromolecular architectures obtained by oxyanionic polymerization: hyperbranched polyglycerols. The viscoelastic behavior of different polyglycerol derivatives was accomplished in the current thesis. In **Chapter 5.1**, the thermo-rheological behavior of a series of hyperbranched polyglycerols (*hb*PG) with a broad range of molecular weights (M_n = 600-106 000 g mol^{-1}) and low polydispersities (M_w/M_n = 1.2-1.8) were investigated in detail with

respect to molecular architecture and molar mass. At low molecular weights, “classical” scaling behavior between zero shear viscosity and molecular weight can be observed, which is reminiscent of dendritic polymers. A more complex exponential behavior can be found for higher molar masses, due to the increasing significance of entanglements of *hb*PGs at a distinct threshold value (20 000 g mol^{-1}). After a modification of *hb*PGs, the viscoelastic behavior of a series of methylated and trimethylsilylated *hb*PGs is presented in ***Chapter 5.2***. The modified structures were analyzed with respect to change in relaxation behavior and thermal properties. Analogous to Chapter 5.1, the entangled regime has been investigated. This work is the result of collaboration with Carina Gillig and Christian Schubert from the group of Professor Christian Friedrich at the Freiburg Materials Research Center (FMF).

Chapter 1: Introduction

1.1: Micro Flow Technology in Polymer Synthesis

Christoph Tonhauser,[1] *Adrian Natalello,*[1] *Holger Löwe,*[1,2] and *Holger Frey**[1]

[1]Institute of Organic Chemistry, Organic and Macromolecular Chemistry, Duesbergweg 10-14 Johannes Gutenberg-University (JGU), D-55099 Mainz, Germany

[2] Institut für Mikrotechnik Mainz GmbH, Carl-Zeiss-Strasse 18-22, 55129 Mainz, Germany.

To be submitted for publication in *Macromolecules Perspectives* **2012**

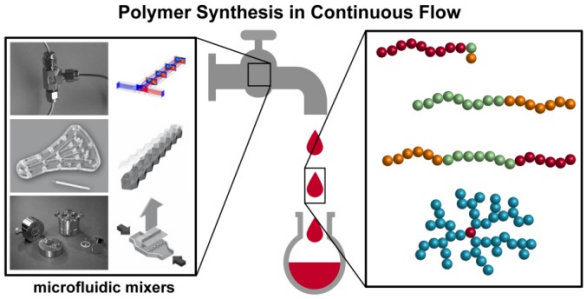

Abstract

Micro flow technology, i.e. the use of microfluidic devices for continuous flow synthesis, represents a highly useful and increasingly popular method in organic chemistry. Recently, an increasing number of polymer synthesis protocols attain benefit from this technique. In particular the control of highly exothermic, fast polymerization reactions can be improved due to the excellent heat and mass transfer within the small dimensions of the microreactors. Continuous flow setups with different micromixer geometries and flow patterns are currently used for the preparation of a large variety of macromolecular architectures by ionic and (controlled) radical polymerization techniques. This perspectives article reviews recent developments in synthetic strategies and reactor design for the homogeneous synthesis of polymeric materials in microflow systems and emphasizes future challenges and potential for applications. Polymer synthesis by radical, anionic, cationic and coordinative polymerization is considered as well as different polymer topologies generated (linear, branched and dendritic architectures).

Introduction

The round-bottom flask is the classical and simple reaction vessel for synthetic chemists to carry out chemical reactions from the milligram to the kilogram scale. A major drawback in this case is the difficult control over highly exothermic reactions due to poor heat dissipation and often "hot spot" formation. In addition, due to the given volume, reactions cannot be stopped right after the desired transformation. These key issues can be overcome by utilizing continuous flow systems, providing efficient heat dissipation properties. In general, micro reaction technology represents a laboratory enrichment for synthetic chemists in both academia and industry.[1] In particular, in the last 20 years the fascinating field of continuous flow synthesis received increasing attention and is still a rapidly growing research area in organic as well as polymer chemistry.[2-5] In addition the topic is included in the curricula at several universities.[6, 7]

"Micro reactor" can be considered as an umbrella term for all small microfluidic devices utilized in continuous flow chemistry. Micro reactors, which are also referred to as "*microstructured reactors*" or flow reactors, encompass various reaction platforms with different mixing geometries.[8-10] The small dimensioned devices offer superior and unique properties, which are unattainable by utilizing conventional reaction vessels. In particular, they enable extremely rapid mixing due to short diffusion pathways. This results in improved mass transport and presents ideal conditions for reactions with very fast kinetics.[10, 11] Furthermore, such reactors represent a very large, specific surface area (surface-area-to-volume ratio) with 10 000 to 50 000 $m^2 m^{-3}$ compared to conventional reactors with 100-1 000 $m^2 m^{-3}$, permitting superior heat exchange properties, which renders fast cooling and heating of continuous flow reactions possible.[12-14] With their efficient thermal management and the remarkable mixing efficiency the formation of side products and hot spots can be suppressed, and the control over highly exothermic reaction can be improved. Additionally, slow reactions can be intensified by increasing temperature and pressure in the micro reactors. Moreover, the small dimensions of the continuous flow reactors improve the safety of the operator who has to handle only small quantities of potentially exothermic, toxic or explosive reaction mixtures, which deemed to be too dangerous to be employed in conventional reactors.[15, 16] In comparison to conventional processes, micro-flow reaction

devices enable facile control and scanning of reaction parameters like temperature, residence time and reactant stoichiometry during the ongoing experiment.

Based on these features, a large variety of applications in different areas of chemistry has been established to date. Continuous flow procedures have been shown to lead to higher selectivity, improved yield, or increased quality of the respective products.[17-19] Moreover, the use of specially engineered or commercially available microreactors[20] under drastic conditions, such as pressurizing or heating the reactor offers access to an enlarged "processing window", which broadens the access to new molecules and materials. For example, single- and multiphase reactions with low-boiling solvent or lower amount of catalyst can be carried out.[21-24]

However, the small dimensions of the flow reactors raise the question, if an implementation in industry with large production scales is possible.[25, 26] Micro reactors are not restricted to completely miniaturized reactors. In general, the challenge is to develop a system with proper dimensions to provide a continuous flow system with increased mixing and heat dissipation properties for the respective reaction. The size of microstructured reactors can be varied from credit card to shoe-box size.[27] In addition, a stable microfluidic system enables production for a longer period of time, thereby generating large quantities of materials ("scale-out" principle). The limitation caused by small product scales can also be overcome by connecting several reactors/subunits with identical conditions in parallel ("numbering-up").[28-31] The availability of such a flexible, economically advantageous continuous-flow system decreases the dependency on the market demand and the required amount of product/intermediate can be synthesized with simultaneously minimizing the storage costs at any time.[32, 33] This presents a tremendous benefit of continuous flow chemistry for industrial processes.[34-36]

Another crucial issue is fouling within the microchannels, which is induced by increasing viscosity and particle formation (e.g., dust, contaminants, and precipitating products). Fast increase of the system pressure and interruption in the continuous flow are caused by this clogging and should be avoided. Reaction conditions have to be adjusted thoroughly during the transfer of a chemical reaction from the conventional batch reactor to a continuous flow process (e.g., temperature, concentration, and pressure).

With increasing access to micro flow systems and continuous improvement of the devices the number of reactions, that have been transferred into continuous flow systems increases rapidly. Oftentimes the microfluidic procedure can reduce the time- and energy-consuming optimization process of reaction parameters and subsequent scale-up compared to the conventional batch reactors. Based on this benefit, combined with increased yield and quality of products as well as chemical selectivity of the reactions, micro flow technology has recently received increasing interest in organic chemistry, which even resulted in industrial applications.[37-53] In particular, recent advances in the preparation of pharmaceutical reagent have to be underlined. Bogdan et al. realized the preparation of ibuprofen, a high-volume anti-inflammatory drug, using an efficient three-step continuous-flow synthesis. Purification as well as the isolation of intermediates were not necessary, which is a significant improvement compared to the conventional synthesis.[54] In an impressive work, Lévesque and Seeberger prepared the anti-malaria drug artemisinin from artemisinic acid in a continuous reactor. This lead to a tremendous reduction of cost, compared to established batch syntheses. This price reduction offers great potential to decrease the high number of deaths (one million per year, worldwide) caused by malaria around the world, by providing low cost medication.[55]

In polymer science micro reaction technology represents an emerging field. Especially highly exothermic polymerizations[56] like living carbanionic polymerization of vinyl monomers can benefit from the continuous flow process with excellent heat and mass transfer. Given the recent enthusiasm in this field, it has to be acknowledged that pioneering reports on anionic polymerization in continuous flow were published by Szwarc and coworkers[57-59] as well as Schulz and coworkers[60, 61] already in the 1960s. Both research groups investigated the reaction kinetics of the anionic styrene polymerization in detail, which benefits from a fast and turbulent mixing process within macroscopic glass tubes. In a pioneering work, this seminal approach was extended by Müller and coworkers, who carried out detailed kinetic analyses of the anionic polymerization of methyl methacrylate in a 4-way jet mixing device, using stopped-flow type experiments.[62-65] In the reports of Schulz et al. and Müller et al. impressive molecular weight control was achieved by simply varying the flow rate ratios or the length of the flow tube. Recently developed continuous flow protocols[66] are based on these fundamental works of Szwarc, Schulz, Müller and coworkers. However, increasing

interest for the preparation of polymeric materials with the micro reaction technology started only in the late 1990s, most probably due to the challenging reaction conditions with high viscosity of polymer solutions and melts.[66-68]

An additional fast developping field of research, which will not be highlighted in this perspective article, is the preparation of polymer particles with different shapes, size and composition by applying micro flow reactors.[69-74] Excellent progress in this field was accomplished by Kumacheva and coworkers. For instance, the development of new strategies for producing microparticles (mono- to multi-phase) in different shapes and morphologies was carried out.[75-79]

Here, we describe perspectives of the micro reaction technology with different types of mixing geometries in the field of homogenous polymer synthesis, where all reagents and products are dissolved throughout the polymerization, and the formation of particles is suppressed. The recent advances in all types of polymerization techniques as well as in the synthesis of complex polymer architectures are highlighted. Furthermore, special catalyzed continuous polymerization processes, which are including the micro reactor material in the reaction mechanisms, show novel access to polymeric materials. Major achievements, recent developments as well as future challenges of micro reaction technology in polymer science will be discussed in detail.

Microfluidic Technology

Microstructured reactors are devices suitable for academic research as well as application in pilot plants[1] and provide various reaction platforms with different mixing geometries.[8-10] The term „microstructured reactor“ represents continuous working flow systems with three dimensional elements in microdimensions. It has to be emphasized, that chemical reactions are physically determined and limited, i.e., the initial step is kinetically controlled and the temperature and concentration of the involved species determine the reaction kinetics. This results in two possibilities for influencing a chemical reaction: (i) Improvement of mass transport by accelerating the mixing procedure, particularly when a chemical reaction is significant faster compared to the mixing time. Furthermore, the backmixing of product with educts should be prevented. (ii) Improvement of heat transfer by rapid cooling or heating of

the reactor. Here, the generation of accumulations, hot-spots, as well as thermal runaways can be reduced significantly.

Thus, suitable reactors or reactor systems have to be provided to carry out a reaction at the kinetic limit. The corresponding systems should generate microstructured fluids but do not have to be necessarily microstructured itself. Thus, the continuous flow chemistry is not limited to small dimensions. One important principle is “adapt your equipment to the chemistry and not vice versa” and several investigations represent, that microreactors can range from credit-card to two-storey house setups (Figure 1).

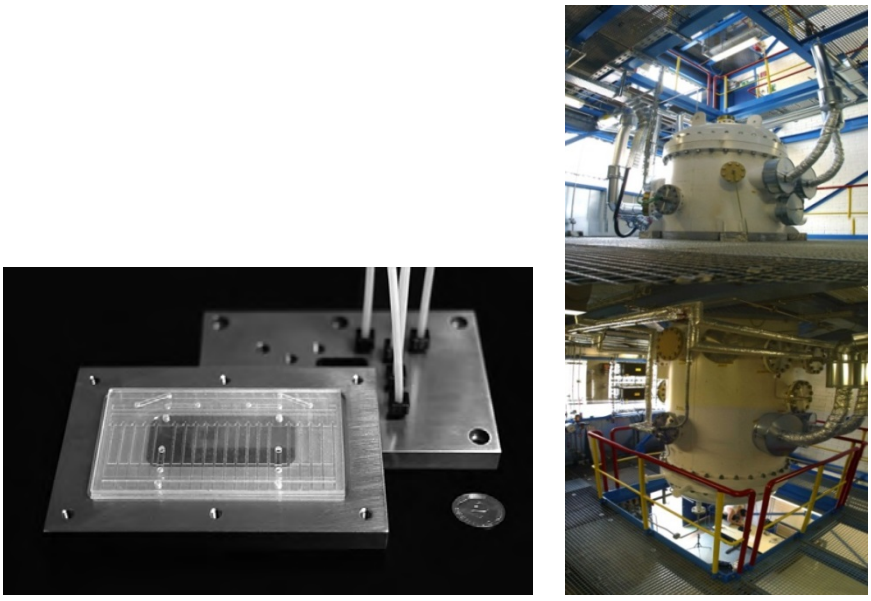

Figure 1. “Microreactors” in different dimensions from a credit-card (left) (mikroglas chemtech GmbH, Germany)[80] to a two-storey house (Evonik, former Degussa, Germany)[81] (right) with microdimensional structures inside.

Taking this into account, this motivates the transfer from conventional batch systems to an individually designed or commercially available microstructured reactor to optimize the reaction parameters and to meet the kinetic limit. Operations, like adding an appropriate solvent, heating the reaction mixture at a certain temperature for a long time, and slow or irregular mixing with a stirring bar is no longer necessary. In the rapid growing area of micro flow technology uncommon reaction conditions can easily be applied. For instance, high pressure and temperature with fast heating or cooling cycles can be afforded in continuous flow setup which might increase yield and selectivity.[82, 83]

In the particular case of high reaction kinetics the complete mixing of the reactants is important to obtain a high yield or selectivity compared to conventional systems. In literature different mixing principles are discussed, which can also be applied in polymer synthesis. In general, the flow rate in microstructured reactors are small (Reynolds number (Re) ≤ 1000, oftentimes below 100) and a lamellar flow can be assumed. In this case the mixing process is dominated by diffusion between pre-shaped fluid layers and the mixing time is only dependent on the fluid film thickness and the diffusion coefficient. Since the diffusion coefficient represents a temperature-dependent and material-specific parameter, an increased mixing efficiency can only be forced if preferably thin fluid layer are realized.
Although contrary opinions exist, the channel-based Lab-on-Chip systems (2-dimensional reactor systems) represent no significant difference compared to 3-dimensional wounded or elongated tube- and capillary reactors. In particular both reactor types show similar flow profiles as well as an increased mass and heat transfer due to similar surface-to-volume ratios. As can be seen in Figure 2 two-dimensional Lab-on-Chip microreactors possess integrated mixers (left), whereas the common setup combines an external mixer with corresponding flow tubes (right). In summary, the often demanded requirement of lateral dimensions in a certain region of micrometers (e.g., ≤ 1000 μm) was randomly chosen and is not based on scientific investigations. Each chemical reaction has to be considered separately and the reactor setup has to be adjusted to the corresponding kinetics.

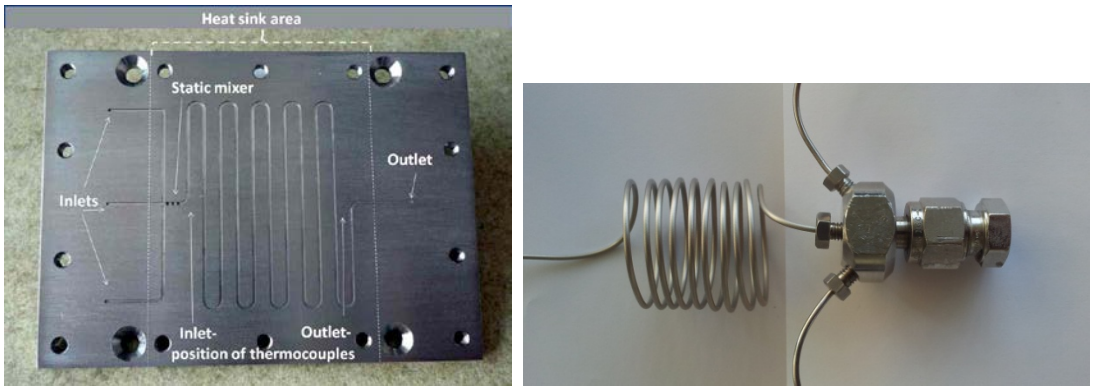

Figure 2. Microreactors with different dimensions: On the left a 2-dimensional micro-reactor with an integrated static mixer [84]and on the right a 3-dimensional micromixer-tube reactor is depicted.

Herein, polymer syntheses in continuous flow utilizing different reactor setups and mixing devices are highlighted. In the following the relevant properties, mixing behavior and characteristics of the utilized mixers will be emphasized.

A classical example for a simple lamination mixer is a commercially available T-piece. Although this type of mixer is easily accessible, it exhibits some disadvantages compared to the more sophisticated lamination mixers. Applying reaction conditions with $Re < 10$ increases the mixing time due to a bilamination of the two reactants. The inefficient mixing is caused by the long pathways of the molecules by diffusion through the complete cross section of the reaction tube. With $Re > 200$ uncontrolled turbulence with pulsation occurs, which hinders the mixing process. Higher Re (> 1000) lead to fluidic jet streams and a controlled mixing process is not possible. Only at Reynolds numbers ~200 a secondary flow pattern creates additional fluid-lamellae to intensify the mixing behavior (Figure 3).[85]

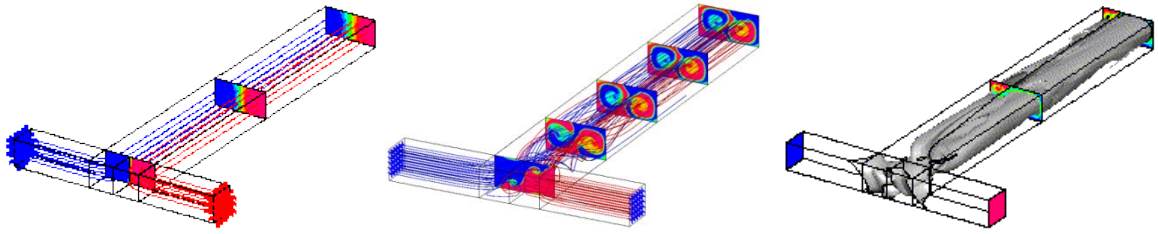

Figure 3. Flow pattern in a T-piece after 2 mm depending on the *Re.* (left) straight laminar und vortex flow, (middle) engulfment and periodic pulsation, (right) chaotic flow with bursts.[86]

In contrast to T-pieces, commercially available multilamination mixers present enhanced mixing patterns. Micrometer thin fluid layers (lamellea) get split up prior to the mixing process and the reactants get alternating combined. The mixing occurs by diffusion between the fluid lamellae, which leads to a rapid mixing within milliseconds due to the ultrathin layers (Figure 4). Such multilamination mixers are also available for high pressure applications.[87]

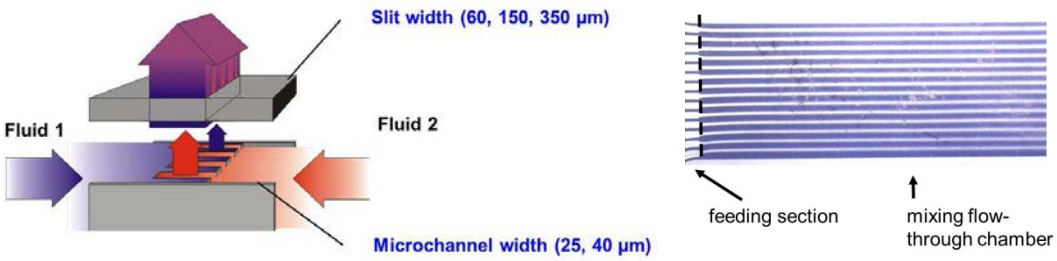

Figure 4. Mulitlamination mixing principal (top) and visualization of laminar flow pattern with colorized and non-colorized water streams (source IMM Institut für Mikrotechnik Mainz GmbH).

Another type of mixing is represented by split-and-recombine mixers (Figure 5), which are especially beneficial for chemical reactions with low viscosity materials. Within this micromixers the fluid lamellae get splited and subsequently recombined. The repetition of this process in each step (n) of the mixers creates 2^n stacked fluid lamellae. Hence a mixer with 8 steps and a hydraulic cross section of 1 mm possess theoretically 512 lamellea with each 2 µm thick. In addition, the process of this serial multilamination shows further dominant fluid-dynamic effects, e.g., formation of secondary stream patterns, which improves the mixing efficiency significantly.

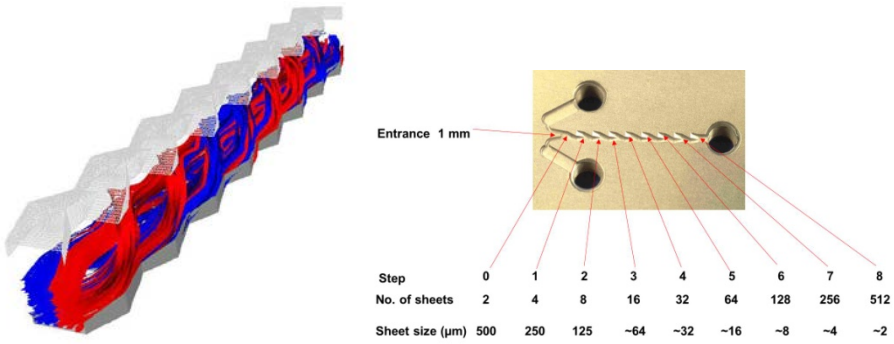

Figure 5. Split-and-recombine micromixer: The flow patern (left) shows the secondary flow instead of multi-lamination and the steps in combination with number of stacked lamellae are depicted in the right image.

In summary, all mixing types show high potential for the transfer of polymerization into continuous flow. In the following section established procedures, current investigations and future challenges in polymer science utilizing different kinds of mixing geometries are discussed.

Homopolymerization by Ionic and Radical Techniques

One central important aspect in current polymer science is the synthesis of well-defined polymers. The molecular weight and molecular-weight distribution (MWD) are the main characteristics governing polymer properties and thus the performance of the material. The preparation of well-defined polymers is essential for numerous applications. A small deviation from the reagent composition (e.g., initiator vs. monomer in controlled polymerization techniques) often affects the properties. Thus, precise control is preferred, which can be achieved by efficient mixing using micro reaction technology.

First reports on continuous preparation of homopolymers were already mentioned in the 1960ies by Szwarc as well as Schulz and coworkers.[57, 61] In these early works, the authors conducted kinetic studies of the anionic styrene polymerization in continuous flow tube reactors. Suprisingly, the area remained mostly untouched in academic research, until the late 1990s, which is marked by the implementation of different polymerization techniques in microreactors. This renaissance evokes the successful synthesis of anionic, cationic, free radical, and controlled radical homopolymerizations, i.e., the homopolymerization of different monomers in continuous flow, which will be outlined in the following section.

In the following, the achievements in ionic polymerization, which represents one of the main principles of chain polymerization, will be discussed. Monomers with carbon-carbon double bonds can propagate by nucleophilic or electrophilic attack. The polymerization exhibits a “living” character if no terminating species are present and the reaction kinetics are highly influenced by the selection of solvent and counter ion. In particular, a more polar solvent causes accelerated reaction kinetics, whereas a control of the highly exothermic reaction becomes demanding[88, 89] and application in industry on large scale is oftentimes challenging. Another essential requirement for the preparation of well-defined polymers with “living” polymerization techniques is a simultaneous initiation, which can be achieved by fast and efficient mixing. Furthermore, the living character demands anhydrous and sealed reaction conditions. Thus, micro reaction technology provides suitable reaction compartments with high mixing efficiencies and hermetically sealed systems to control extreme reaction conditions without losing control. The facile supply of a reaction environment that enables living polymerization without tedious purification steps is a key feature.

The first carbocationic polymerization was transferred in a microfluidic device by Nagaki et al. in 2004. The polymerization of different butyl vinyl ethers within a multilamination micromixer was described and the N-acyliminium cation pool[90, 91] served as an efficient initiator. The polymerization was controlled by the flow rate ratio and was completed within 0.5 s at -78 °C, resulting in decreased polydispersities ($M_w/M_n \geq 1.14$) compared to the batch reactor ($M_w/M_n \geq 2.2$) (Scheme 1). Furthermore, the living character was confirmed by end-capping the polymer with allyltrimethylsilane.[92, 93]

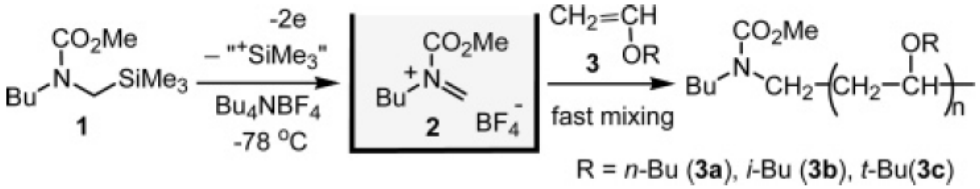

Scheme 1. Preparation of cation pool as initiating species for the continuous carbocationic polymerization of different butyl vinyl ethers.[92]

The challenging reaction conditions (-78 °C) can be avoided by utilizing trifluoromethane sulfonic acid (TfOH) as an initiator. In this case a controlled polymerization can be realized at temperatures of 25 °C.[94] The same setup was used to increase the indane unit content during the polymerization of 1,4-diisopropylbenzene.[95] Paulus et al. studied the microwave-assisted cationic ring-opening polymerization of 2-ethyl-2-oxazoline in a tube reactor. Here, under microwave irradiation complete conversion, but broad MWDs ($M_w/M_n \geq 1.3$ vs. $M_w/M_n = 1.14$ in batch reactions) were achieved, because the flow profile was non-uniform, which results in inefficient mixing.[96]

In addition, anionic polymerizations also is an efficient polymerization technique for the transformation to microfludic processes, especially due to the well-contained reaction zone. Thus, reaction time and experimental effort can be reduced significantly compared to batch reactors.[97]

The preparation of poly(methacrylate)s in the late 1990s by Müller and coworkers demonstrates the high potential for anionic polymerization in continuous flow. Due to the very efficient mixing, the authors obtained well-defined polymeric materials with narrow molecular-weight distributions ($M_w/M_n = 1.04\text{-}1.08$).[63] Although this report could have been an initiation for further works, the next report in this field was not published until 2005 by

Maeda et al.[98]. The authors developed the continuous-flow polymerization of different amino acid anhydrides and compared the results to the corresponding batch reactions. A significant decrease of the PDI value was obtained by utilizing a silicon-based microreactor obtained by dry etching procedure. For instance, the preparation of poly(glutamine) revealed a PDI of 1.17, whereas the batch approach leads to higher values, e.g., 1.56. This underlines the excellent control over the polymerization using microfluidic devices. Employing a decreased flow rate leads to higher residence times and thus molecular weight could gradually be increased (cf. Figure 6). Furthermore, amino acid copolymers consisting of lysine/alanine or lysine/leucine comonomers were synthesized. With respect to biomedical applications, these remarkable results offer a facile and novel access to poly(amino acid)s.[98, 99]

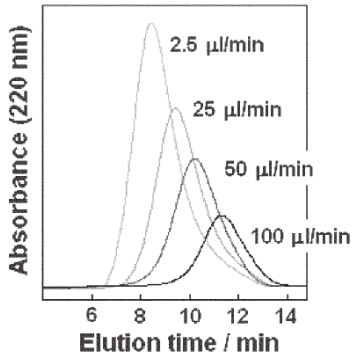

Figure 6. Molecular-weight distributions of poly(lysine)s prepared with different flow rates. Reduction of the flow rate results in prolonged residence times in the microreactor and thus higher molecular weights are obtained.[98]

In our group, the anionic polymerization of poly(styrene) (PS) was transferred to a microstructured reactor. The reactor consisted of capillary flow tubes and an IMM slit interdigital micromixer (inner volume: 15 µL) as mixing unit. The monomer and initiator (*sec.*-butyl lithium) solutions were combined in the micromixer to initiate the anionic polymerization at room temperature in a polar solvent. Using a short outlet tube, PS samples in a broad range of molecular weight (M_n = 2 000–70 000 g mol^{-1}) with narrow molecular-weight distributions (M_w/M_n = 1.09–1.20) were obtained. Compared to the batch reactions, the reaction time could be reduced from hours to several seconds, rendering a facile access to large amounts of well-defined polymers in a short period of time. Furthermore, the adjustment of flow rate ratios leads to different molecular weights in a single experiment

without interrupting the continuous flow process. It has to be mentioned that the complete microreactor interior has to be made of stainless steel, because the living carbanions react with most common materials, e.g. rubber or PTFE sealings.[100]

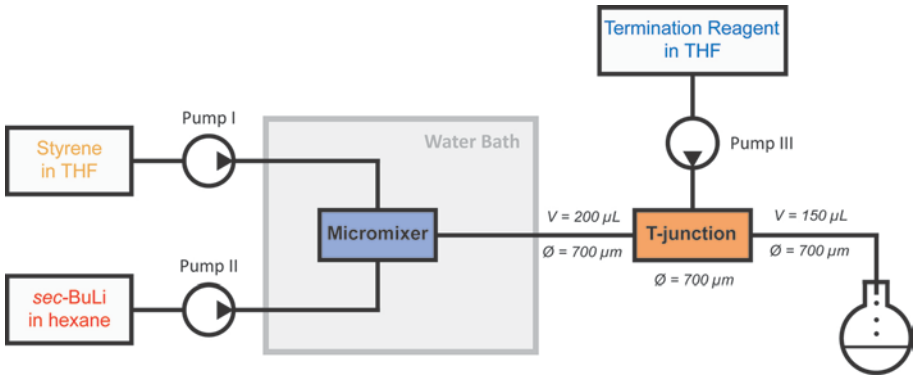

Figure 7. Schematic reactor setup for the quantitative end-functionalization of living poly(styrene) in continuous flow utilizing a HP-IMM micromixer.[101]

This work was extended by investigating the end-capping process of living PS with different reagents in the microreactor. For this purpose a second mixer was added to achieve a direct termination of PS in a continuous process (Figure 7). In particular, living PS was end-capped with specifically tailored glycidyl ethers (e.g., ethoxy ethyl glycidyl ethers (EEGE), isopropylidene glyceryl glycidyl ether (IGG), phenyl-1,3-dioxane glycidyl ether (PDGE), and *N,N*-dibenzyl amino glycidol (DBAG)) to introduce additional hydroxyl or amine functions at the chain termini.[101, 102]

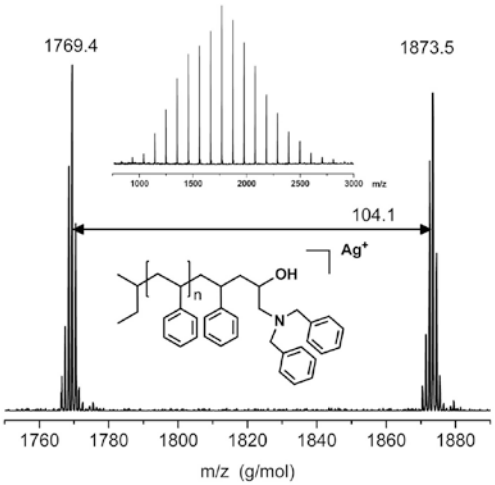

Figure 8. Quantitative end-functionalization of poly(styrene) in continuous flow was confirmed by MALDI-ToF MS. The single distribution mode could be assigned to the desired molecules (here: PS-(DBAG))[102]

The end-functionalized polymers were recovered within several seconds and quantitative end-capping was confirmed in all cases by matrix-assisted laser desorption ionization time-of-flight mass spectrometry (MALDI-ToF MS). An exemplary spectrum of DBAG-functionalized PS is depicted in Figure 8. This continuous end-functionalization provides a valuable method for rapid and cost-efficient polymer screening with respect to novel end-functionalized materials.

Recently, in analogy to the continuous homopolymerization of PS, other research groups extended this concept utilizing different mixing geometries or styrene derivatives.[103, 104] Beers and coworkers investigated the anionic styrene and isoprene polymerization in non-polar solvent (cyclohexane) and low cost aluminium-Kapton microfluidic devices with different 2D flow designs (straight, periodically pinched, obtuse zigzag, and acute zigzag, cf. Figure 9). Polymerizations were carried out at elevated temperatures (60 °C) and high concentrations (up to 42 vol%) and the zigzag channels led to lower PDI values due to passive mixing in the appropriate reactor designs (elastic turbulence and laminar recirculation).[104]

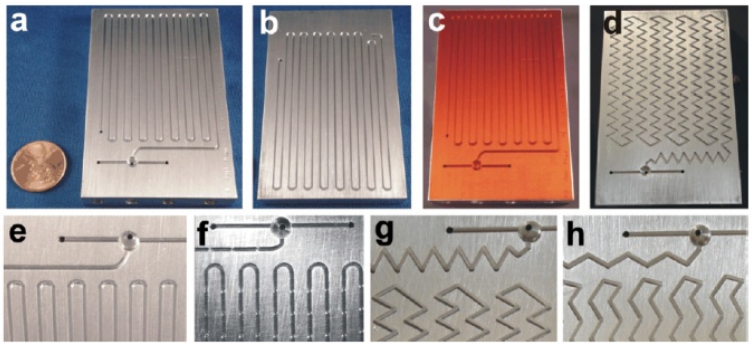

Figure 9. Different 2D designs were cut into aluminum plates on both sides and the reactor was sealed by a Kapton film: (a, b, e) straight, (c) straight sealed with polyimide film, (d) zigzag, (f) periodic pinches (g) acute zigzag, and (h) obtuse zigzag patterns.[104]

Similar to the early works of Müller and coworkers[63], Yoshida et al. studied the homopolymerization of different methacrylates in a syringe-based micromixer equipped with a T-mixer (0.5-1 mm inner diameter (id)). 1,1-diphenylhexyllithium was used as an initiator, and in a controlled manner narrowly distributed polymers were obtained at elevated temperatures from -28 °C to room temperature.[105]

Free radical polymerization can also be applied in micro reaction technology. The main benefit of the transfer to continuous flow is the suppression of the Trommsdorff effect by the superior heat and mass transfer.[106] Due to the increased immobility of the growing polymer chain with higher viscosities, the number of recombination steps decreases and the concentration of reactive chain ends increases, which leads to an increase of the reaction kinetics. This causes an autoacceleration of the polymerization rate resulting oftentimes in the loss of reaction control and the preparation of undefined products. Detailed studies of five different monomers in a free radical polymerization were accomplished by Yoshida et al.[107] The polymerizations were carried out in a T-shaped micromixer with inner dimensions of 250-1000 µm in a highly controlled manner. The authors obtained significant improvement in MWD for the polymerization of benzyl methacrylate, methyl methacrylate (MMA), and butyl methacrylate compared to the corresponding batch reactions. The higher the exothermic propagation reaction, the more effective is the heat dissipation of the micromixer. In the case of poly(butyl acrylate) the MWD could be decreased from approximately 10 in conventional reactors to 3.16 in the continuous flow process (Figure 10). This effect was less pronounced for the free radical polymerization of vinyl benzoate and styrene due to the decreased polymerization rate yielding in a reduced benefit from the efficient heat removal.

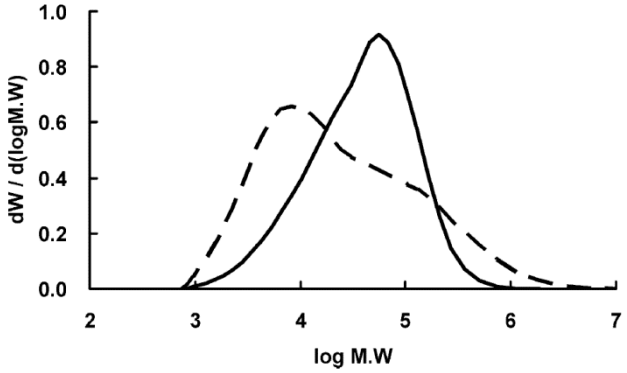

Figure 10. MWDs of poly(butyl acrylate) synthesized in a conventional batch reactor (dashed line) and T-shaped micromixer (solid line).[107]

In addition, the successful implementation of the radical MMA polymerization to an industrial scale was accomplished by Iwasaki et al. With a “numbering-up” approach eight microtube reactors were run in parallel for 6 days and continuous operation with precise control of temperature, molecular weight, and MWD was achieved indicating the inherent

advantage of microflow systems (Figure 11). The pilot plant demonstrates that the continuous free radical polymerization leads to high productivity, for instance 2.5-4 kg within one week with a total flow rate of 60-110 mL/h were obtained.[108] Thus, microchemical plants have a significant potential for applications in polymer industry. Moreover, industrial application of microflow polymerizations with continuously operating pumps are described in several patents.[109-111]

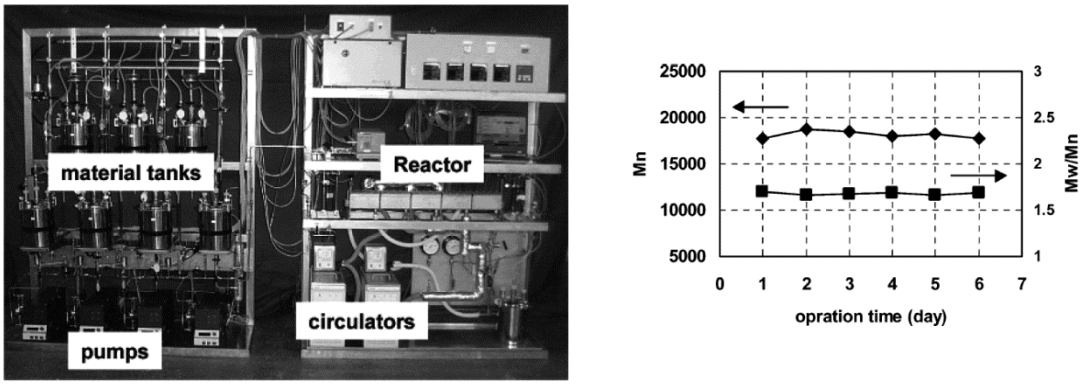

Figure 11. Image of the pilot plant with 8 microtubes in parallel and a total inner volume of 18.4 mL (left) were run for 6 days with precise control of molecular weight and MWD (right).[108]

Since the 1990s, various novel techniques for the controlled synthesis of polymers by radical polymerization were developed. These methods are generally designated “living” or “controlled radical polymerization (CRP)”[112] and they extend the field of standard polymer syntheses procedures in an impressive way. Well-defined polymers with large monomer variation and flexible reaction conditions can be obtained in a facile manner. These important developments can be summarized with three major techniques viz. atomic transfer radical polymerization (ATRP)[113, 114], nitroxide-mediated polymerization (NMP)[115, 116] and reversible addition-fragmentation chain transfer polymerization (RAFT)[117]. Although CRP techniques reveal decreased reaction kinetics one can benefit from micro reaction technology and the challenge to transfer all major CRP techniques to flow systems have been taken up by several research groups.

First reports on the transfer of controlled radical polymerization into continuous flow reaction systems were published by Zhu and coworkers. A continuous column reactor packed with supported CuBr-HMTETA catalyst was utilized for the continuous supported ATRP (C-SATRP)[118] of MMA. The column exhibit good catalyst retention and a long catalytic

reactivity presenting a promising development for industrial ATRP applications.[119] Recently, MMA was also polymerized homogenously in a flow tubular reactor with excellent control over the molecular properties (conversion ≈ 90%, M_n/M_n = 1.06).[120] Beers and coworkers employed an individually fabricated microstructured reactor (Figure 12) for the continuous ATRP of 2-hydroxypropylmethacrylate (HPMA). The system was compared to the batch process[121] and monomer conversion was comparable to bulk reaction kinetics. The molecular variables (M_n = 1 600-12 000 g mol^{-1}, M_n/M_n = 1.19-1.32) were controlled by variation of flow rates, polymerization time, or concentration of the reagents allowing a rapid screening process of polymeric materials with different properties.

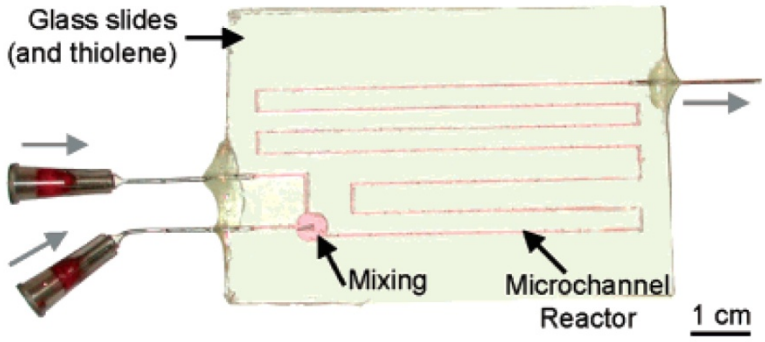

Figure 12. Microstructured reactor for the ARTP of HPMA, constructed by contact photolithography of a thiolene prepolymer with improved solvent resistance compared to PDMS devices. The reactor with one single reaction channel (dimensions 500 μm x 600 μm) is equipped with two inlet channels and one outlet channel. A stir bar is included in the mixing chamber and is driven by a magnetic stir plate. To start the polymerization the solutions of monomer/catalyst and initiator in a water/methanol mixture were added via syringe pumps into the two different inlet channels.[122]

In a more tubular dimension, a rather long continuous reactor (150 m length, id: 2.2 mm) was employed to produce homopolymers of butyl acrylate and styrene by ATRP. Narrow molecular weight distributions and a slightly higher conversion were obtained compared to batch controlled experiments.[123] Further developments, e.g., no purification of reagents, wider inner diameter (4.75 mm), and non-hazardous/inexpensive reducing agent were applied to obtain industrial relevant conditions for the polymerization of butyl acrylate. The clogging problems were decreased by reducing the amount of catalyst to parts per million

(ppm) levels using "activator regenerated by electron transfer" (ARGET) ATRP[124]. An increased amount of reducing agent led to a faster and more robust ARGET ATRP demonstrating the potential for industrial adoption.[125]

Reconsidering microdimensional devices, also other CRP techniques, e.g., NMP, were applied to continuous flow processes. Rosenfeld et al. investigated the high-temperature polymerization of two monomers (styrene and *n*-butyl acrylate) suitable for NMP[126] to increase the control of the reaction. In comparison to lab-scale batch reactors the more exothermic polymerization of *n*-butyl acrylate can benefit of the superior heat release and provide a narrower MWD, whereas styrene shows no difference to the batch processes.[127] This system was utilized to develop an intriguing characterization method for continuous polymer synthesis, namely "continuous online rapid size-exclusion chromatography monitoring of polymerizations" (CORSEMP). This novel GPC characterization method allows the automatic sampling, dilution, injection and analysis every 12 minutes of the raw (co)polymer samples, which are recovered from the reactor outlet. The monitoring in "near real-time" of the molecular weight and MWD shows promising potential for further implementation on academic and industrial level (Figure 13).

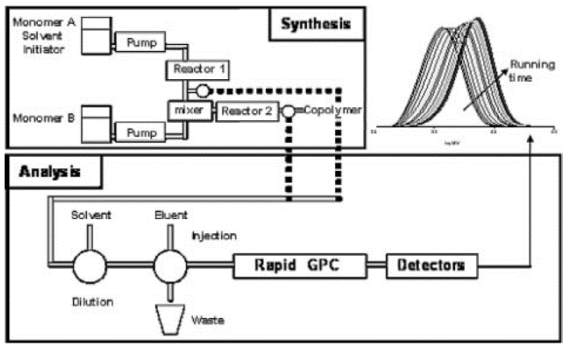

Figure 13. Schematic setup of the CORSEMP representing the continuous polymerization part (top, left) and the analysis section (bottom). The system monitors the molecular weight and the MWD "near real-time" (top, right).

Compared to NMP and ATRP, RAFT polymerization enables the utilization of a wide variety of monomers with applying different chain transfer agents without using transition metal catalysts.[128] Recently, two research groups at the same time published the initial homogeneous RAFT polymerization in continuous flow. Seeberger and coworkers used a syringe-based microreactor for the homogeneous RAFT polymerization of poly(N-

isopropylacrylamide) (PNIPAM) in continuous flow. PNIPAM represents an interesting poly(acrylamide) due to potential applications in the field of biomedicine [129] and stimuli-responsive materials[130]. The microfluidic process reveals a faster polymerization due to the excellent heat transfer with maintaining the control over the polymer parameters (M_n/M_w = 1.15). Similar results were found for microwave assisted RAFT polymerization but the continuous process offers a pronounced scalable and cost-efficient procedure.[131] Hornung et al.[132] successfully conducted solution-phase RAFT polymerization under continuous and segmented flow conditions in a tubular flow reactor (id: 1 000 μm). The comprehensive investigation contains polymerizations under a large variety of conditions. Besides four different monomers (NIPAM, *n*-butyl acrylate (*n*BA), vinyl acetate (VAc), *N,N*-dimethylacrylamide (DMA)), various initiators, solvents, and RAFT agents were employed. High conversions (80-100%) and low polydisperisties (1.15-1.20) could be obtained in both flow modes showing potential for the synthesis of block copolymers in continuous fashion, which will be highlighted in the following section.

In general, controlled radical polymerization exhibits slower reaction kinetics compared to ionic or free radical polymerizations. Due to this, CRPs do not present chemical reactions, which directly benefit from the micro flow technology with its superior heat and mass transfer. Furthermore, additional requirements have to be fulfilled, e.g., the reaction mixture has to be homogeneous at all conversions and temperature ranges, which are applied in the small dimensional reactors. Even a small amount of precipitated material is challenging and can lead to problems for long-term stability of the microfluidic device.[123] However, the reason for the implementation of CRPs in continuous flow is more focused on the development of a simple and economical method for the construction of polymeric material “libraries” that can provide a wide range of well-defined polymers in terms of molecular weight and architecture. Thus, from a scientific and industrial point of view it is advantageous to create a method for facile screening of the relation between polymer architecture, composition and reaction parameters.[122] Scale down can easily be obtained without wasting material during the screening process and therefore the novel developed SEC method , viz., CORSEMP presents an ideal and convenient tool for the rapid analysis of such polymer libraries.

In summary, a large number of monomers have been polymerized homogeneously in various microfluidic devices with different polymerization techniques like anionic, cationic, free radical, and controlled radical polymerization (cf. summary in Table 1). On the one hand the basic investigations of the homopolymers are established in micro reaction technology, but on the other hands future challenges are the implementation of additional monomers for the preparation of homopolymers but also block copolymers and other architectures using continuous flow.

Table 1. Monomers transferred into microstrucutred reactors are listed with corresponding references.

structure	R[a]	name	PM[b]
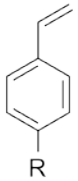	H[100, 101, 103, 104, 107, 123, 127]	styrene	A, F, CRP
		4-*tert*-butoxystyrene	A
	OMe_3[100]	*p*-dimethylsilyl styrene	A
	$SiHMe_2$[103]	*p*-methoxystyrene	A
	OMe[103]	TBDMS sytrene	A
	OTBDMS[c, 103]	*p*-metylthio styrene	A
	SMe[103]	*p*-(1-hexynyl)styrene	A
	-C≡C-Bu[103]		
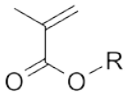	Me[63, 105, 107, 108, 119]	methyl methacrylate	A, F, CRP
	n-Bu[105, 125]	*n*-butyl methacrylate	A, CRP
	t-Bu[105]	*tert*-butyl methacrylate	A
	benzyl[107]	benzyl methacrylate	F
	2-hydroxypropyl[122, 133]	2-hydroxypropyl methacrylate	CRP
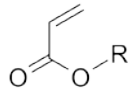	*n*-Bu[63, 107, 123, 127, 132]	*n*-butyl acrylate	A, F, CRP
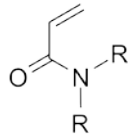	NMe_2[132]	N,N-Dimethyl acrylamide	CRP
	NH-iPr[131, 132]	*N*-isopropyl acrylamide	CRP
	Et[94, 134]	ethyl vinyl ether	C
	n-Bu[92, 95, 134]	butyl vinyl ether	C
	t-Bu[92]	*tert*-butyl ether	C
	i-Bu[92, 94, 134]	isobutyl ether	C
	benzoate[107]	vinyl benzoate	F
	acetoxy[132]	vinyl acetate	CRP

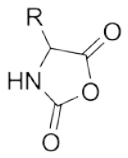	L-Boc-lys[98, 99]	*N-Boc*-L-lysine-NCA[d)]	A
	L-ala[98, 99]	L-alanine-NCA	A
	L-leu[98, 99]	L-leucine-NCA	A
	γ-Bzl-L-glu[99]	γ-benzyl-L-glutamate-NCA	A
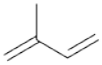	[104]	isoprene	A
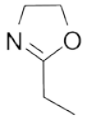	[96]	2-ethyl-2-oxazoline	C

[a]Corresponding residual and/or reference [b]Utilized polymerization technique: carbanionic = A, carbocationic = C, free radical polymerization = F, controlled radical polymerization = CRP, [c]TBDMS = tert-butyl(dimethyl)siloxyl [d)] NCA = *N*-carboxy anhydride and Boc = *tert*-butyloxycarbonyl.

Linear Block Copolymers

The implementation of homopolymerizations in micro reaction technology presents a fundamental research basis (Chapter 3) for the preparation of complex polymeric architectures in microfluidic devices. As can be imagined, the development of linear block copolymers represents the next key target for synthetic chemists and in particular living polymerization techniques provide an ideal platform for the synthesis of multi-block copolymers, since they can be prepared in a one-pot reaction by sequential addition of the desired monomers. By connecting further mixers to the microfluidic device, sequential addition of monomers can be achieved, leading to block copolymers with different block ratio and degree of polymerization. As alternative access, diblock copolymers can be obtained by semi-continuous approaches. Here, a conventionally synthesized macroinitiator can be introduced in the microfluidic devices to initiate the second polymerization or the macroinitiator can be synthesized in continuous flow and utilized in a batch reactor for a subsequent block polymerization. Thus, in many fields of macromolecular chemistry (semi)-continuous flow synthesis of block copolymers were accomplished.

The first reports on carbocationic block copolymerization in flow chemistry was published by Sawamoto and coworkers.[134] The polymerization of different vinyl ether monomers (isobutyl vinyl ether (IBVE), *n*-butyl vinyl ether (NBVE) and ethyl vinyl ether (EVE)) in continuous flow (flow rates 1-4 mL min^{-1}) was investigated. Diblock and triblock copolymers were synthesized by connecting a second and third mixer in sequence for the introduction of monomer 2 and 3, respectively. A schematic setup of the microstructured reactor is depicted in Figure 14

(top). Due to the highly reactive carbocationic intermediates, the polymerization was controlled at -78 °C and short polymerization times of 15-20 seconds per block as well as quantitative yield were obtained. The progress of the block copolymerization was monitored by SEC (Figure 14, bottom). Sequential increase of molecular weights with each monomer addition and narrow MWDs ($M_w/M_n \approx 1.2$) indicating a proper control over the macro-molecular properties.

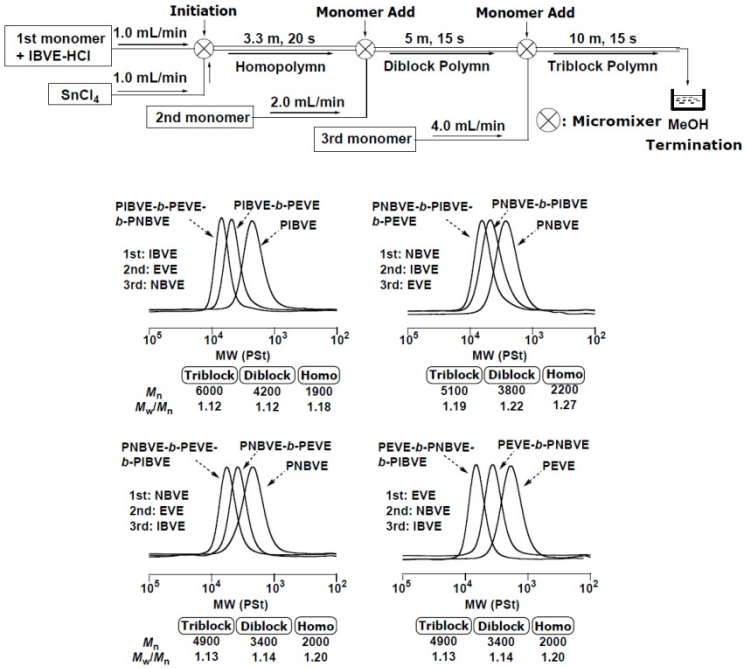

Figure 14. Carbocationic continuous block copolymerization of isobutyl vinyl ether (IBVE), *n*-butyl vinyl ether (NBVE) and ethyl vinyl ether (EVE) in different addition orders carried out in a microstructured reactor with 3 T-shaped micromixers (top). Control over molecular weight and MWD was monitored by SEC (bottom).[134]

Iwasaki et al. carried out diblock copolymer synthesis with different order of monomer addition (monomers: IBVE, NBVE, and EVE). Moreover, the authors were able to increase the reaction temperature to -25 °C by using trifluoromethane-sulfonic acid (TfOH) as initiator.[94] Controlled and rapid synthesis of block copolymerization by anionic polymerization techniques in continuous flow was initially reported by Müller et al. in the late 1990s.[63] In less than 0.6 s a block copolymer of MMA and *n*-BuA (27 000 g mol^{-1}, $M_w/M_n = 1.35$) was obtained in a microfluidic setup with two mixers in sequence. In our group a series of block

copolymers could be prepared in a very short time at room temperature using a microstrucutured reactor with two slit interdigital micromixers[100].

Table 2. Results of the anionic block copolymerization of styrene derivatives in a microstructured reactor, by variation of flow rate ratio different block ratios could be obtained.[100]

sample	S:*t*-BuOS[a]	M_n[b]	M_n[c]	M_n[d]	M_w/M_n[e]
PS-17	0:35	3 600	3 700	4 200	1.21
PS-18	5:5	1 400	1 300	1 500	1.18
PS-19	10:5	1 900	1 900	2 100	1.22
PS-20	22:12	4 400	4 800	4 700	1.17
PS-21	80:30	13 600	13 100	13 600	1.15
PS-22	200:25	25 300	24 700	25 600	1.14

[a]Block ratio styrene (S)/4-*t*-butoxystyrene (*t*-BuOS) adjusted by flow rates; [b]Theoretical value of the number average MWD in g mol^{-1}; [c]Number average of the MWD in g mol^{-1} determined by SEC in tetrahydrofuran; [d]Number average of the MWD in g mol^{-1} determined by multi-angle light scattering (MALLS) in tetrahydrofuran; [e]Polydispersity index determined by MALLS detection in tetrahydrofuran.

The adjustment of block ratios was achieved by variation of flow rate ratio of monomers (styrene and 4-*tert*-butoxystyrene (*t*-BuOS)) and initiator. Well-defined block copolymers were synthesized at room temperature with THF as solvent and molecular weights in the range of 2 000 to 25 000 g mol^{-1} and narrow MWDs (M_w/M_n = 1.1-1.2) were obtained (Table 2). Although the MWDs are not as narrow as those obtained by break seal- and high vacuum-techniques[135] ($M_w/M_n \leq 1.1$), the materials are suitable for most relevant purposes of block copolymers. Nagaki et al.[103] prepared block copolymers in a similar setup using syringe pumps and two T-shaped micromixers in series. The polymerization was carried out at 0–24 °C and two different styrene derivatives (TBDMS-styrene and *p*-dimethylsilyl-styrene) were copolymerized with styrene to synthesize low molecular-weight block copolymers ($M_n \leq 3\,100$ g mol^{-1}). An alternative route to these block copolymers affords the reaction of two different living polymer chains with dichlorosilane.[103] Yoshida and coworker expanded their work by preparing diblock copolymer of different methacrylates. MMA, *n*-Butyl methacrylate (BuMA), and *tert*-butyl methacrylate (*t*-BuMA) were used as monomers to synthesize well defined diblock copolymer without using any additives.[105]

After the successful implementation of anionic polymerizations of methacrylates[105] and styrenes[100, 103, 104] in microfluidic devices, block copolymers consisting of both monomer

types were produced in an integrated flow microreactor system equipped with up to four T-shaped micromixers.[136] In the 1st mixer, styrene was initiated with *sec*-BuLi. Due to the pronounced reactivity of the living chain end, the polymer was end-capped with 1,1-diphenylethylene (DPE) in the 2nd mixer with a high functionalization efficiency (80%). The resulting organolithium species could be used as macroinitiator for methacrylate polymerizations, which were carried out in the 3rd mixer and a subsequent microtube. Block formation was observed by SEC analysis and diblock copolymers with a DPE unit at the junction point and precise adjustable molecular weight properties were recovered (M_n = 3 900–17 000 g mol^{-1}, M_n/M_w = 1.1–1.5, Figure 15).

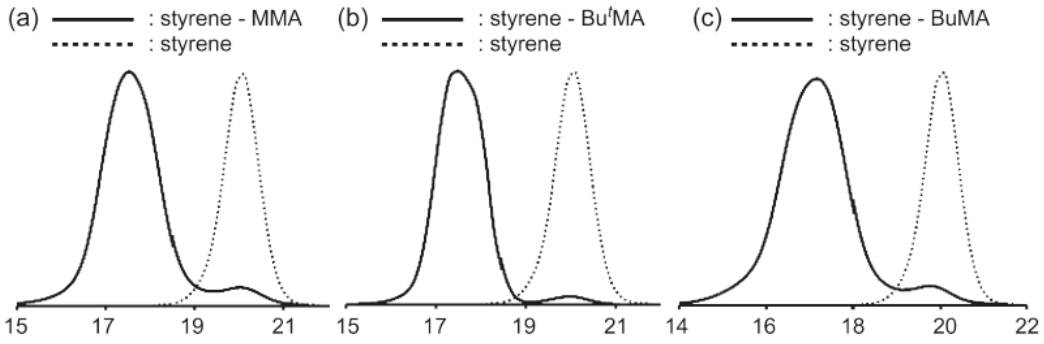

Figure 15. Molecular weight distributions of the block copolymerization of styrene and alkyl methacrylates in continuous flow. In all cases the solid line presents the block copolymer and the dashed line the corresponding PS precursor. a) styrene-MMA, b) styrene-*t*-BuMA, c) styrene-BuMA.[136]

As first monomer styrene or *p*-dimethylsilylstyrene and as second monomer MMA, BuMA, or *t*-BuMA were used to obtain a large variety of different diblock copolymers. To provide the ideal reaction conditions for the different monomers, each part of the system was cooled to the optimized reaction temperature of the corresponding monomer in the range of -28 °C to 24 °C. Moreover, the micro reactor system was expanded with an additional mixer (4th) to prepare PS-(P*t*-BuMA)-poly(alkyl methacrylate) triblock copolymers. The schematic overview of this multiple step continuous flow polymerization is depicted in Figure 16. As third monomer either MMA or BuMA was utilized and the stepwise increase of the molecular weight was observable in SEC. Thus, the continuous polymerization of triblock copolymers was accomplished under easily accessible conditions similar to the carbocationic approaches for diblock copolymers and triblock copolymers mentioned above.[136] These results verify the

living nature of the anionic polymerization in continuous flow and in addition the new and facile access to structurally well-defined block copolymers.

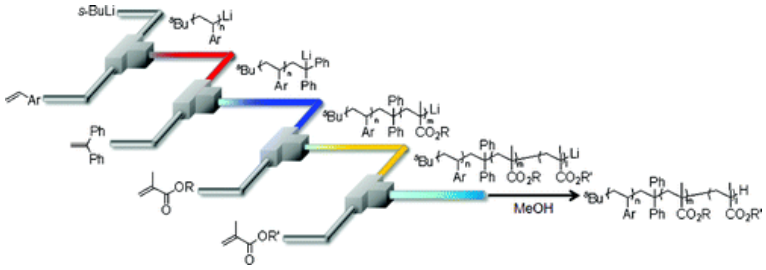

Figure 16. Schematic illustration of a flow micro reactor system for the preparation of triblock copolymers is presented. Living PS gets end-capped with DPE prior to the initiation of two alkyl methacrylate polymerizations in continuous flow.[136]

Very recently, a semi-continuous approach to amphiphilic block copolymers with an addressable amine functionality between the two blocks was accomplished.[102] The first step was a continuous polymerization of styrene in a microstructured reactor with a subsequent quantitative end-capping by *N,N*-dibenzyl amino glycidol (DBAG) as already mentioned above. The attack of the living chain end at the highly strained epoxide ring yields a terminal hydroxyl group. In a second reaction step, the hydroxyl functionalities were utilized to initiate the oxyanionic ring-opening polymerization of ethylene oxide (EO) generating PS-PEO block copolymers with an protected amine group at the block interface. The amine functionality was released by hydrogenolysis and addressability was proven by dye-labeling. The successful coupling demonstrates the intriguing potential of such materials for the generation of switchable, smart surfaces.

Another semi-continuous approach was carried out by Wu et al.[133] In a three-input CRP chip, the controlled radical polymerization (ATRP) of HPMA was started with a PEO macroinitiator (PEO-Br, M_n = 2 900 g mol^{-1}). By applying a constant concentration of all reagents, lower flow rates (240 µL h^{-1}) revealed higher conversion (≤68%) due to the increased reaction time (188 min). Thus, the block length of P(HPMA) can be adjusted via the flow rate. An additional method represents the variation of flow rate ratio between monomer and initiator. By constant total flow rate (450 µL h^{-1}, reaction time: 100 min) a decreasing initiator concentration leads to higher molecular weights but also to a lower conversion. Quantitative initiation was confirmed by SEC analysis due to the disappearance of the macroinitiator

signals. Both methods afford well-defined polymers (M_n = 5 000-13 000 g mol^{-1}) with narrow molecular-weight distributions (M_w/M_n = 1.18-1.30) and afford a facile design and tunability in composition of block copolymers. The already introduced C-SATRP (see Chapter 3) was also utilized from Zhu and coworkers for controlled radical block copolymerizations. Two continuous column reactors packed with supported CuBr-HMTETA catalyst and connected in series were applied for the block copolymerization of MMA and BuMA at 80 °C. Due to residual MMA from the first reactor few MMA units are incorporated in the BuMA block. However, the second block could be adjusted by the flow rate ratio of BuMA and block copolymers with controlled molecular weight can be obtained, which confirms the living manner of the C-SATRP. On the basis of this methodology Barner-Kowollik and coworkers developed a kinetic model for the continuous ATRP synthesis of block-like copolymers enabeling the calculation of sequence distribution as function of chain length in continuous flow reactors (Figure 17).[137]

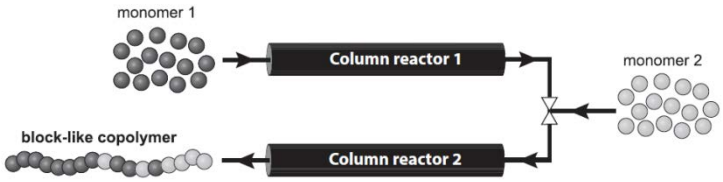

Figure 17. Synthesis of block-like polymers by utilizing continuous supported atomic transfer radical polymerization (C-SATRP).[137]

Haddleton and coworkers utilized ATRP to synthesize block copolymers with tubular flow reactors. As first block MMA and as second block BuMA, benzyl methacrylate (BzMA), or BuA were used whereas the P(MMA)-*block*-P(BzMA) showed the highest conversion (≥ 90%). The report developed a suitable continuous system for an excellent and facile way to continuous ATRP processes.[120]

A nitroxide-mediated block copolymerization of butyl acrylate (BuA) and styrene was carried out in continuous flow and the influence of different lamellar mixing geometries concerning molecular weight and MWD was investigated. Two stainless steel microtube reactors under a constant pressure of 20 bar were used for the polymerization (Figure 18).

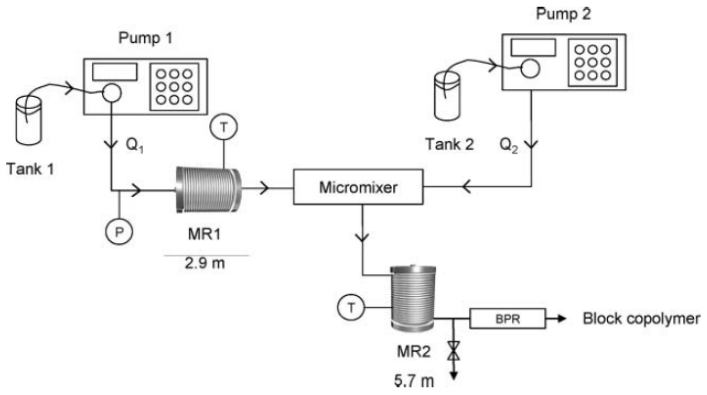

Figure 18. Schematic overview of the microreaction set up of Serra and coworkers for the nitroxide-mediated block copolymerization of BuA and styrene. The setup consists of two micrtube reactors (MR1 and MR2), a micromixer, a pressure sensor P, two temperature probes T and a back pressure regulator (BPR).[138]

Three different geometries of multilamination micromixers with different "form factors" ($F = 1/N(W_C + W_L)$, N number of channels per inlet, W_C = channel width, W_L = slit width) are used to combine the P(BuA) solution[139] with a styrene solution. The efficient mixing leads to higher contact area between the P(BuA) and styrene phases and affords increased conversions and control of styrene polymerization in comparison to batch reactors (no significant increase of M_n and $M_w/M_n = 1.75$[139]). Efficient block formation was confirmed by comparing UV and RI signals of SEC analysis. Moreover, higher form factors of the three different micromixers reveal a decreased BuA incorporation in the second block and narrower MWDs ($M_w/M_n = 1.28$). Furthermore, by changing the flow rate ratio of styrene and P(BuA) from 9.3 to 26.5 µL min^{-1} an increased molecular weight of the second block can easily be achieved. This results can be helpful by optimizing existing micromixers or designing other geometries for a more efficient mixing.[138]

In summary, a large variety of block copolymers were successfully synthesized using micro reaction technology. Cationic, anionic as well as controlled radical polymerization techniques provide access to block copolymers with different molecular properties. Block copolymer synthesis capitalizing micro reaction technology presents the next level prior to the preparation of homopolymers.

Non-Linear Polymer Architectures

Non-linear architectures like hyperbranched, star, or comb polymers as well as dendrimers bear intriguing macromolecular and material properties.[140, 141] Especially, dendrimers represent an emerging class of materials due to distinguishable properties compared to typical polymers (single size, precise molecular weight and number of end groups). In seminal works of Vögtle, Tomalia, Hawker, Fréchet and coworkers the general synthesis strategy including the divergent and convergent approach was discovered.[142-145] Today dendrimers show potential application in a variety of fields, e.g., drug delivery, catalysis, sensor, and light harvesting.[146-148] However, the large scale synthesis of dendrimers is limited due to several tedious and time-consuming synthesis and purification steps, which reduce the industrial potential of the materials. Thus, a fast and rapid synthesis using micro reaction technology is favorable and the comparably low intrinsic viscosity[149, 150] and increased solubility[151, 152] of highly branched polymers are advantageous for transfer to microdimensions.

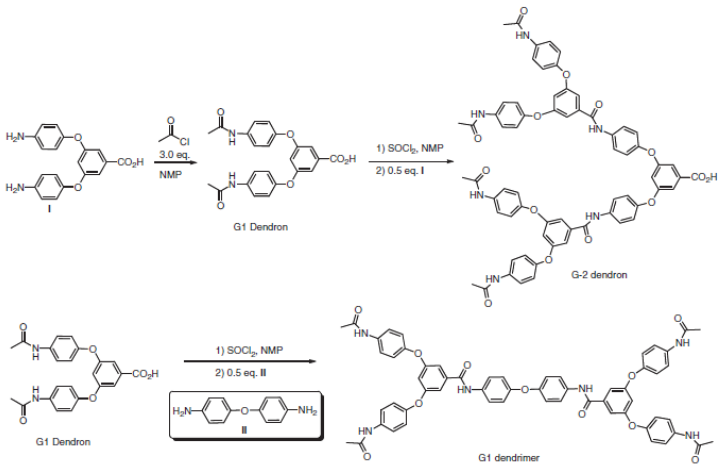

Figure 19. Synthesis of dendritic polyamide in a convergent multistep microreactor approach using a individually designed setup with an IMM interdigital micromixer.[153]

In contrast to the preparation of linear polymers, the continuous flow investigation in the field of complex macromolecular architectures is in its early stage. For example, Liu et al. prepared the first polyamide dendrons and dendrimers (2nd generation) by convergent approach in continuous flow using an IMM interdigital micromixer (Figure 19). Several advantages could be obtained from the implementation to the micromixing process. The reaction time could be decreased from a few hours to minutes indicating reduced

production cost for large scale applications. In addition, the reaction could be carried out at convenient conditions (e.g., room temperature) and access to higher generations of dendrimers might be possible. Moreover, the continuously synthesized dendrimers were directly deposited on functionalized surfaces representing promising applications of protein adsorptions or antimicrobial coatings.

Hyperbranched polymers show similar properties compared to perfectly branched dendrimers and a preparation is enabled without a tedious multistep synthesis protocols.[154] Therefore these materials have been attracted increasing attention in recent years. In particular, the synthesis of hyperbranched polyglycerol by slow monomer addition (SMA) presents a controlled access to biocompatible[155] polymers with randomly branched structure.[156] The synthesis, modification and characterization of this material are investigated in our group intensively.[157-160] Recently, we transferred the ring-opening mulitbranching polymerization (ROMBP) of glycidol into a continuous flow process, where the highly exothermic reaction can benefit from the efficient heat and mass transfer (Figure 20).[161] Compared to classical batch methods, the experimental time and effort could significantly be reduced. Additionally, the highly toxic monomer glycidol can be handled in a safer reaction protocol. Residence times of 10 to 20 minutes were applied and low molecular weights were targeted to keep the overall viscosity low. Quantitative incorporation of the initiator molecule was confirmed by MALDI-ToF MS. Although the molecular weights are limited to 2 000 g mol^{-1} this concept represents a novel and rapid access to hyperbranched polyglycerols, which can be extended to other syntheses of hyperbranched polymers.

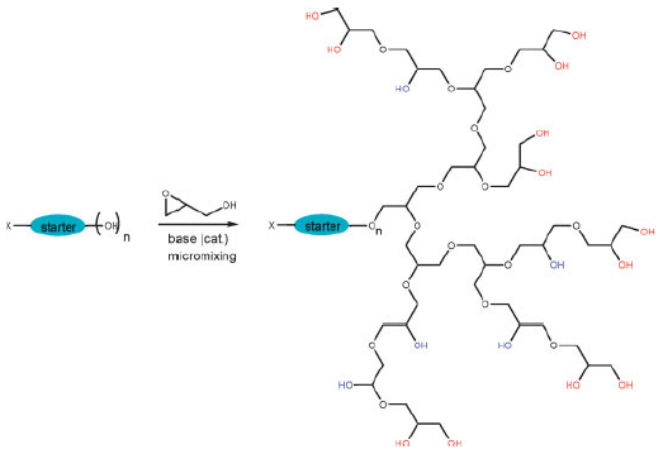

Figure 20. Synthetic access of hyperbranched polyglycerol using a microstrucutured reactor.[66]

The polycondensation of a multifunctional monomer (trialkoxysilane) was conducted in a microreactor setup (caterpillar split-recombine micromixer) and the polymer properties were investigated by changing the residence time. Continuous flow synthesis of branched poly(silsesquioxane)s achieves an increased yield and decreased polydispersities compared to the batch process (M_n = 1 900–11 000 g mol^{-1}, $M_w/M_n \leq 2$).[162]

The ATRP synthesis of branched macromolecular architectures in a tubular microreactor (id: 900 μm) was initially carried out by Bally et al.[163] The authors used the well-known self-condensing vinyl copolymerization (SCVCP) developed by Fréchet et al.[164] and adapted to ATRP by Matyjaszewski et al.[165] The branching efficiency can be optimized with the operating conditions,[166] which is important if a functionalization of the final product is desired. Branched poly(methacrylate)s were synthesized by SCVCP via ATRP in a tubular reactor with 2-(2-bromoisobutyryloxy)-ethyl methacrylate (BIEM) as inimer. The feeding ratio of BIEM was varied between 0 and 5% synthesizing linear and different branched polymers in a controlled manner (M_w/M_n = 1.42–2.15) to conveniently generate a polymer library for screening of various macromolecular characteristics (Figure 21).

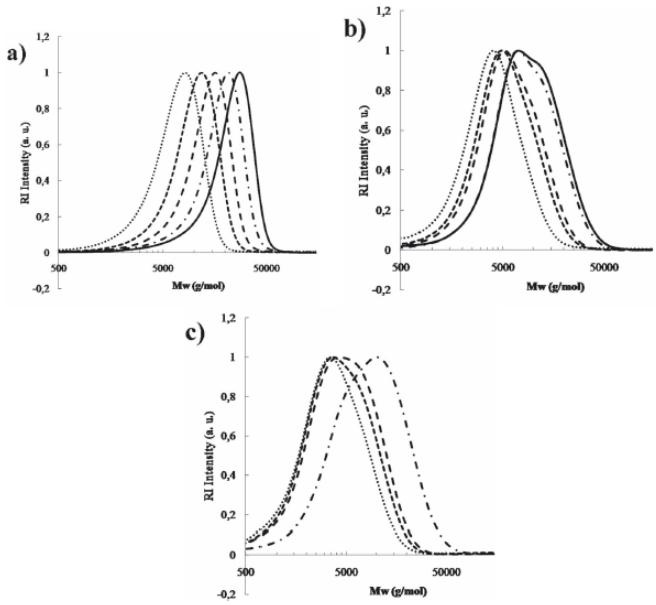

Figure 21. Characterization data from screening experiments with different residence times: 15 min (dotted line), 30 min (short dashed line), 60 min (long dashed line), 120 min (dotted/dashed line), 240 (solid line) and different macromolecular architectures a) linear polymer, b) branched polymer with 2% of BIEM and c) branched polymer with 5% BIEM.[163]

In addition, increased initiation kinetics and the reduced diffusion pathways in the confinement of the microreactor lead to improved branching efficiency, denser polymeric architecture and increased functionality compared to batch reactors.[167] This continuous flow microprocess opens promising perspectives for the synthesis of highly functionalized branched polymers.

Seeberger and coworkers have demonstrated in an elegant way a photofunctionalization of poly(lysine) with glycol-dendrons in continuous flow. In particular, three or nine mannose- or galactose-bearing dendrons were selectively connected to a poly(l-lysine) backbone by a [2+2] photocycloaddition in water. The glycol-conjugated polymer was used as platform to study carbohydrate-pathogen interactions, which show a potential application as a sensitive and selective biosensor for mannose-binding *E.coli*.[168]

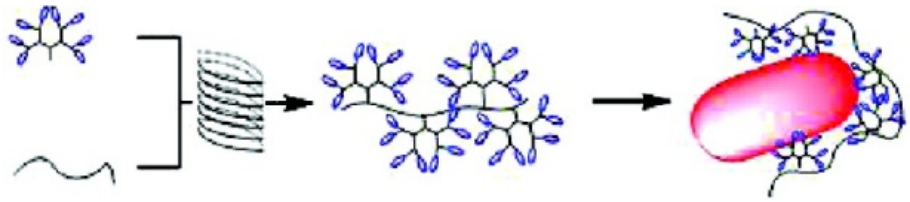

Figure 22. Schematic overview of the efficient and rapid synthesis of glycol-dendronized polylysine in a continuous flow reactor and application as biosensor for mannose-binding *E coli*.[168]

In summary, first attempts for the preparation of non-linear architectures in microreaction processes were successfully carried out. Dendrimers, (hyper)branched and dendronized polymers could be synthesized in continuous flow mostly with superior molecular characteristics compared to the corresponding batch reactions. The facile scale-up and reduction of production costs in combination with promising applications like biosensor or drug delivery systems show the high potential of continuous flow synthesis in terms of macromolecular architectures.

Special-Catalyzed Polymerizations

As indicating above in the last decade several interesting polymerizations techniques have been transferred to continuous flow system for the preparation of various polymer architectures. However, recently a novel synthesis strategy for catalyzed reactions has been developed. In this special cases, the reaction tube is not only the shell respectively the case

in which the reaction solution is passed through, furthermore it represents the necessary catalyst for the polymerization.

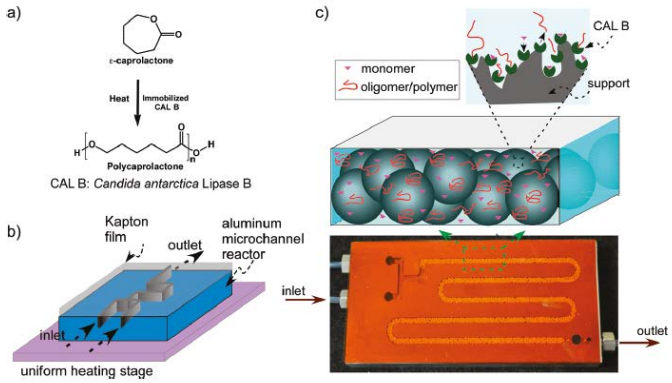

Figure 23. Enzyme-catalyzed polymerization of *ε*-caprolactone in a continuous flow. a) reaction scheme, b) schematic overview of the micoreactor setup. c) image of a reactor used in the study. The zoom in explains the construction and the mechanism of the reaction in the micochannels.[169]

Beers and coworkers designed the first solid supported enzyme-catalyzed polymerization in continuous flow (Figure 23).[169] As a model compound they studied the ring-opening polymerization of *ε*-caprolacton by using immobilized *Candida antartica* Lipase B (CAL B) in the form of Novozym 435 (N435) beads (diameter 400 ± 50 µm) as biocatalyst, which is commercially available. The polymerization was carried out in the temperature range from 55–100 °C and compared to the corresponding reaction in a batch system. The apparent rate of reaction is at least one order of magnitude higher due to the special reaction conditions in the microreactor. As a consequence of the small diameter (2 mm width, 1 mm depth) of the reaction tube the reactants are forced to be in contact with the enzyme and due to the high surface-to-volume ratio more active sites of the enzyme are available during the course of the reaction. The results are promising, especially with regard to future applications, like screening reactions for different catalytic systems.

In another report Beers and coworkers investigated a microchannel-confined surface-initiated polymerization technique (µSIP) to synthesize gradient polymer brush layers of poly 2-hydroxyethyl methacrylate (PHEMA) by ATRP (Figure 24).[170] Therefore the authors prepared an initiator functionalized monolayer on the surface of a silicon microchannel. As

expected there is a linear correlation of the thickness of the polymer brushes and the distance from the inlet to the outlet (representing the length of the initiator functionalized silicon microchannel) and consequently with the reaction time.

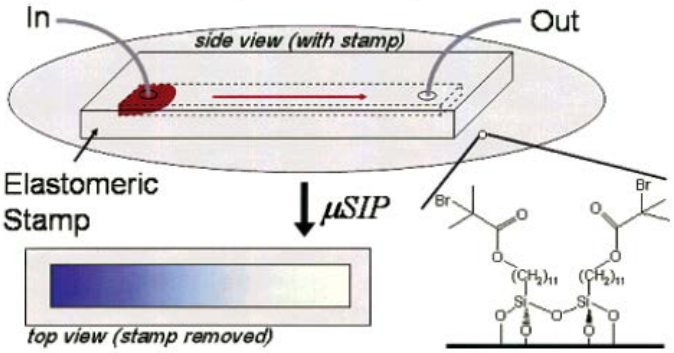

Figure 24. Syntheses of gradient polymer brush by µSIP.[170]

In a further thematically encouraging study Beers and coworkers were able to synthesize statistical copolymer brushes of *n*-butyl methacrylate (BMA) and 2-(*N*,*N*-dimethylamino)ethyl methacrylate (DMAEMA) with a gradient structure in a modified continuous flow setup.[171]

To date, it is not possible to perform a living radical polymerization of vinylchloride (VC) with an inner-sphere radical process, e.g. ATRP. The corresponding intermediate of VC (i.e., I-CH_2-CH(Cl)-X, with I: initiator and X: halide of the Initiator) is not reactive enough towards the Cu(I) species to start the polymerization.[172] In 2001 Percec and coworkers developed a novel strategy for the polymerization of VC in an almost controlled fashion by using I-CH_2-Ph-CH_2-I/Cu(0)/ 2,2'-bipyridyl as initiator system at a temperature of 130 °C. The observed monomer conversion was in the most cases lower than 40% due to the formation of inactive species via chain transfer to monomer. Hence, the authors obtained a linear correlation of M_n to monomer conversion and simultaneous decrease of the molecular weight distribution ($M_w/M_n \approx 1.5$).[173] The Cu^0 initiated polymerization presents a breakthrough in terms of VC polymerization and consequently Percec and coworkers established the outer-sphere single-electron-transfer living radical polymerization (SET-LRP).[174, 175] A variety of monomers were investigated and high molecular weights (M_n > 1 kg mol^{-1}) with narrow MWDs as well as negligible bimolecular termination at room temperature were achieved. Compared to inner-sphere radical processes the SET-LRP shows high reaction kinetics due to decreased activation energy.[176] These outstanding polymerization properties especially with regards to

the high reaction rates inspired Hutchinson and coworkers to transfer this new LRP method to a microfluidic system for the polymerization of methyl acrylate (MA) in dimethyl sulfoxide (DMSO).[177] Inexpensive and commercially available cupper tubes were used as initiator, which obviously offer a large surface area and hence efficient catalysis (Figure 25). Additionally, the authors demonstrated the pronounced living character of the continuous flow LRP-experiment by further chain extensions experiments.

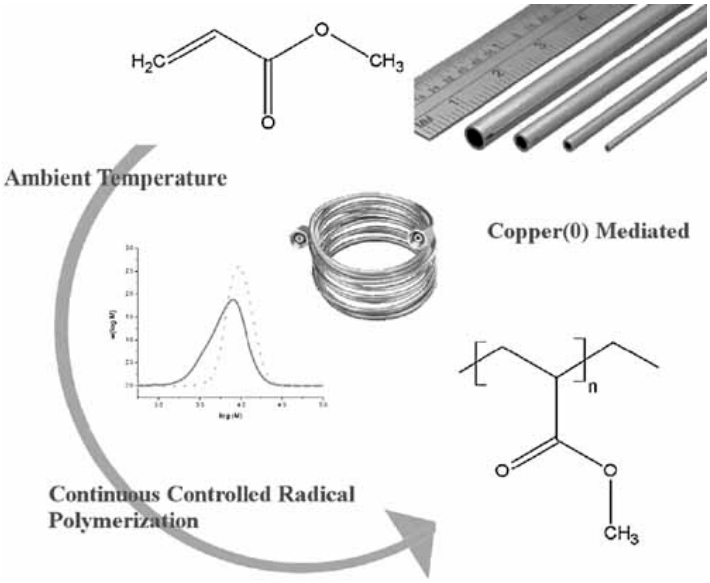

Figure 25. Polymerization of methyl acrylate in DMSO at room temperature by SET-LRP in continuous flow.[177]

Further studies in a continuous tank reactor underline the high potential of this reaction, especially in terms of possible industrial scaled processes.[178]

Very recently, Hutchinson and coworkers improved the synthesis of poly(methyl acrylate) (PMA) in continuous flow.[179] Inspired by ARGET ATRP,[180] they studied the influence of ascorbic acid in SET-LRP in both, batch and continuous flow systems. In conventional reactors ascorbic acid was added to the catalyst, which leads to an enormous boost of the reaction, accompanied with a loss of control ($M_w/M_n \approx 3.3 \pm 0.2$). To avoid this undesired effect the reaction was initiated with the copper wire and in a second step, the wire was removed and ascorbic acid was added. The mixture of existing copper specie and ascorbic acid in the reaction was sufficient to possess an increased control of the reaction. Moreover, the reaction was amplified with increasing reaction control. The reaction conversion was up to 95% and MWDs of 1.20 were obtained.

Based on this knowledge, the ascorbic acid stimulated SET-LRP was investigated in detail by transferring the corresponding polymerization to a special designed reactor (Figure 26). After initiating the reaction in a copper tube (id: 1.6 mm), ascorbic acide was added by a T-mixer and the polymerization proceeds in a stainless steel tube which leads to polymers with decreased copper content of less than 10^2 ppm.

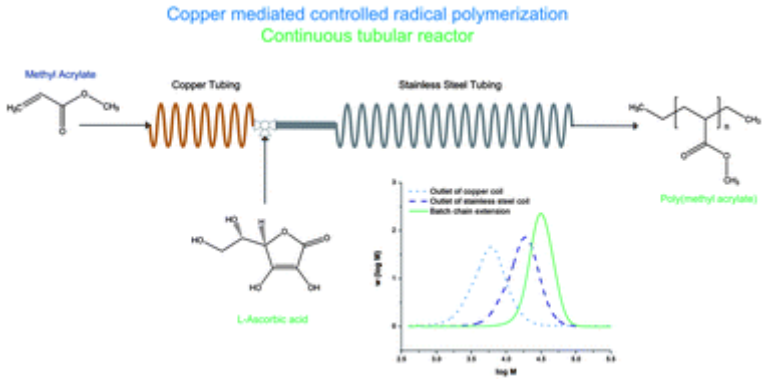

Figure 26. Copper mediated SET-LRP of methyl acrylate in the presence of ascorbic acid using a continuous flow microreactor[179]

From an economic point of view, iron represents a more attractive metal due to its lower price and lower toxicity compared to copper. In 2010 Wang and Matyjaszewski demonstrated in an impressive work an ATRP of methyl methacrylate (MMA) using $FeBr_2$ as catalyst in the absence of additional ligands.[181] Certain polar solvents not only dissolve the catalyst, additionally the solvents might operate as ligand for the catalyst and adjust the catalytic activity. First time in 2011 this approach was transferred to the SET-LRP in continuous flow by Chen et al. The polymerization of acrylonitrile (AN) using iron tubes (Fe^0) as catalyst and 2-bromopropionitrile (BPN) as initiator without any ligands was investigated.[182] The linear correlation between the molecular weights of the resulting polymers with conversion suggests, that the polar solvents like *N*-methyl-2-pyrrolidone (NMP) and *N,N*-dimethylformamide (DMF) could act as ligands in this system. In batch reactors the authors verified the living nature of the continuously synthesized PAN by subsequent block copolymerization of MMA.

In summary, this paragraph about recently developed strategies for the *in situ* catalyzed polymerization in microstructured reactors present a current overview and shows the high potential of continuous flow devices. New polymerization techniques are managed to be transferred to a continuous flow system with promising results. Not only due to the already

and often discussed benefits owed by the special design, but also for the less synthetic effort for screening reactions to find the best synthetic conditions.

Conclusion and Outlook

Micro flow technology represents a valuable reaction platform for polymer synthesis. The reported works on ionic as well as (controlled) radical polymerization techniques benefit from the small dimensions with excellent heat and mass transfer. Furthermore, the advantageous conditions in microreactors lead to higher conversions and reduced reaction times. Individually designed microreators provide a hermetically sealed system, which is ideal for ionic polymerizations given the related sensitive process. Besides the continuous synthesis of linear polymers, particular progress has been made for the preparation of complex non-linear architectures. For example, pathways to dendrimers, (hyper)branched and dendronized polymer with reduced experimental effort were accomplished and offer polymeric materials with high definion considering the molecular weight distribution. This enables facile access to polymeric materials with architectural variation and structural design.

Although micro flow technology is established in polymer science, some key issues have to be investigated in the future. For possible applications both in academia and industry, scientists will have to deal with a certain focus on the following key questions: Does the polymerization take place within the micromixer or in the subsequent delay tube? When is the earliest point to obtain the product without wasting reaction time and experimental effort?

In addition to the scientific benefit, in a university setting the utilization of microflow processes afford educational benefit due to the small scale experiments and the similarity to technical procedures that are often continuous. The exploration of potential of continuous approaches that are so far only achieved in large-scale production in industry can be accomplished within the microstructured reactors using very small amounts of reagents. Moreover, the continuous flow synthesis enables rapid screening of reaction parameters. Thereby, microflow systems are valuable tools for the optimization of reaction conditions. Additionally, the preparation of a large number of polymer samples with different molar

masses by variation of flow rate ratios of monomer and initiator in just one reaction setup can be achieved conveniently, rendering microflow devices a rapid experimental tool.
Recently, a tubular reactor was used directly as a catalyst in continuous flow. This shows first approaches to go beyond the borders of batch systems. Future challenges are the transfer of peculiar and unexploited polymerizations into microstructured reactors, which cannot be carried out easily under conventional conditions. In addition, the scope of the current technology can be advanced by combination of different polymerization techniques or the synthesis of multiple block copolymers with sequential addition of (metastable) monomers. The implementation of post-polymerization reactions seems to be another promising prospect to reduce reaction time and purification steps compared to the conventional procedures. Although the micro processes are partially prone to clogging of the microchannels, current investigations show the high potential of microflow processes for academic and industrial applications. The current challenges and the promise of the microdimensions will undoubtedly inspire polymer scientists for more research in this fascinating area.

Acknowledgments

C.T. thanks MPGC (Max Planck Graduate Center with Johannes Gutenberg-University) for a scholarship. C.T. and A.N. acknowledge the Excellence Initiative (DFG/GSC 266) for fellowships and financial support.

Biographies

Christoph Tonhauser received his diploma degree in chemistry from the Johannes Gutenberg-Universität Mainz in 2009. After a temporary stay at the Polymer Science and Engineering Department, University of Massachusetts in Amherst in the group of E. Bryan Coughlin, he is currently working on his PhD thesis in the group of Holger Frey. His research focuses on the preparation of functional polymers in microstructured reactors. He currently holds a scholarship from the Max-Planck Graduate Center (MPGC) and a fellowship of the MAINZ graduate school of excellence.

Biographies of co-authors are deleted due to privacy protection.

Lebensläufe der Co-Autoren wurden aus datenschutzrechtlichen Gründen entfernt.

References

1. Hessel, V.; Renken, A.; Schouten, J. C.; Yoshida, J.-i., *Micro Process Engineering : A Comprehensive Handbook*. Wiley-VCH: Weinheim, 2009.
2. Ehrfeld, W.; Hessel, V.; Löwe, H., *Microreactors: New Technology for Modern Chemistry*. Wiley-VCH: Weinheim, 2000.
3. Hessel, V.; Löwe, H.; Müller, G.; Kolb, G., *Chemical Micro Process Engineering 1 + 2. Fundamentals, Modeling and Reactions/Processes and Plants*. Wiley-VCH: Weinheim, 2005.
4. Kockmann, N.; Brand, O.; Feder, G. K., *Micro Process Engineering*. Wiley-VCH: Weinheim, 2006.
5. Kenis, P. J. A.; Ismagilov, R. F.; Whitesides, G. M. *Science* **1999,** 285, (5424), 83-85.
6. Gorges, R.; Taubert, T.; Klemm, W.; Scholz, P.; Kreisel, G.; Ondruschka, B. *Chem. Eng. Technol.* **2005,** 28, (3), 376-379.
7. Greener, J.; Tumarkin, E.; Debono, M.; Dicks, A. P.; Kumacheva, E. *Lab Chip* **2012,** 12, (4), 696-701.
8. Hessel, V.; Hardt, S.; Löwe, H.; Schönfeld, F. *AlChE J.* **2003,** 49, (3), 566-577.
9. Hardt, S.; Schönfeld, F. *AlChE J.* **2003,** 49, (3), 578-584.
10. Hessel, V.; Löwe, H.; Schönfeld, F. *Chem. Eng. Sci.* **2005,** 60, (8-9), 2479-2501.
11. Nguyen, N.-T.; Wu, Z. *J. Micromech. Microeng.* **2005,** 15, (2), R1.
12. Jäckel, K. P., Microsystem Technology for Chemical and Biological Microreactors. In *DECHEMA Monographs*, W.Ehrfeld, Ed. VCH: Weinheim, 1996; Vol. 132, p 29.
13. Morini, G. L. *Int. J. Therm. Sci.* **2004,** 43, (7), 631-651.
14. Chun, J.-H.; Lu, S.; Lee, Y.-S.; Pike, V. W. *The Journal of Organic Chemistry* **2010,** 75, (10), 3332-3338.
15. Veser, G. *Chem. Eng. Sci.* **2001,** 56, (4), 1265-1273.
16. Ehrfeld, W.; Hessel, V.; Kiesewalter, S.; Löwe, H.; Richter, T.; Schiewe, J. In Microreaction Technology - IMRET 3: Proceedings of the 3rd International Conference on Microreaction Technology, Berlin, 2000; Ehrfeld, W., Ed. Springer: Berlin, 2000; p 14.
17. Jähnisch, K.; Hessel, V.; Löwe, H.; Baerns, M. *Angew. Chem. Int. Ed.* **2004,** 43, (4), 406-446.
18. Wörz, O.; Jäckel, K.-P.; Richter, T.; Wolf, A. *Chem. Eng. Technol.* **2001,** 24, (2), 138-142.

19. Wörz, O.; Jäckel, K.-P.; Richter, T.; Wolf, A. *Chem. Ing. Tech.* **2000,** 72, (5), 460-463.

20. Gavriilidis, A.; Angeli, P.; Cao, E.; Yeong, K. K.; Wan, Y. S. S. *Chem. Eng. Res. Des.* **2002,** 80, (1), 3-30.

21. Hessel, V. *Chem. Eng. Technol.***2009,** 32, (11), 1655-1681.

22. Fraga-Dubreuil, J.; Comak, G.; Taylor, A. W.; Poliakoff, M. *Green Chemistry* **2007,** 9, (10), 1067-1072.

23. Kiwi-Minsker, L.; Renken, A. *Catal. Today* **2005,** 110, (1-2), 2-14.

24. Fernandez-Suarez, M.; Wong, S. Y. F.; Warrington, B. H. *Lab Chip* **2002,** 2, (3), 170-174.

25. de Mello, A.; Wootton, R. *Lab Chip* **2002,** 2, (1), 7N-13N.

26. Jensen, K. F. *Chem. Eng. Sci.* **2001,** 56, (2), 293-303.

27. Löwe, H.; Hessel, V. In 8th International Conference on Chemical & Process Engineering, Ischia, Italy, 2007; Ischia, Italy, 2007.

28. Thayer, A. M. *Chem. Eng. News* **2005,** 83, 43-47.

29. Iwasaki, T.; Yoshida, J.-I. In *Numbering-up of microreactors for radical polymerization*, Proceedings of 8th International Conference on Microreaction Technology, Atlanta USA, 2005; Atlanta USA, 2005.

30. Pennemann, H.; Hessel, V.; Löwe, H. *Chem. Eng. Sci.* **2004,** 59, (22/23), 4789-4794.

31. Wörz, O.; Jäckel, K. P.; Richter, T.; Wolf, A. In *Topical Conference Preprints*, Process Miniaturization - IMRET 2: 2nd International Conference on Microreaction Technology, New Orleans, USA, 1998; Ehrfeld, W.; Rinard, I. H.; Wegenge, R. S., Eds. American Institut of Chemical Engineers: New Orleans, USA, 1998; p 183.

32. Hessel, V.; Löwe, H. *Chem. Ing. Tech.* **2002,** 74, (1-2), 17-30.

33. Hessel, V.; Löwe, H. *Chem. Ing. Tech.* **2002,** 74, (3), 185-207.

34. Pennemann, H.; Watts, P.; Haswell, S. J.; Hessel, V.; Löwe, H. *Org. Process Res. Dev.* **2004,** 8, (3), 422-439.

35. Hessel, V.; Löwe, H.; Müller, A.; Kolb, G., *Chemical Process Engineering - Processing and Plants*. Wiley-VCH: Weinheim, 2005.

36. Hessel, V.; Löwe, H.; Stange, T. *Lab Chip* **2002,** 2, (1), 14N-22N.

37. Wiles, C.; Watts, P. *Green Chemistry* **2012,** 14, (1), 38-54.

38. Watts, P.; Wiles, C. *Chem. Commun.* **2007**, (5), 443-467.

39. Hessel, V.; Löwe, H. *Chem. Eng. Technol.* **2005,** 28, (3), 267-284.

40. Mason, B. P.; Price, K. E.; Steinbacher, J. L.; Bogdan, A. R.; McQuade, D. T. *Chem. Rev.* **2007,** 107, (6), 2300-2318.

41. Wiles, C.; Watts, P., *Micro Reaction Technology in Organic Synthesis*. CRC Press Inc.: Boca Raton, 2011.

42. Watts, P.; Haswell, S. J. *Chem. Soc. Rev.* **2005,** 34, (3), 235-246.

43. Fletcher, P. D. I.; Haswell, S. J.; Pombo-Villar, E.; Warrington, B. H.; Watts, P.; Wong, S. Y. F.; Zhang, X. *Tetrahedron* **2002,** 58, (24), 4735-4757.

44. Wiles, C.; Watts, P.; Haswell, S. J.; Pombo-Villar, E. *Lap Chip* **2001,** 1, 100 - 101.

45. Wiles, C.; Watts, P.; Haswell, S. J.; Pombo-Villar, E. *Lab Chip* **2001,** 1, (2), 100-101.

46. Burns, J. R.; Ramshaw, C. *Chem. Eng. Res. Des.* **1999,** 77, (3), 206-211.

47. Wiessmeier, G.; Honicke, D. *J. Micromech. Microeng.* **1996,** 6, (2), 285.

48. Greenway, G. M.; Haswell, S. J.; Morgan, D. O.; Skelton, V.; Styring, P. *Sensors Actuators B: Chem.* **2000,** 63, (3), 153-158.

49. Skelton, V.; Greenway, G. M.; Haswell, S. J.; Styring, P.; Morgan, D. O.; Warrington, B. H.; Wong, S. Y. F. *Analyst* **2001,** 126, (1), 11-13.

50. Haswell, S. J.; Middleton, R. J.; O'Sullivan, B.; Skelton, V.; Watts, P.; Styring, P. *Chem. Commun.* **2001**, (5), 391-398.

51. Geyer, K.; Codée, J. D. C.; Seeberger, P. H. *Chem. Eur. J.* **2006,** 12, (33), 8434-8442.

52. Geyer, K.; Seeberger, P. H. *Helv. Chim. Acta* **2007,** 90, (2), 395-403.

53. Ratner, D. M.; Murphy, E. R.; Jhunjhunwala, M.; Snyder, D. A.; Jensen, K. F.; Seeberger, P. H. *Chem. Commun.* **2005**, (5), 578-580.

54. Bogdan, A. R.; Poe, S. L.; Kubis, D. C.; Broadwater, S. J.; McQuade, D. T. *Angew. Chem. Int. Ed.* **2009,** 48, (45), 8547-8550.

55. Lévesque, F.; Seeberger, P. H. *Angew. Chem. Int. Ed.* **2012,** 51, (7), 1706-1709.

56. Brandrup, J.; Immergut, E. H.; Grulke, E. A., *Polymer Handbook*. Wiley: New York, 1999.

57. Geacintov, C.; Smid, J.; Szwarc, M. *J. Am. Chem. Soc.* **1962,** 84, (13), 2508-2514.

58. Bhattacharyya, D. N.; Lee, C. L.; Smid, J.; Szwarc, M. *J. Am. Chem. Soc.* **1963,** 85, (5), 533-539.

59. Bhattacharyya, D. N.; Lee, C. L.; Smid, J.; Szwarc, M. *J. Phys. Chem.* **1965,** 69, (2), 612-623.

60. Hostalka, H.; Figini, R. V.; Schulz, G. V. *Macromol. Chem. Phys.* **1964,** 71, (1), 198-203.

61. Barnikol, W. K. R.; Schulz, G. V. *Die Makromolekulare Chemie* **1963,** 68, (1), 211-215.

62. Baskaran, D.; Müller, A. H. E. *Macromolecules* **1997,** 30, (7), 1869-1874.

63. Hofe, T.; Maurer, A.; Müller, A. H. E. *GIT Labor-Fachz.* **1998,** 42, 1127.

64. Marcarian, X.; Falk, L.; Müller, A. H. E. *DECHEMA Monographs* **1988,** 134, 577.

65. Baskaran, D.; Müller, A. H. E.; Sivaram, S. *Macromolecules* **1999,** 32, (5), 1356-1361.

66. Wilms, D.; Klos, J.; Frey, H. *Macromol. Chem. Phys.* **2008,** 209, (4), 343-356.

67. Hessel, V.; Löwe, H.; Serra, C.; Hadziioannou, G. *Chem. Ing. Tech.* **2005,** 77, (11), 1693-1714.

68. Bally, F.; Serra, C. A.; Hessel, V.; Hadziioannou, G. *Chem. Eng. Sci.* **2011,** 66, (7), 1449-1462.

69. Ohm, C.; Fleischmann, E.-K.; Kraus, I.; Serra, C.; Zentel, R. *Adv. Funct. Mater.* **2010,** 20, (24), 4314-4322.

70. Ohm, C.; Kapernaum, N.; Nonnenmacher, D.; Giesselmann, F.; Serra, C.; Zentel, R. *J. Am. Chem. Soc.* **2011,** 133, (14), 5305-5311.

71. Steinbacher, J. L.; McQuade, D. T. *J. Polym. Sci., Part A: Polym. Chem.* **2006,** 44, (22), 6505-6533.

72. Quevedo, E.; Steinbacher, J.; McQuade, D. T. *J. Am. Chem. Soc.* **2005,** 127, (30), 10498-10499.

73. Bouquey, M.; Serra, C.; Berton, N.; Prat, L.; Hadziioannou, G. *Chem. Eng. J.* **2008,** 135S, S93-S98.

74. Rossow, T.; Heyman, J. A.; Ehrlicher, A. J.; Langhoff, A.; Weitz, D. A.; Haag, R.; Seiffert, S. *J. Am. Chem. Soc.* **2012,** 134, (10), 4983-4989.

75. Kumacheva, E.; Garstecki, P., *Microfluidic Reactors for Polymer Particles*. Wiley: West Sussex, 2011.

76. Jagadeesan, D.; Nasimova, I.; Gourevich, I.; Starodubtsev, S.; Kumacheva, E. *Macromol. Biosci.* **2011,** 11, (7), 889-896.

77. Nie, Z.; Li, W.; Seo, M.; Xu, S.; Kumacheva, E. *J. Am. Chem. Soc.* **2006,** 128, (29), 9408-9412.

78. Xu, S.; Nie, Z.; Seo, M.; Lewis, P.; Kumacheva, E.; Stone, H. A.; Garstecki, P.; Weibel, D. B.; Gitlin, I.; Whitesides, G. M. *Angew. Chem. Int. Ed.* **2005,** 44, (5), 724-728.

79. Nie, Z.; Xu, S.; Seo, M.; Lewis, P. C.; Kumacheva, E. *J. Am. Chem. Soc.* **2005,** 127, (22), 8058-8063.

80. Knitter, R.; Dietrich, T. R., *Microfabrication in ceramic and glass*. Wiley-VCH: 2006; Vol. 5, p 353-385.

81. Bayer, T.; Kinzl, M., *Industrial applications in Europe*. Wiley-VCH: 2006; Vol. 5, p 415-438.

82. Löb, P.; Hessel, V.; Krtschil, U.; Löwe, H. *chimica oggi - Chemistry Today* **2006,** 24, (2), 46-50.

83. Hessel, V. *Chem. Eng. Technol.* **2007,** 30, (3), 289.

84. Löwe, H.; Axinte, R. D.; Breuch, D.; Hofmann, C. *Chem. Eng. J.* **2009,** 155, 548-550.

85. Kockmann, N.; Engler, M.; Woias, P. *Chem. Ing. Tech.* **2004,** 76, (12), 1777-1783.

86. Kockmann, N., *Transport Phenomena in Micro Process Engineering*. Springer: 2007.

87. IMM-Catalogue. **2007,** Volume V.

88. Baskaran, D.; Müller, A. H. E. *Prog. Polym. Sci.* **2007,** 32, (2), 173-219.

89. Hsieh, H. L.; Quirk, R. P., *Anionic Polymerization: Principles And Practical Applications*. Marcel Dekker Inc: New York, 1996.

90. Yoshida, J.-i.; Suga, S.; Suzuki, S.; Kinomura, N.; Yamamoto, A.; Fujiwara, K. *J. Am. Chem. Soc.* **1999,** 121, (41), 9546-9549.

91. Suga, S.; Suzuki, S.; Yamamoto, A.; Yoshida, J.-i. *J. Am. Chem. Soc.* **2000,** 122, (41), 10244-10245.

92. Nagaki, A.; Kawamura, K.; Suga, S.; Ando, T.; Sawamoto, M.; Yoshida, J.-i. *J. Am. Chem. Soc.* **2004,** 126, (45), 14702-14703.

93. Yoshida, J.; Nagaki, A.; Iwasaki, T.; Suga, S. *Chem. Eng. Technol.* **2005,** 28, (3), 259-266.

94. Iwasaki, T.; Nagaki, A.; Yoshida, J.-i. *Chem. Commun.* **2007**, (12), 1263-1265.

95. Iwasaki, T.; Yoshida, J.-i. *Macromol. Rapid Commun.* **2007,** 28, (11), 1219-1224.

96. Paulus, R. M.; Erdmenger, T.; Becer, C. R.; Hoogenboom, R.; Schubert, U. S. *Macromol. Rapid Commun.* **2007,** 28, (4), 484-491.

97. Hadjichristidis, N.; Iatrou, H.; Pispas, S.; Pitsikalis, M. *J. Polym. Sci., Part A: Polym. Chem.* **2000,** 38, (18), 3211-3234.

98. Honda, T.; Miyazaki, M.; Nakamura, H.; Maeda, H. *Lab Chip* **2005,** 5, (8), 812-818.

99. Miyazaki, M.; Honda, T.; Nakamura, H.; Maeda, H. *Chem. Eng. Technol.* **2007,** 30, (3), 300-304.

100. Wurm, F.; Wilms, D.; Klos, J.; Löwe, H.; Frey, H. *Macromol. Chem. Phys.* **2008,** 209, (11), 1106-1114.

101. Tonhauser, C.; Wilms, D.; Wurm, F.; Berger-Nicoletti, E.; Maskos, M.; Löwe, H.; Frey, H. *Macromolecules* **2010,** 43, (13), 5582-5588.

102. Tonhauser, C.; Obermeier, B.; Mangold, C.; Löwe, H.; Frey, H. *Chem. Commun.* **2011,** 47, (31), 8964-8966.

103. Nagaki, A.; Tomida, Y.; Yoshida, J.-i. *Macromolecules* **2008,** 41, (17), 6322-6330.

104. Iida, K.; Chastek, T. Q.; Beers, K. L.; Cavicchi, K. A.; Chun, J.; Fasolka, M. J. *Lab Chip* **2009,** 9, (2), 339-345.

105. Nagaki, A.; Tomida, Y.; Miyazaki, A.; Yoshida, J.-I. *Macromolecules* **2009,** 42, (13), 4384-4387.

106. Tieke, B., *Macromoleculare Chemie*. Wiley-VCH: Weinheim, 2005.

107. Iwasaki, T.; Yoshida, J.-I. *Macromolecules* **2005,** 38, (4), 1159-1163.

108. Iwasaki, T.; Kawano, N.; Yoshida, J.-i. *Org. Process Res. Dev.* **2006,** 10, (6), 1126-1131.

109. Marcarian, X.; Navarro, C.; Falk, L.; Pla, F. EP0913187, 1999.

110. Pysall, D.; Wachsen, O.; Bayer, T.; Wulf, S. US2002128416, 2003.

111. Marcarian, X.; Navarro, C.; Falk, L.; Pla, F. US2002128416, 2003.

112. Matyjaszewski, K., *Controlled/Living Radical Polymerization: Progress in ATRP, NMP and RAFT*. Am. Chem. Soc.: Washington, DC, 2000.

113. Wang, J.-S.; Matyjaszewski, K. *J. Am. Chem. Soc.* **1995,** 117, (20), 5614-5615.

114. Kato, M.; Kamigaito, M.; Sawamoto, M.; Higashimura, T. *Macromolecules* **1995,** 28, (5), 1721-1723.

115. Georges, M. K.; Veregin, R. P. N.; Kazmaier, P. M.; Hamer, G. K. *Macromolecules* **1993,** 26, (11), 2987-2988.

116. Hawker, C. J.; Bosman, A. W.; Harth, E. *Chem. Rev.* **2001,** 101, (12), 3661-3688.

117. Chiefari, J.; Chong, Y. K.; Ercole, F.; Krstina, J.; Jeffery, J.; Le, T. P. T.; Mayadunne, R. T. A.; Meijs, G. F.; Moad, C. L.; Moad, G.; Rizzardo, E.; Thang, S. H. *Macromolecules* **1998,** 31, (16), 5559-5562.

118. Zhu, S.; Shen, Y.; Pelton, R. H. Supported Controlled Radical Polymerization and Continuous Packed Cloumn Reactor Technology. U.S. Patent No. 2,307,438, 2000.

119. Youqing Shen; Shiping Zhu; Robert Pelton. *Macromol. Rapid Commun.* **2000,** 21, (14), 956-959.

120. Noda, T.; Grice, A. J.; Levere, M. E.; Haddleton, D. M. *Eur. Polym. J.* **2007,** 43, (6), 2321-2330.

121. Save, M.; Weaver, J. V. M.; Armes, S. P.; McKenna, P. *Macromolecules* **2002,** 35, (4), 1152-1159.

122. Wu, T.; Mei, Y.; Cabral, J. T.; Xu, C.; Beers, K. L. *J. Am. Chem. Soc.* **2004,** 126, (32), 9880-9881.

123. Müller, M.; Cunningham, M. F.; Hutchinson, R. A. *Macromol. React. Eng.* **2008,** 2, (1), 31-36.

124. Jakubowski, W.; Matyjaszewski, K. *Angew. Chem. Int. Ed.* **2006,** 45, (27), 4482-4486.

125. Chan, N.; Boutti, S.; Cunningham, M. F.; Hutchinson, R. A. *Macromol. React. Eng.* **2009,** 3, (5-6), 222-231.

126. Yin, M.; Krause, T.; Messerschmidt, M.; Habicher, W. D.; Voit, B. *J. Polym. Sci., Part A: Polym. Chem.* **2005,** 43, (9), 1873-1882.

127. Rosenfeld, C.; Serra, C.; Brochon, C.; Hadziioannou, G. *Chem. Eng. Sci.* **2007,** 62, (18-20), 5245-5250.

128. Lowe, A. B.; McCormick, C. L. *Prog. Polym. Sci.* **2007,** 32, (3), 283-351.

129. Guan, Y.; Zhang, Y. *Soft Matter* **2011,** 7, (14), 6375-6384.

130. Kawaguchi, H.; Kisara, K.; Takahashi, T.; Achiha, K.; Yasui, M.; Fujimoto, K. *Macromol. Symp.* **2000,** 151, (1), 591-598.

131. Diehl, C.; Laurino, P.; Azzouz, N.; Seeberger, P. H. *Macromolecules* **2010,** 43, (24), 10311-10314.

132. Hornung, C. H.; Guerrero-Sanchez, C.; Brasholz, M.; Saubern, S.; Chiefari, J.; Moad, G.; Rizzardo, E.; Thang, S. H. *Org. Process Res. Dev.* **2011,** 15, (3), 593-601.

133. Wu, T.; Mei, Y.; Xu, C.; Byrd, H. C. M.; Beers, K. L. *Macromol. Rapid Commun.* **2005,** 26, (13), 1037-1042.

134. Ouchi, M.; Inagaki, N.; Ando, T.; Sawamoto, M. *Poly. Prepr. (Div. Polym. Chem.)* **2005,** 46, 939-940.

135. Hadjichristidis, N.; Pispas, S.; Floudas, G., *Block Copolymers: Synthetic Strategies, Physical Properties, and Applications*. John Wiley & Sons, Inc.: 2003.

136. Nagaki, A.; Miyazaki, A.; Yoshida, J.-i. *Macromolecules* **2010,** 43, (20), 8424-8429.

137. Dervaux, B.; Junkers, T.; Barner-Kowollik, C.; Du Prez, F. E. *Macromol. React. Eng.* **2009,** 3, (9), 529-538.

138. Rosenfeld, C.; Serra, C.; Brochon, C.; Hadziioannou, G. *Lab Chip* **2008,** 8, (10), 1682-1687.

139. Rosenfeld, C.; Serra, C.; Brochon, C.; Hessel, V.; Hadziioannou, G. *Chem. Eng. J.* **2008,** 135, S242-S246.

140. Hadjichristidis, N.; Pitsikalis, M.; Pispas, S.; Iatrou, H. *Chem. Rev.* **2001,** 101, (12), 3747-3792.

141. Nikos Hadjichristidis; Akira Hirao; Yasuyuki Tezuka; Prez, F. D., *Complex Macromolecular Architectures: Synthesis, Characterization, and Self-Assembly*. Jon Wiley & Sons: 2011.

142. Buhleier, E.; Wehner, W.; Vögtle, F. *Synthesis* **1978,** 2, 155.

143. Tomalia, D. A.; Baker, H.; Dewald, J.; Hall, M.; Kallos, G.; Martin, S.; Roeck, J.; Ryder, J.; Smith, P. *Polym. J.* **1985,** 17, (1), 117-132.

144. Hawker, C. J.; Frechet, J. M. J. *J. Am. Chem. Soc.* **1990,** 112, (21), 7638-7647.

145. Hawker, C.; Frechet, J. M. J. *J. Chem. Soc., Chem. Commun.* **1990**, (15), 1010-1013.

146. Liu, M.; Fréchet, J. M. J. *Pharm. Sci. Technol. Today* **1999,** 2, (10), 393-401.

147. Bosman, A. W.; Janssen, H. M.; Meijer, E. W. *Chem. Rev.* **1999,** 99, (7), 1665-1688.

148. Baker, J. R.; Quintana, A.; Piehler, L.; Banazak-Holl, M.; Tomalia, D.; Raczka, E. *Biomed. Microdevices* **2001,** 3, (1), 61-69.

149. Tomalia, D. A.; Naylor, A. M.; Goddard, W. A. *Angew. Chem., Int. Ed.* **1990,** 29, (2), 138-175.

150. Mourey, T. H.; Turner, S. R.; Rubinstein, M.; Frechet, J. M. J.; Hawker, C. J.; Wooley, K. L. *Macromolecules* **1992,** 25, (9), 2401-2406.

151. Hawker, C. J.; Lee, R.; Frechet, J. M. J. *J. Am. Chem. Soc.* **1991,** 113, (12), 4583-4588.

152. Wooley, K. L.; Fréchet, J. M. J.; Hawker, C. J. *Polymer* **1994,** 35, (21), 4489-4495.

153. Liu, S.; Chang, C.-H. *Chem. Eng. Technol.* **2007,** 30, (3), 334-340.

154. Yan, D.; Gao, C.; Frey, H., *Hyperbranched Polymers: Syntheses, Properties and Applications*. J. Wiley Publishers: New York and London 2011.

155. Kainthan, R. K.; Janzen, J.; Levin, E.; Devine, D. V.; Brooks, D. E. *Biomacromolecules* **2006,** 7, (3), 703-709.

156. Sunder, A.; Hanselmann, R.; Frey, H.; Mülhaupt, R. *Macromolecules* **1999,** 32, (13), 4240-4246.

157. Wilms, D.; Schömer, M.; Wurm, F.; Hermanns, M. I.; Kirkpatrick, C. J.; Frey, H. *Macromol. Rapid Commun.* **2010,** 31, (20), 1811-1815.

158. Wilms, D.; Wurm, F.; Nieberle, J.; Böhm, P.; Kemmer-Jonas, U.; Frey, H. *Macromolecules* **2009,** 42, (9), 3230-3236.

159. Tonhauser, C.; Wilms, D.; Korth, Y.; Frey, H.; Friedrich, C. *Macromol. Rapid Commun.* **2010,** 31, (24), 2127-2132.

160. Schüll, C.; Frey, H. *ACS Macro Letters* **2012,** 1, (4), 461-464.

161. Wilms, D.; Nieberle, J.; Klos, J.; Löwe, H.; Frey, H. *Chem. Eng. Technol.* **2007,** 30, (11), 1519-1524.

162. Kessler, D.; Löwe, H.; Theato, P. *Macromol. Chem. Phys.* **2009,** 210, (10), 807-813.

163. Bally, F.; Serra, C. A.; Brochon, C.; Hadziioannou, G. *Macromol. Rapid Commun.* **2011,** 32, (22), 1820-1825.

164. Fréchet, J. M. J.; Henmi, M.; Gitsov, I.; Aoshima, S.; Leduc, M. R.; Grubbs, R. B. *Science* **1995,** 269, (5227), 1080-1083.

165. Matyjaszewski, K.; Gaynor, S. G.; Müller, A. H. E. *Macromolecules* **1997,** 30, (23), 7034-7041.

166. Mori, H.; Seng, D. C.; Lechner, H.; Zhang, M.; Müller, A. H. E. *Macromolecules* **2002,** 35, (25), 9270-9281.

167. Bally, F.; Ismailova, E.; Brochon, C.; Serra, C. A.; Hadziioannou, G. *Macromolecules* **2011,** 44, (18), 7124-7131.

168. Laurino, P.; Kikkeri, R.; Azzouz, N.; Seeberger, P. H. *Nano Lett.* **2011,** 11, (1), 73-78.

169. Kundu, S.; Bhangale, A. S.; Wallace, W. E.; Flynn, K. M.; Guttman, C. M.; Gross, R. A.; Beers, K. L. *J. Am. Chem. Soc.* **2011,** 133, (15), 6006-6011.

170. Xu, C.; Wu, T.; Drain, C. M.; Batteas, J. D.; Beers, K. L. *Macromolecules* **2005,** 38, (1), 6-8.

171. Xu, C.; Barnes, S. E.; Wu, T.; Fischer, D. A.; DeLongchamp, D. M.; Batteas, J. D.; Beers, K. L. *Adv. Mater.* **2006,** 18, (11), 1427-1430.

172. Queffelec, J.; Gaynor, S. G.; Matyjaszewski, K. *Macromolecules* **2000,** 33, (23), 8629-8639.

173. Asandei, A. D.; Percec, V. *J. Polym. Sci., Part A: Polym. Chem.* **2001,** 39, (19), 3392-3418.

174. Percec, V.; Popov, A. V.; Ramirez-Castillo, E.; Monteiro, M.; Barboiu, B.; Weichold, O.; Asandei, A. D.; Mitchell, C. M. *J. Am. Chem. Soc.* **2002,** 124, (18), 4940-4941.

175. Rosen, B. M.; Percec, V. *Chem. Rev.* **2009,** 109, (11), 5069-5119.

176. Percec, V.; Guliashvili, T.; Ladislaw, J. S.; Wistrand, A.; Stjerndahl, A.; Sienkowska, M. J.; Monteiro, M. J.; Sahoo, S. *J. Am. Chem. Soc.* **2006,** 128, (43), 14156-14165.

177. Chan, N.; Cunningham, M. F.; Hutchinson, R. A. *Macromol. Rapid Commun.* **2011,** 32, (7), 604-609.

178. Chan, N.; Cunningham, M. F.; Hutchinson, R. A. *Polym. Chem.* **2012,** 3, (2), 486-497.

179. Chan, N.; Cunningham, M. F.; Hutchinson, R. A. *Polym. Chem.* **2012,** 3, (5), 1322-1333.

180. Jakubowski, W.; Min, K.; Matyjaszewski, K. *Macromolecules* **2005,** 39, (1), 39-45.

181. Wang, Y.; Matyjaszewski, K. *Macromolecules* 43, (9), 4003-4005.

182. Chen, H.; Zhang, M.; Yu, M.; Jiang, H. *J. Polym. Sci., Part A: Polym. Chem.* **2011,** 49, (22), 4721-4724.

1.2: A Road Less Traveled to Functional Polymers: Epoxide Termination in Living Carbanionic Polymer Synthesis

Christoph Tonhauser and *Holger Frey*

Institute of Organic Chemistry, Organic and Macromolecular Chemistry, Duesbergweg 10-14
Johannes Gutenberg-University (JGU), D-55099 Mainz, Germany

Published in *Macromolecular Rapid Communications* **2010**, *31*, 1938–1947

Epoxide derivatives are highly promising candidates for the functionalization of living anionic polymers. This type of compound not only introduces one single hydroxyl, but multiple functionalities. Macromolecular engineering, industrial applications and a novel continuous reaction strategy for the rapid synthesis of different end-functional polymers are presented.

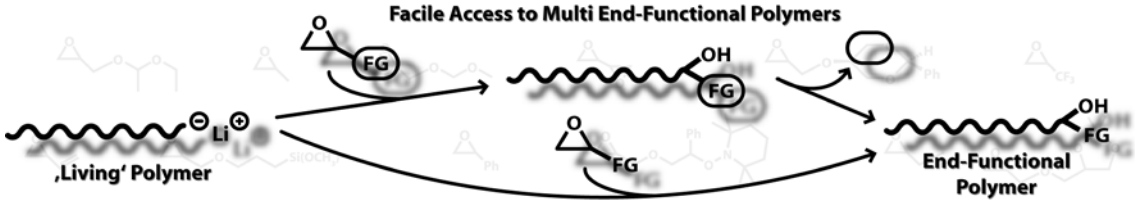

Keywords: anionic polymerization; continuous flow synthesis; epoxide; functionalization of polymers; structure; termination

Abstract

Functional polymers possess tremendous potential both in academia and in industry. In particular, oxiranes offer manifold possibilities for the introduction of single hydroxyl or multiple orthogonal functionalities in carbanionic polymerization. Here, we present a brief overview of the fascinating possibilities arising from the employment of common as well as individually designed epoxide derivatives for the synthesis of end-functional polymers. Continuous flow techniques can be utilized for the rapid generation and screening of

precisely defined hydroxyl-modified polymers. The utilization of functionalized polymers as precursors for the formation of complex macromolecular architectures (e.g., miktoarm star polymers) is summarized and potential applications as well as future perspectives are discussed.

Christoph Tonhauser received his diploma degree in chemistry from the Johannes Gutenberg- University Mainz in 2009. After a temporary stay at the Polymer Science and Engineering Department, University of Massachusetts in Amherst in the group of E. Bryan Coughlin, he is currently working on his Ph.D. thesis in the group of Holger Frey. His research focuses on the preparation of functional polymers in microstructured reactors. He currently holds a scholarship from the Max-Planck Graduate Center (MPGC) and a fellowship of the MAINZ graduate school of excellence.

Biography of co-author is deleted due to privacy protection.

Lebenslauf des Co-Autors wurden aus datenschutzrechtlichen Gründen entfernt.

Introduction

Anionic polymerization remains an important and powerful method to prepare well-defined macromolecules with low polydispersity and precisely defined molecular weights, despite all recent advances in the area of controlled radical polymerization. The majority of synthetic strategies to functional polymers via carbanionic polymerization is based on pioneering work by Szwarc in the 1950s.[1-3] The absence of chain termination and chain transfer reactions, referred to as *living* character, provides a highly capable approach to generate specifically chain-end-functionalized polymers with tailored structure and quantitative end-functionalization.[4]

End-functional polymers possess vast potential as macromolecular precursors, since many functional groups can (directly or after modification, e.g., deprotonation) initiate further polymerization reactions or chain extension, branching, and linking reactions with other chains or functional reagents.[5] This variety of post-polymerization reactions provides a synthetic toolbox to realize advanced and often unusual macromolecular architectures with intriguing physical and chemical properties[6] (e.g., block copolymers, star-branched, comb-like, linear-hyperbranched, and cyclic polymers). Furthermore, the interfacial interaction between functional polymers and surfaces can be adjusted by varying the terminal functionality or architecture of the corresponding polymer. Thus, the nature and position of functionalities permits modification of surface properties (e.g., adhesion[7], wettability, biocompatibility, chemical resistance, and hydrophobicity), which is interesting with respect to various applications.[8]

There are two possible, fundamentally different strategies to obtain polymers with a functional terminus. One pathway leading to quantitative end-functionalization is based on the use of functional initiators.[9] While quantitative functionalization is inherent to this strategy, limited availability and oftentimes severe solubility problems of the respective initiators restrict broad application of this technique. Therefore, the most widely used strategy is the transformation of anionic living chain ends into functional end groups by using electrophilic substrates as termination reagents. Facile access to termination reagents combined with highly sophisticated reaction techniques to control the reactive carbanions lead to high degrees of functionalization.[10, 11] Numerous functionalization reactions were

introduced and studied by Quirk et al. in pioneering work. The authors presented the termination of alkyllithium-initiated living polymers with special reagents to implement various functionalities, such as carboxy[12], aldehyde[13], amino[14], sulfonate[15], and thiol[16], using different electrophilic reagents like carbon dioxide, N-formylmorpholine, protected α-halo-ϖ-aminoalkanes, or thiiranes. High degrees of functionalization were achieved by optimizing parameters like solvent, temperature, concentration, stoichiometry as well as the use of additional promoters.[5]

A more general approach to a wide variety of end-functional polymers is realized by using universal methodologies. Common termination reagents for the carbanionic chain termini include chlorosilane derivatives containing protected[17] or unprotected[18] functional groups. For instance, DeSimone and coworkers demonstrated the high potential of this general functionalization approach by introducing primary aliphatic amines and alcohols at the terminal position of different carbanionic polymers.[19] With one additional synthetic step unprotected functionalities can be conveniently introduced. First, dimethylchlorosilane was used as a capping reagent to obtain a terminal silyl hydride function. In the second step, several unprotected functionalities were introduced by hydrosilylation. This method allows facile access to a variety of end-functional polymers with identical molecular weight and permits to investigate the influence of a single end group.[20-23] Based on this approach, Bellas and Rehahn established a novel universal method for block copolymer synthesis by chemoselective stepwise coupling of two living polymer chains using a heterobifunctional chlorosilane.[24, 25]

A second class of common termination reagents are the diphenylethylene (DPE) derivatives, which are widely used as efficient termination agents of living carbanionic polymers.[5, 26-28] By definition, the reaction of DPE with a living polymer is not a termination, and strictly speaking it has to be specified as ‘living functionalization reaction’, since the polymer chain remains active for further reactions after the functionalization step. The expression ‘termination reagent’, as used for chlorosilane derivatives, is only appropriate, if the active site of a DPE-functionalized polymer is terminated with an additional reagent. Furthermore, miscellaneous DPE-derivatives have been utilized as coupling reagent to obtain complex macromolecular architectures.[29-32]

In polymer chemistry, the highly strained epoxides are well-known for their use as monomers in homo-[33] and copolymerization[34] to obtain a large variety of polyethers that are relevant for a vast number of applications. However, the application of epoxide derivatives as termination reagents for living carbanionic polymers has been investigated to a lesser extent. After nucleophilic attack of the living carbanionic chain end at the epoxide and subsequent ring-opening, one single (in most cases a secondary) hydroxyl functionality is obtained. However, this step can also release other (formerly hidden or protected) functionalities. In this paper, we summarize the state of the art regarding carbanionic polymer synthesis combined with epoxide derivatives as terminating reagents. We will first summarize the synthesis of mono- and multi-end-functionalized polymers with (non-) protected, common epoxides. In the subsequent sections we will focus on novel synthetic strategies, using acetal-protected glycidyl ethers as well as continuous flow techniques. We will furthermore highlight the potential of end-functional polymers in the synthesis of complex macromolecular architectures (e.g., block copolymers, miktoarm, and ABC star polymers).

Mono-functionalization by Epoxide Derivatives

Epoxide derivatives are versatile compounds and one field of particular interest is the utilization in carbanionic polymerization. Due to the high ring strain[35], epoxides arereactive towards nucleophilic attack by living carbanions. Lithium as a common counter ion in carbanionic polymerization does not lead to further propagation of epoxides due to the strong oxygen-lithium aggregation, providing to precisely one terminal unit. This was first mentioned by Furukawa et al. in a groundbreaking study of ethylene oxide (EO) polymerization employing different counter ions.[36] Therefore, termination of carbanionic polymerization and lithium counter ions with epoxide derivatives leads to hydroxyl-functionalized polymers with high degrees of functionalization.

Chain-end-functionalization with Ethylene Oxide (EO)

The possibility to utilize epoxide derivatives as termination reagents for polymer carbanions was first pointed out as early as 1959 by Richards and Szwarc. In their fundamental work two carbanionic end groups per poly(styrene) (PS) chain were generated by α-methyl styrene

"tetramer" with sodium as a counter ion, and the 'living' polymer was terminated with EO, propylene oxide, or water. Although detailed characterization was difficult at that time, the authors confirmed a high degree of functionalization after 'killing' the 'living' polymers (Figure 1).[37] They state in this paper that ''the red solution of ''living'' PS (…)was divided into two portions, one being 'killed' by addition of a trace of water and the other by EO.'' Figure 1 shows a table from this seminal 1959 paper, in which the use of both EO aswell as PO was pioneered for functional termination.

TABLE 1.—DETERMINATION OF END —OH GROUPS IN POLYMERS BY ZEREWITINOV TECHNIQUE

type of polymer	m.w. from [η]	number of OH group per polymer molecule
polystyrene A, " killed " by ethylene oxide	11,300	2·08
polystyrene A, " killed " by propylene oxide	11,300	1·85
polystyrene A, " killed " by water	11,300	none
polyethylene oxide initiated by α-methyl styrene tetramer	~10,000	2·3

Figure 1. Pioneering results by Richards and Szwarc from their seminal paper on the end-functionalization of living carbanionic polymer chains ''killed'' with epoxide derivatives.[37] Copyright 1959, The Royal Society of Chemistry.

In the following years the hydroxyl functionalization of poly(styryl)lithium with EO was investigated in several studies, motivated by two fundamental questions: (i) which degrees of functionalization are obtainable?; (ii) Does oligomerization of EO at the terminal position occur? All analytical techniques available at that time for the characterization of the terminal groups (end-group titration, SEC, vapor pressure osmometry, NMR-analysis, TLC) were utilized to answer these questions. Epoxide termination was found to represent a highly efficient functionalization method (> 99%), and the absence of EO-propagation at the hydroxyl-functionalized polymer was confirmed by ^{13}C NMR investigations.[38] The extension of characterization methods by the development of matrix-assisted laser desorption ionization time-of-flight mass spectrometry (MALDI-ToF MS) in the late 1980s increased the detection possibilities dramatically. In the case of identical detection intensities of functionalized and non-functionalized polymers, MALDI-ToF MS provides an important tool to confirm quantitative functionalization of all polymer chains formed by obtaining a spectrum with a single distribution mode corresponding to the added masses of end groups,

counter ion, and monomer units, respectively.[39] Related to the improved characterization possibilities,

newconclusions were drawn, since MALDI-ToF MS permits to detect small quantities of side products. Quirk et al. demonstrated possible oligomerization in the presence of Li-counter ions only when employing high excess of EO (tenfold) and prolonged reaction times (up to 4 weeks).[40-42] By using such exceptional reaction conditions, the formation of PS terminated with 2-3 EO-units was detected (Figure 2). At the same time a slightly increased oligomerization probability was found for the poly(butadienyl)lithium species compared to poly(styryl)lithium samples, as reported by Ji et al.[43] Currently, MALDI-ToF MS represents one of the most important methods for the characterization of polymers with functional termini. In combination with other characterization methods, the degree of polymerization and the extent of functionalization can be unequivocally established. However, alkyl-initiated polymerization of styrene[38], butadiene[43] and 1,3-cyclohexatriene[44] terminated with EO under common reaction conditions leads to quantitative end-functionalization without oligomerization of the oxirane.

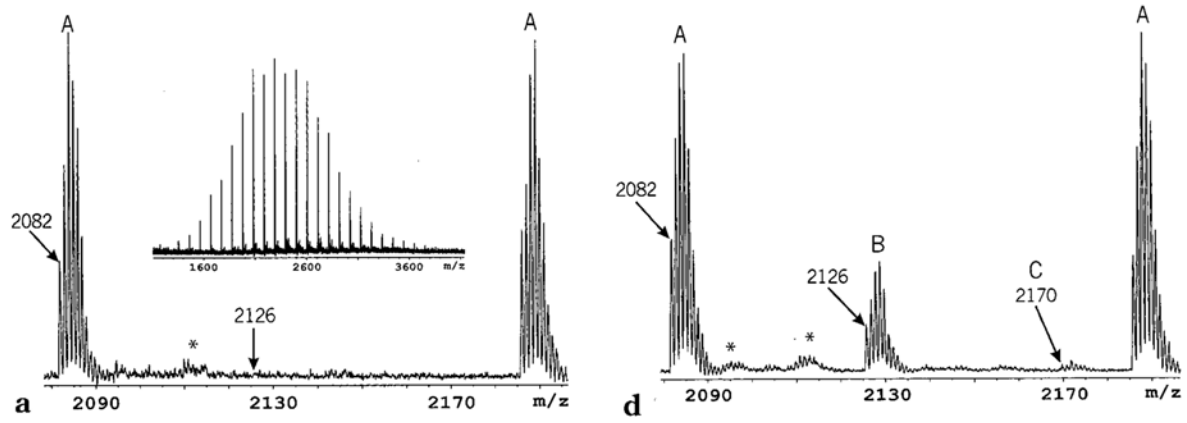

Figure 2. MALDI-ToF spectra of poly(styryl)lithium functionalized with one (A) two (B) three (C) EO units (reaction conditions a: 4 equiv. 12 h; b: 10 equiv. 4 weeks); *broad signals corresponding to fragments of the polymer with Ag^{+}[40] Copyright 2002, American Chemical Society.

Functionalization with Other Alkylene Oxides

As a result of the fundamental studies on the synthesis of v-hydroxyethylated polymers, several functionalized and non-functionalized epoxide derivatives have been employed as

termination reagents (Scheme 1 and 2). Obviously, reaction with asymmetrically substituted epoxide derivatives may lead to two different products. The living chain end attacks primarily the less hindered region due to steric effects and in the case of PO (Scheme 1a) the reaction with the least substituted methylene group is nearly regioselective with a yield of 97%. This was confirmed by use of ^{13}C-methyl-labeled PO. The degree of functionalization (93%) is decreased in the case of PO by the proton transfer between methyl group and living chain end, which results in impurities caused by non-functionalized PS.[45] In contrast, functionalization reaction of the next higher homolog, 1-butene oxide (BO, Scheme 1b), provides 99% functionalization with quantitative, regiospecific attack of poly(styryl)lithium at the least substituted carbon of the epoxide ring to form the corresponding secondary alcohol. Compared to PO, a decreased amount of non-functionalized PS was obtained due to the steric and electronic effects in the pending ethyl group with respect to the hydrogen transfer from the methylene group adjacent to the epoxide ring.[46] In addition to the common characterization methods, detailed MALDI-ToF studies of a number of different epoxides were carried out.[47] In summary, the efficiency of functionalization with respect to non-functionalized epoxide derivatives can be deduced from the aforementioned reports as follows: EO > BO > PO. Another less efficient termination reaction using an oxirane is the termination of living PS with 1,1,1-trifluoro-2,3-epoxypropane (Scheme 1c), affording a degree of functionalization of 57%.[48]

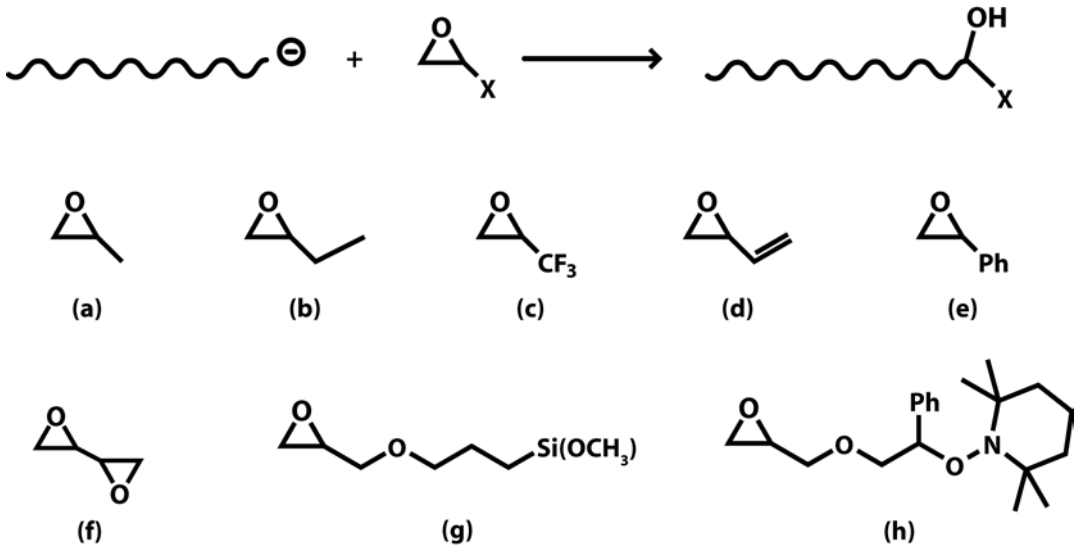

Scheme 1. Functionalization of living carbanionic polymers with non-protected epoxide derivatives (a–h) leads to a variety of end groups that permit further transformation or polymerization reactions.

Implementation of Various Functionalities

Epoxide Derivatives with Non-protected Functionalities

Introducing synthesis procedures utilizing specific epoxide derivatives permits the implementation of additional functionalities in terminal position adjacent to the hydroxyl group. To this end, the employed functional groups located at the epoxide ring must tolerate the harsh reaction conditions of anionic polymerization. If this is not the case, they have to be equipped with sufficiently base-stable protecting groups. This intriguing approach will be described in the ensuing paragraph.

As one of the first reported examples, the termination with 3,4-epoxy-1-butene (Scheme 1d) introduces a terminal vinyl group with an efficiency of 95%. The attack of the living chain end results in three different butenol-functionalized polymers, depending on the reaction site, leading to the 3,4-, 4,3- or 1,4-adduct, respectively. However, each polymer possessed the desired functionalities, and by altering the reaction conditions (adding lithium salt or Lewis-bases, solvent, temperature) the ratio of products could be controlled and even limited to one specific product. In addition, dehydration of the end groups presents an efficient route to diene-functionalized macromonomers for the synthesis of grafted polymer brushes.[49] The synthesis of hydroxyl end-functional polymers utilizing styrene oxide (SO, Scheme 1e) as termination reagents was first carried out by Shimura and Lin.[50] However, detailed studies by Quirk et al. showed that the reaction results not only in functional and proton-terminated polymers, but also in other byproducts such as dimeric and trimeric polymers. The formation of these undesired macromolecules can be almost fully suppressed by adding THF as a Lewis base, leading to reduced association of living polymer chain ends. In this case, high degrees of functionalization (>99%) can be obtained.[51, 52] The regiochemistry of this reaction is affected by steric (polymer chain) and electronic (electron-delocalization) factors[53]. Thus, both substitution products, primary and secondary alcohols, were formed in equal parts. Based on these results, it is obvious that different functional groups should be introducible by using a variety of para-substituted SO derivatives. Recently, this method has been exploited for the convergent living anionic polymerization, a technique based on in situ chain-end functionalization and polymerization of dendritic PSs with 4-vinyl styrene oxide as termination reagent. This procedure leads to low polydispersity, hyperbranched PS with

hydroxyl groups at each branch point, as demonstrated in elegant work by Bender and Knauss.[54]

In an important work Quirk et al. introduced 1,3-butene diepoxide (Scheme 1f) as a coupling reagent. The diepoxide was reacted with an excess of poly(styryl)lithium to form PS with two adjacent, in-chain hydroxyl groups. After purification the successful coupling reaction was confirmed by NMR and MALDI-ToF measurements.[55] Another interesting approach is the reaction of poly(styryl)lithium and poly(butadienyl)lithium with 3-glycidoxypropyltrimethoxysilane (Scheme 1g), which leads to high degrees of functionalization by adding lithium alkoxides.[56] According to the authors, the trialkoxysilyl-functionalized polymers can be used as dispersion agent for silica particles. The end-functional polymers enhance polymer-filler interactions, leading to reinforced elastomers.[57, 58] However, nucleophilic attack of the carbanionic chain end at the trimethoxysilane group is a highly likely side reaction of the termination with this functional termination agent.

Glycidyl Ethers with Protected Functionalities

Epoxide derivatives containing protected functionalities must fulfill certain criteria for the utilization as termination reagents in carbanionic polymer synthesis. A convenient synthetic route to such epoxides and a simple post polymerization step to release the protective group is desirable. However, the most important criterion is the mandatory stability of the protecting group against the extremely basic conditions of carbanionic polymerization. Glycidyl ethers containing various protective groups represent an important class of compounds meeting these criteria. Several acetal- or ketal-protected glycidyl ethers, namely ethoxy ethyl glycidyl ether (EEGE)[59], 1,2-isopropylene glyceryl glycidyl ether (IGG)[60] and 2-phenyl-1,3-dioxane glycidyl ether (PDGE)[39], have been utilized by our group in recent work to demonstrate the rapid generation of multihydroxyl end-functional PSs. The respective glycidyl ethers are shown in Scheme 2.

A novel polymerization-termination sequence which enables quantitative functionalization of the living carbanions by employing a continuous operating microflow system based on a micromixer and conventional HPLC equipment was developed in our laboratories. A high pressure slit interdigital multilamination micromixer (HP-IMM, internal volume 15 mL) with excellent heat dissipation and efficient mixing was used. Monomer and initiator (i.e., styrene

and *sec*-butyllithium) were pumped into the micromixer to obtain a rapid and simultaneous start of the polymerization.[61]

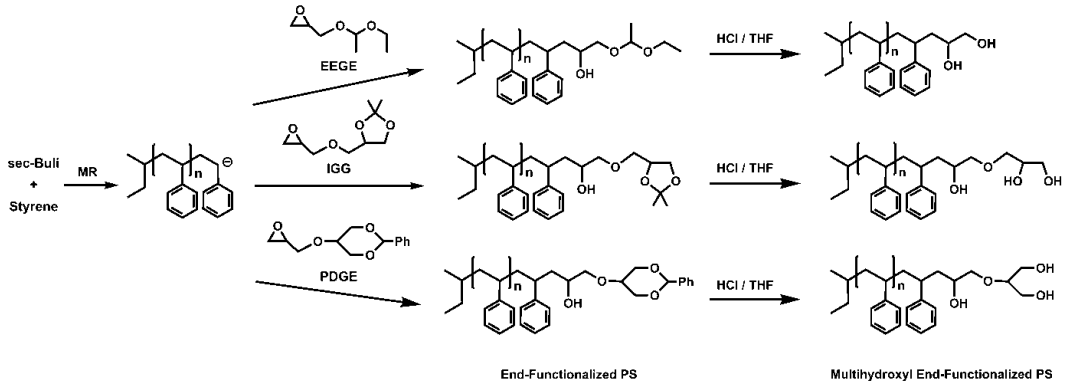

Scheme 2. Chemical structure of glycidyl ethers employed as termination reagents in living anionic polymerization. The terminationstrategies shown permit the generation of 2–3 hydroxyl termini at the chain end.[39]

In a T-mixer connected to the micromixer the corresponding glycidyl ether was introduced to the living poly(styryl)lithium anions to terminate the polymer within the continuous flow. In this manner quantitatively end-functionalized polymer samples were recovered from the outlet tube of the reactor. The schematic reactor set-up is depicted in Figure 3. In a second synthetic step multiple hydroxyl end groups were released by acidic hydrolysis. The narrowly distributed polymers exhibit quantitative functionalization and regioselectivity, confirmed by detailed SEC, MALDI-ToF and NMR investigation. Adjusting the reaction parameters (e.g., ratio of flow rates) during the continuous polymerization permitted good control of the molecular weights, and well-defined end-functional polymers were obtained within several seconds. Due to the continuous process, the approach affords a rapid and cost-efficient materials´ screening with respect to novel end-functionalized polymers offering a wide range of material properties.[39]

Termination with methoxy methyl glycidyl ether (MMO) in a conventional reaction set-up was realized by Hillmyer and coworkers in 2004 and will be discussed in the following paragraph.[62, 63] The authors used the end-functional polymer as a precursor for the synthesis of miktoarm star polymers. Wang and Huang demonstrated a similar approach to star polymers utilizing EEGE as capping reagent in 2007.[64, 65]

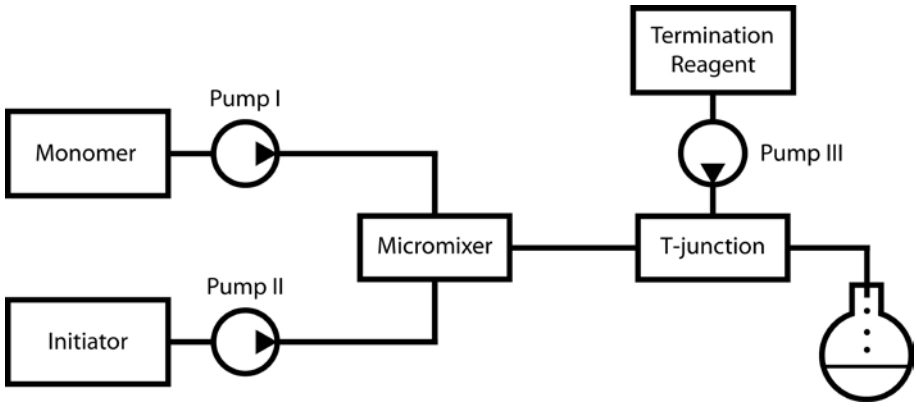

Figure 3. Schematic reactor set-up for continuous end-functionalization of poly(styryl)-lithium utilizing different glycidyl ethers. Micromixer: HP-IMM.[39]

Epoxide Termination for Macromolecular Engineering and Complex Architectures

In the previous paragraphs, a large variety of functionalization reactions with epoxide derivatives has been discussed. On the one hand the end-functional polymers can exhibit various peculiar chemical and physical properties as such, but on the other hand the functional groups can obviously be used for further post-polymerization reactions. In particular, the hydroxyl-groups of the epoxy-terminated polymers can be utilized in subsequent oxy-anionic polymerization steps. This renders the macromolecules useful as precursors for the synthesis of complex macromolecular architectures. In the following, various post-polymerization reactions that rely on the end-functional polymers as macroinitiators are described.

Amphiphilic block copolymer synthesis capitalizing on epoxide terminated PS as precursor was performed already in 1959 in pioneering work by Richards and Szwarc.[37] As a second monomer EO was added to α,ϖ-hydroxyl-functionalized PS with sodium as a counter ion to form a block copolymer after stirring the solution for one week. The block copolymer was characterized by UV/Vis spectroscopy. The precipitation behavior of the material in various solvents was also characterized. Further attempts with PO and SO as monomers did not lead to block copolymers in high yields due to chain transfer reactions to the epoxides in the course of the polymerization. In a similar procedure, more than 30 years later PS-PEO block copolymers were synthesized and their potential application as stabilizer in emulsion polymerizations was demonstrated by Jialanella et al. The effect of different block lengths as well as the anchor unit/stabilizer block ratios were studied on the basis of polymerization

kinetics and particle size.[66] Monohydroxyl-functionalized PS, using PO as a second monomer represents a pathway to well-defined block copolymers with narrow molecular weight distributions (< 1.08) containing PO blocks with up to 12 000 g mol^{-1}. The effects of different counter ions (Na/K, Rb, and Cs) as well as crown ethers were also investigated. Chain transfer to PO leads to a significant amount of poly(propylene oxide) (PPO) and hydroxyl-terminated diblock copolymer, but due to rapid proton transfer reactions between active alkoxides and dormant hydroxylated species[67, 68] the block copolymer grows continuously. Therefore, the growth of the block copolymer is not impeded by chain transfer processes and the pure, narrow distributed block copolymer can be separated from PPO homo polymer by precipitation.[69]

Kobatake et al. reported the synthesis of end-functional polymers by termination of poly(butadienyl)lithium with an alkoxamine functionalized epoxide (2,2,6,6,-tetramethyl-1-(2-glycidyloxy-1-phenylethoxy)piperidine, Scheme 1h). This termination reaction offers facile access to macroinitiators for living (nitroxide-mediated) and free radical polymerizations (Figure 4).

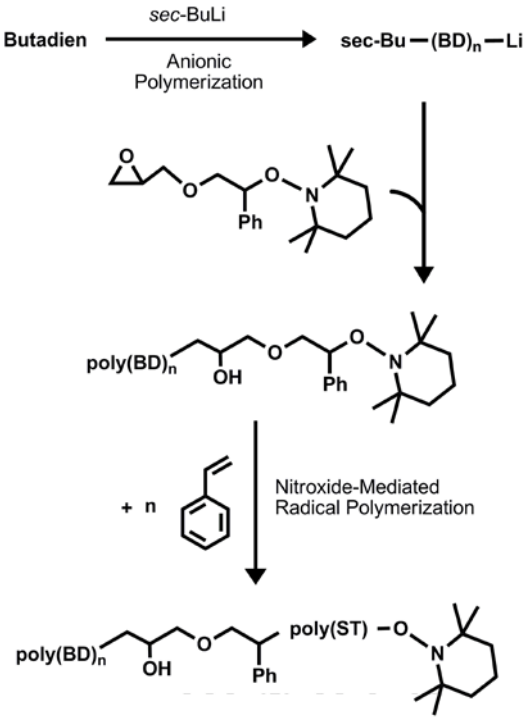

Figure 4. Synthetic strategy to poly(butadiene-b-styrene) by endfunctionalization and subsequent nitroxide-mediated radical polymerization.[70]

To this end the authors developed an alternative and favorable synthetic strategy to promote the synthesis of transparent impact poly(styrene)s (TIPS), consisting of a blend containing PS and PB-PS block copolymers. In the industrial two-step procedure PB-PS blocks, generated by laborious anionic polymerization are blended with PS homopolymers. Simple addition of the macroinitiator to the radical polymerization of styrene lowers the experimental effort and cost compared to the common synthetic strategy for the synthesis of TIPS and bears interesting potential for industrial application.[70, 71]

Complex macromolecular architectures like miktoarm star polymers with three different arms were synthesized by Li et al.[62], Saito et al.[63], and Wang and Huang[64, 65], as mentioned before. The synthetic strategy of ABC miktoarm star triblock copolymers consisting of poly(ethyl ethylene) (PEE), poly(ethylene oxide) (PEO), and poly(perfluoro-propylene oxide) (PFPO) relies on two anionic polymerization steps, followed by one effective polymer-polymer coupling reaction (Figure 5). As junction molecule MMO was used to obtain a hydroxyl group and a protected hydroxyl group at one chain end of poly(butadiene) (PBD). Catalytic hydrogenation leads to end-functional PEE, which was used as macroinitator for the synthesis of a PEE-*b*-PEO block copolymer with a protected hydroxyl group at the block interface. After deprotection of this hydroxyl group a third polymer chain (mono acyl chloride end-capped PFPO) was attached via a polymer-polymer coupling reaction.[62]

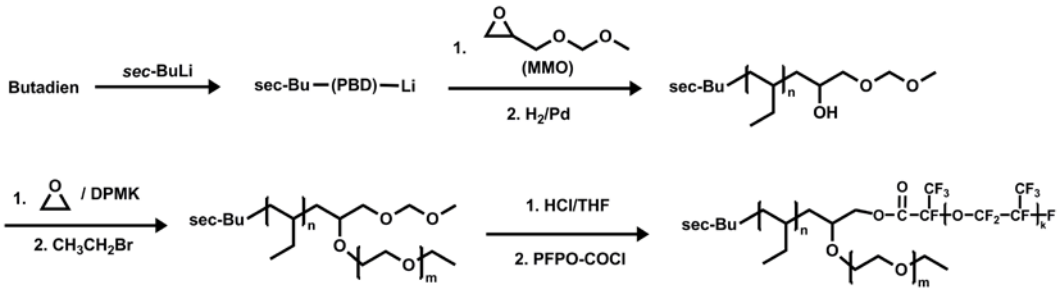

Figure 5. Synthetic strategy to synthesize a (PEE)(PEO)(PFPO) miktoarm star ter-polymer.[62]

Such ABC miktoarm star polymers exhibit interesting solution behavior and micellar structures due to the "triple philicity" with three immiscible components: the first being a water-soluble, the second a hydrocarbon, and the third a hydro- and oleophobic, fluorinated polymer chain. The formation of different structures in aqueous solution was investigated by

cryo-transmission electron microscopy (cryo-TEM). Figure 6 shows several cryo-TEM images and the proposed schematic structures. Depending on the block length the formation of various structures as multicompartment micelles, extended wormlike structures with segmented cores and nanostructured bilayer vesicles was observed.[72] This example demonstrates the remarkable potential of miktoarm star architectures for the formation of multicompartment structures.

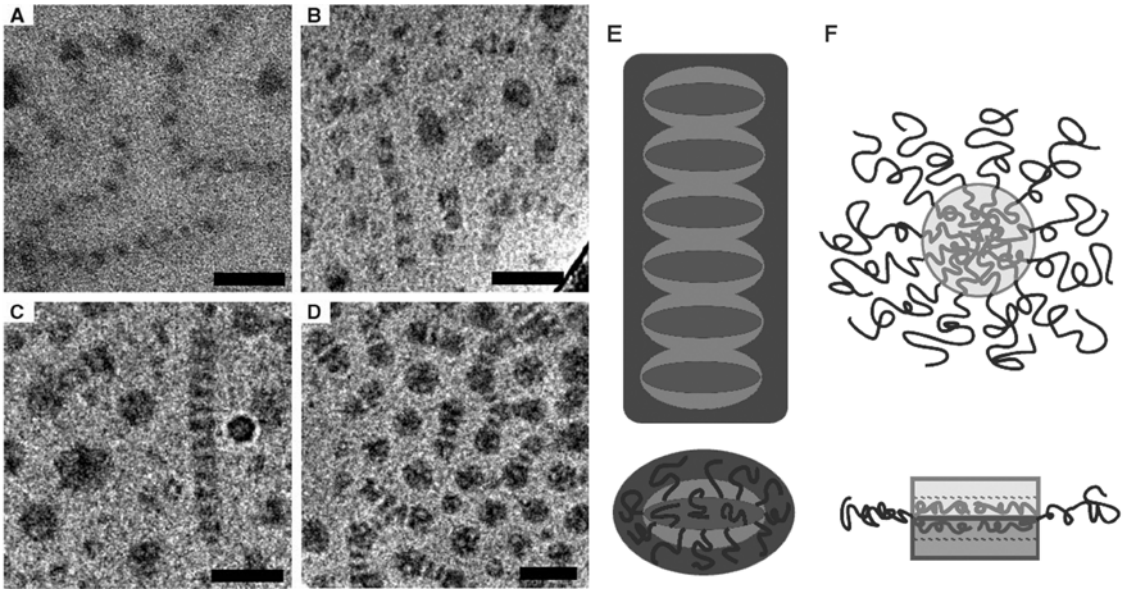

Figure 6. (A–D) Cryo-TEM images of ABC miktoarm star triblock copolymers with corresponding schematic drawings of micellar structures. (E) Individual micelle and the stacking into a string (in A). (F) Side and end-on views of proposed chain packing for segemented ‘‘worms’’(in B–D)[72] Copyright 2004, American Chemical Society.

The investigation of a second ABC miktoarm star polymer, which was synthesized using the hydroxyl group at the juncture of PEE and PEO to initiate the ring opening polymerization (ROP) of γ-methyl-ε-caprolactone leads to similar results with respect to the microphase behavior in aqueous solution.[63]

A similar approach to ABC miktoarm star polymers was used by Wang and Huang. The authors terminated the living anionic polymerization of PS with EEGE and utilized this polymer in two subsequent steps as a macroinitiator for the ROP of either EO and EEGE or EO and ε-CL to generate two well-defined ABC-miktoarm star polymers. In a subsequent

reaction step the poly(EEGE) arm was deprotected, using acidic hydrolysis to recover a linear poly(glycerol) polymer chain.[64, 65]

Higashihara et al. synthesized end-functional PS chains with 1,3-butadienyl end groups, which were quantitatively converted into epoxides via epoxidation. Different numbers of epoxy functions were generated [$PS(EO)_n$ with n = 4, 8, 16] to react with living poly(styryl)lithium and create 5- or 9-arm star polymers. The coupling reaction was highly efficient, leading to well-defined star-branched PSs. Furthermore, the linking points are equipped with hydroxyl groups that can be used for additional reactions.[73] As mentioned before, another approach generating hydroxyl groups at junction points was demonstrated recently by Bender and Knauss.[54] The convenient synthetic strategy is presented in Figure 7. The dendritically branched PS with one hydroxyl group at each branch point was synthesized by slow monomer addition of 4-vinylstyrene oxide and styrene to poly(styryl)lithium. The formation of the hydroxyl group in this insitu chain-end functionalization/polymerization process was confirmed by titrimetric analysis.

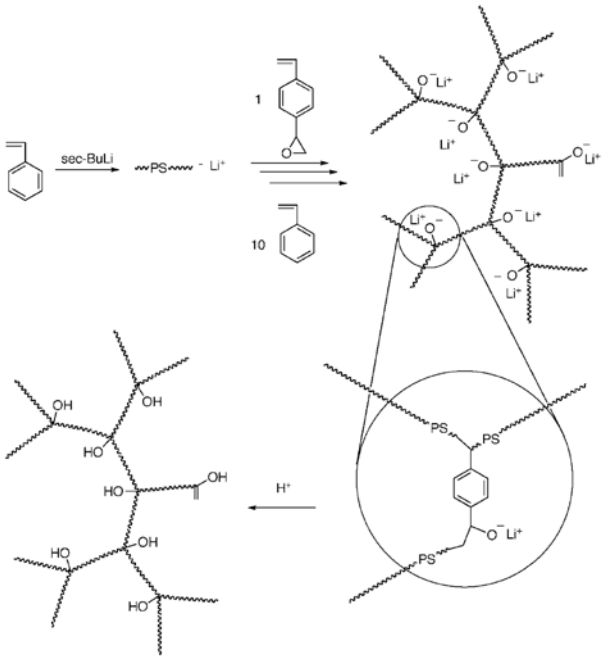

Figure 7. Synthetic strategy for hyperbranched PSs with one hydroxyl group at each junction point synthesized by convergent ‘‘living’’ anionic polymerization.[54] Copyright 2009, American Chemical Society.

Based on these few examples, the intriguing potential of polymers terminated with functional epoxides for the creation of novel well-defined polymer architectures that exhibit

non-conventional supramolecular order in solution and in the solid state is clearly visible. Star polymers with 3 chemically different, immiscible arms (ABC stars) represent just one promising example.

Conclusion

Although pioneering work was already carried out as early as 1959, the termination of living carbanionic polymers by epoxides still represents “a road less traveled” This overview summarizes the past and present activities in this area, demonstrating the high potential of epoxide derivatives. Functional epoxides permit to introduce a large variety of different terminal functionalities in different positions of the polymer (e.g., in-chain or terminal). A promising procedure based on micromixing has been introduced, which provides a tool for rapid screening of functionalized polymers by adjusting flow rates, stoichiometry, monomer, and termination reagents. The availability of a broad variety of well-defined end-functional polymers gives the opportunity to use those as precursors in the formation of complex macromolecular architectures (e.g., miktoarm star polymers, ABC stars), but also in applications requiring surface or interface-attachment. However, numerous other and also novel tailor-made epoxide derivatives are still less explored and clearly offer great potential. It is interesting to note that in most reported studies styrene was utilized as a monomer. However, it is a safe bet that there is high potential for the preparation of other carbanionic polymer structures by expanding the synthesis to different monomers which are suitable for carbanionic polymerization (e.g., acrylates, dienes, etc.).

In summary, it is obvious that the full potential of oxirane-based termination agents has by no means tapped yet and their use for the termination of anionic polymerization will increase and result in unusual macromolecular architectures and novel materials for future applications.

Acknowledgements: C. T. thanks the *MPGC (Max Planck Graduate Center mit der Johannes Gutenberg-Univesity))* as well as the *MAINZ Graduate Class of Excellence* for fellowships and financial support. H.F. acknowledges the SFB 625 (From Single Molecules to Materials) supported by the DFG for valuable support as well as the FCI (Fonds der Chemischen Industrie).

References

[1] M. Szwarc, *Nature* 1956, *178*, 1168.

[2] M. Szwarc, *J. Polym. Sci., Part A: Polym. Chem.* 1998, *36*, ix.

[3] D. Baskaran, A. H. E. Müller, *Prog. Polym. Sci.* 2007, *32*, 173.

[4] R. P. Quirk, D. L. Pickel, "Anionic Synthesis of Chain-End Functionalized Polymers. Scope, Limitations and Recent Advances", in *Living and Controlled Polymerization*, J. Jagur-Grodzinski, Ed., Nova Science Publisher, New York 2006, p. 235.

[5] R. P. Quirk, H. L. Hsieh, "Functionalized Polymers and Macromonomers", in *Anionic Polymerization: Principles And Practical Applications*, D.E. Hudgin, Ed., Marcel Dekker Inc, New York 1996, p. 261.

[6] N. Hadjichristidis, M. Pitsikalis, S. Pispas, H. Iatrou, *Chem. Rev.* 2001, *101*, 3747.

[7] J. Wang, R. Stark, M. Kappl, H.-J. Butt, *Macromolecules* **2007**, *40*, 2520.

[8] L. R. Hutchings, A. P. Narrianen, R. L. Thompson, N. Clarke, I. Ansari, *Polym. Int.* **2008**, *57*, 163.

[9] A. Hirao, M. Hayashi, *Acta Polym.* **1999**, *50*, 219.

[10] N. Hadjichristidis, H. Iatrou, S. Pispas, M. Pitsikalis, *J. Polym. Sci., Part A: Polym. Chem.* **2000**, *38*, 3211.

[11] K. Takenaka, A. Hirao, S. Nakahama, *Polym. Int.* **1995**, *37*, 291.

[12] R. P. Quirk, J. Yin, L. J. Fetters, *Macromolecules* **1989**, *22*, 85.

[13] R. P. Quirk, J. X. Kuang, *Polym. Int.* **1994**, *33*, 181.

[14] K. Ueda, A. Hirao, S. Nakahama, *Macromolecules* **1990**, *23*, 939.

[15] R. P. Quirk, J. Kim, *Macromolecules* **1991**, *24*, 4515.

[16] R. P. Quirk, M. Ocampo, M. J. Polce, C. Wesdemiotis, *Macromolecules* **2007**, *40*, 2352.

[17] T. E. Long, L. W. Kelts, S. R. Turner, J. A. Wesson, T. H. Mourey, *Macromolecules* **1991**, *24*, 1431.

[18] M. O. Hunt, A. M. Belu, R. W. Linton, J. M. DeSimone, *Macromolecules* **1993**, *26*, 4854.

[19] M. A. Peters, A. M. Belu, R. W. Linton, L. Dupray, T. J. Meyer, J. M. DeSimone, *J. Am. Chem. Soc.* **1995**, *117*, 3380.

[20] R. Lund, S. Plaza-GarciÌa, A. AlegriÌa, J. Colmenero, J. Janoski, S. R. Chowdhury, R. P. Quirk, *Macromolecules* **2009**, *42*, 8875.

[21] R. P. Quirk, J. Janoski, S. R. Chowdhury, C. Wesdemiotis, D. E. Dabney, *Macromolecules* **2009**, *42*, 494.

[22] R. P. Quirk, H. Kim, M. J. Polce, C. Wesdemiotis, *Macromolecules* **2005**, *38*, 7895.

[23] R. P. Quirk, J. Janoski, M. Olechnowicz, H. Kim, D. E. Dabney, C. Wesdemiotis, *Macromol. Symp.* **2009**, *283-284*, 78.

[24] V. Bellas, M. Rehahn, *Macromol. Chem. Phys.* **2009**, *210*, 320.

[25] V. Bellas, M. Rehahn, *Macromol. Rapid Commun.* **2007**, *28*, 1415.

[26] R. P. Quirk, T. Yoo, Y. Lee, J. Kim, B. Lee, "Application of 1,1-Diphenylethylene Chemistry in Anionic Synthesis of Polymers with Controlled Structure", in *Adv. Polym. Sci.*, Springer Verlag, Berlin 2000, p. 67.

[27] R. P. Quirk, Y. Wang, *Polym. Int.* **1993**, *31*, 51.

[28] J. Kim, S. Kwak, K. U. Kim, K. H. Kim, J. C. Cho, W. H. Jo, D. Lim, D. Kim, *Macromol. Chem. Phys.* **1998**, *199*, 2185.

[29] T. Higashihara, K. Sugiyama, H.-S. Yoo, M. Hayashi, A. Hirao, *Macromol. Rapid Commun.* **2010**, *31*, 1031.

[30] A. Hirao, M. Hayashi, S. Loykulnant, K. Sugiyama, S. W. Ryu, N. Haraguchi, A. Matsuo, T. Higashihara, *Prog. Polym. Sci.* **2005**, *30*, 111.

[31] R. P. Quirk, T. Yoo, B. Lee, *J. M. S. -Pure Appl. Chem.* **1994**, *31*, 911.

[32] T. Fujimoto, H. Zhang, T. Kazama, Y. Isono, H. Hasegawa, T. Hashimoto, *Polymer* **1992**, *33*, 2208.

[33] B. Obermeier, F. Wurm, H. Frey, *Macromolecules* **2010**, *43*, 2244.

[34] C. Mangold, F. Wurm, B. Obermeier, H. Frey, *Macromol. Rapid Commun.* **2010**, *31*, 258.

[35] A. S. Pell, G. Pilcher, *Trans. Faraday Soc.* **1965**, *61*, 71.

[36] J. Furukawa, T. Saegusa, T. Tsuruta, G. Kakogawa, *Macromol. Chem. Phys.* **1960**, *36*, 25.

[37] D. H. Richards, M. Szwarc, *Trans. Faraday Soc.* **1959**, *55*, 1644.

[38] R. P. Quirk, J. J. Ma, *J. Polym. Sci., Part A: Polym. Chem.* **1988**, *26*, 2031.

[39] C. Tonhauser, D. Wilms, F. Wurm, E. Berger-Nicoletti, M. Maskos, H. Löwe, H. Frey, *Macromolecules* **2010**, *43*, 5582.

[40] R. P. Quirk, R. T. Mathers, C. Wesdemiotis, M. A. Arnould, *Macromolecules* **2002**, *35*, 2912.

[41] R. P. Quirk, Y. Guo, C. Wesdemiotis, M. A. Arnould, *Polymer* **2004**, *45*, 3423.

[42] C. Wesdemiotis, M. A. Arnould, Y. Lee , R. P. Quirk, *Polym. Prepr. (Am. Chem. Soc., Div. Polym. Chem.)* **2000**, *41*, 629.

[43] H. Ji, N. Sato, W. K. Nonidez, J. W. Mays, *Polymer* **2002**, *43*, 7119.

[44] R. P. Quirk, F. You, C. Wesdemiotis, M. A. Arnould, *Macromolecules* **2004**, *37*, 1234.

[45] R. P. Quirk, G. M. Lizarraga, *Macromolecules* **1998**, *31*, 3424.

[46] R. P. Quirk, Q. Ge, M. A. Arnould, C. Wesdemiotis, *Macromol. Chem. Phys.* **2001**, *202*, 1761.

[47] M. A. Arnould, M. J. Polce, R. P. Quirk, C. Wesdemiotis, *Int. J. Mass Spectrom.* **2004**, *238*, 245.

[48] R. P. Quirk, T. H. Cheong, K. Jiang, D. L. Gomochak, T. J. Yoo, K. T. Andes, R. T. Mathers, *Macromol. Symp.* **2003**, *195*, 69.

[49] R. P. Quirk, D. L. Gomochak, C. Wesdemiotis, M. A. Arnould, *J. Polym. Sci., Part A: Polym. Chem.* **2003**, *41*, 947.

[50] Y. Shimura, W.-S. Lin, *J. Polym. Sci., Part A: Polym. Chem.* **1970**, *8*, 2171.

[51] R. P. Quirk, H. Hasegawa, D. L. Gomochak, C. Wesdemiotis, K. Wollyung, *Macromolecules* **2004**, *37*, 7146.

[52] R. P. Quirk, D. L. Pickel, H. Hasegawa, *Macromol. Symp.* **2005**, *226*, 69.

[53] M. M. Kayser, P. Morand, *Can. J. Chem.* **1980**, *58*, 302.

[54] J. T. Bender, D. M. Knauss, *Macromolecules* **2009**, *42*, 2411.

[55] R. P. Quirk, A. Contractor, M. J. Polce, C. Wesdemiotis, *Macromol. Chem. Phys.* **2006**, *207*, 2280.

[56] R. P. Quirk, K. Jiang, *Polym. Prepr. (Am. Chem. Soc., Div. Polym. Chem.)* **2001**, *42*, 27.

[57] US 5652310 (1997), The Goodyear Tire & Rubber Company, Akron, OH, invs.: W.-L. Hsu, A. F. Halasa.

[58] US 5665812 (1997), Michelin, Clermont-Ferrand Cedex, FR, invs.: J.-N. Gorce, G. Labauze.

[59] A. O. Fitton, J. Hill, D. E. Jane, R. Millar, *Synthesis* **1987**, 1140.

[60] F. Wurm, J. Nieberle, H. Frey, *Macromolecules* **2008**, *41*, 1909.

[61] F. Wurm, D. Wilms, J. Klos, H. Löwe, H. Frey, *Macromol. Chem. Phys.* **2008**, *209*, 1106.

[62] Z. Li, M. A. Hillmyer, T. P. Lodge, *Macromolecules* **2004**, *37*, 8933.

[63] N. Saito, C. Liu, T. P. Lodge, M. A. Hillmyer, *Macromolecules* **2008**, *41*, 8815.

[64] G. Wang, J. Huang, *Macromol. Rapid Commun.* **2007**, *28*, 298.

[65] G. Wang, J. Huang, *J. Polym. Sci., Part A: Polym. Chem.* **2008**, *46*, 1136.

[66] G. L. Jialanella, E. M. Firer, I. Piirma, *J. Polym. Sci., Part A: Polym. Chem.* **1992**, *30*, 1925.

[67] X.-S. Feng, D. Taton, E. L. Chaikof, Y. Gnanou, *J. Am. Chem. Soc.* **2005**, *127*, 10956.

[68] P. J. Flory, *J. Am. Chem. Soc.* **1940**, *62*, 1561.

[69] R. P. Quirk, G. M. Lizarraga, *Macromol. Chem. Phys.* **2000**, *201*, 1395.

[70] S. Kobatake, H. J. Harwood, R. P. Quirk, D. B. Priddy, *Macromolecules* **1998**, *31*, 3735.

[71] S. Kobatake, H. J. Harwood, R. P. Quirk, D. B. Priddy, *Macromolecules* **1997**, *30*, 4238.

[72] Z. Li, E. Kesselman, Y. Talmon, M. A. Hillmyer, T. P. Lodge, *Science* **2004**, *306*, 98.

[73] T. Higashihara, M. Kitamura, N. Haraguchi, K. Sugiyama, A. Hirao, J.-H. Ahn, J.-S. Lee, *Macromolecules* **2003**, *36*, 6730.

Chapter 2: Continuous Flow End-Functionalization

2.1: Multihydroxyl-Functional Polystyrenes in Continuous Flow

Christoph Tonhauser,[1] *Daniel Wilms,*[1] *Frederik Wurm,*[1] *Elena Berger-Nicoletti,*[1] *Michael Maskos,*[2,3] *Holger Löwe*[1] and *Holger Frey*[1*]

[1]Institute of Organic Chemistry, Organic and Macromolecular Chemistry, Duesbergweg 10-14 Johannes Gutenberg-University Mainz, 55099 Mainz, Germany

[2]Institute of Physical Chemistry, Johannes Gutenberg-University Mainz, 55099 Mainz, Germany

[3]Federal Institute for Material Research and Testing BAM, Unter den Eichen 87, 12205 Berlin, Germany

Published in *Macromolecules* ***2010*** *43*, 5582-5588

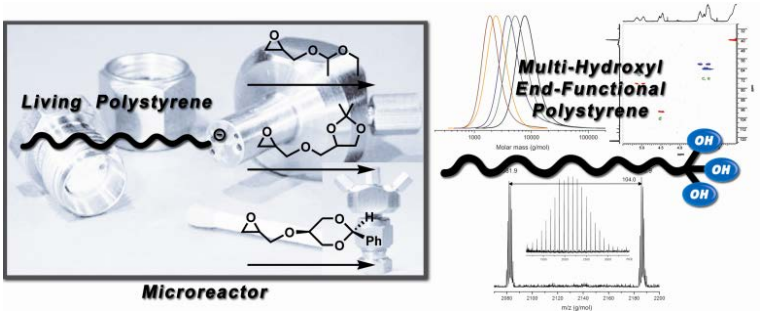

Keywords: end-functionalization, glycidyl ether, microstructured reactor, micromixing, anionic polymerization, epoxide termination, functional polymers

Abstract

We describe the synthesis of end-functionalized poly(styrene)s by living anionic polymerization in a microstructured reactor via termination by acetal-protected functional epoxides. Initiation of styrene polymerization by alkyllithium takes place in a micromixing device with efficient heat and mass transfer properties. A newly developed continuous polymerization-termination sequence enabled quantitative functionalization of the living

carbanions by nucleophilic displacement with different, specifically designed glycidyl ethers (ethoxy ethyl glycidyl ether (EEGE), 1,2-isopropylidene glyceryl glycidyl ether (IGG), and *trans*-2-phenyl-1,3-dioxane glycidyl ether (PDGE)). Upon acidic hydrolysis the end-capped poly(styrene)s release multiple hydroxyl groups (2-3) at the chain end. Temperature and flow rates have been varied to control molecular weights and to optimize the reaction conditions for maximum polymerization and termination efficiency. The polymers were analyzed in detail using NMR spectroscopy, size exclusion chromatography (SEC), and MALDI-ToF MS. Molecular weights of the samples prepared ranged between 1800 and 9000 g/mol. For all of the novel termination agents full termination was confirmed by MALDI-ToF MS. The approach presented is applicable for a large variety of monomers that are polymerizable by carbanionic polymerization.

Introduction

Carbanionic polymerization is a highly useful technique for the synthesis of polymers with precisely adjustable molecular weights and low polydispersity. Its living character along with negligibility of chain transfer/termination reactions further permits the preparation of specifically chain-end-functionalized polymers. Since Michael Szwarc's pioneering works in the 1950s,[1] both academic and industrial interests have been focusing on the exploration of new synthetic strategies to a large variety of well-defined functional macromolecules.[2] Polymers with functional termini offer vast potential due to the possibilities resulting from reversible ionic association, further chain extension, branching, and (cross)linking with polyfunctional reagents or other polymer chains as well as for the initiation of subsequent polymerizations. Advanced macromolecular architectures with unique structural and physical properties[3,4] (for instance, block copolymers, comblike, cyclic, linear-hyperbranched[5] and star-branched polymers) can be elegantly obtained from well-defined functional polymer precursors.

A large variety of intriguing materials with supramolecular properties that depend on the nature and position (terminal or in-chain) of the functional groups has been developed.[6] As the interaction at polymer-polymer interfaces in blends or between polymers and surfaces can be tailored by the polymer architecture, functional polymers possess enormous potential for a variety of industrial and academic applications[7], e.g., dispersion of fillers[8], transparent impact polystyrene-polybutadiene blends (TIPS)[9] and for the modification of surface properties, that is, adhesion, wettability, biocompatibility, chemical resistance, and hydrophobicity.[10]

Two general strategies are employed to synthesize well-defined, end-functional polymers by living carbanionic polymerization: (i) use of a (usually protected) functional initiator and/or (ii) termination of the polymerization with an electrophilic reagent bearing the desired functionality. Using functional initiators permits quantitative functionalization and facile synthesis of telechelic polymers with (different) functional groups. However, their availability is limited, and solubility in solvents suitable for carbanionic polymerization may sometimes be poor. The termination strategy (ii) has been employed in most cases. Quirk and co-workers have optimized the latter approach by realizing a variety of termination

reactions via selective adjustment of reaction parameters like temperature, solvent, and additives to obtain a maximum degree of functionalization.[11]

The most widely used termination reagents are chlorosilane derivatives.[6, 12] As an alternative, the reaction with functional diphenylethylenes (DPE) has become popular,[4,13] since the polymer chains remain active for further extension (living functionalization reaction) unless a termination agent is added. Various epoxides[14] have also been used, particularly ethylene oxide (EO), however, in fewer cases than the highly established chlorosilane termination method. Epoxides are of particular interest for the termination of carbanionic polymerization, since they combine pronounced chemical versatility with high reactivity toward nucleophilic attack due to the effect of ring strain. Furthermore, the lithium counterion common in carbanionic polymerization is known to prevent further propagation in epoxide polymerization due to the strong oxygen-lithium aggregation.[15] Quirk et al. took advantage of this behavior in elegant work to realize quantitatively hydroxyl-terminated poly(styrene) (PS) by reaction of the living chain end with ethylene oxide (EO).[16] Also, propylene oxide[17] and 1,2-epoxybutane[18] have been employed as termination reagents during the past two decades to introduce a single secondary hydroxyl group at the chain end. Additional functionalities can be implemented by using epoxide derivates with protected or unprotected functional groups, depending on the stability toward the highly aggressive living carbanions.[19,20]

Glycidyl ethers, a peculiar class of epoxide derivatives, have only been marginally referred to as termination reagents for living carbanionic polymerizations. In an elegant work, Hillmyer et al. reported the termination with methoxy methylene glycidyl ether (MMO) and subsequent use of the generated bis-hydroxy functional polymer as macroinitiators for preparation of ABC miktoarm star terpolymers[21] with unusual morphologies[22]. In a similar manner, Huang et al. prepared three-arm star polymers using ethoxy ethyl glycidyl ether (EEGE) as a termination reagent.[23]

Here we report on the development of an efficient and versatile synthesis protocol for the preparation of well-defined poly(styrene)s with multiple hydroxyl end groups, using different glycidyl ethers with acetal structures, namely ethoxy ethyl glycidyl ether (EEGE), 1,2-isopropylidene glyceryl glycidyl ether (IGG) and *trans*-2-phenyl-1,3-dioxane glycidyl ether (PDGE) as termination reagents. In accordance with the rapid approach to precisely defined

living poly(styrene) chains previously published by our group,[24] we employed a microstructured reaction system[25] for sequential initiation/polymerization/functionalization within very short times, taking advantage of the dedicated heat and mass transfer characteristics, which are particularly favorable for living polymerization techniques requiring rapid mixing of initiator and monomer as well as efficient heat release due to pronounced exothermic character.[24, 26]

Recent studies demonstrate the successful implementation of several polymerization techniques in microdimensional devices, e.g., free radical,[27] controlled radical,[28] anionic,[24,29] and cationic[30] polymerizations. Beers et al. performed the anionic polymerization of styrene in a low-cost aluminum-kapton microfluidic device investigating different 2D designed flow channels.[31] Pertinent advances have also been achieved in the field of hyperbranched polymers[32] and dendrimers.[33]

However, only little attention has been paid to the potential of continuously operating microstructured reactors for the sequential synthesis of multiple functionalized polymers and the anionic polymerization of vinylmonomers with subsequent functionalization in continuous flow. Within the scope of our investigations, we concentrated on the development of a versatile process for the rapid synthesis of novel tailor-made end-functional polymers by living carbanionic polymerization, using specifically designed glycidyl ethers as termination reagents that release multiple hydroxyl groups upon facile acidic hydrolysis. An overview of the epoxides employed and the functionalization strategies introduced is shown in Scheme 1.

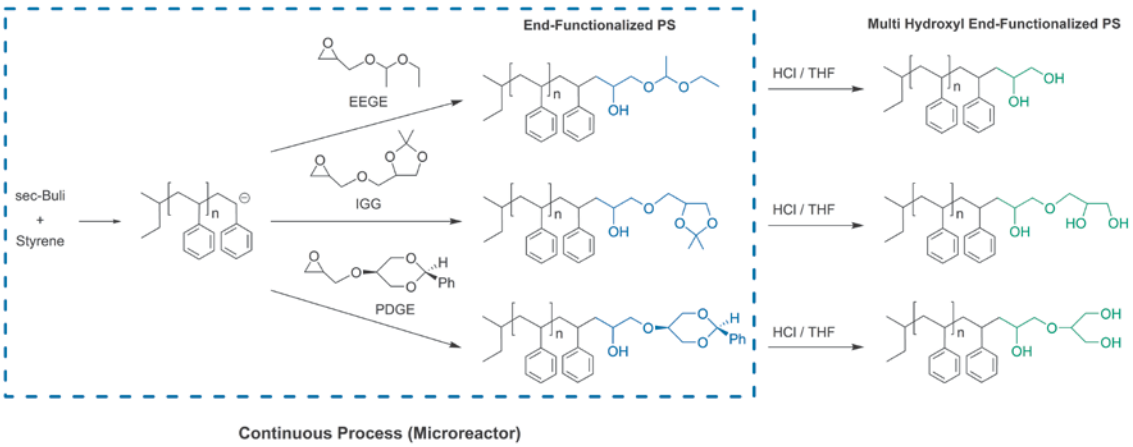

Scheme 1. Semi-continuous synthesis of multi-hydroxyl end-functionalized poly(styrene) using a microstructured reactor (HP-IMM)

Experimental Section

Reagents. All solvents and reagents were purchased from Acros Organics and used as received unless otherwise stated. Tetrahydrofuran (THF) for polymerization was distilled from sodium/benzophenone under reduced pressure (cryo-transfer). Styrene was dried over calcium hydride (CaH_2) and cryo-transferred prior to use. *sec*-Butyllithium (*sec*-BuLi, 1.3M, Acros) was used as received, and the concentration of the initiator was determined by the Gilman double titration method.[34] *n*-Hexane and CaH_2 were purchased from Fluka and used as received. Chloroform-*d* and benzene-d_6 were purchased from Deutero GmbH and stored over molecular sieves (3Å).

Instrumentation. ^{1}H NMR spectra were recorded at 400 MHz on a Bruker AMX 400 and were referenced internally to residual proton signals of the deuterated solvent ($CDCl_3$, benzene-d_6). Field desorption mass spectra were measured on a Finnigan MAT 95. Size exclusion chromatography (SEC) measurements were carried out in THF on an instrument consisting of a Waters 717 plus autosampler, a TSP Spectra Series P 100 pump, a set of three PSS SDV columns (104/500/50 Å), and RI and UV detectors. All SEC diagrams rely on the RI detector signal, and the molecular weights refer to linear poly(styrene) (PS) standards provided by Polymer Standards Service. Matrix-assisted laser desorption and ionization time-of-flight (MALDI-ToF) measurements were performed on a Shimadzu Axima CFR MALDI-TOF mass spectrometer using dithranol (1,8,9-trishydroxyanthracene) as matrix.

Synthesis of Glycidyl Ethers. *Ethoxy Ethyl Glycidyl Ether* (EEGE, **1**). EEGE was synthesized as reported by Fitton et al.[35] Glycidol was added to an excess of ethyl vinyl ether and catalytic amounts of *p*-toluenesulfonic acid to obtain the desired product (yield: 90%).

DL-1,2-Isopropylidene Glyceryl Glycidyl Ether (IGG, **2**). IGG was synthesized according to a recently published procedure[36] by phase-transfer reaction of epichlorohydrin and solketal (isopropylidene glycerol) in benzene and 50% KOH solution as solvents. Tetrabutyl-ammonium bromide (TBAB) was added and served as catalyst (yield: 51%).

trans-2-Phenyl-1,3-dioxane Glycidyl Ether (PDGE, **3**). 4.1 g (23 mmol) of 5-hydroxy-2-phenyl-1,3-dioxane (HPD)[37] was dissolved in 20 mL of benzene, 20 mL of 50% KOH, and 0.74 g (2.3 mmol) of TBAB were added. After cooling the mixture to 10 °C, epichlorohydrin was slowly added via syringe. The reaction mixture was stirred at room temperature for 48 h, diluted with diethyl ether, and washed three times with water, saturated aqueous $NaHCO_3$, and

saturated aqueous NaCl. After drying over $MgSO_4$, diethyl ether and excess epichlorohydrin were removed *in vacuo*. The crude product was purified via column chromatography (silica, chloroform:ethyl acetate 5:1, R_f = 0.45). 1.5 g (6.3 mmol, yield: 30%) of PDGE was obtained and characterized by ^{1}H NMR spectroscopy and field desorption mass spectrometry (FD-MS). ^{1}H NMR (300 MHz, C*D*Cl$_3$, δ in ppm): 7.43 (m, 5H, C$_6$*H*$_5$), 5.57 (s, 1H, C*H* acetal), 4.37 (m, 2H, C*H*$_2$ 1,3-dioxane), 4.08 (m, 2H, C*H*$_2$ 1,3-dioxane), 3.97 (dd, 1H, C*H*$_2$ glycidol), 3.55 (q, 1H, C*H*$_2$ glycidol), 3.46 (m, 1H), 3.24 (m, 1H, C*H* epoxide), 2.83 (t, 1H, C*H*$_2$ epoxide), 2.68 (q, 1H, C*H*$_2$ epoxide). ^{13}C NMR (75 MHz, C*D*Cl$_3$, δ in ppm): 138.0 (quart. *C* aromatic), 128.9 (*C*H aromatic), 128.2 (*C*H aromatic), 126.1 (*C*H aromatic), 101.3 (tert. *C*H acetal), 71.0 (*C*H 1,3-dioxane) 69.4 (*C*H$_2$ 1,3-dioxane) 68.6 (*C*H$_2$), 51.2 (*C*H epoxide), 44.2 (*C*H$_2$ epoxide). FD-MS: 235.9 g/mol.

Microstructured Reactor. A continuous flow reaction setup (Figure 1) equipped with a micromixer was employed for the synthesis of end-functionalized poly(styrene)s. A stainless steel high-pressure slit interdigital micromixer (HP-IMM, provided by the Institut für Mikrotechnik Mainz (IMM)) with an internal volume of 15 µL was used for fast and efficient mixing of monomer and initiator realized by multilamination mixing mode, combined with geometric and hydrodynamic focusing.[38] The micromixer was immersed in a water bath at predefined temperature and equipped with two reactant inlets and one outlet. After mixing of monomer and initiator within several milliseconds, the reaction mixture passed a short stainless steel capillary residence tube (for details cf. Figure 1) and was combined with the corresponding glycidyl ether (separate flow tube) in a T-junction (diameter = 700 µm). The residence tube behind the T-junction was connected to a degassed vessel for sample collection. Flow rates were controlled via HPLC pumps (Knauer WellChrom K-501, inert 10 mL pump heads with ceramic inlays).

Synthesis of Hydroxyl-Functionalized Poly(styrene)s. *Exemplary Synthesis Procedure for PS-EEGE-3*. Prior to the polymerization reaction, THF was pumped through the microstructured reactor setup for 10 min at 0.5 mL min^{-1} via all three HPLC pumps to rinse off residual impurities. The water bath was kept at room temperature, and a solution of purified styrene (1.5 M) in dry THF was kept under argon in a flask covered with a septum. Into a second flask containing dry hexane, 3.8 mL *sec*-BuLi was added via syringe directly before starting the reaction (0.05 M). The third flask contained a solution of purified EEGE (0.1 M) in THF. The three flasks were connected to the HPLC pumps via PTFE tubes transfixed through the septa.

The connection tube between micromixer and T-junction was 50 cm in length and 700 µm in diameter, corresponding to an internal volume of 200 µL. A schematic overview of the general setup is shown in Figure 1.

Prior to the polymerization start, pump II (initiator) was activated and the assembly was flushed with *sec*-BuLi solution to eliminate residual impurities. In order to initiate the continuous process, pumps I (monomer) and II (initiator) were activated with flow rates of 1 mL min^{-1}. After the characteristic reddish color appeared at the outlet, pump III was activated with a flow rate of 1 mL min^{-1} to combine the termination reagent and the reaction mixture within the T-junction. Full monomer conversion was achieved after 6 s, and the end-capped polymer was recovered from a short outlet tube (50 cm length, 700 µm diameter, internal volume 200 µL) connected to the T-junction. PS-EEGE-3 was precipitated into methanol and dried in vacuum at room temperature for 12 h.

All polymer samples prepared have been produced by an analogous procedure. Adjusting the flow rates via the control elements of the HPLC pumps or selecting different concentrations permits convenient variation of molecular weights of the materials prepared.

Synthesis of Multihydroxyl-Functionalized Poly(styrene). 500 mg of the end-capped PS was dissolved in 20 mL of THF and 3 mL of 2M HCl. After refluxing of the solution for 8 h, the reaction mixture was diluted with chloroform and washed with saturated aqueous $NaHCO_3$ and water. After drying the organic phase with $MgSO_4$, all solvents ($CHCl_3$, THF) were removed under reduced pressure. The samples were precipitated into MeOH and dried at room temperature for 12 h.

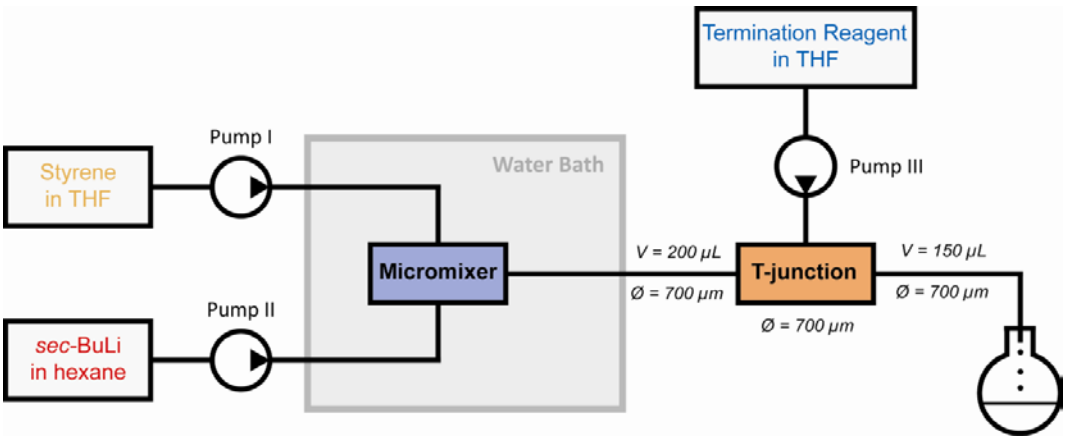

Figure 1. Schematic reactor setup for polymerization of styrene with direct subsequent termination by glycidyl ethers (micromixer: HP-IMM).

Results and Discussion

Three different glycidyl ethers (Figure 2) with acetal or ketal protecting group were used to terminate the living anionic poly(styrene) chains in continuous flow, aiming at novel multi-hydroxyl end-functionalized polymer structures: EEGE (**1**), IGG (**2**), and PDGE (**3**), a novel glycidyl ether that was prepared from epichlorohydrin using TBAB as a phase transfer catalyst. This compound offers the unique possibility to introduce one secondary and two primary protected hydroxyl groups via a single functionalization/deprotection sequence.

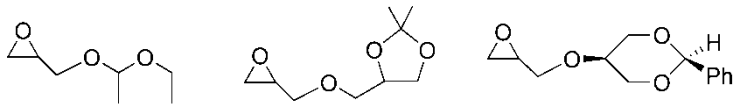

EEGE (**1**) IGG (**2**) PDGE (**3**)

Figure 2. Glycidyl ethers/acetals used as termination reagents in the continuous polymerization-termination sequences.

The different epoxide termination agents were obtained in high purity (see Supporting Information, Figures S7 and S8), which is essential for quantitative chain-end functionalization of living carbanionic polymers. Strong aggregation of the lithium counterion with alkoxides prevents further oxyanionic propagation,[15] rendering the synthesized glycidyl ethers suitable for quantitative and simultaneous end-capping of the living carbanions.

Utilization of the micromixer-based reaction system permits rapid reactant mixing and offers the possibility to apply reaction conditions (room temperature) that are not applicable in conventional glass equipment. Thus, significantly faster reaction kinetics can be realized. The technique is feasible, unless very high molecular weights are required. The stainless steel setup shows excellent chemical resistance toward the highly aggressive carbanions and hence provides an ideal platform for rapid living anionic polymerization sequences. For comparison, classical batch methods for carbanionic polymerizations are often labor-intensive and in many cases require “high vacuum” or “break-seal” methods as well as individually manufactured glass reactors.[39] Residence times required for full conversion of styrene in the micromixer-based system are generally below 15 s without loss of control over the polymerization compared to oftentimes prolonged reaction times of typically 2-3 h in batch reactors. The temperature dependency of the continuous flow polymerization has

also been studied by increasing the temperature to 60 °C. However, no significant deviation with respect to the polymer properties (M_n, PDI) has been observed.

Initiation of styrene polymerization with *sec*-BuLi in the micromixer at room temperature, using THF as a solvent, results in an extremely fast propagation reaction ($t_{1/2}$ < 0.5 s).[40] Full monomer conversion is achieved within seconds[24, 26] before the living chain ends are reacted with the unsubstituted carbon of the highly strained epoxide ring. A short outlet tube (for details cf. Figure 1) is sufficient for reaction of all living polymer chains with the termination reagent before leaving the reactor. A color change of the reaction mixture (reddish to light yellow), resulting from the termination of living carbanions, can be observed.

Table 1. Characterization data of end-functionalized PS samples prepared by anionic polymerization with subsequent termination in a microstructured reaction setup.

sample	T /°C	t [a)]	M_n [b)]	M_n [c)]	M_n/M_w [c)]
PS-EEGE-1	25	12	1900	1800	1.14
PS-EEGE-2	40	12	1900	1900	1.15
PS-EEGE-3	40	10	3100	3000	1.14
PS-EEGE-4	25	5	4300	3900	1.13
PS-EEGE-5	40	8	3800	4500	1.26
PS-EEGE-6	50	8	3800	6400	1.18
PS-IGG-1	25	6	1900	1900	1.22
PS-IGG-2	60	12	2500	2300	1.18
PS-IGG-3	25	12	2600	2900	1.28
PS-IGG-4	25	8	3800	4100	1.29
PS-IGG-5	25	10	3900	5000	1.21
PS-IGG-6	60	8	5000	5300	1.23
PS-IGG-7	25	8	5200	7700	1.22
PS-PDGE-1	25	12	2800	3600	1.26
PS-PDGE-2	25	12	5000	4100	1.36
PS-PDGE-3	25	8	7500	8800	1.24

[a)]Residence time in seconds [b)]Theoretical value of the number average of the molecular weight in g·mol^{-1}
[c)]Molecular weight in g·mol^{-1} and molecular-weight distribution characterized by SEC in THF.

By adjusting the ratio of styrene and *sec*-BuLi flow rates, the degree of polymerization was readily varied during the ongoing experiment. Thus, the micromixing device provides convenient access to a variety of structurally different polymers without modifying the setup

within one run. Subsequent to the continuous polymerization/functionalization sequence, the protecting groups are cleaved by acidic hydrolysis to afford multihydroxyl end-functionalized polymers.

Characterization by size exclusion chromatography (SEC) yielded reasonable agreement between theoretical and experimental molecular weights, revealing narrow to moderate and monomodal molecular-weight distributions (MWDs) (M_w/M_n < 1.30, mostly < 1.25; Table 1). No dependence of molecular weights and PDI on the temperature was observed in the temperature range between 25 and 60 °C.

Figure 3 depicts the SEC diagrams of IGG-terminated poly(styrene)s with monomodal MWDs, evidencing the remarkable degree of control over the polymerization under the applied continuous flow conditions.

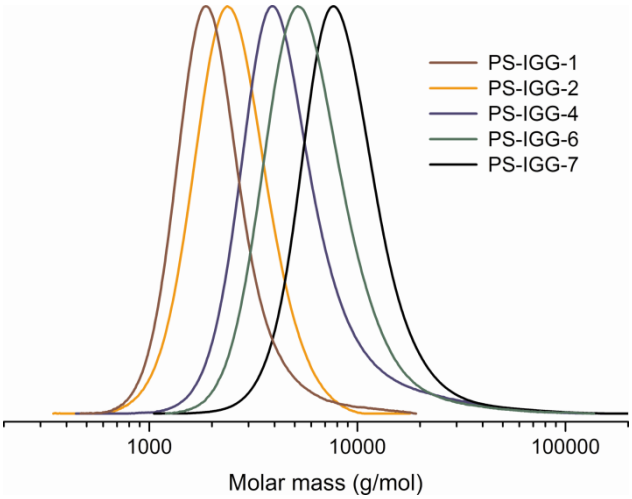

Figure 3. MWDs determined via SEC of selected PS-IGG samples (THF, RI-Signal).

The MWDs of the epoxide-terminated polymers obtained by the continuous approach presented herein are generally slightly broader than those realizable in classical batch reactors (typically < 1.1, often 1.01-1.03).A possible explanation can be found in the slightly incontinuous flow of the HPLC pumps, which results in temporary deviations from the adjusted stoichiometry. Taking into account the significantly reduced experimental effort using the continuous device, the micromixer-based system provides an alternative for carbanionic batch polymerization, when very narrow MWDs with PDIs below 1.05 do not represent a necessity, as it applies for a wide variety of applications.[41]

^{1}H NMR spectroscopy was employed to study the functionalization as well as monomer conversion. Figure 4 (bottom) represents the ^{1}H NMR spectrum of PS-EEGE-2. The expected

signals reflecting the poly(styrene) backbone (aromatic signals at 7.3-6.3 ppm and aliphatic signals at 2.6-0.8 ppm) are clearly visible. Referencing the respective signals to the six methyl proton signals of the initiator *sec*-BuLi (0.72 ppm) permits to estimate the functionalization efficiency. The acetalic proton (4.38 ppm) of the end group attached to the polymer generates a readily distinguishable signal that can be separately integrated. The respective values were close to 1 in all cases, indicating a high degree of functionalization. However, end-group analysis using ^{1}H NMR spectroscopy becomes increasingly problematic at elevated molecular weights due to the diminishing end-group signal intensity.

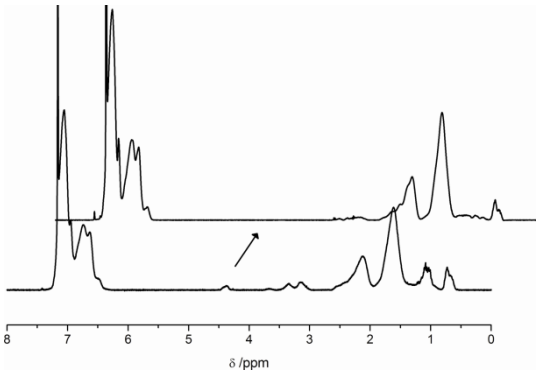

Figure 4. ^{1}H-NMR spectra of PS-EEGE: (bottom: PS-EEGE-2, top: deprotected PS-EEGE-2 (PS-EEGE$_d$-2); both spectra were measured in benzene-d_6 as solvent.

It is known from the literature that the regiochemistry of reactions between living poly(styrene) and epoxide compounds depends on the steric and electronic nature of the termination reagent.[17-20] For instance, the reactions of poly(styryl)lithium with propylene oxide and 1,2-butene oxide are regioselective due to pronounced steric effects of the methyl or ethyl group, respectively. Nucleophilic attack at the least hindered carbon atom predominantly results in formation of the secondary alcohol. In contrast, when employing styrene oxide as a termination reagent, no regioselectivity can be observed due to the parallel influence of both steric and electronic effects. In the case of reacting poly-(styryl)lithium with the different glycidyl ethers reported herein, regioselectivity was expected due to the steric hindrance of the bulky moieties attached to the epoxide ring. Two-dimensional (2D) NMR spectroscopy was employed to gain insight with respect to the selectivity of the reactions. Figure 5 represents a section of the HSQC spectrum of PS-EEGE-2 in benzene-d_6 after reaction with trifluoroacetic anhydride (TFAA), adding a small amount of pyridine-d_5 as acid scavenger to prevent cleavage of the protecting group. The cross peaks **b**,

generated by the methine groups, are shifted downfield (5.0-5.5 ppm) in the corresponding ^{1}H NMR spectrum due to ester formation. Owing to the presence of a mixture of diastereomers, two distinct methine signals are generated. The absence of any downfield-shifted methylene signals (blue) indicates that regioselective attack of poly(styryl)lithium took place exclusively at the least hindered carbon atom of EEGE, and thus no primary alcohol was formed. Furthermore, the ^{1}H-^{1}H-COSY spectrum (see Supporting Information Figure S5) illuminates the coupling between **b** and adjacent methylene groups **a** and **c**. Taking into account the additional steric constraints of the other termination reagents, similarly regioselective nucleophilic displacement reactions can be safely assumed for all epoxide termination reagents of this study.

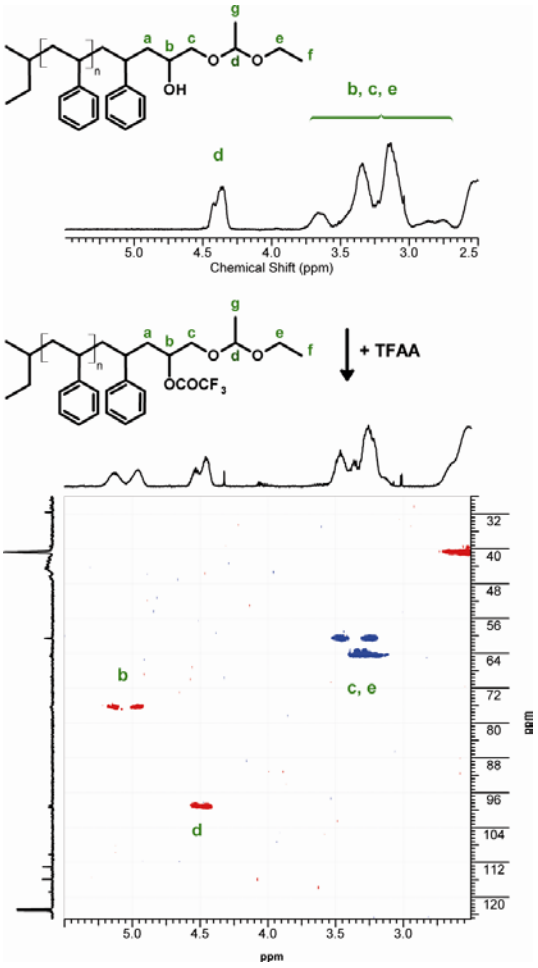

Figure 5. Top: Section of ^{1}H NMR spectrum of PS-EEGE-2. Bottom: HSQC spectrum of PS-EEGE-2 after reaction with trifluoroacetic anhydride (TFAA). Phase information is given by coloration of cross peaks (red: methyl, methine; blue: methylene).

The spectra of both the protected and deprotected polymer (PS-EEGE-2) are depicted in Figure 4. Complete disappearance of the acetalic proton d (4.38 ppm) as well as the methyl group signals (1.06) confirms quantitative deprotection of the acetalic end groups. It has to be emphasized that the deprotection times are considerably prolonged compared to water-soluble polymers[42], which can be explained by the nonpolar character of the poly(styrene) backbone, shielding the acetal group from the deprotecting reagent. Additional NMR spectra of PS-IGG and PS-PDGE polymers before and after deprotection are given in Figures S3 and S4 of the Supporting Information. As expected, no significant change in molecular weight and MWD has been observed after cleavage of the protecting groups (SEC).

As indicated above, NMR spectra cannot provide sufficient proof for quantitative terminal functionalization of the polymers, particularly at elevated degrees of polymerization. Matrix-assisted laser desorption/ionization time-of-flight mass spectrometry (MALDI-ToF MS) as a crucial characterization method for the detailed investigation of end-functional polymers was thus applied in order to obtain unequivocal evidence for the high functionalization efficiency of the method. Quantitative functionalization of poly(styrene)s capped with the three different glycidyl ethers was demonstrated by MALDI-ToF MS, using silver trifluoro-acetate as cationizing agent and dithranol (1,8,9-trishydroxyanthracene) as matrix. Figure 6 shows two MALDI-ToF spectra of IGG- and PDGE-terminated poly(styrene). The spectrum of PS-IGG (left) reveals only one distribution mode, which is unambiguously assigned to IGG-functionalized poly(styrene). The most intense isotopic mass species appear 3 units higher than the monoisotopic peak, and one representative mass peak at *m/z* 2541.6 corresponds to the 21-mer of PS-IGG-3 (C_4H_9-$(C_8H_8)_{21}$-$C_9H_{17}O_4$·Ag^+); calculated isotopic mass = 2541.4 Da. Similar conclusions apply for the spectrum on the right, representing PS-PDGE-1 with a single distribution mode that can clearly be assigned to the desired polymer. The representative mass peak (28mer: C_4H_9-$(C_8H_8)_{21}$-$C_{13}H_{17}O_4$·Ag^+, 3317.7 Da) is in very good agreement with the calculated value (3317.8 Da). In both cases the mass difference between each signal represents the molecular mass of the monomer (104.1 Da). Furthermore, it has to be emphasized that peaks corresponding to the protonated, non-functional poly(styrene) (PS-H: 22mer = 2457.4 Da or 31mer = 3394.7 Da) are absent in both spectra, confirming the quantitative functionalization of poly(styrene) with IGG and PDGE.

In order to confirm that nonfunctionalized PS-chains would be detected in the presence of the functionalized PS-samples, mixtures containing end-functional and nonfunctional poly(styrene)s have been subjected to MALDI-ToF measurements. In this case, in 1:1 blends nearly identical detection intensities of both series of signals were observed (see Supporting Information Figure S9), and therefore similar desorption and ionization properties of the different poly(styrene) types can be safely assumed.

MALDI-ToF investigation of the PS-EEGE sample series confirmed quantitative functionalization, resulting in analogous single molecular weight distributions (see Supporting Information Figure S6). Detailed MALDI-ToF studies with the deprotected polymers confirmed results of the ^{1}H NMR spectra, evidencing successful cleavage of the protecting groups and full functionalization (see Supporting Information Figure S6).

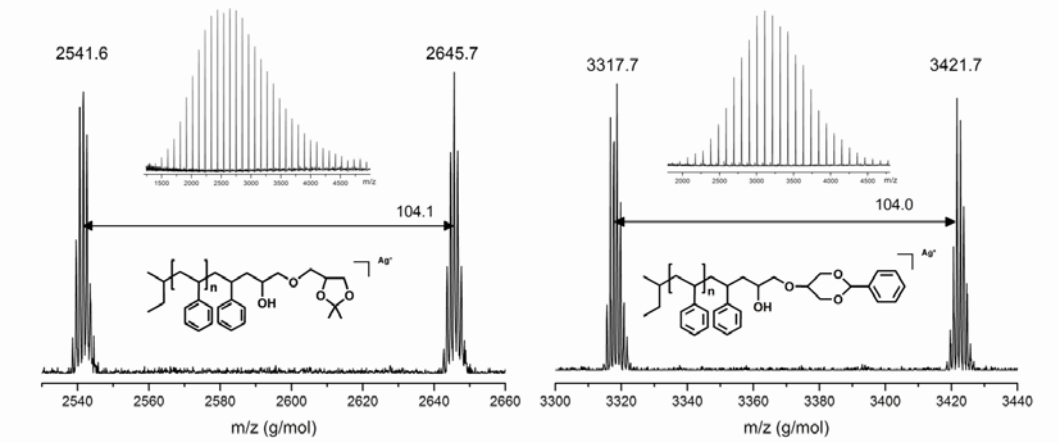

Figure 6. MALDI-ToF mass spectra of end-functionalized poly(styrene) synthesized in continuous flow: PS-IGG-3 (left), PS-PDGE-1 (right).

Conclusion

We have developed a semicontinuous strategy for the rapid preparation of multihydroxyl-functional poly(styrene)s, capitalizing on the high stability of the acetal-protecting groups of the protected glycidyl ethers toward strong bases. The synthetic approach presented relies on a continuously operating microstructured reaction device for living carbanionic polymerization and termination with specifically tailored glycidyl ethers, followed by deprotection of the introduced end-group moieties.

Adjustment of molecular weights as well as chemical nature of the end group can be achieved by alteration of the flow rates in a single experiment without interrupting the

continuous flow process. Full styrene monomer conversion was achieved within several seconds by working at room temperature in a polar solvent, usually THF. The functional polymers were thus obtained in very short reaction times without having to resort to tedious postpolymerization protocols or purification steps in order to yield pure and quantitatively functionalized materials. The acetal and ketal protecting groups of the employed termination reagents are stable toward the highly reactive carbanions and can be cleaved under acidic conditions.

The general termination methodology presented herein also provides a method for rapid and cost-efficient polymer screening with respect to novel end-functionalized materials. By tailoring the glycidyl ethers by means of standard organic synthesis protocols, a large variety of terminal units at vinyl polymers with multiple end groups and intriguing properties can be realized. The respective materials can be further used as macroinitiators for complex macromolecular architectures, such as miktoarm star polymers, block copolymers, and graft polymers. Depending on monomer and termination reagent, such end-functional polymers are also promising for the specific adjustment of surface and interfacial properties.Use of several monomer/termination reagent combinations can rapidly afford polymer libraries, permitting to screen a wide range of material properties (wettability, hydrophobicity, chemical resistance, biocompatibility). A detailed study of other carbanionic polymerization reactions with respect to protected glycidyl ether termination and functionalization is currently in progress and will be reported in due course.

Acknowledgment

C. T. thanks the POLYMAT Graduate Class of Excellence as well as MPGC (Max Planck Graduate Center with Johannes Gutenberg-University) for fellowships and financial support. D. W. acknowledges the Fonds der Chemischen Industrie (FCI) for a Ph. D. fellowship. We also thank the IMM (Institut für Mikrotechnik Mainz) for providing the micromixer equipment.

Supporting Information

The following Figures represent characterization results obtained by NMR spectroscopy, size exclusion chromatography and MALDI-ToF mass spectrometry:

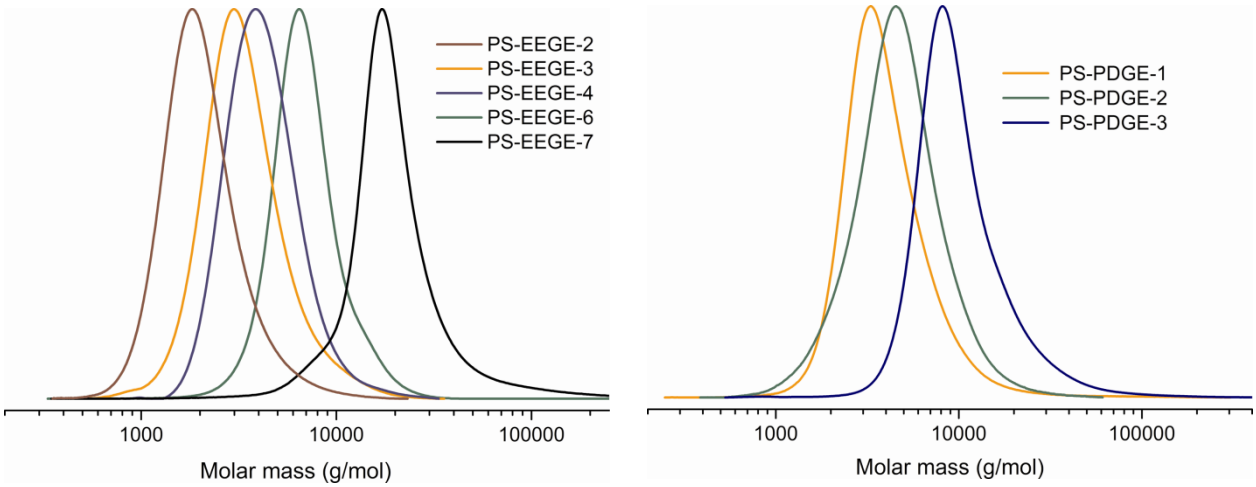

Figure S1. SEC curves of selected PS-EEGE (left) and PS-PDGE (right) samples (THF, RI-Signal).

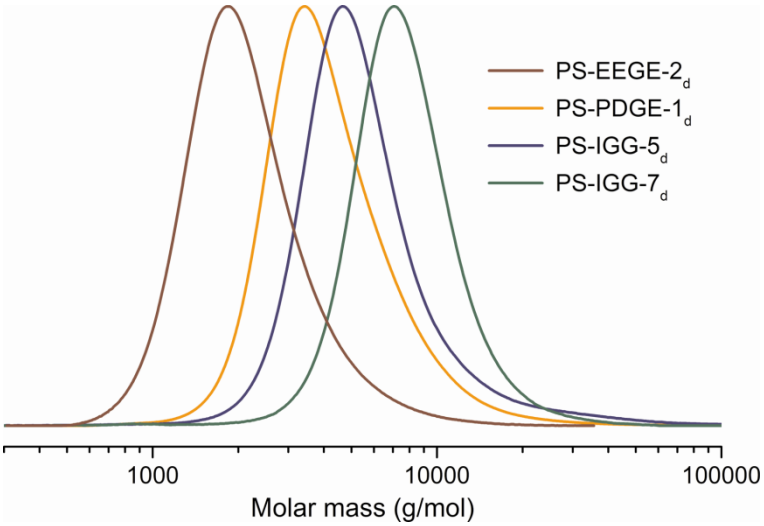

Figure S2. SEC-curves of deprotected poly(styrene)s (PS-EEGE$_d$, PS-IGG$_d$, PS-PDGE$_d$)

Table 1. SEC characterization data of multi-hydroxyl end-functionalized PS samples prepared by an additional cleavage step.

sample	M_n [a)]	M_n/M_w [a)]
PS-EEGE-2d	1700	1.18
PS-EEGE-3d	3400	1.19
PS-EEGE-5d	4800	1.27
PS-IGG-5d	5000	1.21
PS-IGG-7d	7700	1.22
PS-PDGE-1d	3700	1.26

[a]Molecular weight in g·mol^{-1} and molecular weight distribution characterized by SEC in THF.

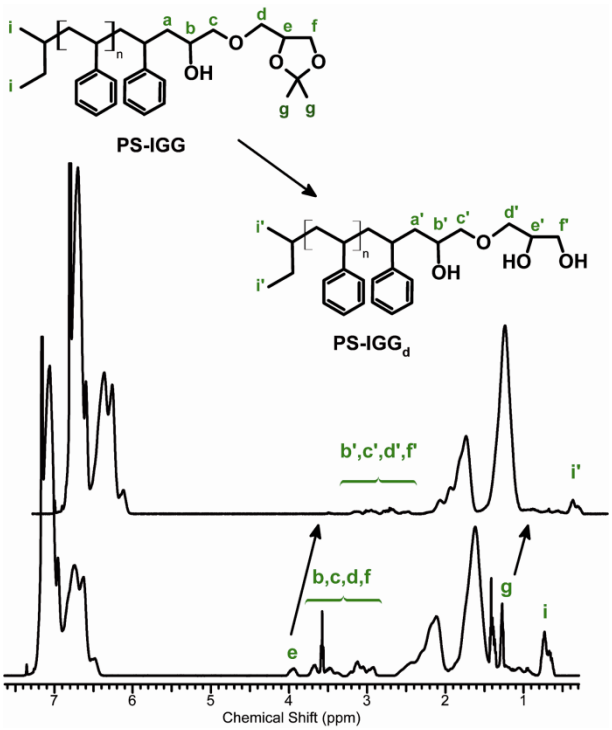

Figure S3. ^{1}H NMR spectra of PS-IGG: bottom: PS-IGG-1, top: PS-IGG-7$_d$; both spectra were measured in benzene-d_6 as solvent.

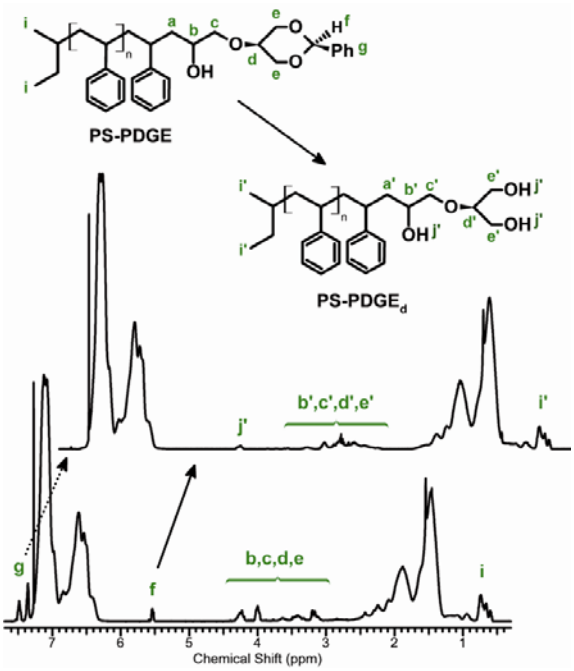

Figure S4. ^{1}H NMR spectra of PS-PDGE: bottom: PS-PDGE-1, top: PS-PDGE-1$_d$; both spectra were measured in chloroform-*d* as solvent.

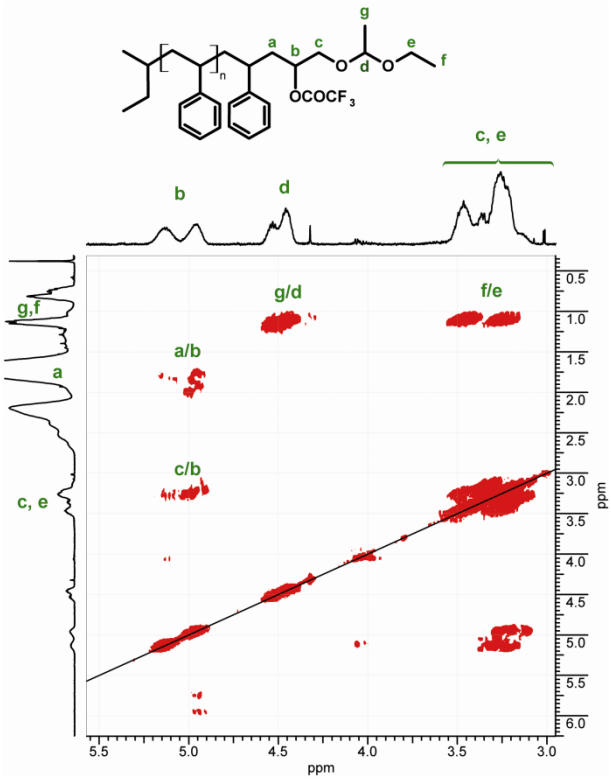

Figure S5. ^{1}H-^{1}H-COSY spectrum of PS-EEGE-2 with corresponding assignment of ^{1}H coupling.

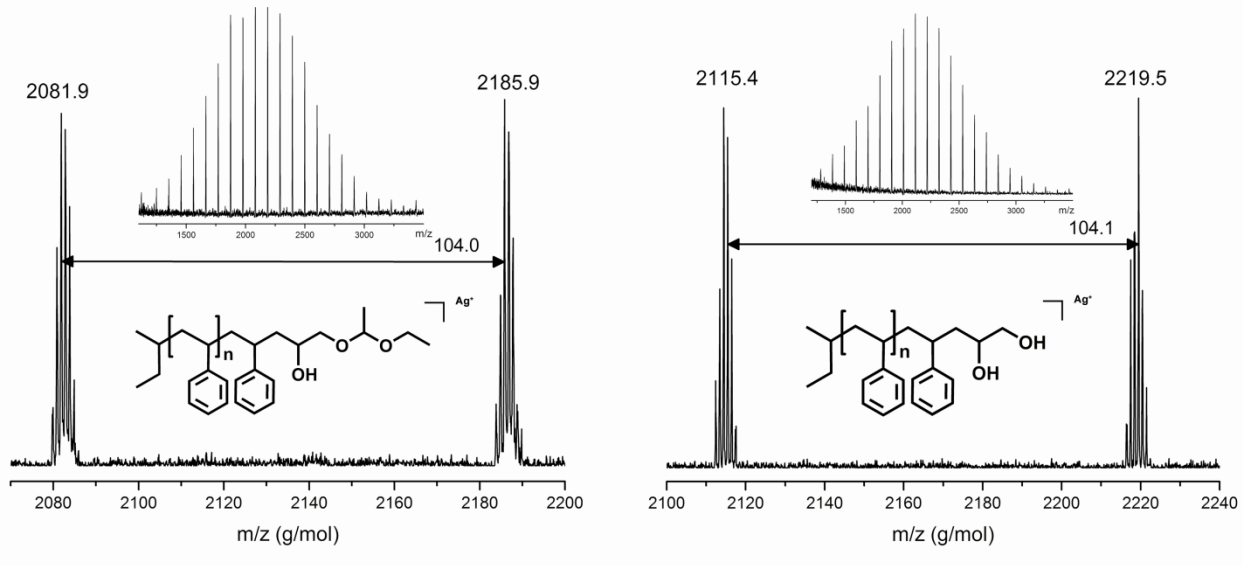

Figure S6. MALDI-ToF mass spectra of PS-EEGE-1 (left) and PS-EEGE-2_d (right) representing quantitative termination and deprotection of poly(styrene) synthesized in continuous flow.

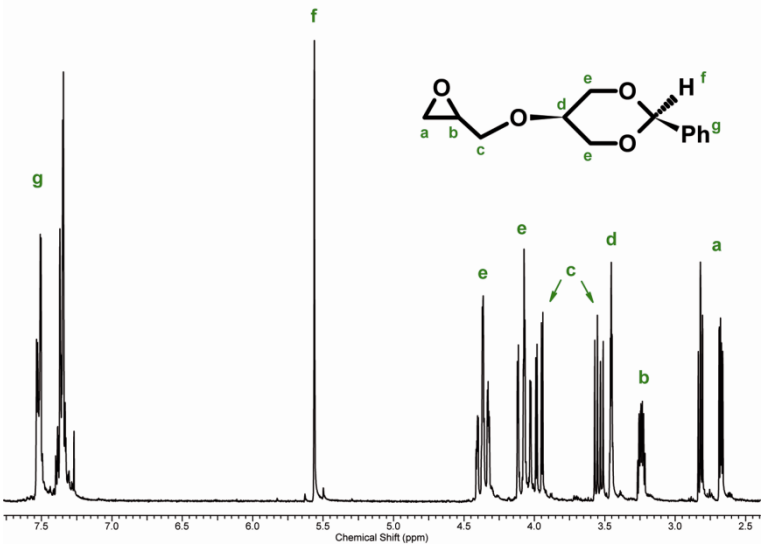

Figure S7. ^{1}H NMR spectrum of trans-2-phenyl-1,3-dioxane glycidyl ether (PDGE) in $CDCl_3$.

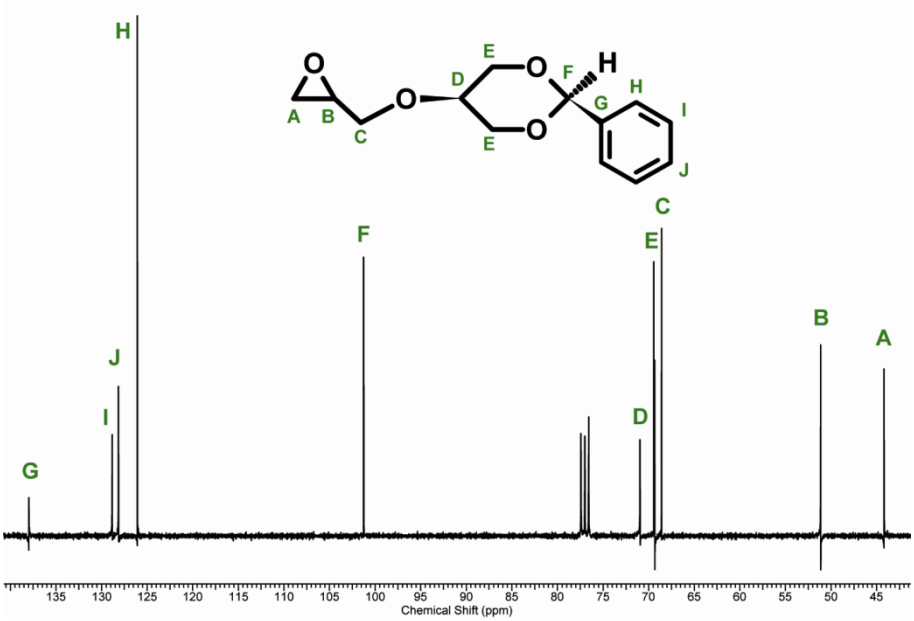

Figure S8. ^{13}C NMR spectrum of trans-2-phenyl-1,3-dioxane glycidyl ether (PDGE) in $CDCl_3$.

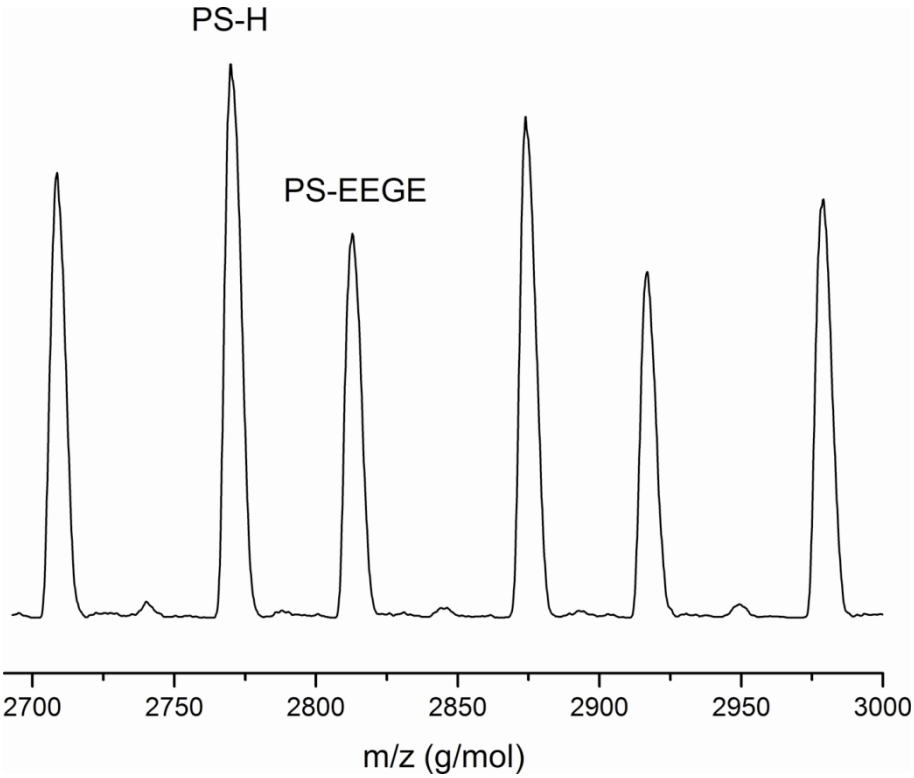

Figure S9. MALDI-ToF Spectrum of a mixture containing PS-EEGE and PS-H in a 1:1 ratio.

References

(1) Szwarc, M. *Nature* **1956,** 178, 1168–1169.

(2) Quirk, R. P.; Pickel, D. L. Anionic Synthesis of Chain-End Functionalized Polymers. Scope, Limitations and Recent Advances. In *Living and Controlled Polymerization*; Jagur-Grodzinski, J., Ed.; Nova Science Publishers: Hauppauge, NY, 2006; pp 235-255.

(3) Hadjichristidis, N.; Iatrou, H.; Pitsikalis, M.; Mays, J. *Prog. Polym. Sci.* **2006,** 31, 1068–1132.

(4) (a) Hirao, A.; Hayashi, M. *Acta Polym.* **1999,** 50, 219–231. (b) Higashihara, T.; Sugiyama, K.; Yoo, H.-S.; Hayashi, M.; Hirao, A. Macromol. Rapid Commun. 2010, DOI: 10.1002/marc.200900773.

(5) (a) Marcos, A. G.; Pusel, T. M.; Thomann, R.; Pakula, T.; Okrasa, L.; Geppert, S.; Gronski, W.; Frey, H. *Macromolecules* **2006,** 39,971–977. (b) Barriau, E.; Marcos, A. G.; Kautz, H.; Frey, H. *Macromol. Rapid Commun.* **2005,** 26, 862–867. (c) Wurm, F.; Nieberle, J.; Frey, H. *Macromolecules* **2008,** 41, 1184–1188.

(6) Hadjichristidis, N.; Pitsikalis, M.; Pispas, S.; Iatrou, H. *Chem. Rev.* **2001,** 101, 3747–3792.

(7) Quirk, R. P.; Gomochak, D. L. *Rubber Chem. Technol.* **2003,** 76,812–831.

(8) Quirk, R. P.; Jiang, K. *Polym* Prepr. *(Div. Polym. Chem.)* **2001,** 42, 27–28.

(9) Kobatake, S.; Harwood, H. J.; Quirk, R. P.; Priddy, D. B. *Macromolecules* **1998,** 31, 3735–3739.

(10) Hutchings, L. R.; Narrianen, A. P.; Thompson, R. L.; Clarke, N.; Ansari, I. *Polym. Int.* **2008,** 57, 163–170.

(11) Quirk, R. P.; Hsieh, H. L. Functionalized Polymers and Macromonomers. In *Anionic Polymerization: Principles And Practical Applications*; Hudgin, D. E., Ed.; Marcel Dekker: New York, 1996; pp 261-306.

(12) Peters, M. A.; Belu, A. M.; Linton, R. W.; Dupray, L.; Meyer, T. J.; DeSimone, J. M. *J. Am. Chem. Soc.* **1995,** 117, 3380–3388.

(13) Quirk, R. P.; Yoo, T.; Lee, Y.; Kim, J.; Lee, B. Application of 1,1-Diphenylethylene Chemistry in Anionic Synthesis of Polymers with Controlled Structure. In Advances in Polymer Science; Springer-Verlag: Berlin, 2000; Vol. 153, pp 67-162.

(14) Quirk, R. P.; Cheong, T. H.; Jiang, K.; Gomochak, D. L.; Yoo, T. J.; Andes, K. T.; Mathers, R. T. *Macromol. Symp.* **2003,** 195, 69–74.

(15) Furukawa, J.; Saegusa, T.; Tsuruta, T.; Kakogawa, G. *Macromol. Chem. Phys.* **1960,** 36 (1), 25–39.

(16) Quirk, R. P.; Ma, J. J. *J. Polym. Sci*., *Part A: Polym. Chem.* **1988,** 26, 2031–2037.

(17) Quirk, R. P.; Lizarraga, G. M. *Macromolecules* **1998,** 31, 3424–3430.

(18) Quirk, R. P.; Ge, Q.; Arnould, M. A.; Wesdemiotis, C. *Macromol. Chem. Phys.* **2001,** 202, 1761–1767.

(19) Quirk, R. P.; Gomochak, D. L.; Wesdemiotis, C.; Arnould, M. A. *J. Polym. Sci., Part A: Polym. Chem.* **2003,** 41 (7), 947–957.

(20) Quirk, R. P.; Hasegawa, H.; Gomochak, D. L.; Wesdemiotis, C.; Wollyung, K. *Macromolecules* **2004,** 37, 7146–7155.

(21) (a) Li, Z.; Hillmyer, M. A.; Lodge, T. P. *Macromolecules* **2004,** 37,8933–8940. (b) Saito, N.; Liu, C.; Lodge, T. P.; Hillmyer, M. A. *Macromolecules* **2008,** 41, 8815–8822.

(22) (a) Li, Z.; Kesselman, E.; Talmon, Y.; Hillmyer, M. A.; Lodge, T. P. *Science* **2004,** 306, 98–101. (b) Li, Z.; Hillmyer, M. A.; Lodge, T. P. *Langmuir* **2006,** 22, 9409–9417.

(23) Wang, G.; Huang, J. *J. Polym. Sci., Part A: Polym. Chem.* **2008,** 46,1136–1150.

(24) Wurm, F.; Wilms, D.; Klos, J.; Löwe, H.; Frey, H. *Macromol. Chem. Phys.* **2008,** 209, 1106–1114.

(25) (a) Hessel, V.; Renken, A.; Schouten, J. C.; Yoshida, J.-I. *Micro Process Engineering : A Comprehensive Handbook*; Wiley-VCH: Weinheim, 2009. (b) Jähnisch, K.; Hessel, V.; Löwe, H.; Baerns, M. *Angew. Chem*., *Int. Ed.* **2004,** 43, 406–446. (c) Wilms, D.; Klos, J.; Frey, H. *Macromol. Chem. Phys.* **2008,** 209, 343–356. (d) Hessel, V.; Löwe, H.; Serra, C.; Hadziioannou, G. *Chem. Ing. Tech.* **2005,** 77,1693–1714.

(26) Nagaki, A.; Tomida, Y.; Yoshida, J.-I. *Macromolecules* **2008,** 41,6322–6330.

(27) (a) Iwasaki, T.; Yoshida, J.-I. *Macromolecules* **2005,** 38, 1159–1163. (b) Serra, C.; Sary, N.; Schlatter, G.; Hadziioannou, G.; Hessel, V. *Lab Chip* **2005,** 5, 966–973.

(28) (a) Rosenfeld, C.; Serra, C.; Brochon, C.; Hadziioannou, G. *Chem. Eng. Sci.* **2007,** 62, 5245–5250. (b) Wu, T.; Mei, Y.; Cabral, J. T.; Xu, C.; Beers, K. L. *J. Am. Chem. Soc.* **2004,** 126, 9880–9881. (c) Wu, T.; Mei, Y.; Xu, C.; Byrd, H. C. M.; Beers, K. L. *Macromol. Rapid Commun.* **2005,** 26, 1037–1042.

(29) (a) Miyazaki, M.; Honda, T.; Nakamura, H.; Maeda, H. *Chem. Eng. Technol.* **2007,** 30, 300–304. (b) Nagaki, A.; Tomida, Y.; Miyazaki, A.; Yoshida, J.-I. *Macromolecules* **2009,** 42, 4384–4387.

(30) (a) Nagaki, A.; Kawamura, K.; Suga, S.; Ando, T.; Sawamoto, M.; Yoshida, J.-I. *J. Am. Chem. Soc.* **2004,** 126, 14702–14703. (b) Iwasaki, T.; Nagaki, A.; Yoshida, J.-I. *Chem. Commun.* **2007**,1263–1265. (c) Iwasaki, T.; Yoshida, J.-I. *Macromol. Rapid Commun.* **2007,** 28, 1219–1224. (d) Ouchi, M.; Inagaki, N.; Ando, T.; Sawamoto, M. *Polym. Prepr. (Div. Polym. Chem.)* **2005,** 46, 939–940.

(31) Iida, K.; Chastek, T. Q.; Beers, K. L.; Cavicchi, K. A.; Chun, J.; Fasolka, M. J. *Lab Chip* **2009,** 9, 339–345.

(32) Wilms, D.; Nieberle, J.; Klos, J.; Löwe, H.; Frey, H. *Chem. Eng. Technol.* **2007,** 30, 1519–1524.

(33) Liu, S.; Chang, C.-H. *Chem. Eng. Technol.* **2007,** 30, 334–340.

(34) Gilman, H.; Haubein, A. H. *J. Am. Chem. Soc.* **1944,** 66, 1515–1516.

(35) Fitton, A. O.; Hill, J.; Jane, D. E.; Millar, R. *Synthesis* **1987**, 1140–1142.

(36) Wurm, F.; Nieberle, J.; Frey, H. *Macromolecules* **2008,** 41, 1909–1911.

(37) Carlsen, P. H. J.; Sorbye, K.; Ulven, T.; Aasbo, K. *Acta Chem. Scand.* **1996,** 50, 185–187.

(38) Hessel, V.; Hardt, S.; Löwe, H.; Schönfeld, F. *AlChE J.* **2003,** 49,566–577.

(39) Hadjichristidis, N.; Iatrou, H.; Pispas, S.; Pitsikalis, M. *J. Polym. Sci., Part A: Polym. Chem.* **2000,** 38, 3211–3234.

(40) (a) Geacintov, C.; Smid, J.; Szwarc, M. *J. Am. Chem. Soc.* **1962,** 84,2508–2514. (b) Bhattacharyya, D. N.; Lee, C. L.; Smid, J.; Szwarc, M. *J. Am. Chem. Soc.* **1963,** 85, 533–539. (c) Bhattacharyya, D. N.; Lee, C. L.; Smid, J.; Szwarc, M. *J. Phys. Chem.* **1965,** 69, 612–623.

(41) Lynd, N. A.; Hillmyer, M. A. *Macromolecules* **2005,** *38*, 8803–8810.

(42) Mangold, C.; Wurm, F.; Obermeier, B.; Frey, H. *Macromol. Rapid Commun.* ***2010*** 31, (3), 258-264.

Chapter 3: Macromolecular Architectures

3.1: Introducing an Amine Functionality at the Block Junction of Amphiphilic Block Copolymers by Anionic Polymerization Strategies

Christoph Tonhauser,[1] *Boris Obermeier,*[1] *Christine Mangold,*[1] *Holger Löwe*[1,2] and *Holger Frey**[1]

[1]Institute of Organic Chemistry, Organic and Macromolecular Chemistry, Duesbergweg 10-14 Johannes Gutenberg-University (JGU), D-55099 Mainz, Germany

[2]Institut für Mikrotechnik Mainz GmbH, Carl-Zeiss-Strasse 18-22, 55129 Mainz, Germany.

Published in *Chemical Communications* **2011**, *47*, 8964-8966

In a semicontinuous anionic procedure amino in-chain functionalization of amphiphilic block copolymer (PS-(NH_2)-PEO) were obtained and reactivity was proofed by addressing a fluorescent dye to the active site.

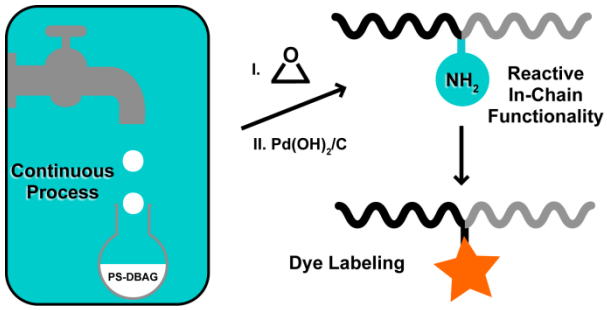

Abstract

A series of block copolymers bearing a single amino in-chain functionality was synthesized via anionic polymerization of styrene and ethylene oxide. By means of both a conventional and a continuous setup, living poly(styrene) was quantitatively end functionalized with an oxirane (DBAG) prior to the polymerization of the poly(ethylene oxide) segment. The in-chain amine was conjugated with a fluorescent dye.

Anionic polymerization represents an important technique to synthesize well-defined macromolecules with in-chain and chain-end functionalities.[1] The established procedure for the introduction of end-functional groups requires universal capping reagents, e.g., diphenylethylene (DPE)[2] or chlorosilane[3] derivatives. Epoxides possess great potential as termination agents for the implementation of a single hydroxyl group or multiple orthogonal functionalities with high degrees of functionalization, as we reviewed recently.[4] Furthermore, the polymerization-termination sequence can be transferred to continuous flow, utilizing microstructured reactors.[5]

The introduction of exactly one in-chain functionality directly at the interface between the two blocks of diblock copolymers can be realized by termination reagents exhibiting two functional groups, i.e., one to initiate the anionic polymerization of the following block, while the other functional group is stable or protected towards the polymerization conditions and can subsequently be modified. Such unique polymer architectures represent a fascinating class of compounds, which can be utilized as precursors for macromolecular architectures[6] like miktoarm star polymers[7] and H-shaped polymers.[8] With respect to self-assembly, in-chain functionalized polymers offer intriguing properties and potential for applications[9] due to the defined position of the single in-chain functional group.[10]

Functionalization methods via living polymerization techniques often require sophisticated synthesis procedures. Recently, Quirk and co-workers introduced a DPE derivative bearing a SiH-group at the junction point as a general functionalization method.[11] The facile combination of oxy- and carbanionic polymerizable monomers can be achieved by using epoxide derivatives as capping reagents, due to the emerging hydroxyl group. To date this functionalization methodology provides an in-chain hydroxyl group leading to ABC miktoarm star polymers.[12]

Here, we present the first introduction of exactly one amino functionality at the interface of an amphiphilic block copolymer in a facile three step synthesis, starting with a microfluidic process in the first step. The benzyl protected amino group as well as a hydroxyl group were introduced by end capping “living” poly(styrene) with the specially designed epoxide (*N,N*-dibenzyl amino glycidol, DBAG)[13] as a termination agent. Polymerization of the second block (poly(ethylene oxide)) and deprotection of the amino group by hydrogenolysis resulted in the desired poly(styrene)-*block*-poly(ethylene oxide) copolymer (PS-*b*-PEO) bearing an amino

group at the block junction. As a proof of principle a fluorescent dye has been attached to the in-chain amine (Scheme 1).

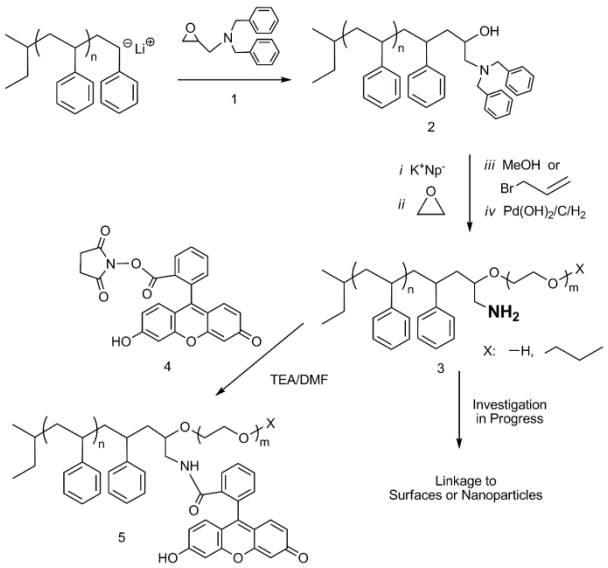

Scheme 1 Synthetic strategy for in-chain amino-functionalized, amphiphilic block copolymers (PS-(NH_2)-*b*-PEO).

Alkyllithium initiated poly(styrene) (PS) polymerization was terminated with a recently developed oxirane (DBAG, **1**)[13] in continuous flow. This microfluidic process was carried out in a microstructured reactor (Scheme S1) with an interdigital micromixer[14], providing fast and efficient mixing of the reagents, due to multilamination.[5] By altering flow rate ratios of monomer and initiator solution a series of chain-end functionalized polymers can be obtained rapidly during the ongoing reaction (see Table S1). Analogous reactions were carried out in classical batch reactors. The functionalization efficiency of all end functional polymers was verified by matrix-assisted laser desorption/ionization time-of-flight mass spectrometry (MALDI-ToF MS), a crucial characterization method for end group analysis. Fig. 1 presents the MALDI-ToF spectrum of polymer #1 (Table 1) with only one distribution mode, which can be assigned to DBAG-functionalized PS (**2**) with silver as a counterion (small sub-distribution: PS-DBAG·Li^+ at 1776 g mol^{-1}). This result confirms the previously reported high functionalization efficiency of termination reactions with epoxide derivatives and the addition of exactly one epoxide per polymer chain, which is due to the strong lithium–oxygen aggregation.[1, 4, 5]

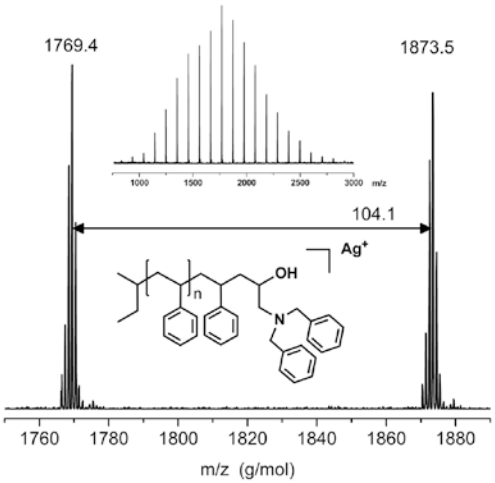

Fig. 1: MALDI-ToF spectrum of PS-DBAG (#1), cationizing agent: silver trifluoro acetate, matrix: dithranol.

Utilizing **1** as capping reagent provides a facile introduction of two orthogonal functionalities. After termination a hydroxyl group is available for subsequent reactions and a protected amino group can be released by hydrogenolysis. Conventional and continuously synthesized polymers in the range of 2–20 kg mol^{-1} with narrow molecular weight distributions (MWDs) were obtained and characterized by size exclusion chromatography (SEC), MALDI-ToF MS and NMR spectroscopy (#1–6, Table 1, see also SI). The MWDs of the polymers synthesized by the continuous end capping process are slightly broader compared to the classical batch reactor ($M_w/M_n \leq 1.20$). A faintly discontinuous flow from the HPLC pumps leading to temporary deviations from the adjusted stoichiometry might be an explanation. However, experimental time and effort are significantly reduced in the micro-flow system, providing a fast access to the end functionalized polymer and for a large variety of applications extremely narrow MWDs ($M_w/M_n \leq 1.05$) are not required.

The introduction of a hydroxyl group at the chain terminus allowed the utilization of PS-DBAG as a macroinitiator for the anionic ring opening polymerization of ethylene oxide to obtain an amphiphilic poly(styrene)-*block*-poly(ethylene oxide) copolymer with a protected amine moiety at the block junction. Characterization data of all block copolymers with PS/PEO ratios of 1–12 are shown in Table 1 (#8–15). Successful polymerization can be monitored by SEC. Fig. 2 shows the MWDs of precursors and block copolymers demonstrating a clearly visible shift of the molecular weight from 4.3 to 10.5 kg mol^{-1} (#7 and #13). To demonstrate an additional possibility of functionalization two block copolymers

were terminated with allyl bromide at the PEO block terminus (#11 and #12). This allyl function can be employed for further reactions, e.g., the covalent conjugation with Si–H or S–H-functionalized macro- or low molecular weight molecules resulting in novel architectures, which is subject of ongoing studies.

Table 1: Characterization data of PS-DBAG and in-chain functionalized PS-*b*-PEO prepared by anionic polymerization.

#	polymer[a]	M_n[b]	PDI[b]	PEO/PS[a]
1	PS_{20}-(DBAG)[c]	2200	1.19	-
2	PS_{45}-(DBAG)[c]	5000	1.18	-
3	PS_{122}-(DBAG)[c]	13000	1.12	-
4	PS_{199}-(DBAG)[c]	20000	1.19	-
5	PS_{21}-(DBAG)[d]	2400	1.06	-
6	PS_{26}-(DBAG)[d]	2700	1.06	-
7	PS_{40}-(DBAG)[d]	4300	1.06	-
8	PS_{21}-(DBAG)-*b*-PEO_{102}[e]	8100	1.07	2.0
9	PS_{40}-(DBAG)-*b*-PEO_{95}[e]	8800	1.07	1.0
10	PS_{21}-(DBAG)-*b*-PEO_{130}[e]	9600	1.06	2.6
11	PS_{26}-(DBAG)-*b*-PEO_{155}[f]	10500	1.08	2.5
12	PS_{40}-(DBAG)-*b*-PEO_{185}[f]	12800	1.09	1.9
13	PS_{40}-(DBAG)-*b*-PEO_{341}[e]	20700	1.07	3.7
14	PS_{20}-(DBAG)-*b*-PEO_{727}[e]	24000[g]	1.18[g]	6.4
15	PS_{33}-(DBAG)-*b*-PEO_{909}[e]	28400[g]	1.18[g]	12.1
16	PS_{21}-(NH_2)-*b*-PEO_{130}	8100	1.14	3.0
17	PS_{21}-(NH_2)-*b*-PEO_{102}	8100	1.17	2.4
18	PS_{40}-(NH_2)-*b*-PEO_{185}	13000	1.18	2.0
19	PS_{40}-(NH-Fl)-*b*-PEO_{185}	14700	1.09	2.0

[a]calculated by ^{1}H NMR, [b]molecular weight in g·mol^{-1} and MWD characterized by SEC in THF (PS-standard), [c]synthesized in microstructured reactor, [d]synthesized in conventional reactor, [e]terminated with methanol, [f]terminated with allyl bromide, [g]due to low solubility in THF characterized by SEC in $CHCl_3$ (PS-standard).

To obtain the in-chain amine functionality at the block junction, the benzyl protecting groups have to be released by hydrogenolysis. The reaction was catalyzed by palladium hydroxide on activated carbon ($Pd(OH)_2$/C) and carried out in a solvent mixture of THF/MeOH/H_2O.[13] The progress of the deprotection can be monitored by ^{13}C NMR spectroscopy. Disappearance of the methylene signals of the benzyl protective groups at 139.5 ppm confirms the quantitative deprotection of the amino group (Fig. S11). Table 1 summarizes the

characterization data of the in-chain amine-functionalized block copolymers (PS-(NH_2)-*b*-PEO, **3**). MWDs (#16-18) are slightly increased compared to the protected polymers, most probably due to additional interaction between the amino group and the SEC column material (Fig. S12).

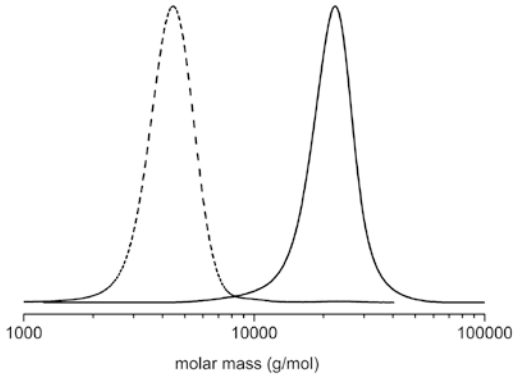

Fig. 2: SEC traces of precursor (PS-DBAG, #7, dashed line) and amphiphilic block copolymer (PS-DBAG-*b*-PEO, #13, solid line).

The access to novel in-chain amine-functionalized block copolymers is important for a large variety of applications (e.g. tailoring of surface properties or the synthesis of miktoarm star polymers). First studies to demonstrate the selective reactivity of the amino group were carried out by attaching a fluorescent dye to the block interface. The activated *N*-hydroxy-succinimide ester of fluorescein (NHS-Fl, **4**) as an active compound for reactions with amino functions was synthesized by DCC coupling according to literature.[15] The coupling of polymer #12 with end capped hydroxyl function and NHS-Fl was carried out under basic conditions in DMF. After purification of the fluorescein-labeled block copolymer (PS-(NH-Fl)-*b*-PEO, **5**) SEC measurements revealed a decreased polydispersity compared to PS-(NH_2)-*b*-PEO (Fig. S12) and a strong UV signal at an absorption wavelength of 500 nm, evidencing the successful fluorescein linkage (Fig. S13). In addition, fluorescence spectra of the fluorescein-NHS ester, PS-(NH-Fl)-*b*-PEO and a mixture of PS-(DBAG)-*b*-PEO and the active ester were recorded in ethanol (each $2 \cdot 10^{-4}$ M). The spectra of the mixture (536 nm) and the active ester (535 nm) exhibit similar fluorescence maxima, whereas in the case of the dye-labeled block copolymer the maximum shows a significant blue shift (519 nm). This shift results from the decreasing polarity in the direct environment of the dye due to the attached block copolymer (Fig. 3).[16]

This efficient implementation of a fluorescent dye to the junction of an amphiphilic block copolymer demonstrates the high potential of the central amine for a large variety of coupling reactions. Detailed work in this area is currently in progress.

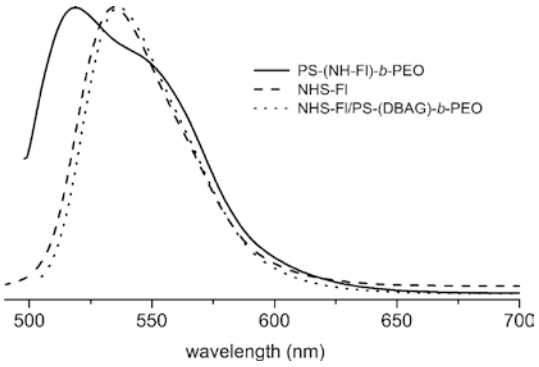

Fig. 3: Fluorescence spectra of PS-(NH-Fl)-*b*-PEO (#19, solid line), NHS-Fl (dashed line) and a mixture of PS-DBAG-*b*-PEO (#12) and NHS-Fl (dotted line) with λ_{ex} = 490, 511 and 512 nm respectively in ethanol medium ($2 \cdot 10^{-4}$ M).

Using a micromixer-based system we have developed a semicontinuous process for in-chain functionalized PS-*b*-PEO amphiphilic block copolymers, capitalizing on the rapid capping reaction of epoxide derivatives. The continuous, quantitative functionalization of living PS with a special designed epoxide (DBAG) afforded a macroinitiator for the oxyanionic polymerization of ethylene oxide. The resulting amphiphilic block copolymer bears exactly one protected amine functionality at the block junction, which was released by hydrogenolysis. The reactivity of the amine was investigated by addressing an active fluorescein ester (NHS-Fl). This successful coupling demonstrates the intriguing potential of such materials for the generation of switchable, smart surfaces. In addition, the polymers can be specifically adjusted on surface areas of nanoparticles to enhance their surface properties, which are subject of future research.

Acknowledgment

We thank MPGC (Max Planck Graduate Center with Johannes Gutenberg-University) and the Excellence Initiative (DFG/GSC 266) for fellowships and financial support (C.T and C.M). B.O. thanks the Fond der Chemischen Industrie (FCI) for a fellowship.

Supporting Information

Experimental Section

Reagents

All solvents and reagents were purchased from Acros Organics or Sigma Aldrich and used as received unless otherwise stated. Chloroform-d_1 was purchased from Deutero GmbH. Tetrahydrofuran (THF) was distilled from sodium/benzophenone under reduced pressure (cryo-transfer). Styrene was dried over calcium hydride (CaH_2) and cryo-transferred prior to use. Cyclohexane was cryo-transferred from *n*-buthyllithium/DPE. *sec*-Butyllithium (*sec*-BuLi, 1,3 M, Acros) was used as received and the concentration of the initiator was determined by the Gilman double titration method.[17] *N,N*-Dibenzyl amino glycidol (DBAG) was synthesized as reported previously.[13]

Instrumentation

^{1}H NMR spectra were recorded at 300 MHz or 400 MHz on a Bruker AC300 or Bruker AMX 400 respectively and were referenced internally to residual proton signals of the deuterated solvent. Size exclusion chromatography (SEC) measurements were carried out in THF or $CHCl_3$ on an instrument consisting of a Waters 717 plus auto sampler, a TSP Spectra Series P 100 pump, a set of three PSS SDV columns (104/500/50 Å), RI- and UV-detectors (absorption wavelength: 254 nm or 500 nm). All SEC diagrams show the RI detector signal unless otherwise stated, and the molecular weight refer to linear poly(styrene) (PS) standards provided by Polymer Standards Service (PSS). Matrix-assisted laser desorption/ionization time-of-flight (MALDI-ToF) measurements were performed on a Shimadzu Axima CFR MALDI-TOF mass spectrometer using silver trifluoroacetate as cationizing agent and dithranol (1,8,9-trishydroxy-anthracene) as a matrix. UV/vis spectroscopy was measured on a JASCO V-630 UV-VIS spectrophotometer and fluorescence was accomplished on a JASCO PL 6200 spectrofluorometer.

Microstructured Reactor

A continuous flow reaction setup (Scheme S1) equipped with a micromixer was employed for the synthesis of DBAG-functionalized poly(styrene) as reported previously.[5,18] A stainless steel high pressure slit interdigital micromixer (HP-IMM, provided by the Institut für Mikrotechnik Mainz (IMM)) with an internal volume of 15 µL was used for fast and efficient mixing of monomer and initiator realized by multilamination mixing mode, combined with geometric and hydrodynamic focusing.[19] The micromixer was immersed in a tempered water bath (room temperature) and equipped with two reactant inlets and one outlet. After mixing of monomer and initiator (within several milliseconds), the reaction mixture passed a short stainless steel capillary residence tube and was combined with DBAG (separate flow tube) in a T-mixer (ø = 700 µm). The residence tube behind the T-mixer was connected to a degassed vessel for sample collection. Flow rates were controlled via HPLC pumps (Knauer WellChrom K-501, inert 10 mL pump heads with ceramic inlays).

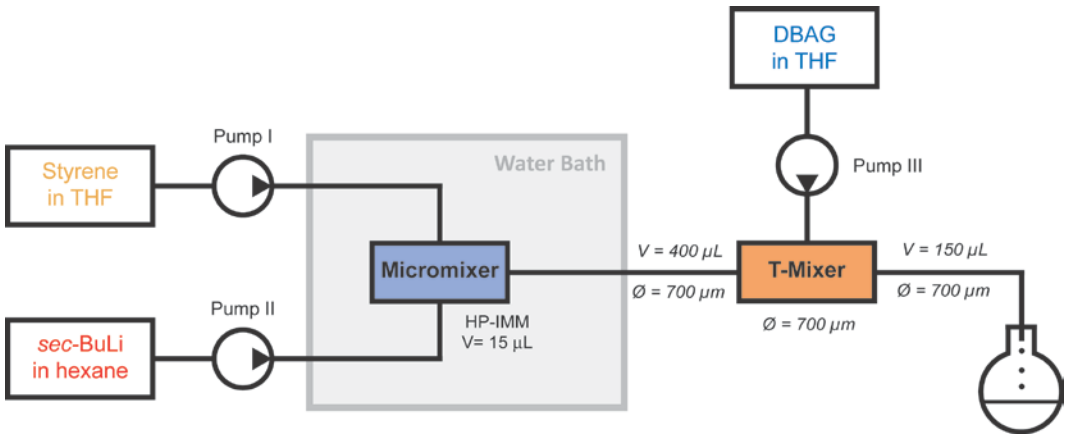

Scheme S1: Schematic reactor setup continuous polymerization-termination processes. Monomer: styrene; initiator: *sec*-BuLi; capping reagent: DBAG; micromixer: HP-IMM.

Continuous Synthesis of PS-DBAG

Exemplary synthesis procedure for PS_{33}-(DBAG) (#S2, Table S1): Prior to the polymerization reaction, THF was pumped through the microstructured reactor setup (Scheme S1) for 10 min with a flow rate of 0.5 mL·min^{-1} at each HPLC pump to rinse off residual impurities. A

solution of purified styrene (1.47 M) in dry THF was kept under argon in a flask covered with a septum. Into a second flask equipped with dry hexane, 4.0 mL *sec*-BuLi was added via syringe directly before starting the reaction (0.05 M). The third flask contained a solution of purified DBAG in THF (0.1 M). The three flasks were connected to the HPLC pumps via PTFE tubes transfixed through the septa. To eliminate residual impurities prior to the polymerization start, pump II was activated and the assembly was flushed with the *sec*-BuLi solution. In order to initiate the continuous process, pumps I (monomer) and II (initiator) were activated each with flow rates of 1 mL·min^{-1}. After the characteristic reddish color appeared at the outlet, pump III was activated with a flow rate of 1 mL·min^{-1} to combine the DBAG-solution and the living poly(styrene) within the T-mixer. Full monomer conversion was achieved after 12 s, and the end-capped polymer was recovered from a short outlet tube connected to the T-junction. PS_{33}-DBAG was precipitated several times in methanol to remove residual DBAG. The final product was dried in vacuum at room temperature for 12 h. All polymer samples (Table S1) prepared by the continuous end capping process have been produced by an analogous procedure. Adjusting the flow rate via the control elements of the HPLC pumps or using different concentrations permits convenient variation of molecular weight. ^{1}H NMR (400 MHz, $CDCl_3$, δ in ppm): 7.50-6.18 (PS aromatic), 3.66 (m, 2H, C*H*$_2$-Ph), 3.48-3.20 (m, 3H, C*H*$_2$-Ph, C*H*-OH), 2.6-0.80 (PS backbone), 0.79-0.50 (m, 6H, (C*H*$_3$-CH$_2$-CH-C*H*$_3$)). ^{13}C NMR (100 MHz, $CDCl_3$, δ in ppm): 145.5 (PS aromatic.), 138.46 (aromatic Carbon subst. protecting group), 128.0 (PS aromatic), 125.6 (PS aromatic), 64.6 (*C*H-OH), 60.2-58.9 (*C*H$_2$-NR$_2$), 58.2 (N-(*C*H$_2$)$_2$), 47.1-41.0 (*C*H$_2$ backbone), 40.3 (*C*H backbone), 31.5 (CH$_3$-*C*H), 29.9 (CH$_3$-*C*H), 18.5 (*C*H$_3$), 11.2 (*C*H$_3$).

Conventional Procedure for PS-DBAG

Vacuum-distilled styrene (5 g, 48 mmol) was dissolved in dry cyclohexane (30 mL), cooled to 0 °C and the polymerization was initiated with the corresponding amount of *sec*-BuLi (1.3 M, 1.28 mL). The red-colored reaction mixture was stirred for 20 h at 40 °C. After a small amount of THF (~1-2 mL) was cryo-transferred to the reaction mixture, DBAG (2 eq.) was introduced via syringe to terminate the polymerization and the dark red color disappeared immediately. The solution was stirred for further 20 h and precipitated several times into MeOH to obtain 5 g (90%) PS-DBAG (**2**). ^{1}H NMR (400 MHz, $CDCl_3$, δ in ppm): 7.50-6.18 (PS

aromatic), 7.32 (m, 4H, meta- of protective benzyl groups), 3.66 (m, 2H, C*H*$_2$-Ph), 3.48-3.20 (m, 3H, C*H*$_2$-Ph, C*H*-OH), 2.6-0.80 (PS backbone), 0.79-0.50 (m, 6H, (C*H*$_3$-CH$_2$-CH-C*H*$_3$)). ^{13}C NMR (100 MHz, $CDCl_3$, δ in ppm): 145.5 (PS aromatic.), 138.5 (aromatic, protecting group), 129.0-125.0 (PS aromatic), 64.6 (*C*H-OH), 60.2-58.9 (*C*H$_2$-NR$_2$), 58.2 (N-(*C*H$_2$)$_2$), 47.1-41.0 (*C*H$_2$ backbone), 40.3 (*C*H backbone), 31.5 (CH$_3$-*C*H), 29.9 (CH$_3$-*C*H), 18.5 (*C*H$_3$), 11.2 (*C*H$_3$).

Table S1: Characterization data of PS-DBAG samples synthesized in continuous flow.

#	polymer[a]	M_n[b]	PDI[b]
1[c]	PS_{20}-(DBAG)	2200	1.19
2[c]	PS_{45}-(DBAG)	5000	1.18
3[c]	PS_{122}-(DBAG)	13000	1.12
4[c]	PS_{199}-(DBAG)	20000	1.19
S1	PS_{27}-(DBAG)	3100	1.25
S2	PS_{33}-(DBAG)	3700	1.19
S3	PS_{34}-(DBAG)	3700	1.17
S4	PS_{37}-(DBAG)	3800	1.15
S5	PS_{52}-(DBAG)	5900	1.15
S6	PS_{68}-(DBAG)	7500	1.15
S7	PS_{74}-(DBAG)	8200	1.14

[a]calculated by ^{1}H NMR, [b]molecular weight in g mol^{-1} and MWD characterized by SEC in THF (PS-Standard), [c]already listed in the main publication (Table 1).

Synthesis of PS-(DBAG)-*b*-PEO

500 mg PS-DBAG (#6) were dissolved in dry THF in a 100 mL Schlenk flask and titrated with potassium naphthalide (0.1 M) until a slight green color maintained. The monomer ethylene oxide (EO, 1 mL) was cryo-transferred into a graduated ampoule and subsequently into the reaction flask at approximately -80 °C. The greenish color disappeared rapidly. The reaction mixture was heated up to 60 °C and stirred for 24 h. The polymerization was terminated with either degassed methanol or freshly distilled allyl bromide (2 eq.) and precipitated in cold diethyl ether. Drying in vacuum at room temperature leads to 1.3 g PS-(DBAG)-*b*-PEO. Yield: 94%. ^{1}H NMR (400 MHz, $CDCl_3$, δ in ppm): 7.35-6.24 (PS aromatic), 7.22 (m, 4H, meta- of protective benzyl groups), 5.90[a] (m, 1H, CH$_2$-C*H*=CH$_2$), 5.26[a] (dq, 1H, CH=C*H*$_2$), 5.17[a] (dq, 1H, CH=C*H*$_2$), 4.02[a] (dt, 2H, C*H*$_2$-CH=CH$_2$), 3.86-3.38 (PEO backbone), 2.5-0.80 (PS backbone),

0.79-0.50 (m, 6H, (C*H*$_3$-CH$_2$-CH-C*H*$_3$)). ^{13}C NMR (100 MHz, $CDCl_3$, δ in ppm): 145.1 (PS aromatic.), 139.3 (aromatic, protecting group), 134.7[a] (CH$_2$-*C*H=CH$_2$), 128.7-125.5 (PS aromatic), 117.0[a] (CH=*C*H$_2$), 72.1 (*C*H-OH), 70.5 (PEO backbone), 69.3 (Core-PEO-*C*H$_2$) 61.1[b] (*C*H$_2$-OH) 59.5-59.1 (*C*H$_2$-NR$_2$), 59.0 (N-(*C*H$_2$)$_2$), 47.1-41.0 (PS-*C*H$_2$ backbone), 40.3 (PS-*C*H backbone).

[a]allyl bromide-terminated polymers, [b]methanol-terminated polymers.

Synthesis of PS-(NH$_2$)-*b*-PEO

Catalytic hydrogenolysis of PS-(DBAG)-*b*-PEO was carried out as described previously.[2] The polymer (500 mg) was dissolved in a solvent mixture of 40 mL of THF, 20 mL of MeOH and 20 mL of H_2O (2:1:1) and 100 mg palladium hydroxide (10-20 wt%) on activated carbon ($Pd(OH)_2$/C) were added. The reaction mixture was stirred for 5 days at 40 bar H_2. After removal of the catalyst by filtration over Celite and removal of solvent under reduced pressure PS-(NH$_2$)-*b*-PEO was obtained. Strong adhesion of the amphiphilic block copolymer as well as the amino function to $Pd(OH)_2$/C resulted in yields of 50-70%. ^{1}H NMR (400 MHz, $CDCl_3$, δ in ppm): 7.35-6.24 (PS aromatic), 4.05-3.29 (PEO backbone), 2.5-0.80 (PS backbone), 0.79-0.50 (m, 6H, (C*H*$_3$-CH$_2$-CH-C*H*$_3$)). ^{13}C NMR (100 MHz, $CDCl_3$ δ in ppm): 145.3 (PS aromatic), 128.9-125.5 (PS aromatic), 73.0 (*C*H-CH$_2$-NH$_2$), 70.5 (PEO backbone), 49.8 (*C*H$_2$-NH$_2$), 47.1-41.0 (PS-*C*H$_2$ backbone), 40.2 (PS-*C*H backbone).

Synthesis of NHS-Fl

2-(6-Hydroxy-3-oxo-3*H*-xanthen-9-yl)-benzoic acid 2,5-dioxo-pyrrolidin-1-yl ester (*N*-hydroxysuccinimide ester of fluorescein) was synthesized as reported previously.[15] The reduced DMF solution was purified by flash chromatography using first petroleum ether/ethyl acetate (20:80) and then MeOH/$CHCl_3$(30:70). ^{1}H NMR (300 MHz, DMSO-d_6, δ in ppm): 8.35 (d, 1H), 8.08-7.84 (m, 2H), 7.67 (d, 1H), 6.78 (d, 2H), 6.67-6.44 (m, 4H), 2.72 (s, 4H).

Synthesis PS-(NH-Fl)-b-PEO

50 mg ($4 \cdot 10^{-3}$ mmol) PS-(NH_2)-*b*-PEO was dissolved in 5 mL of DMF. 2.6 mg ($6 \cdot 10^{-3}$ mmol, 1.5 eq.) NHS-Fl and triethylamine (TEA) were added and the reddish reaction mixture was stirred for 24 h. The reaction was neutralized with acetic acid and purified by preparative chromatography (solvent: $CHCl_3$). Yield: 30 mg (58%). ^{1}H NMR (300 MHz, DMSO-d_6, δ in ppm): 7.44-6.29 (PS aromatic), 4.05-3.23 (PEO backbone), 2.5-0.77 (PS backbone), 0.79-0.5 (m, 6H, (CH_3-CH_2-CH-CH_3)).

UV/vis and Fluorescence Spectroscopy

The investigation of PS-(NH-Fl)-*b*-PEO (#19), NHS-Fl and a mixture of NHS-Fl and PS-(DBAG)-*b*-PEO (#12) was started with the measurement of absorption spectra to indentify the maximum transition wavelength of each sample (Table S2). This wavelength was adjusted as excitation wavelength for fluorescence measurements. All samples were measured in ethanol solution ($2 \cdot 10^{-4}$ M) and Table S2 presents absorption as well as fluorescence maxima.

Table S2: Maxima of absorption and fluorescence measurements.

sample	λ_{abs} [a]	λ_{fl} [b]
NHS-Fl	511	535
PS-(NH-Fl)-*b*-PEO	490	519
PS-(DBAG)-*b*-PEO /NHS-Fl	512	536

[a]maximum of absorption spectrum in nm, [b]maximum of fluorescence spectrum in nm.

Additional Characterization Spectra:

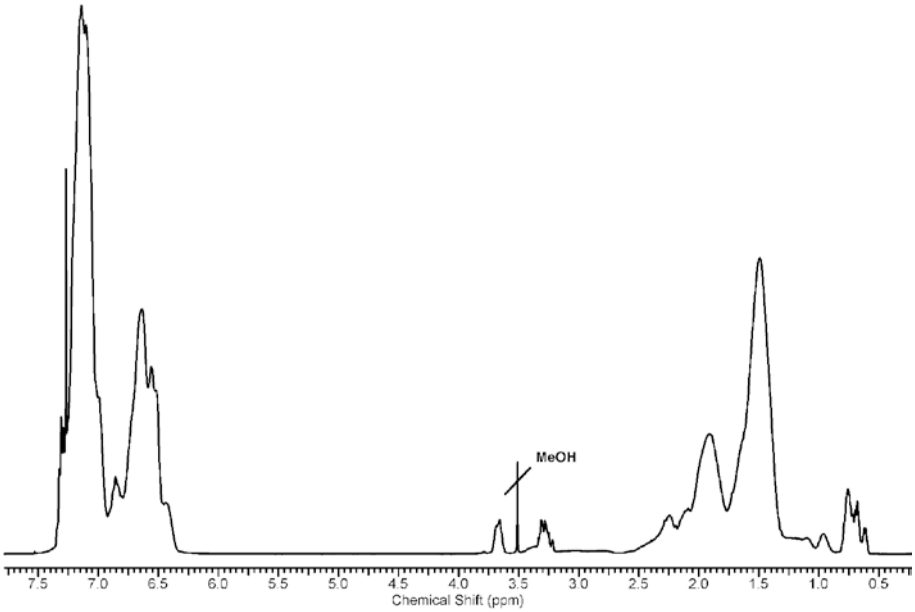

Fig. S1. ^{1}H NMR spectrum of PS-DBAG (#6)

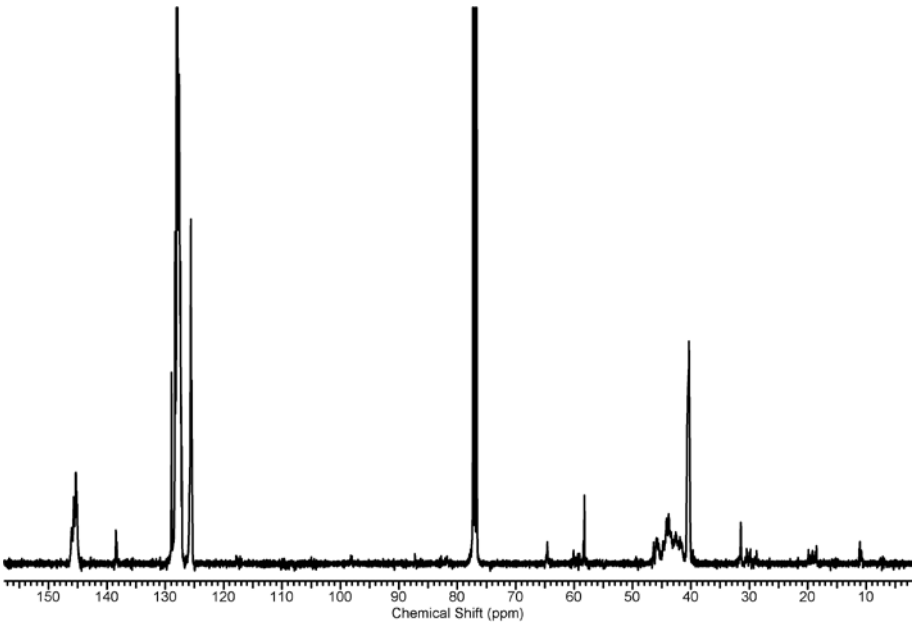

Fig. S2. ^{13}C NMR spectrum of PS-DBAG (#6)

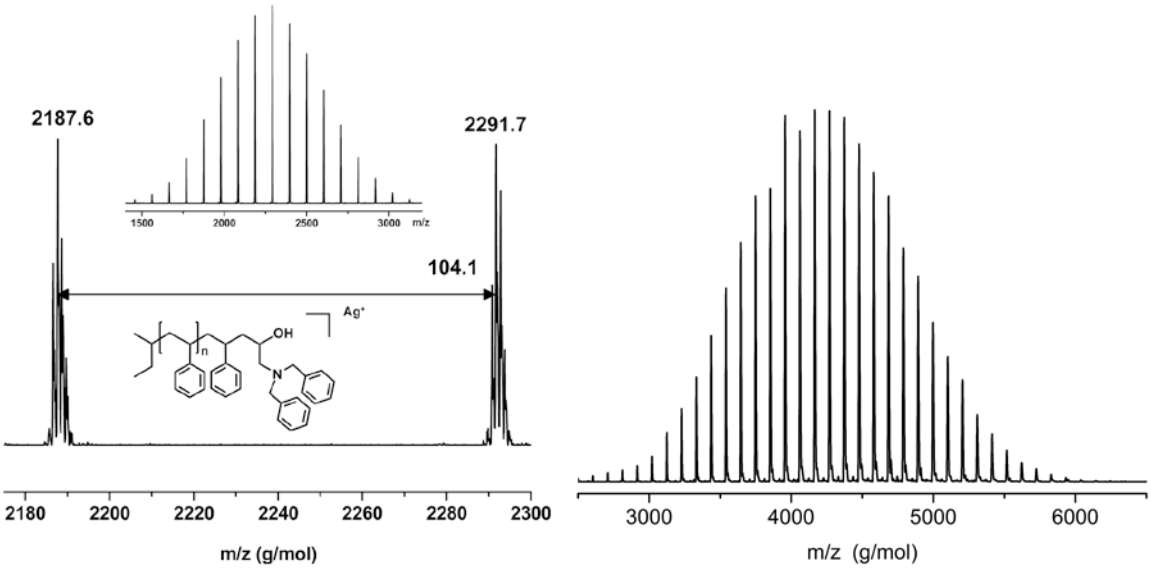

Fig. S3. MALDI-ToF spectra of PS-DBAG synthesized via conventional procedure. Left spectra: #5 with enlarged region, right spectra: #7. Cationizing agent: silver trifluoro acetate, matrix: dithranol.

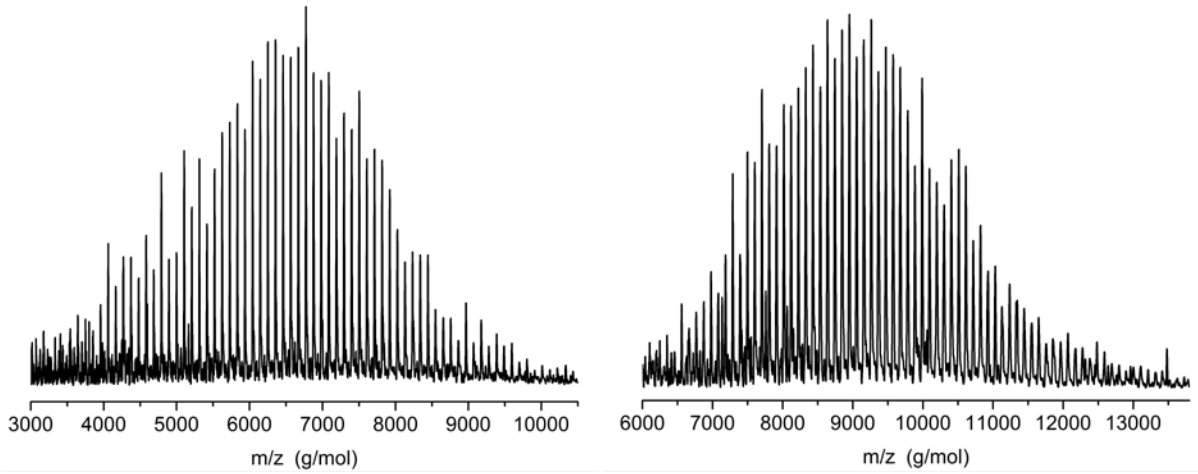

Fig. S4. MALDI-ToF spectra of PS-DBAG synthesized in continuous flow. Left spectra: #S6 in Table S1, right spectra: #3. Cationizing agent: silver trifluoro acetate, matrix: dithranol.

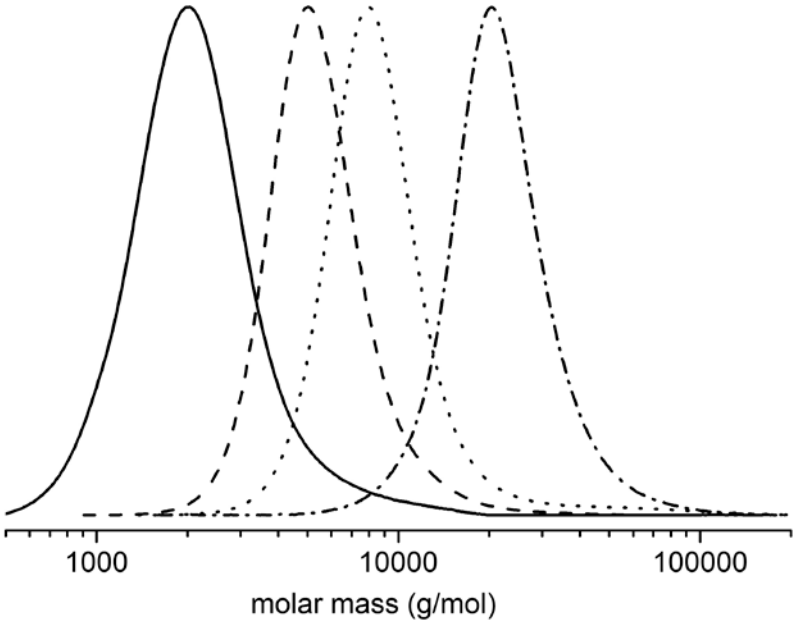

Fig. S5. SEC traces of PS-DBAG (continuous procedure): #1 (solid line), #2 (dashed line), #S6 (dotted line) and #4 (dashed/dotted line).

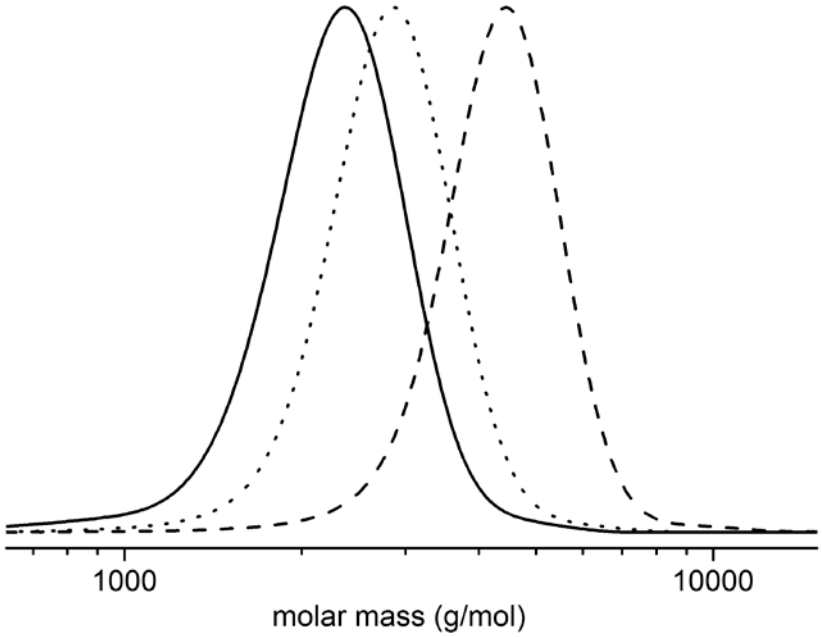

Fig. S6. SEC traces of PS-DBAG (conventional procedure): #5 (solid line), #6 (dotted line), #7 (dashed line).

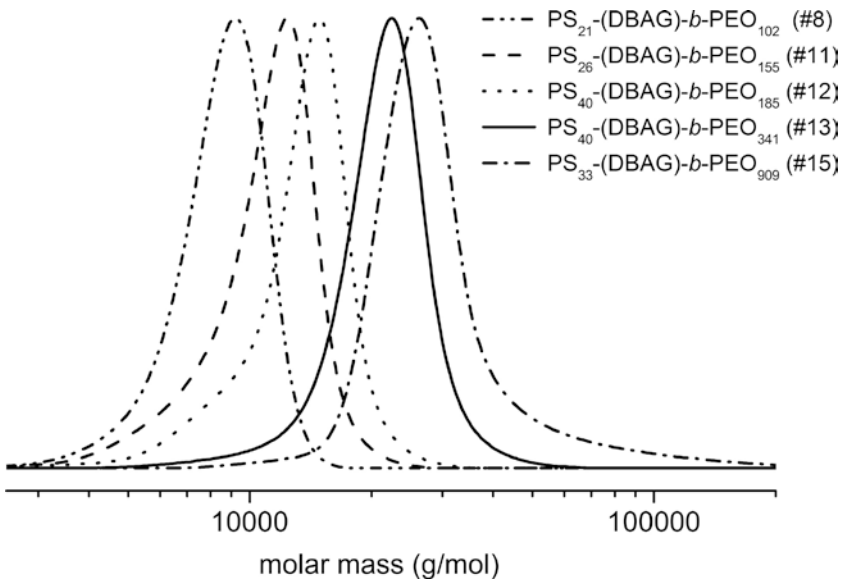

Fig. S7. SEC traces of PS-(DBAG)-*b*-PEO.

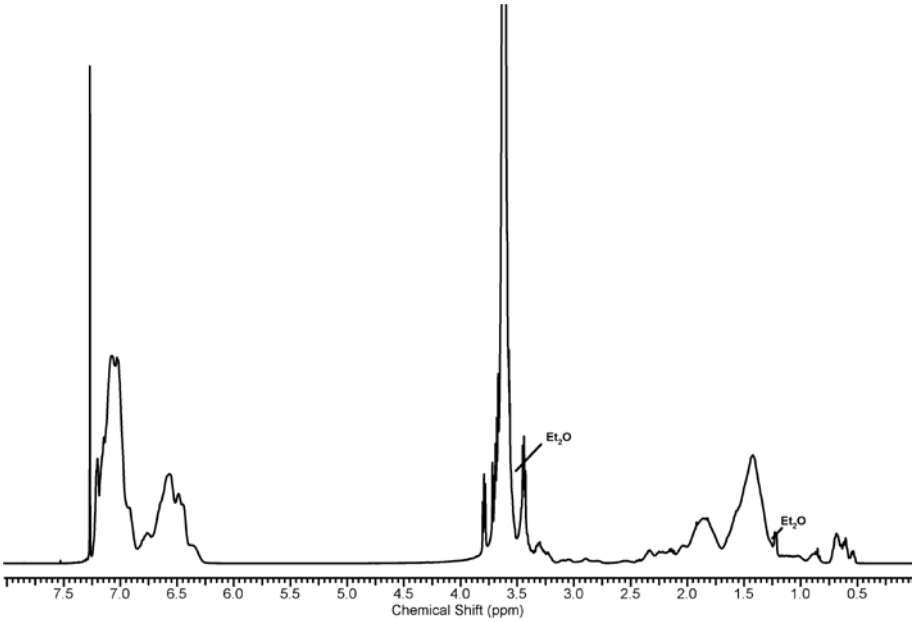

Fig. S8. ^{1}H NMR spectrum of PS-DBAG-*b*-PEO (#10).

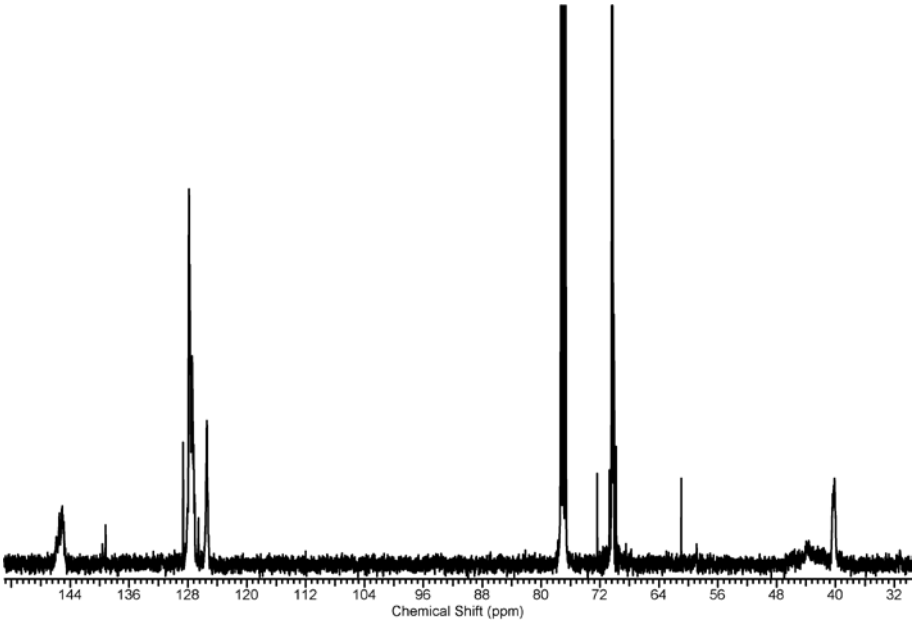

Fig. S9. ^{13}C NMR spectrum of PS-DBAG-*b*-PEO (#10).

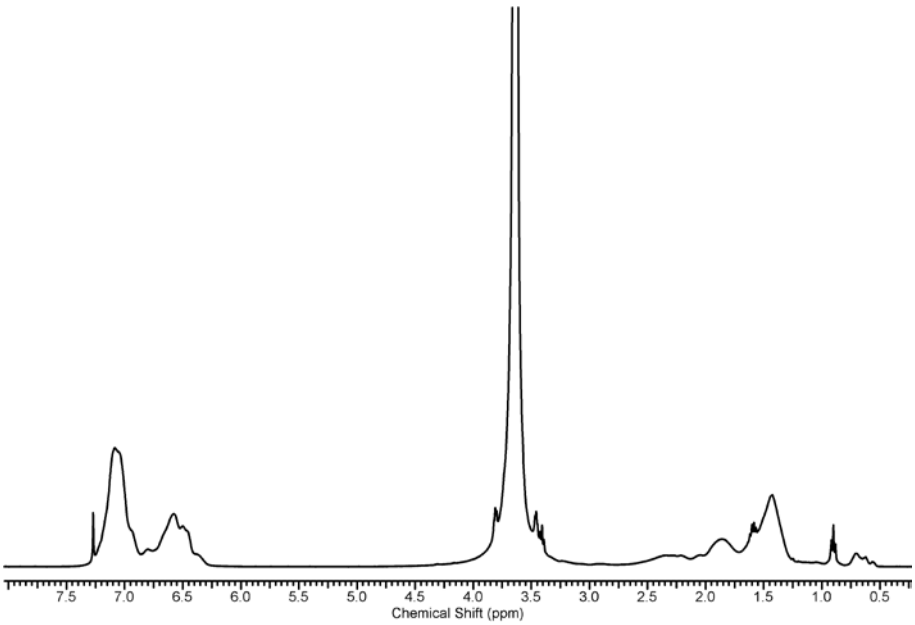

Fig. S10. ^{1}H NMR spectrum of PS-(NH_2)-*b*-PEO (#17).

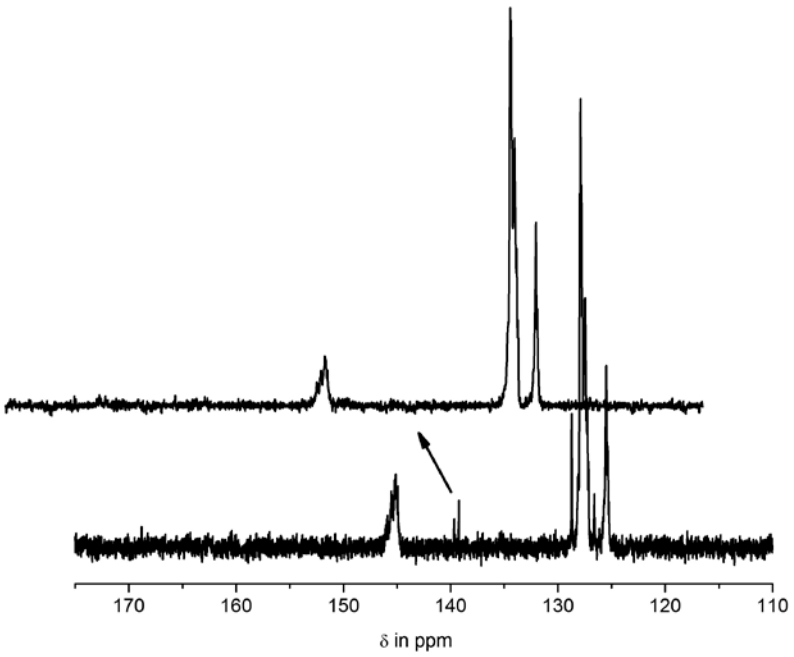

Fig. S11. ^{13}C NMR spectrum of PS-(DBAG)-*b*-PEO (#14, bottom) and PS-(NH_2)-*b*-PEO (#17, top).

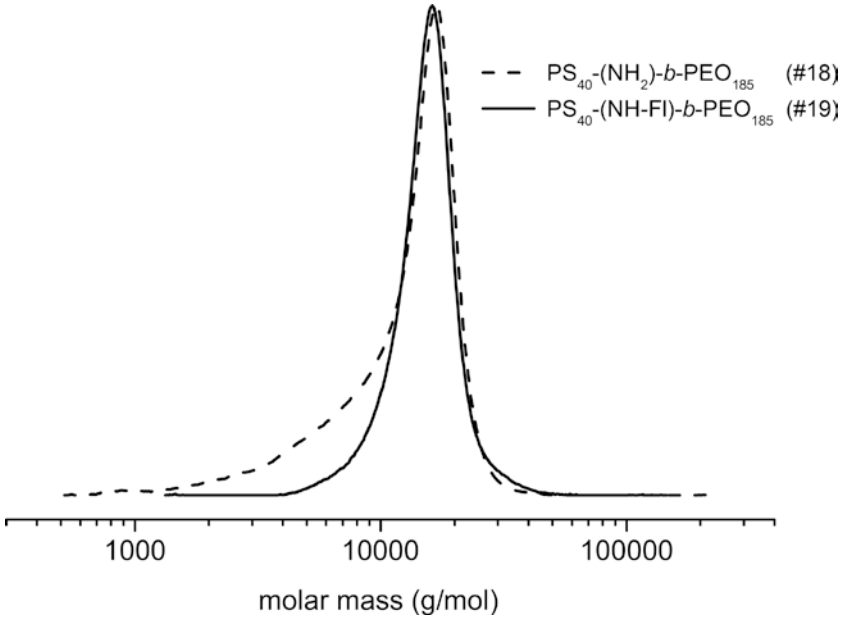

Fig. S12. SEC traces of PS-(NH_2)-*b*-PEO (#18, dashed line) and PS-(NH-Fl)-*b*-PEO (#19, solid line). The polydispersity of #19 is decreased compared to #18, which might be due to lower interaction between the column material and the fluorescent dye in comparison with the amino functionality.

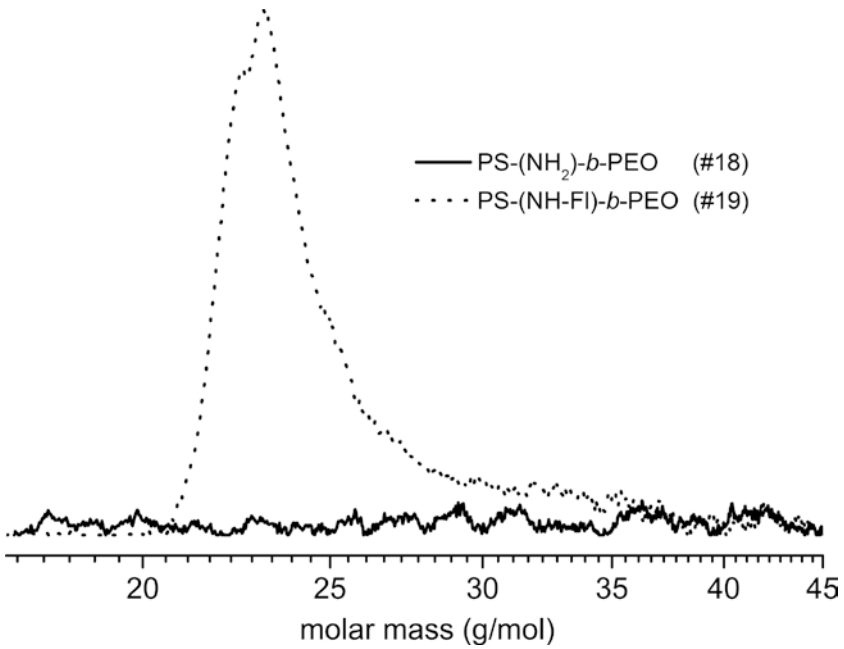

Fig. S13. SEC traces of PS-(NH_2)-*b*-PEO (#18, solid line) and PS-(NH-Fl)-*b*-PEO (#19, dotted line) with UV-signals at an absorption wavelength of 500 nm. The difference in signal strength (#19 strong signal, #18 no signal observable) indicating the successful incorporation of fluorescein at the block copolymer.

References

1 R. P. Quirk and H. L. Hsieh, *Anionic Polymerization: Principles And Practical Applications*, Marcel Dekker Inc, New York, 1996.

2 (a) R. P. Quirk, T. Yoo, Y. Lee, J. Kim and B. Lee, in *Advances in Polymer Science*, Springer Verlag, Berlin, 2000, vol. 153, pp. 67–162; (b) A. Hirao, M. Hayashi and N. Haraguchi, Macromol. *Rapid* Commun., 2000, **21**, 1171–1184.

3 M. A. Peters, A. M. Belu, R. W. Linton, L. Dupray, T. J. Meyer and J. M. DeSimone, J. Am. Chem. Soc., 1995, **117**, 3380–3388.

4 C. Tonhauser and H. Frey, Macromol. *Rapid* Commun., 2010, **31**, 1938–1947.

5 C. Tonhauser, D. Wilms, F. Wurm, E. Berger-Nicoletti, M. Maskos, H. Löwe and H. Frey, *Macromolecules*, 2010, **43**, 5582–5588.

6 (a) A. Hirao, M. Hayashi, S. Loykulnant, K. Sugiyama, S. W. Ryu, N. Haraguchi, A. Matsuo and T. Higashihara, Prog. Polym. Sci., 2005, **30**, 111–182; (b) N. Hadjichristidis, M. Pitsikalis, S. Pispas and H. Iatrou, Chem. Rev., 2001, **101**, 3747–3792.

7 (a) N. Hadjichristidis, J. Polym. Sci., *Part A:* Polym. Chem., 1999, **37**, 857–871; (b) A. Abouelmagd, K. Sugiyama and A. Hirao, *Macromolecules*, 2011, **44**, 826–834.

8 S. Perny, J. Allgaier, D. Cho, W. Lee and T. Chang, *Macromolecules*, 2001, **34**, 5408–5415.

9 (a) X. Wang, Y. Zhang, Z. Zhu and S. Liu, Macromol. *Rapid* Commun., 2008, **29**, 340–346; (b) J. Yang, X. Lou, J. G. Spiro and M. A. Winnik, *Macromolecules*, 2006, **39**, 2405–2412; (c) J. T. Goldbach, T. P. Russell and J. Penelle, *Macromolecules*, 2002, **35**, 4271–4276; (d) C. Cheng and N.-L. Yang, *Macromolecules*, 2010, **43**, 3153–3155.

10 T. Haliloglu, R. Balaji and W. L. Mattice, *Macromolecules*, 1994, **27**, 1473–1476.

11 W.-B. Zhang, B. Sun, H. Li, X. Ren, J. Janoski, S. Sahoo, D. E. Dabney, C. Wesdemiotis, R. P. Quirk and S. Z. D. Cheng, *Macromolecules*, 2009, **42**, 7258–7262.

12 N. Saito, C. Liu, T. P. Lodge and M. A. Hillmyer, *Macromolecules*, 2008, **41**, 8815–8822.

13 B. Obermeier, F. Wurm and H. Frey, *Macromolecules*, 2010, **43**, 2244–2251.

14 P*rovided by the Institut für Mikrotechnik, Mainz (http://www.imm-mainz.de/)*.

15 J. Gao, P. Wang and R. W. Giese, Anal. Chem., 2002, **74**, 6397–6401.

16 L. Wang, Y. Shao, J. Zhang and M. Anpo, Opt. Mater., 2006, **28**, 1232–1234.

17 H. Gilman and A. H. Haubein, *Journal of the American Chemical Society*, 1944, **66**, 1515-1516.

18 F. Wurm, D. Wilms, J. Klos, H. Löwe and H. Frey, *Macromolecular Chemistry and Physics*, 2008, **209**, 1106-1114.

19 V. Hessel, S. Hardt, H. Löwe and F. Schönfeld, *AIChE Journal*, 2003, **49**, 566-577.

3.2: Water-Soluble Poly(vinyl ferrocene)-b-Poly(ethylene oxide) Diblock and Miktoarm Star Polymers

Christoph Tonhauser,[1] *Markus Mazurowski,*[2] *Matthias Rehahn,*[2] *Markus Gallei**[2] and *Holger Frey**[1]

[1]*Institute of Organic Chemistry, Organic and Macromolecular Chemistry, Duesbergweg 10-14 Johannes Gutenberg-University (JGU), D-55099 Mainz, Germany*

[2]*Ernst-Berl Institute for Chemical Engineering and Macromolecular Science, Darmstadt University of Technology, Petersenstraße 22, D-64287 Darmstadt, Germany*

Published in *Macromolecules* ***2012***, *45, 3409-3418*

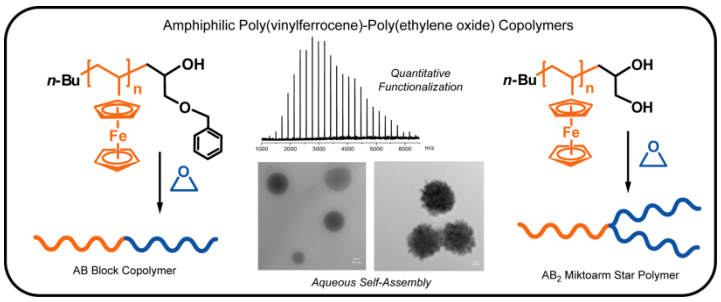

Keywords: polyvinylferrocene, anionic polymerization, epoxide termination, miktoarm star polymers, metal-containing polymers

Abstract

We describe the synthesis of water-soluble diblock and miktoarm star polymers consisting of poly(vinylferrocene) (PVFc) and poly(ethylene oxide) (PEO) blocks. First, end-functionalized poly(vinylferrocene) was generated by end-capping the living carbanionic PVFc chains with benzyl glycidyl ether (BGE) or ethoxy ethyl glycidyl ether (EEGE). Acidic hydrolysis of the EEGE-terminated PVFc partially oxidized the PVFc backbone. However, the dihydroxyl end-functional PVFc was obtained in quantitative yields by hydrogenolysis of the BGE-terminated PVFc. A series of block copolymers and AB_2 miktoarm star copolymers was obtained in a

second polymerization step, utilizing the respective end-functionalized PVFc as a macroinitiator for the ring-opening polymerization (ROP) of ethylene oxide. All polymers were analyzed in detail, using NMR spectroscopy and size-exclusion chromatography (SEC). Online SEC-viscosimetry as well as MALLS was carried out, confirming the formation of miktoarm structures. Quantitative functionalization and subsequent removal of the acetal and benzyl protective groups, respectively were confirmed by MALDI–ToF mass spectrometry. Molecular weights of the end-functionalized PVFcs range between 1000 and 3600 g mol^{-1}, and block copolymers with 10 000 to 50 000 g mol^{-1} overall molar masses were synthesized. In addition, the water-soluble block copolymers were investigated by differential scanning calorimetry (DSC) and thermogravimetric analysis (TGA). For characterization of the morphology in aqueous solution, transmission electron microscopy (TEM) was performed, showing micelles and multicompartment micellar structures.

Introduction

Ferrocene-containing polymers offer a promising combination of different characteristic features such as redox, catalytic, mechanical, semiconductive, photophysical, optoelectronic, and magnetic properties.[1-7] Furthermore, these polymers demonstrate high potential for applications in fields like amperometric glucose/L-glutamate sensors, as demonstrated by Hale et al., who attached a ferrocene unit to a flexible polysiloxane backbone. The resulting polymer can be utilized as an efficient electron-transfer relay system (glucose oxidase/electrode) to improve the sensor response time.[8] Biosensors containing the ferrocene/ferrocenium redox couple and a carbon electrode are highly explored.[9-14] Moreover, ferrocene-containing materials show promise for various biomedical application[15], e.g., as antimalarial-[16] or anticancer-active drugs.[17-20]

The first synthesis of polymers containing ferrocene units dates back to the 1950s and was based on radical and step growth polymerization techniques. However, at this time no single material with well-defined structure and high molecular weight could be obtained, due to side reactions, low solubility, and insufficient chemical stability of the formed products.[21-26] This limitation was overcome by the seminal discovery of the controlled living ring-opening polymerization (ROP) of *ansa*-metallocenophanes by Manners and co-workers,[27,28] which leads to high-molecular-weight poly(ferrocenylsilanes) (PFS). Manifold PFS-based (both, linear and hyperbranched) block copolymers, star polymers, and graft copolymers were developed utilizing this synthetic pathway.[29-34] These polymers exhibit various intriguing self-assembled nanostructures in bulk and solution (e.g., micelles, rods, and nanotubes).[34-39]

Other established ferrocene-based monomers are ferrocenylmethyl methacrylates (FMMA)[40-42] and vinylferrocene (VFc)[43-45], which possess a high stability toward thermal treatment and atmospheric exposure. The latter monomer (VFc) can be utilized to attach ferrocene units to a preformed polymer backbone.[46] First reports dealing with anionic polymerization of vinylferrocene were published by Nuyken et al. in the 1990s.[43] The authors not only synthesized PVFc homopolymes, but also described PVFc block copolymers (comonomers: methyl methacrylate, styrene, and propylene sulfide) with narrow molecular-weight distributions. Similar procedures were used by Durkee[47] and Higashihara[44] to synthesize PVFc-based block copolymers with poly(isoprene) and poly(isobutylene),

respectively. "Living" radical homo- and block copolymerization of VFc with styrene – mediated by TEMPO – was developed by our group.[48] Most of those block copolymers exhibit low-molecular-weight PVFc blocks only. In the case of controlled radical chain growth, side reactions prevent the formation of longer PVFc blocks, while for living anionic approaches this is due to tremendously decreasing reactivity of the living chains with increasing chain length.[44] Recently, however, we could demonstrate that reactivation of the "sleeping" state formed by the anionic chain termini can be achieved by adding a mixture of 1,1-dimethylsilacyclobutane (DMSB) and 1,1-diphenylethylene (DPE) (activating agent and end-capping reagent, respectively), yielding well-defined block copolymers.[45, 49] This method is known as the so-called "carbanion pump" technique.[50, 51] The synthetic strategy provides access to a large variety of well-defined block copolymers in a broad range of molecular weights.

Despite all recent progress in this field, well-defined amphiphilic or water-soluble ferrocene-based block copolymers have hardly been reported in literature.[52, 53] Manners and coworkers developed two synthetic routes to PFS-*b*-poly(ethylene oxide) (PFS-*b*-PEO) block copolymers. In a first approach, SiH-functionalized PEO was utilized as a macroinitiator for the transition metal-catalyzed ROP of dimethylsila[1]-ferrocenophanes[54] and second two homopolymers (PEO, PFS) were combined with a bis(terpyridine)ruthenium(II) complex.[55] The former strategy reveals spherical structures, whereas the latter leads to intriguing rod-like micelles in aqueous media, due to deviating crystallization behavior of the two organometallic block copolymers.

The established route for amphiphilic block copolymers with a PEO-block (combination of oxy- and carbanionic polymerization) relies on the termination of living carbanionic polymers with ethylene oxide.[56, 57] By utilizing epoxide derivatives as capping reagents, a wide variety of end-functionalized polymers can be obtained, either with a single hydroxyl group or multiple orthogonal functionalities.[58-60] Subsequently, the terminal functionalities can be used to initiate the synthesis of well-defined polymer architectures (e.g., in-chain functionalized block copolymers,[61, 62] star polymers,[63, 64] or hyperbranched polymers[65]). To the best of our knowledge, epoxide termination has not been used for PVFc to obtain end-functional polymers to date. Therefore, the initial goal of this work was to develop a strategy for the combination of PVFc and PEO by sequential monomer addition (oxy- and carbanionic

polymerization). A facile approach to amphiphilic metal-containing block copolymers without suffering from the redox-lability of VFc was the foremost objective of this work.

In this contribution, we describe a powerful and versatile synthetic strategy to novel amphiphilic organometallic macromolecular architectures containing PVFc blocks (Scheme 1). PEO was employed as the polar component in this initial study.[66] In the first step of the reaction sequence "living" poly(vinylferrocene) anions were end-capped with benzyl glycidyl ether (BGE) to obtain one hydroxyl group and one benzyl-protected hydroxyl group at the chain termini (PVFc-BGE, **1**). The terminal hydroxyl group was then utilized to initiate anionic ring-opening polymerization (AROP) of ethylene oxide, affording a series of poly(vinylferrocene)-*block*-poly(ethylene oxide) copolymers (PVFc-BGE-PEO, **4**). After release of the second hydroxyl group of PVFc-BGE, **1**, by hydrogenolysis, on the other hand, the resulting dihydroxyl end-functionalized PVFc (PVFc-$(OH)_2$, **2**) was used as a macroinitiator for polymerization of EO. This approach resulted in a series of novel AB_2 miktoarm star polymers containing two hydrophilic PEO blocks (PVFc-$(PEO)_2$, **3**). The materials have been characterized in detail and studied regarding their thermal stability and aqueous self-assembly.

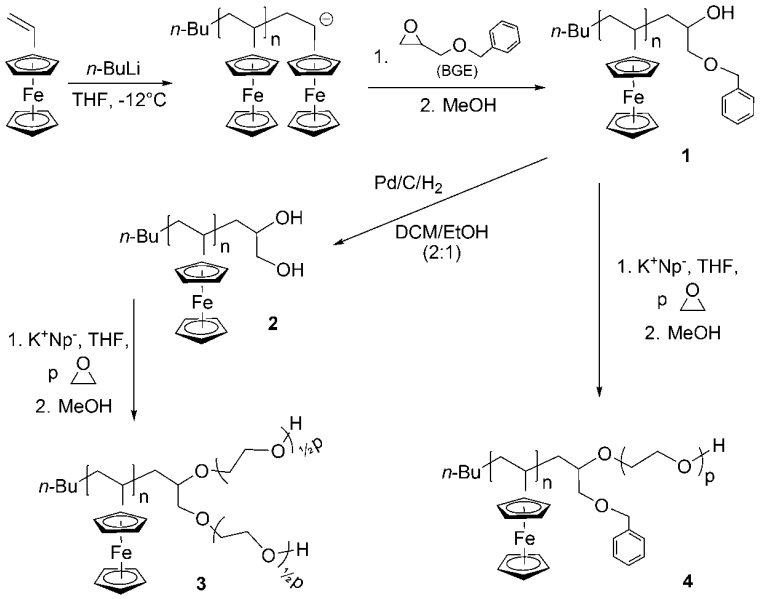

Scheme 1. Synthetic strategy to amphiphilic ferrocene-containing block copolymers (PVFc-BGE-PEO, **4**) and AB_2 miktoarm star polymers (PVFc-$(PEO)_2$, **3**). (K^+Np^-: potassium naphthalide, BGE: benzyl glycidyl ether)

Experimental Section

Reagents. All solvents and reagents were purchased from Acros Organics or Sigma-Aldrich and used as received, unless otherwise stated. Chloroform-d_1 was purchased from Deutero GmbH. Tetrahydrofuran (THF) was distilled from sodium/benzophenone under reduced pressure (cryo-transfer) prior to the addition of 1,1-diphenylethylene and *n*-BuLi as well as a second cryo-transfer. Benzyl glycidyl ether (BGE) and ethoxy ethyl glycidyl ether (EEGE) were dried over calcium hydride (CaH_2) or trioctylaluminium 2-3 times and cryo-transferred prior to use. Vinylferrocene (VFc) was synthesized according to a recently published procedure.[49]

Instrumentation. All syntheses were carried out under an atmosphere of nitrogen or argon, using the Schlenk technique or a glovebox equipped with a Coldwell apparatus. ^{1}H NMR spectra were recorded at 300 or 400 MHz on a Bruker AC300 or Bruker AMX 400, respectively and are referenced internally to residual proton signals of the deuterated solvent. Size exclusion chromatography (SEC) measurements were carried out in $CHCl_3$ on an instrument consisting of a Waters 717 plus autosampler, a TSP Spectra Series P 100 pump, a set of three MZ SDV columns (10^4/500/50 Å), RI- and UV-detectors (absorption wavelength: 254 nm). All SEC diagrams show the RI detector signal unless otherwise stated, and the molecular weight refer to linear poly(styrene) (PS) standards provided by Polymer Standards Service (PSS). In addition, SEC was performed with THF as the mobile phase (flow rate 1 mL min^{-1}) on a Mixed Gel column set from PL (PL Mixed Gel B, PL Mixed Gel C, PL Mixed Gel D) or an SDV column set from PSS (SDV 1000, SDV 100000, SDV 1000000) at 30 °C. Here, calibration was carried out using poly(styrene) (PS; from Polymer Standard Service (PSS), Mainz) and PVFc (self-made) calibration standards.[49] For the SEC-MALLS experiments, a system composed of a Waters 515 pump (Waters, Milford, CT), a TSP AS100 auto sampler, a Waters column oven, a Waters 486 UV detector operating at 254 nm, a Waters 410 RI-detector, and a DAWN DSP light scattering detector (Wyatt Technology, Santa Barbara, CA) was used. For data acquisition and evaluation of the light-scattering experiments, Astra version 4.73 (Wyatt Technology, Santa Barbara, CA) was used. The light-scattering instrument was calibrated using pure toluene, assuming a Rayleigh ratio of $9.78 \cdot 10^{-6}$ cm^{-1} at 690 nm. An injection volume of 118 µL, a sample concentration of 1-2 g L^{-1}, a column temperature of 35 °C, and a THF flow rate of 1 mL min^{-1} was used, and SEC analysis was performed on a high resolution column set from PSS (SDV 5 µm 10^6 Å, SDV 5 µm 10^5 Å, SDV

5 µm 1000 Å). The online viscosity was analyzed in THF at room temperature on linear M column (UV, RI, visco, and light scattering detectors) by PSS-company in Mainz.

Matrix-assisted laser desorption and ionization time-of-flight (MALDI-ToF) measurements were performed on a Shimadzu Axima CFR MALDI-ToF mass spectrometer equipped with a nitrogen laser delivering 3 ns laser pulses at 337 nm. Dithranol (1,8,9-trihydroxyanthracene) was used as a matrix. Samples were prepared by dissolving the polymer in THF at a concentration of 10 g L^{-1}. A 10 µL aliquot of this solution was added to 10 µL of a 10 g L^{-1} solution of the matrix. A 1 µL aliquot of the mixture was applied to a multistage target to evaporate THF and create a thin matrix/analyte film. The samples were measured in linear or reflection mode of the spectrometer. DSC curves were recorded on a Perkin-Elmer DSC 8500. TGA measurements were conducted on a Perkin-Elmer Pyris 6 TGA. A Philips EM420 transmission electron microscope (TEM) using a LaB_6 cathode at an acceleration voltage of 120 kV was used to obtain TEM images. TEM grids (carbon film on copper, 300 mesh) were obtained from Electron Microscopy Sciences Hatfield, PA, USA. Additional TEM experiments were carried out using a Zeiss EM 10 electron microscope operating at 80 kV. In all cases no staining was necessary. As autoclave a high-pressure laboratory autoclave Model II form Carl Roth GmbH + Co. KG was used.

Poly(vinylferrocene)benzyl glycidyl ether (PVFc-BGE, 1). *Exemplary Synthesis Procedure for PVFc$_4$-BGE.* In an ampule equipped with a stirring bar, 520 mg (2.45 mmol) neat VFc was dissolved in 12 mL of dry THF and the solution was cooled to −12 °C. A 325 µL (0.52 mmol) sample of a 1.6 M solution of *n*-BuLi in hexane was added quickly. The solution was stirred for 3 h to ensure complete conversion. A sample was taken for SEC measurement. After that time 3.9 mL of freshly distilled BGE (2.59 mmol, 5 equiv concerning the living chain ends) were added via a syringe. The solution was allowed to warm up to room temperature and stirred for 2 h. A small amount of degassed methanol was added and the reaction mixture was poured into a 10-fold excess of methanol. The end-functionalized PVFc precipitated quantitatively and was collected by filtration, washed with methanol, and dried *in vacuo* (yield: quantitative).

^{1}H NMR (300 MHz, C*D*Cl$_3$, δ in ppm): 7.51–7.08 (m, BGE aromatic), 4.61–3.25 (br, PVFc aromatic –C*H*-), 2.71–0.73 (br, PVFc backbone –C*H*$_2$–C*H*–). ^{13}C NMR (75 MHz, CDCl$_3$, δ in ppm): 128.4 (BGE aromatic) 127.8 (BGE aromatic) 95.8 (PVFc C_{quat}) 70.3–64.5 (PVFc

aromatic), 43.0 (PVFc backbone CH_2–*C*H), 32.1 (PVFc backbone *C*H_2–CH) 22.7 (PVFc initiator *C*H_2) 14.2 (PVFc initiator *C*H_3).

Poly(vinylferrocene)-(OH)$_2$ (PVFc-(OH)$_2$, 2). The reaction flask (laboratory autoclave) was filled with 500 mg (0.19 mmol) of **1**, 40 mL of DCM, 20 mL of EtOH, and 100 mg of palladium catalyst on activated carbon (Pd/C, 10%). The flask was flushed with hydrogen (50–80 bar) and stirred for 72 h. Subsequently the catalyst was removed by filtration over Celite, and the solvent was removed *in vacuo*. PVFc-$(OH)_2$ was obtained by precipitation in methanol and drying *in vacuo*. Strong interaction of the polymer with Pd/C resulted in yields of 50–70% only. ^{1}H NMR (300 MHz, C*D*Cl_3, δ in ppm): 4.61–3.25 (br, PVFc aromatic –C*H*–), 2.71–0.73 (br, PVFc backbone C*H*$_2$–C*H*). ^{13}C NMR (75 MHz, $CDCl_3$, δ in ppm): 96.0 (PVFc C_{quat}) 70.8–64.5 (PVFc aromatic), 43.7 (PVFc backbone CH_2–*C*H), 32.4 (PVFc backbone *C*H_2–CH) 22.8 (PVFc initiator *C*H_2) 14.3 (PVFc initiator *C*H_3).

Poly(vinylferrocene)-*b*-poly(ethylene oxide) (PVFc-BGE-PEO, 4). *Exemplary Synthesis Procedure for PVFc$_4$-BGE-PEO$_{92}$.* The terminally functionalized polymer **1** (280 mg, 0.15 mmol) was dissolved in 20 mL of THF and the hydroxyl group was deprotonated by titration with potassium naphthalide (K^+Np–, 0.5 M, 0.35 mL) until a slightly greenish color remained. Ethylene oxide (EO, 0.88 g, 20 mmol) was cryo-transferred into a graduated ampule and subsequently into the reaction flask at approximately -80 °C. The greenish color disappeared rapidly. The reaction mixture was heated up to 60 °C and stirred for 24-48 h. The polymerization was terminated with degassed methanol. PVFc-BGE-PEO was obtained as a bright yellow powder using precipitation in cold diethyl ether and drying *in vacuo* at room temperature (yield: 91%). ^{1}H NMR (400 MHz, $CDCl_3$, δ in ppm): 4.68–3.74 (br, PVFc aromatic –C*H*–), 3.96–2.77 (br, PEO backbone C*H*$_2$–C*H*$_2$) 2.71–0.73 (br, PVFc backbone C*H*$_2$–C*H*). ^{13}C NMR (100 MHz, $CDCl_3$, δ in ppm): 95.7 (PVFc C_{quat}) 72.4 (BGE: –*C*H_2–), 71.7–68.6 (PEO backbone *C*H_2–*C*H_2), 68.6–65.6 (PVFc aromatic –C*H*–), 61.0 (CH_2–OH), 32.9–28.5 (PVFc backbone *C*H_2–CH).

Poly(vinylferrocene)-*b*-(poly(ethylene oxide))$_2$ (PVFc-(PEO)$_2$, 3). *Exemplary Synthesis Procedure for PVFc$_{11}$-(PEO$_{61}$)$_2$.* A 200 mg (0.08 mmol) of **2** were utilized as macroinitiator for the anionic polymerization of EO analogous to the preparation of **4**. A THF solution of **2** was titrated by K^+Np– and EO (0.88 g, 20 mmol) was added. The reaction mixture was stirred for 24 h at 60 °C and was terminated with degassed methanol. Precipitation in cold diethyl ether

and drying *in vacuo* yields PVFc-$(PEO)_2$ as bright yellow powder (yield: 90%). ^{1}H NMR (400 MHz, $CDCl_3$, δ in ppm): 4.68–3.92 (br, PVFc aromatic –C*H*–), 3.90–2.97 (br, PEO backbone CH_2–CH_2) 2.84–0.63 (br, PVFc backbone CH_2–C*H*). ^{13}C NMR (100 MHz, $CDCl_3$, δ in ppm): 95.7 (PVFc C_{quat}) 72.5 (core, –CH_2–), 71.5–68.4 (PEO backbone CH_2–CH_2), 68.9–65.8 (PVFc aromatic –C*H*–), 61.2 (CH_2–OH), 33.1–28.7 (PVFc backbone CH_2–CH).

Results and Discussion

A. Synthesis of Linear and Star-Shaped PVFc-*block*-PEO Copolymers.

A series of block copolymers and AB_2 miktoarm star polymers containing one PVFc block and either one or two PEO blocks have been prepared by living anionic polymerization. Vinylferrocene was synthesized as described in literature[49], and the polymerization was initiated by *n*-BuLi. To the best of our knowledge, neither water-soluble PVFc block copolymers have been synthesized, nor has epoxide termination been used in the context of the carbanionic synthesis of PVFc to date. As it is known from the epoxide-termination of poly(styrene),[58, 67] the strong coordination of the lithium counterion with alkoxides prevents undesired further propagation and direct oxyanionic polymerization.[59, 68] The living anionic polymerization of VFc was terminated by the addition of two different epoxide derivatives, i.e., benzyl glycidyl ether (BGE) and ethoxy ethyl glycidyl ether (EEGE), thereby generating a first hydroxyl group at the chain termini. In both cases, a second hydroxyl group can be released, utilizing different deprotection protocols (hydrogenolysis and acidic hydrolysis, respectively). Initially EEGE was utilized as the end-capping reagent to obtain mono- and dihydroxyl end-functional PVFcs, because we assumed facile and rapid release of the second hydroxyl group by acidic hydrolysis, and because of its high stability toward the aggressive reaction conditions of carbanionic polymerization (Scheme S1).

A series of PVFc-EEGEs was synthesized and characterized by SEC (Figure 1) and MALDI–ToF MS. Table 1 summarizes the molecular weights determined by SEC, using PS and PVFc standards. The difference between these values increases with increasing molecular weights. PVFc chains show considerably smaller hydrodynamic volumes compared to PS samples with similar molar mass, due to the very compact chain conformation of the ferrocene-containing polymer.[49] According to the MALDI–ToF results the end-capping process was not

quantitative. The highest degree of functionalization for the PVFc-EEGE was approximately 80% (Figure S1, Supporting Information). In addition, acidic hydrolysis of this polymer even under mild reaction conditions afforded yields of less than 50% dihydroxyl end-functionalized polymer (cf. MALDI–ToF MS: Figure S2, Supporting Information). Partial oxidation of the iron centers, which are located laterally to the polymer backbone, occurred. As a simple indication of the undesired oxidation process a color change of the reaction mixture from amber yellow to green was observed.

Table 1. Characterization data of PVFc-EEGE

no.	polymer	M_n[a]	M_n[b]	M_w/M_n[b]
I	$PVFc_8$-EEGE[c]	1 500	1 800	1.17
II	$PVFc_{16}$-EEGE[c]	1 700	3 500	1.20
III	$PVFc_{37}$-EEGE[c]	3 400	8 000	1.26

[a]Molecular weight determined by SEC in g mol^{-1}(PS standards, THF). [b]Molecular weight in g mol^{-1} and molecular-weight distribution characterized by SEC in THF (PVFc standards[49]). [c]Degree of polymerization calculated by SEC (PVFc standards).

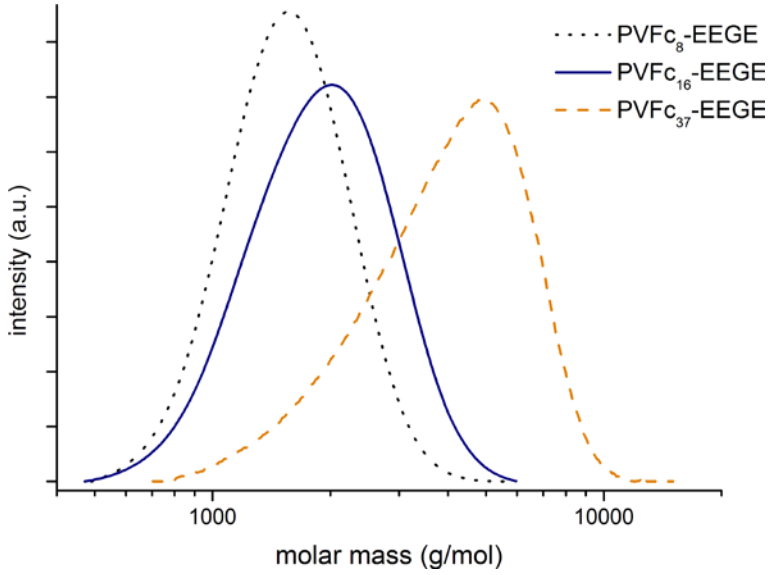

Figure 1. MWDs determined via SEC of PVFc-EEGE samples #I-III (THF, RI-Signal, PS standard).

As an alternative synthetic pathway, BGE instead of EEGE was utilized as protected epoxide derivative for the termination step. The reaction was terminated with a 5-fold excess of BGE to introduce simultaneously (i) an active hydroxyl group and (ii) a benzyl-protected hydroxyl group at the chain terminus. In contrast to the former strategy the second hydroxyl group

can be released by hydrogenolysis, and hence without the unwanted oxidizing processes. The BGE end-functionalized polymers were precipitated in methanol and characterized using SEC, ^{1}H NMR spectroscopy and MALDI–ToF MS. The corresponding characterization data are summarized in Table 2.

Table 2. Characterization data of the PVFc-BGE samples

no.	polymer[c]	M_n[a]	M_n[b]	M_w/M_n[b]
1	$PVFc_4$-BGE	860	980	1.07
2	$PVFc_5$-BGE	1 180	1 110	1.07
3	$PVFc_{11}$-BGE	1 150	2 630	1.09
4	$PVFc_{13}$-BGE	1 510	3 050	1.11
5	$PVFc_{16}$-BGE	1 990	3 650	1.10

[a]Molecular weight determined by SEC in g·mol^{-1} (THF, PS standards). [b]Molecular weight in g·mol^{-1} and molecular-weight distribution characterized by SEC in THF (PVFc standards[49]). [c]Degree of polymerization calculated by SEC (PVFc standards).

^{1}H NMR spectra were recorded in $CDCl_3$ (Figure S3 Supporting Information, bottom). A characteristic challenge of the NMR spectra of PVFc polymers in general is the appearance of very broad and unstructured resonances (see Supporting Information).[49] Nevertheless, the successful end-capping reaction with benzyl glycidyl ether could be verified, since the signal of the benzylic proton (7.49–7.25 ppm) is separated from the polymer signals. Unfortunately, the unstructured resonances in the PVFc spectra prevent accurate integration of the initiator signals, and therefore precise end-group analysis based on NMR spectroscopy is complicated. MALDI–ToF MS has been utilized instead to carry out a precise end-group analysis. The respective measurements of PVFc-BGE demonstrate quantitative terminal functionalization of PVFc with BGE. Figure 2 shows the MALDI–ToF mass spectrum of $PVFc_{16}$-BGE as an example (no. 5, Table 2). The spectrum reveals only one distribution mode, which can unequivocally be assigned to BGE-functionalized poly-(vinylferrocene) (1). This confirms the high functionalization efficiency of epoxide derivatives for the end-capping of PVFc. In the spectrum shown, representative signals are enlarged. The mass peak at m/z 2768.0 corresponds to the 12-mer of PVFc- BGE ($C_4H_9(C_{12}H_{12}Fe)_{12}C_{10}H_{13}O_2$; calculated value, 2767.2 g mol^{-1}). Showing a constant mass difference (molecular mass of the monomer repeating unit: 212.1 g mol^{-1}) between each signal, the complete spectrum is in good agreement with the calculated values. Furthermore, it should be emphasized that no signals corresponding

to the mass peak of proton-terminated, and thus unfunctionalized PVFc ($C_4H_9(C_{12}H_{12}Fe)_{13}H$; calculated value, 2815.1 g mol^{-1}) can be observed in the MALDI–ToF spectrum, which again supports quantitative BGE functionalization. The MALDI–ToF investigation of all PVFc-BGE samples (see Table 2) confirmed the high functionalization efficiency of the BGE end-capping method (see Supporting Information, Figure S4).

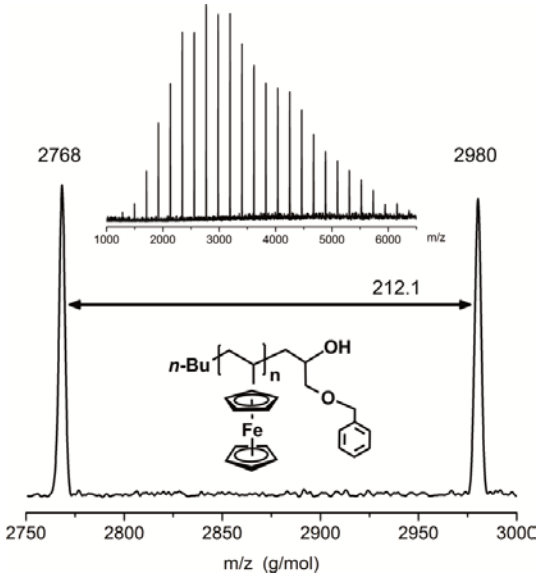

Figure 2. MALDI–ToF spectrum of PVFc16-BGE (no. 5, Table 2) synthesized by anionic polymerization and a termination process with BGE as end-capping reagent; matrix, dithranol.

All synthesized PVFc samples showed a narrow and monomodal molecular-weight distribution (M_w/M_n = 1.09–1.11) and average molecular weights in the range of 770–1760 g mol^{-1} (vs PS standards[69]) and 980-3650 g mol^{-1} (vs PVFc standards) according to SEC results (cf. Figure 3 and Table 2). Because of the aforementioned misleading values of the molar masses when evaluated using PS standards, it is necessary to consider molecular weights determined by SEC using PVFc standards (~500–50 000 g mol^{-1}). In summary, monohydroxyl end-functional PVFc samples were obtained in quantitative yields.

As mentioned above, the benzyl protecting group can now be released by catalytic hydrogenolysis to obtain dihydroxyl end-functionalized poly(vinyferrocene)s (PVFc-$(OH)_2$, **2**). By adjusting several parameters including solvent, time, and temperature the reaction conditions were optimized. Using the polar solvent mixture of dichloromethane and ethanol (2:1), Pd/C as a catalyst, and a hydrogen pressure of 50–80 bar, the best hydrogenolysis

results were obtained.[70] The progress of the deprotection reaction was monitored by ^{1}H and ^{13}C NMR spectroscopy. Figure S3 , Supporting Information shows ^{1}H NMR spectra of PVFc before (PVFc-BGE, no. 4) and after (PVFc-$(OH)_2$) the release of the benzyl groups. The disappearance of the aromatic proton signals in the δ = 7.49–7.25 ppm region confirms successful deprotection. ^{13}C NMR analysis verifies the results additionally, as the disappearance of the aromatic signals in the region between 127.4 and 128.9 ppm is evident (Figure S5, Supporting Information).

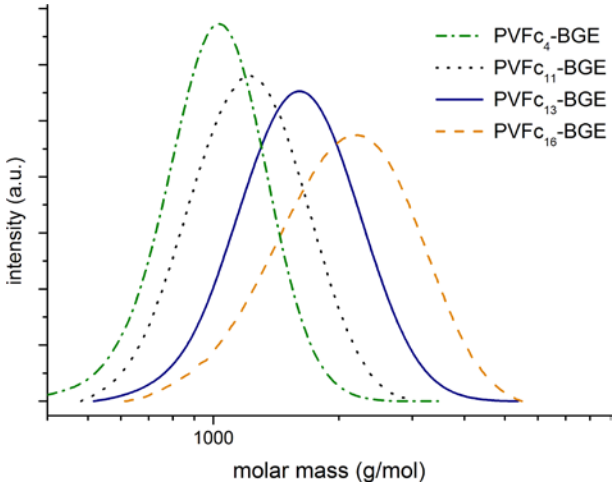

Figure 3. MWDs determined via SEC of selected PVFc-BGE samples no. 1 and no. 3-5 of Table 2 (THF, RI-Signal, PS standard).

MALDI–ToF MS was employed to verify successful and quantitative removal of the benzyl group. Figure 4 shows an overlay of the MALDI–ToF spectra recorded before ($PVFc_{16}$-BGE, no. 5) and after ($PVFc_{16}$-$(OH)_2$) hydrogenolysis. A shift of the signals to lower masses is observed, indicating successful removal of the protecting group. The upper right part of Figure 4 depicts a magnification of the spectrum in the region between 1900 and 2500 g mol^{-1}, which highlights the expected shift (90.1 g mol^{-1} for the leaving group C_7H_7). Furthermore, it has to be emphasized that only the desired distribution mode can be observed in the MALDI–ToF spectrum of $PVFc_{16}$-$(OH)_2$, but no signals corresponding to the $PVFc_{16}$-BGE, even if the same experimental conditions were used as for the analysis of $PVFc_{16}$-BGE (cf. Figure S6, Supporting Information). SEC characterization of PVFc-$(OH)_2$ samples (Table S1 and Figure S7, Supporting Information) underlined narrow molecular-weight distributions (M_w/M_n = 1.09–1.15, THF, PS standards). The molecular weights as

determined for these polymers using SEC are in good agreement with their protected counterparts.

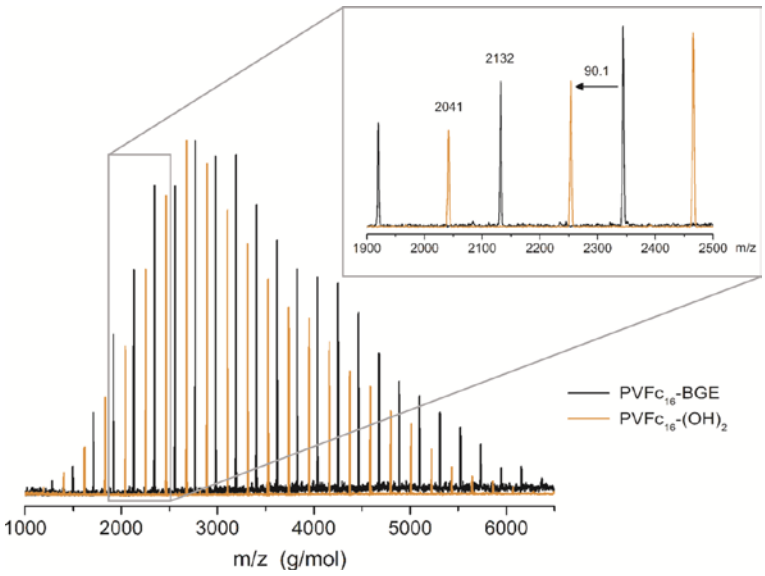

Figure 4. Overlay of MALDI ToF mass spectra $PVFc_{16}$-BGE (Table 2 sample no. 5, black) and the respective $PVFc_{16}$-$(OH)_2$ (Table S1 sample no. S4, orange). The magnification highlights the successful release of the benzyl protecting group.

The successful synthesis of two different end-functionalized poly(vinylferrocene)s with either one or two terminal hydroxyl groups paves the way to different PVFc-based block copolymer architectures.[57] To illustrate the potential of the approach, some representative amphiphilic PVFc block copolymers and AB_2 miktoarm star polymers have been prepared. The detailed results will be discussed in the following sections.

Linear (PVFc-BGE)-b-PEO diblock copolymer ***4***. BGE-endcapped PVFc was used as an initiator and EO as a monomer. The polymerization of EO is usually initiated by cesium or potassium alkoxides.[71–74] In our present case, the initiating species for EO polymerization is a potassium alkoxide, which was obtained by potassium naphthalide titration: The slightly greenish colored reaction mixture was cooled to −70 °C, and the corresponding amount of EO was added. After stirring the reaction mixture for 24 h at 60 °C, the copolymer (**4**) was precipitated into cold diethyl ether. The material was obtained in high yields (91%). After drying a bright yellow powder was obtained. When dissolving the powder in water, successful incorporation of the PVFc block is already visually indicated by the absence of precipitated PVFc homopolymer. Block copolymers in the range of 10 000 to 50 000 g mol^{-1} with a constant PVFc block of 1 000 g mol^{-1} were synthesized to investigate the influence of

varying PEO block length on the copolymer properties. ^{1}H NMR spectroscopy was employed to study the block copolymer structure and composition. However, similar to the spectra of PVFc homopolymers, broad and unstructured signals are observed throughout, due to limited chain mobility. Nevertheless, the main signals of the two different polymer blocks can clearly be distinguished. The expected signals reflecting the PVFc backbone appear at 2.7-0.7 ppm. The signals of the PEO backbone and the ferrocene units overlap in the region between 4.5 and 3.0 ppm. In addition, ^{13}C NMR analyses were carried out. The signals of both blocks (PVFc: backbone 34–29 ppm; ferrocene units 68–65 ppm; PEO 73–69 ppm) are clearly visible in analogy to the ^{1}H NMR spectrum. The presence of all expected signals in ^{1}H and ^{13}C NMR analysis confirms the successful synthesis of the desired diblock copolymers (Table 3 and Figure S8, Supporting Information).

Table 3. Characterization data of block copolymers PVFc-BGE-PEO and AB_2 miktoarm star polymers PVFc-$(PEO)_2$.

no.	polymer[a]	M_n[b]	M_n[c]	M_w/M_n[c)]
6	$PVFc_4$-BGE-PEO_{92}	10 000	10 000	1.11
7	$PVFc_4$-BGE-PEO_{206}	20 000	20 000	1.12
8	$PVFc_4$-BGE-PEO_{795}	43 000	37 000	1.07
9	$PVFc_4$-BGE-PEO_{1045}	44 000	48 000	1.06
10	$PVFc_{11}$-$(PEO_{61})_2$	11 000	8 000	1.19
11	$PVFc_{11}$-$(PEO_{73})_2$	11 000	9 000	1.25
12	$PVFc_{13}$-$(PEO_{273})_2$	25 000	27 000	1.10
13	$PVFc_{13}$-$(PEO_{420})_2$	50 000	40 000	1.10

[a]PVFc: degree of polymerization corresponds to the protected precursor (nos. 1-10), PEO: degree of polymerization determined by SEC [b]Theoretical value of the number-average of the molecular weight in g mol^{-1} [c]Molecular weight in g mol^{-1} and molecular-weight distribution characterized by SEC in $CHCl_3$ (PS standard).

NMR characterization provides important information about the copolymers, but final proof of successful block formation is not possible by this technique. Thus, SEC was applied to study all polymer samples subsequent to the work up procedure. Figure 5 presents the MWDs of a diblock copolymer (no. 8) and the corresponding precursor PVFc-BGE (no. 1), demonstrating efficient block formation. A characteristic shift of the molecular weights from approximately 2 000 to 40 000 g mol^{-1} can be observed. Since the PEO block does not induce

a signal in the UV detector, the pronounced UV absorption of the block copolymers evidence successful incorporation of the PVFc chains. The corresponding characterization data for all copolymers are listed in Table 3 (no. 6–9) and the respective SEC traces are depicted in Figure S9, Supporting Information. In comparison, theoretical values of the molecular weight agree well with SEC results, showing good control of the polymerization process.

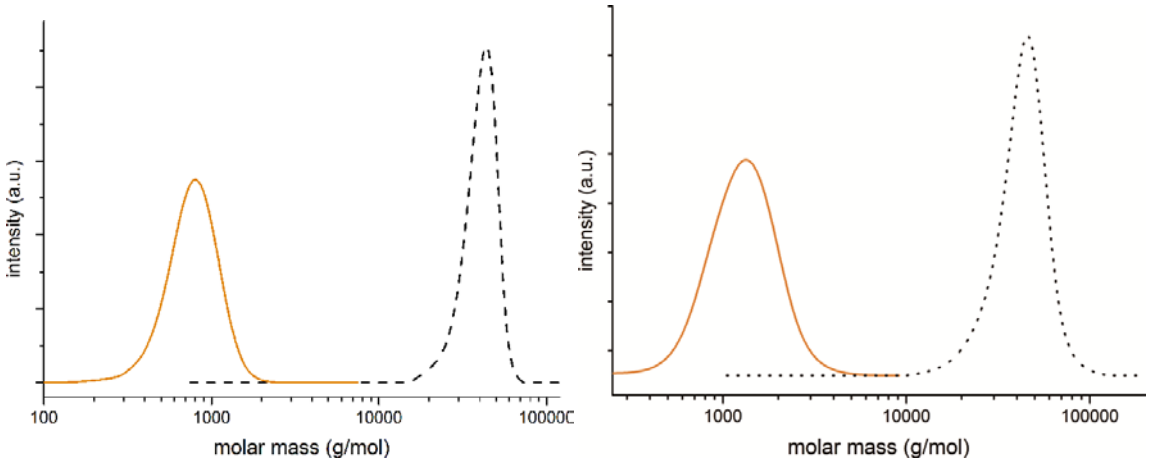

Figure 5. Linear block copolymer formation evidenced by UV-signals in SEC. MWDs of $PVFc_4$-BGE and $PVFc_4$-BGE-PEO_{795} (no. 1 and no. 13, left) as well as $PVFc_{13}$-$(OH)_2$ and $PVFc_{13}$-$(PEO_{420})_2$ (corresponds to no. 4 and no. 18, right). (CHCl3, PS standard).

It has to be emphasized that all synthesized polymers show excellent water solubility. By dissolving the bright yellow product in water, the formation of a clear, slightly amber colored solution is observed. In addition, UV–Vis spectra have been measured in $CHCl_3$ and H_2O, showing the characteristic strong absorption[75] of PVFc between 400 and 450 nm (Figure S10, Supporting Information). Comparable solubility properties are not observed for any other amphiphilic ferrocene-containing polymer published so far.[55]

The use of BGE as the capping reagent provides facile access to terminal orthogonal hydroxyl functionalities. The first hydroxyl group can directly be applied for further reactions (as shown herein) and the second hydroxyl group can be released by hydrogenolysis. The presented synthetic strategy generates block copolymers with a single protected functionality at the block junction, which is suitable for additional reactions subsequent to the release of the benzyl group. It may be worth mentioning that also ABC block copolymers with poly(vinylferrocene) segment should be available in this manner. Detailed studies

employing the functionality at the interface yielding novel macromolecular architectures are subject of future research.

*PVFc-(PEO)$_2$ AB$_2$ Miktoarm Star Polymer **3***. After the successful release of the benzyl group, PVFc-(OH)$_2$ was subsequently used as a difunctional macroinitiator-functionalized PVFc, offering access to water-soluble AB$_2$ miktoarm star polymers. The procedure was carried out similar to the linear block copolymer synthesis, and both hydroxyl groups were deprotonated using potassium naphthalide prior to the addition of EO. Because of the rapid cation-exchange equilibrium (compared to the propagation), both hydroxyl groups can be expected to react with the monomer units in the same manner and with the same propagation rate.[76] In comparison to PVFc-PEO block copolymers, similar reaction conditions with 24–48 h reaction time, 60 °C and an identical work up procedure was applied to obtain PVFc-(PEO)$_2$ (3) miktoarm star polymers as a bright yellow powder. As expected, the materials are water-soluble as well.

Molecular weights in the range of 8 000 to 40 000 g mol^{-1} with low PDIs (Mw/Mn < 1.25) were synthesized. The corresponding characterization data of all PVFc-(PEO)$_2$ samples are also summarized in Table 3 (no. 10–13, cf. Figure S11, Supporting Information). All signals of ^{1}H NMR and ^{13}C NMR spectra can be assigned to the respective hydrogens and carbons of PVFc-(PEO)$_2$ and are analogous to the respective linear block copolymers. Because of high molecular weights and therefore low signal intensity of the junction carbons, no significant difference between linear block and miktoarm star polymers was observable in NMR spectroscopy (cf. Figure S12, Supporting Information). To confirm block formation, in Figure 5 the SEC results obtained from the miktoarm star polymer no. 13 and the dihydroxyl PVFc-precursor are combined. In analogy to the linear block copolymer a molecular weight shift from 3 000 to 40 000 g mol^{-1} can be observed and the presence of an intense UV absorption in SEC analysis indicates successful incorporation of the PVFc block into the 3-arm star polymer. Again, the comparison of experimentally observed and theoretically expected values for molar masses demonstrates good control over molecular weights. In contrast to the linear block copolymers the SEC results underestimate the molecular weights slightly. This is due to the macromolecular architecture of the star-shaped polymer, which shows a reduced hydrodynamic volume compared to linear block copolymer with similar contour length.[77, 78]

It is obvious that it is a key issue, whether the formation of the miktoarm structures has been achieved. Additional information on the polymers was obtained by investigating two selected samples with conventional SEC, SEC–MALLS and SEC online viscometry. The corresponding results are listed in Table 4. Characterization by light-scattering demonstrated similar molecular weights for both samples (block and star polymer), whereas in the case of the conventional SEC (linear PS standards) the molecular weight of the star polymer was strongly underestimated. This is obviously a consequence of the decreased hydrodynamic volume of the star-shaped polymer. In addition, the data of the viscosity detector present a distinct difference between linear and star shaped polymers concerning the intrinsic viscosity (see Table 4 and Figure S13, Supporting Information). These results support the successful synthesis of ferrocene-containing AB_2 miktoarm star polymers, i.e., growth of both PEO arms, and mirror the different hydrodynamic volume of linear and miktoarm star polymer prepared.

Table 4. Characterization data of a selected block copolymer PVFc-BGE-PEO and an AB_2 miktoarm star polymer PVFc-$(PEO)_2$ (conventional SEC vs. SEC-MALLS).

no.	polymer	M_n[a]	M_w[a]	M_w/M_n[a]	M_w[b]	$[\eta]$[c]
6	$PVFc_4$-BGE-PEO_{92}	9 600	12 200	1.27	9 700	17.3
10	$PVFc_{11}$-$(PEO_{61})_2$	6 800	8 100	1.19	9 900	8.7

[a]Number-average and weight-average of molecular weight in g mol^{-1} and molecular-weight distribution characterized by SEC in THF, [b]Weight-average of molecular weight in g mol^{-1} characterized by SEC-MALLS in THF,[79] [c]Intrinsic viscositsy determined by SEC on-line viscosity measurements in THF.

B. Properties of Linear and Star-Shaped PVFc-*block*-PEO Copolymers.

The main objective of this work was the development of a versatile synthetic strategy to generate water-soluble block copolymers containing PVFc blocks. Nevertheless, first results of preliminary studies of their behavior in solution, thermal properties and morphological characteristics will be given in the following.

DSC measurements of both types of block copolymers (linear and AB_2 star polymers) have been performed to evaluate the effect of the different chain architectures. The long PEG chain of both polymer structures provides clearly visible glass transition temperatures (T_g: ~−50 °C) and melting points (T_m: ~ 60 °C), whereas the T_g of the PVFc chains, which is expected in the region of approximately 200 °C,[49] could not be observed. This is most

probably due to the low weight fraction of the PVFc blocks (2–25%). However, an increased stability of the synthesized polymeric structures was observed by TGA analysis. The degradation threshold compared to PEO homopolymers (380–400 °C[80, 81]) was slightly higher for the organometallic structures (420 °C).

As mentioned above, all presented PVFc-PEO structures show water solubility (see Figure S10, Supporting Information). This is of interest, since amphiphilic ferrocene-containing block copolymers based on poly(ferrocenylsilane) can form redox-active micelles, allowing e.g., for the storage and release of encapsulated drugs in aqueous media.[82–85] The morphologies of block and miktoarm star copolymers in solution were studied by transmission electron microscopy (TEM) using the drop-casting method. The polymers were initially dissolved in THF. Subsequent slow addition of water by a syringe pump was employed to lock the core structures ("frozen micelles") as described by Eisenberg et al.[86] To obtain the micelles in pure water, the organic cosolvent was gradually eliminated by dialysis. One drop of the aqueous solution ($c \approx 0.5$ g L^{-1}) was deposited on a carbon-coated copper TEM grid. The water was allowed to evaporate under vacuum, before the polymer structures on the grid were investigated by TEM.

Representative images of PVFc-BGE-PEO and PVFc-$(PEO)_2$ (M_n of approximately 40 000 g mol^{-1}) are shown in Figure 6A–C. As expected for the given block ratios with rather small content of the insoluble PVFc block and high content of PEO, micellar structures were observed. The diameters of the spherical aggregates varied between 100 and 400 nm. Neither the shape nor the diameters show a difference, comparing the TEM images of block copolymers and AB_2 miktoarm star polymers. However, the TEM images of star polymers with lower molecular weight (sample no. 11, ~10 000 g mol^{-1}) exhibit a spherical structure consisting of several agglomerated spherically shaped micelles (Figure 6D–F). In Figure 6F an intriguing microphase separation within the block copolymer micelles can be distinguished. Obviously, the dark regions represent the cores of the micelles consisting of PVFc, whereas the brighter regions in proximity represent the PEO blocks. In addition, rather uniform diameter of the micelles of approximately 100 nm can be observed. In our current understanding, the appearance of different agglomerated micelles depends on the molecular weight of the block copolymers and the fraction of PVFc.

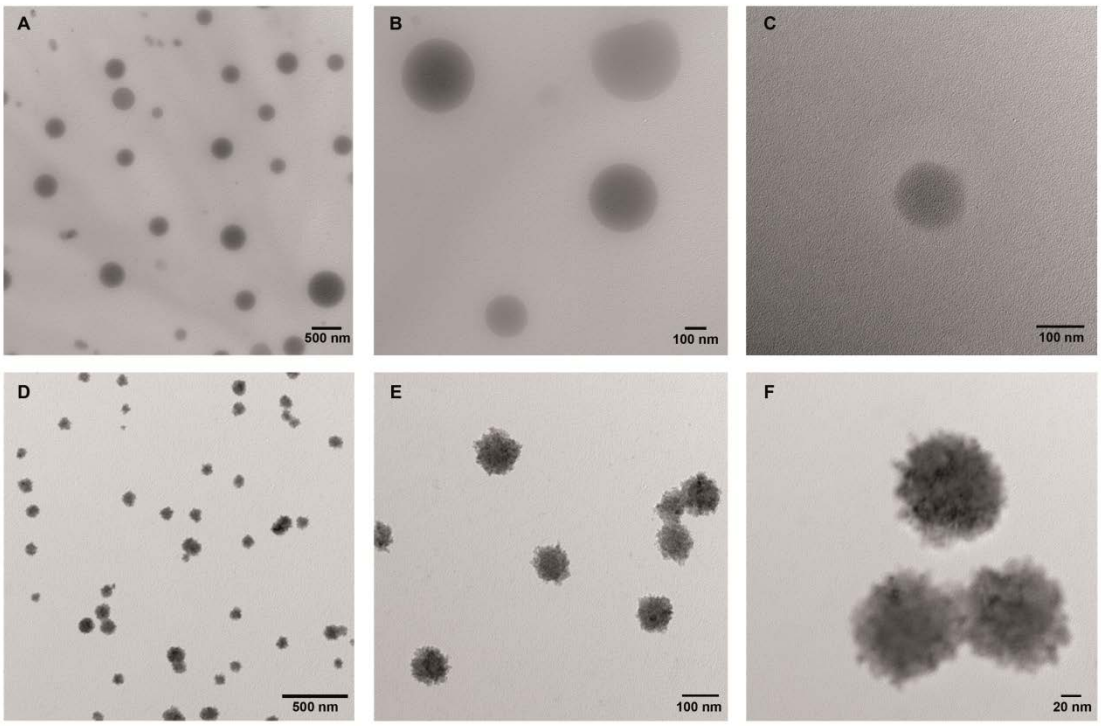

Figure 6. TEM images of PVFc-BGE-PEO block copolymers and PVFc-$(PEO)_2$ star polymers prepared from aqueous solution using the drop-casting method. (A and B: $PVFc_{13}$-$(PEO_{420})_2$, no. 13, C: $PVFc_4$-BGE-PEO_{795}, no. 8, D-F: $PVFc_{11}$-$(PEO_{73})_2$, no. 11).

Furthermore, the degree of crystallization of the high molecular weight PEO in the initially swollen and subsequently dried shell of the micelle might play a role for the formation of the structures observed. Morphologies and potential application (e.g., redox-active micelles) of block copolymers with increasing PVFc ratio are currently investigated in a systematic manner and will be presented in forthcoming work.

Conclusion

A synthetic pathway to water-soluble block copolymers and AB_2 miktoarm star polymers containing a poly(vinyl ferrocene) (PVFc) block and either one or two poly(ethylene oxide) (PEO) blocks has been developed. For the first time, the combination of carb- and oxyanionic polymerization has been implemented for poly(vinylferrocene), utilizing a protected epoxide derivative as end-capping reagent. Two different glycidyl ethers (BGE and EEGE) were employed for the functional end-capping of the PVFc block. In order to switch from the PVFc block to PEO, a procedure had to be developed that permits to overcome the redox-

sensitivity of the metalcontaining PVFc block. The benzyl glycidyl ether (BGE) was found to be the best suited capping reagent, since cleavage of the benzyl protecting group by hydrogenolysis does not lead to degradation of the PVFc polymer chain in contrast to the acidic treatment, which is necessary to remove the acetal protecting group of EEGE. Quantitative end-capping (and deprotection) led to mono and dihydroxyl end-functionalized PVFc, as evidenced by MALDI–ToF MS. In the following step, the respective polymers have been used as macroinitiators for the ring-opening polymerization of ethylene oxide to obtain a series of water-soluble PVFc-BGE-PEO block copolymers and PVFc-$(PEO)_2$ AB_2 miktoarm star polymers with molecular weights in the range of 8 000 to 50 000 g mol^{-1}, as confirmed by a combination of SEC, SEC–MALLS and online viscosimetry. These metal-containing amphiphilic block copolymers exhibit good solubility in water, and the synthetic pathway provides an efficient approach to watersoluble and redox-active complex polymer architectures. First studies dealing with the morphologies in aqueous solution showed agglomerated micelle structures. The general synthetic pathway demonstrated herein provides a facile route to a large variety of macromolecular architectures containing PVFc blocks combined with polyether chains. In view of the versatile application potential for water-soluble ferrocene-containing compounds, the presented structures are promising materials for bio-organometallic applications,[15,17] which are currently investigated.

Acknowledgments

C.T. thanks MPGC (Max Planck Graduate Center with Johannes Gutenberg-University) and the Excellence Initiative (DFG/GSC 266) for a scholarship and financial support. The authors would like to thank the Landesoffensive zur Entwicklung Wissenschaftlich-ökonomischer Exzellenz (LOEWE Soft Control) for financial support of this work. We acknowledge Daniela Held und Michael Krämer (PSS company Mainz) for detailed SEC analysis and online viscosity measurements. Support in performing the SEC analyses by Marion Trautmann (PVFc) is acknowledged.

Supporting Information

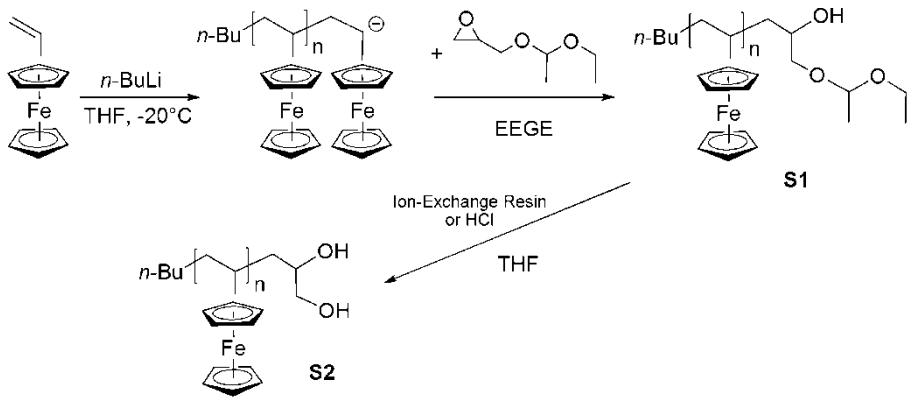

Scheme S1. Initial planned synthetic strategy to dihydroxyl functional PVFc by end capping of living PVFc with EEGE and subsequent release of the protecting group by acidic hydrolysis.

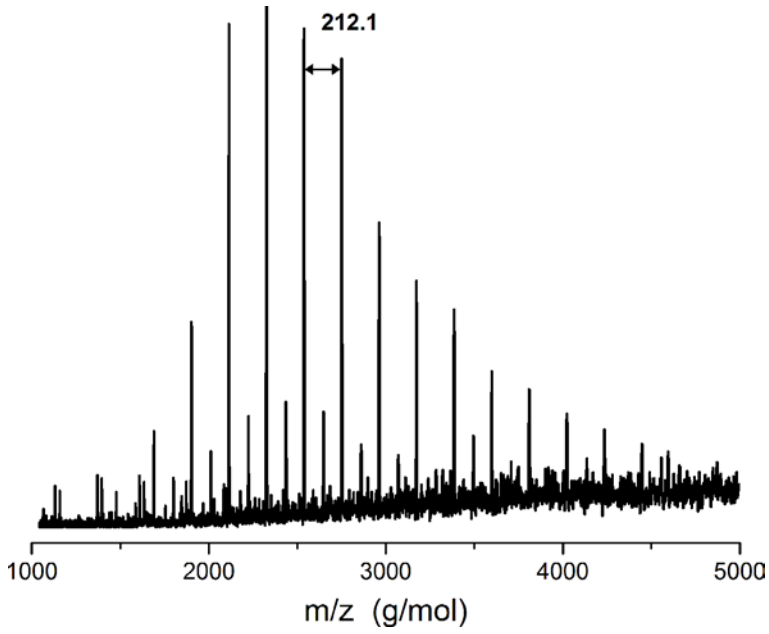

Figure S1. MALDI-ToF spectrum of PVFc-EEGE (no. I in Table 1). Main distribution can be assigned to PVFc-EEGE and sub distribution represents PVFc-H/K^+ (Matrix: dithranol)

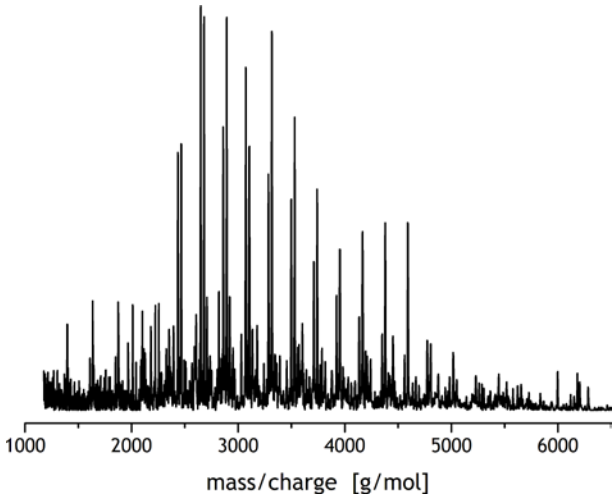

Figure S2. MALDI-ToF spectrum of deprotected PVFc-EEGE. One distribution can be assigned to PVFc-EEGE and a second distribution with similar intensity represents PVFc-$(OH)_2$ (Matrix: dithranol)

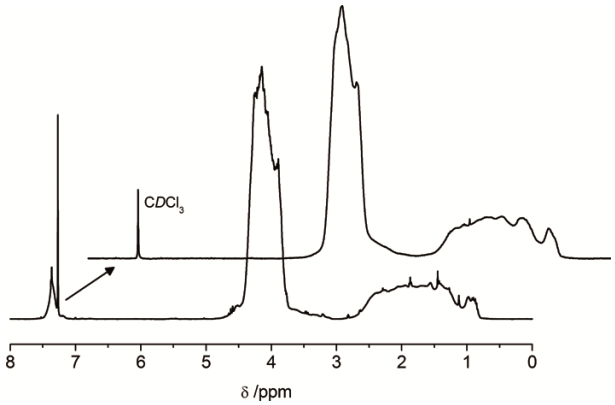

Figure S3. ^{1}H NMR spectra (300 MHz, C*D*Cl_3) of PVFc-BGE (no. 4, bottom) and corresponding PVFc-$(OH)_2$ (top).

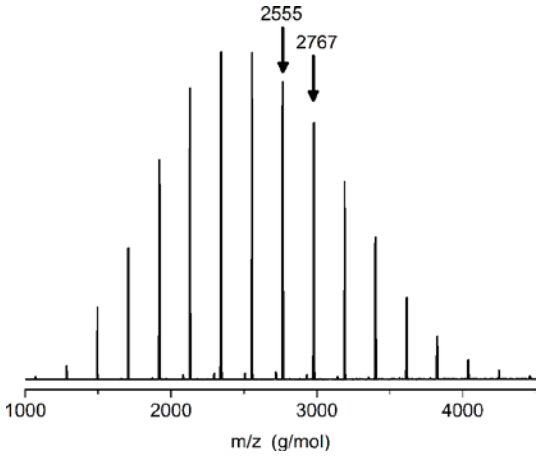

Figure S4. MALDI-ToF spectrum of $PVFc_{11}$-BGE (no. 3) (Matrix: dithranol).

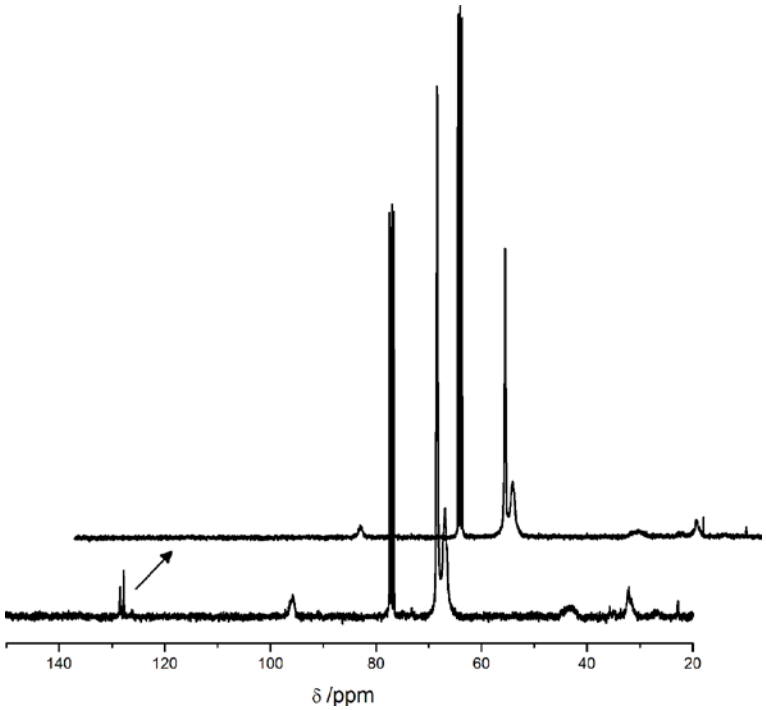

Figure S5. ^{13}C NMR spectra (300 MHz, C*D*Cl_3) of PVFc-BGE (no. 4, bottom) and PVFc-$(OH)_2$ (top); the benzyl protective groups have been cleaved.

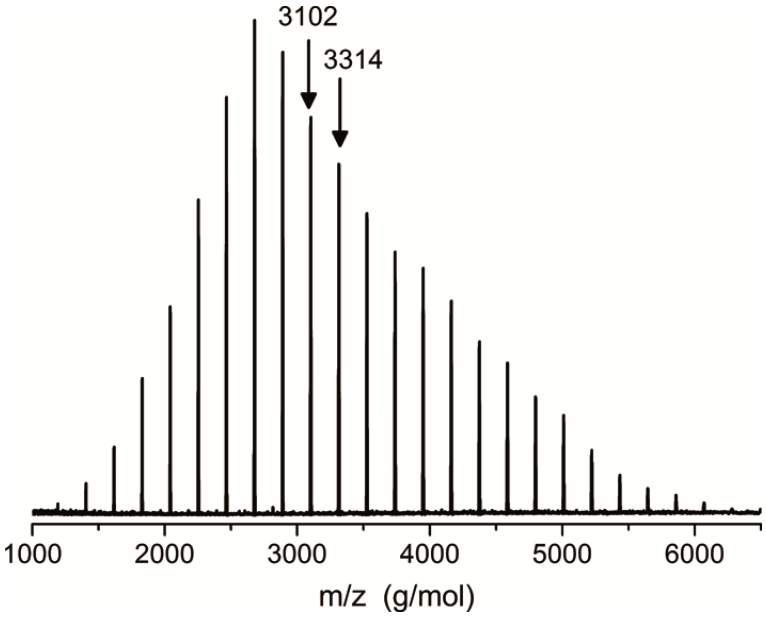

Figure S6. MALDI-ToF spectrum of $PVFc_{16}$-$(OH)_2$ (Matrix: dithranol).

Table S1. Characterization data of PVFc-$(OH)_2$

no.	polymer[b]	M_n[a]	M_w/M_n[a]
S1	$PVFc_{11}$-$(OH)_2$[c)]	1 390	1.09
S2	$PVFc_{11}$-$(OH)_2$[c)]	1 360	1.09
S3	$PVFc_{13}$-$(OH)_2$[d)]	1 520	1.10
S4	$PVFc_{16}$-$(OH)_2$[e)]	2 500	1.11
S5	$PVFc_{16}$-$(OH)_2$[e)]	2 140	1.15

[a]Molecular weight in g·mol^{-1} and molecular-weight distribution characterized by SEC in THF (PS standards), [b]SEC results after hydrogenolysis of the corresponding samples of Table 2 no. 3[c)], no. 4[d)], and no. 5[e)]

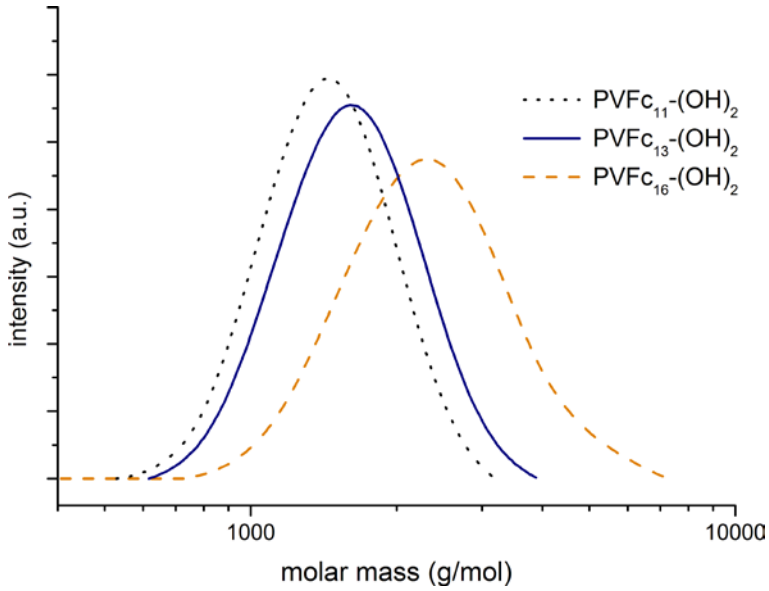

Figure S7. SEC traces of selected PVFc-$(OH)_2$ samples of Table S1 (no. S1, no. S3, and no. S5, THF, PS-Standards).

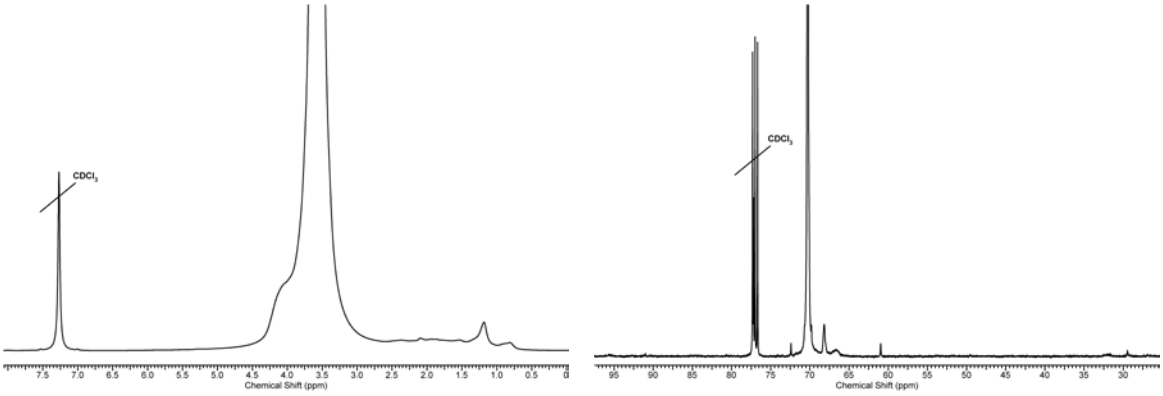

Figure S8. NMR spectra of $PVFc_4$-BGE-PEO_{92} (no. 6) measured in deuterated chloroform (^{1}H NMR, left and ^{13}C NMR, right)

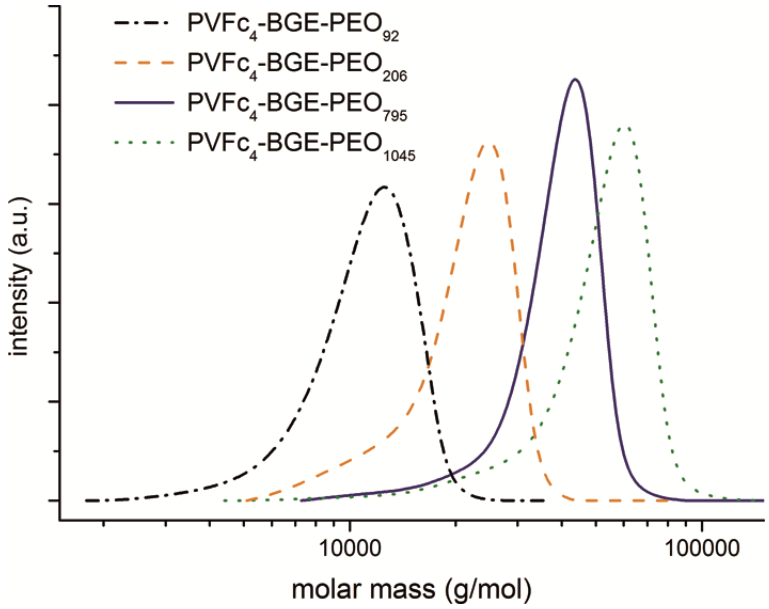

Figure S9. MWDs of PVFc-BGE-PEO samples ($CHCl_3$, UV-Signal. PS standard).

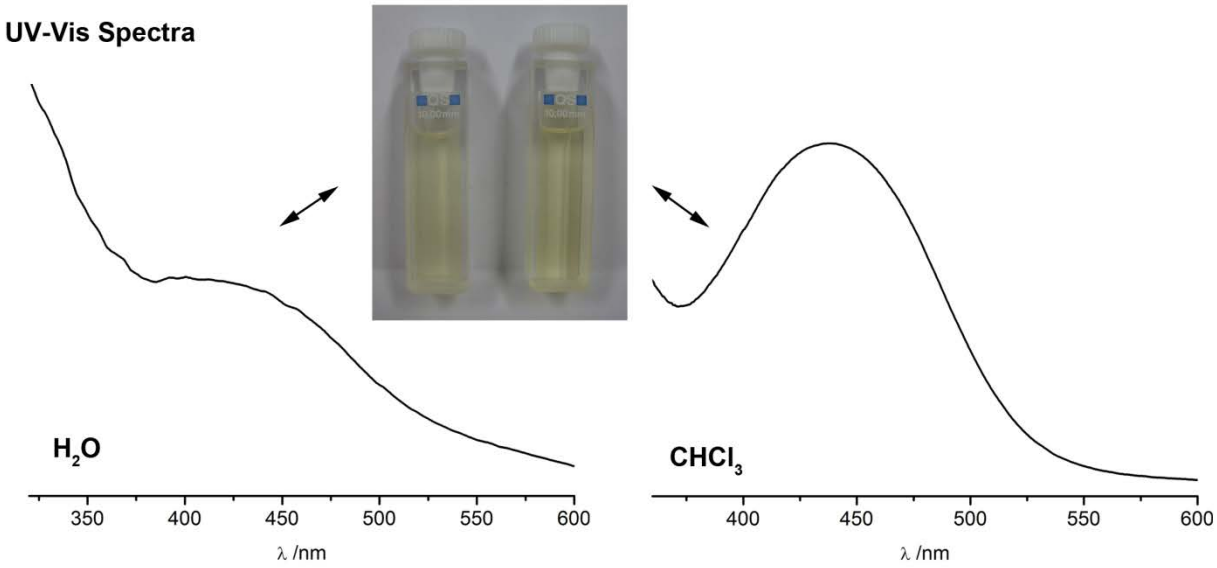

Figure S10. UV-Vis Spectra of $PVFc_4$-BGE-PEO_{92} in different solvents (H_2O and $CHCl_3$). The typical absorption of PVFc can be observed in both spectra between 400 and 450 nm (λ_{H2O} = 420 nm; λ_{CHCl3} = 438 nm) and matches previously reported absorption spectra of PVFc (λ_{DCM} = 440 nm).[75] The images show the bright yellow solutions of $PVFc_4$-BGE-PEO_{92} in H_2O (left) and $CHCl_3$ (right).

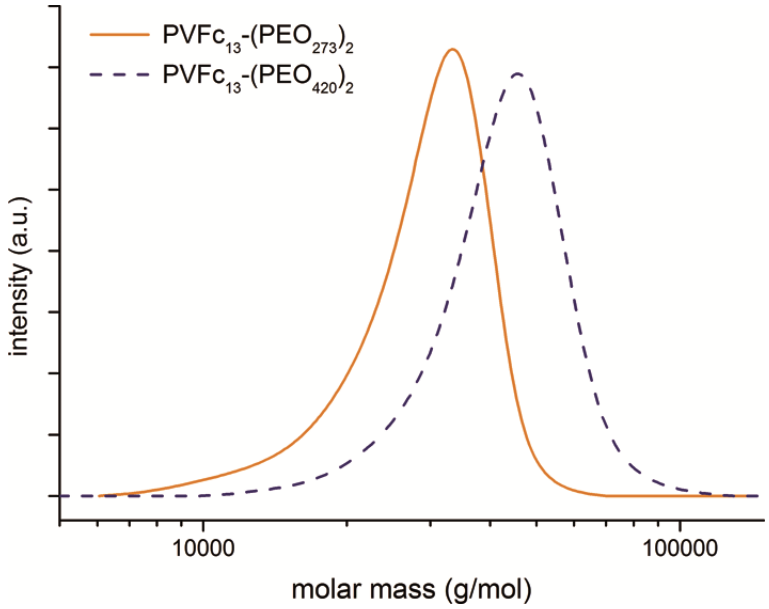

Figure S11. SEC traces of PVFc-$(PEO)_2$ (no. 10, no. 12, #13) ($CHCl_3$, PS standards).

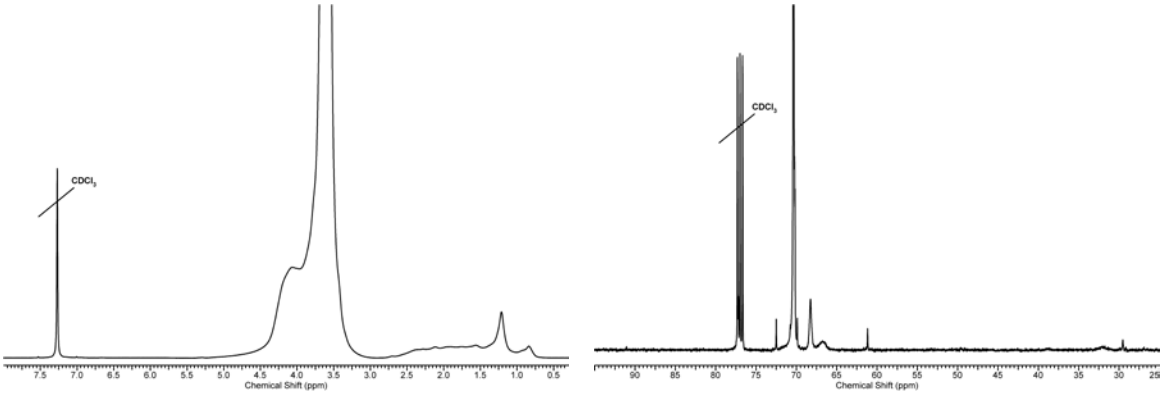

Figure S12. NMR spectra of $PVFc_{11}$-$(PEO_2)_{61}$ (no. 10) measured in deuterated chloroform (^{1}H NMR, left and ^{13}C NMR, right).

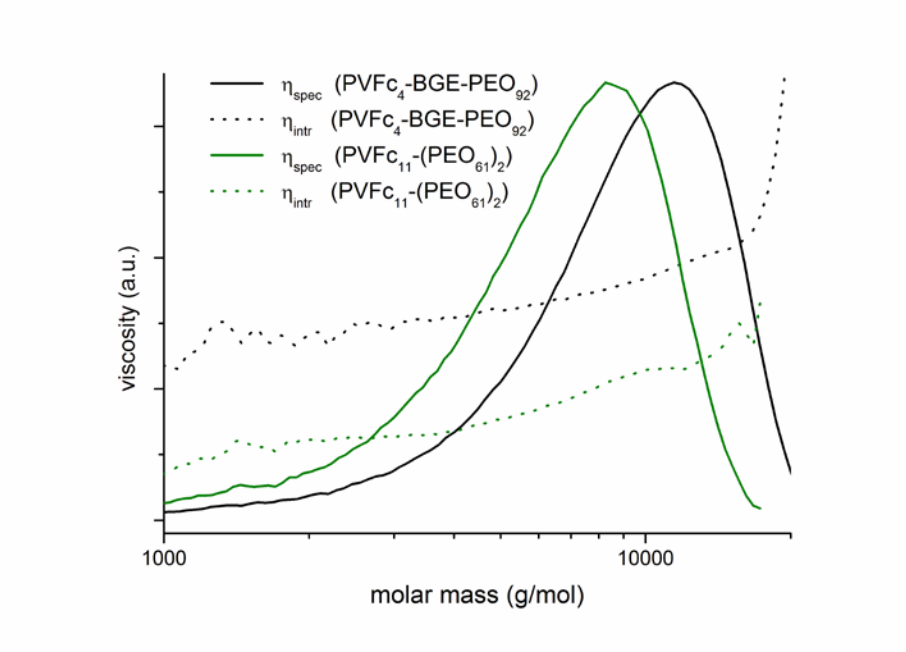

Figure S13. Intrinsic and specific viscosity of $PVFc_4$-BGE-PEO_{92} and $PVFc_{11}$-$(PEO_2)_{61}$ analyzed by SEC online viscosity measurements (THF, universal calibaration)

References

(1) Whittell, G. R.; Manners, I. *Adv. Mater.* **2007,** 19, (21), 3439-3468.

(2) Abd-El-Aziz, A. S.; Manners, I., *Frontiers in Transition Metal-Containing Polymers*. Wiley-Interscience: Hoboken, NJ, 2007.

(3) Manners, I., *Synthetic Metal-Containing Polymers*. VCH: Weinheim, Germany. 2004.

(4) Wöhrle, D.; Pomogailo, A. D., *Metal Complexes and Metals in Macromolecules: Synthesis, Structure and Properties*. Wiley-VCH: Weinheim, Germany, 2003.

(5) Carraher, C. E.; Abd-El-Aziz, A. S.; Pittman, C.; Sheats, J.; Zeldin, M. *A Half Century of Metal and Metalloid Containing Polymers*; Wiley: New York, 2003.

(6) Rehahn, M. Organic-Inorganic Hybrid Polymers. In *Synthesis of Polymers*, Schlüter, A.-D., Ed.; Wiley-VCH: Weinheim, Germany, 1999; p 319.

(7) Smith, T. M.; Nelson, G. L. *Polym. Adv. Technol.* **2006,** 17 (9–10), 746–753.

(8) Hale, P. D.; Inagaki, T.; Karan, H. I.; Okamoto, Y.; Skotheim, T. A. *J. Am. Chem. Soc.* **1989,** 111 (9), 3482–3484.

(9) Tatsuma, T.; Saito, K.; Oyama, N. *Anal. Chem.* **1994,** 66 (7), 1002–1006.

(10) Saito, T.; Watanabe, M. *React. Funct. Polym.* **1998,** 37 (1–3), 263–269.

(11) Saito, T.; Watanabe, M. *Polym. J.* **1999,** 31 (11–2), 1149–1154.

(12) Patel, H.; Li, X.; Karan, H. I. *Biosens. Bioelectron.* **2003,** 18 (8), 1073–1076.

(13.) Gülce, A.; Gülce, H. *J. Biochem. Bioph. Methods* **2005,** 62 (1), 81–92.

(14) Cass, A. E. G.; Davis, G.; Francis, G. D.; Hill, H. A. O.; Aston, W. J.; Higgins, I. J.; Plotkin, E. V.; Scott, L. D. L.; Turner, A. P. F. *Anal. Chem.* **1984,** 56 (4), 667–671.

(15) van Staveren, D. R.; Metzler-Nolte, N. *Chem. Rev.* **2004,** 104(12), 5931–5986.

(16) Biot, C.; Pradines, B.; Dive, D. Ferroquine: A Concealed Weapon. In *Apicomplexan Parasites*; Wiley-VCH Verlag GmbH & Co. KGaA: Weinheim, Germany, 2011; pp 397–411.

(17) Top, S.; Vessières, A.; Leclercq, G.; Quivy, J.; Tang, J.; Vaissermann, J.; Huché, M.; Jaouen, G. *Chem. Eur. J.* **2003,** 9 (21), 5223–5236.

(18) Top, S.; Dauer, B.; Vaissermann, J.; Jaouen, G. *J. Organomet. Chem.* **1997,** 541 (1–2), 355–361.

(19) Köpf-Maier, P.; Köpf, H.; Neuse, E. W. *Angew. Chem., Int. Ed.* **1984,** 23 (6), 456–457.

(20) Ornelas, C. *New J. Chem.* **2011,** 35 (10), 1973–1985.

(21) Arimoto, F. S.; Haven, A. C. *J. Am. Chem. Soc.* **1955,** 77 (23), 6295–6297.

(22) Neuse, E. W.; Rosenberg, H. *J. Macromol. Sci., Rev. Macromol. Chem.* **1970,** 4 (1), 1–145.

(23) Neuse, E. W. *J. Macromol. Sci., Chem.* **1981,** 16 (1), 3–72.

(24) Withers, H. P.; Seyferth, D.; Fellmann, J. D.; Garrou, P. E.; Martin, S. *Organometallics* **1982,** 1 (10), 1283–1288.

(25) Walter, S. *Russ. Chem. Rev.* **1991,** 60 (7), 784.

(26) Brandt, P. F.; Rauchfuss, T. B. *J. Am. Chem. Soc.* **1992,** 114 (5), 1926–1927.

(27) Foucher, D. A.; Tang, B. Z.; Manners, I. *J. Am. Chem. Soc.* **1992,** 114 (15), 6246–6248.

(28) Manners, I. *Can. J. Chem.* **1998,** 76 (4), 371–381.

(29) Hirano, T.; Yoo, H.-S.; Ozama, Y.; Abou El-Magd, A.; Sugiyama, K.; Hirao, A. *J. Inorg. Organomet. Polym.* **2010,** 20 (3), 445–456.

(30) Hudson, R. D. A. *J. Organomet. Chem.* **2001,** 637–639, 47–69.

(31) Gilroy, J. B.; Patra, S. K.; Mitchels, J. M.; Winnik, M. A.; Manners, I. *Angew. Chem., Int. Ed.* **2011,** 50 (26), 5851–5855.

(32) Wurm, F.; Frey, H. *Prog. Polym. Sci.* **2011,** 36 (1), 1–52.

(33) Wurm, F.; Villanueva, F. J. L.; Frey, H. *J. Polym. Sci., Part A: Polym. Chem.* **2009,** 47 (10), 2518–2529.

(34) Bellas, V.; Rehahn, M. *Angew. Chem., Int. Ed.* **2007,** 46 (27), 5082–5104.

(35) Wurm, F.; Hilf, S.; Frey, H. *Chem. Eur. J.* **2009,** 15 (36), 9068–9077.

(36) Massey, J. A.; Winnik, M. A.; Manners, I.; Chan, V. Z. H.; Ostermann, J. M.; Enchelmaier, R.; Spatz, J. P.; Müller, M. *J. Am. Chem. Soc.* **2001,** 123 (13), 3147–3148.

(37) Mohd Yusoff, S. F.; Gilroy, J. B.; Cambridge, G.; Winnik, M. A.; Manners, I. *J. Am. Chem. Soc.* **2011,** 133 (29), 11220–11230.

(38) Eloi, J.-C.; Rider, D. A.; Cambridge, G.; Whittell, G. R.; Winnik, M. A.; Manners, I. *J. Am. Chem. Soc.* **2011,** 133 (23), 8903–8913.

(39) Qian, J.; Guerin, G.; Lu, Y.; Cambridge, G.; Manners, I.; Winnik, M. A. *Angew. Chem., Int. Ed.* **2011,** 50 (7), 1622–1625.

(40) Pittman, C. U.; Lai, J. C.; Vanderpool, D. P. *Macromolecules* **1970,** 3 (1), 105–107.

(41) Gallei, M.; Schmidt, B. V. K. J.; Klein, R.; Rehahn, M. *Macromol. Rapid Commun.* **2009,** 30 (17), 1463–1469.

(42) Herfurth, C.; Voll, D.; Buller, J.; Weiss, J.; Barner-Kowollik, C.; Laschewsky, A. *J. Polym. Sci., Part A: Polym. Chem.* **2012,** 50 (1), 108–118.

(43) Nuyken, O.; Burkhardt, V.; Hübsch, C. *Macromol. Chem. Phys.* **1997,** 198 (11), 3353–3363.

(44) Higashihara, T.; Faust, R. *Macromolecules* **2007,** 40 (21), 7453–7463.

(45) Gallei, M.; Tockner, S.; Klein, R.; Rehahn, M. *Macromol. Rapid Commun.* **2010,** 31 (9–10), 889–896.

(46) Chauhan, B. P. S.; Rathore, J. S. *J. Am. Chem. Soc.* **2005,** 127(16), 5790–5791.

(47) Durkee, D. A.; Eitouni, H. B.; Gomez, E. D.; Ellsworth, M. W.; Bell, A. T.; Balsara, N. P. *Adv. Mater.* **2005,** 17 (16), 2003–2006.

(48) Baumert, M.; Fröhlich, J.; Stieger, M.; Frey, H.; Mülhaupt, R.; Plenio, H. *Macromol. Rapid Commun.* **1999,** 20 (4), 203–209.

(49) Gallei, M.; Klein, R.; Rehahn, M. *Macromolecules* **2010,** 43 (4), 1844–1854.

(50) Kloninger, C.; Rehahn, M. *Macromolecules* **2004,** 37 (5), 1720–1727.

(51) Zundel, T.; Baran, J.; Mazurek, M.; Wang, J.-S.; Jerome, R.; Teyssie, P. *Macromolecules* **1998,** 31 (9), 2724–2730.

(52) Wang, X.-S.; Winnik, M. A.; Manners, I. *Macromol. Rapid Commun.* **2002,** 23 (3), 210–213.

(53) Schacher, F. H.; Elbert, J.; Patra, S. K.; Mohd Yusoff, S. F.; Winnik, M. A.; Manners, I. *Chem. □Eur. J.* **2012,** 18 (2), 517–525.

(54) Resendes, R.; Massey, J.; Dorn, H.; Winnik, M. A.; Manners, I. *Macromolecules* **2000,** 33 (1), 8–10.

(55) Gohy, J.-F.; Lohmeijer, B. G. G.; Alexeev, A.; Wang, X.-S.; Manners, I.; Winnik, M. A.; Schubert, U. S. *Chem. Eur. J.* **2004,** 10(17), 4315–4323.

(56) Hillmyer, M. A.; Bates, F. S. *Macromolecules* **1996,** 29 (22), 6994–7002.

(57) Natalello, A.; Tonhauser, C.; Berger-Nicoletti, E.; Frey, H. *Macromolecules* **2011**, *44*, 9887–9890.

(58) Tonhauser, C.; Frey, H. *Macromol. Rapid Commun.* **2010,** 31(22), 1938–1947.

(59) Tonhauser, C.; Wilms, D.; Wurm, F.; Berger-Nicoletti, E.; Maskos, M.; Löwe, H.; Frey, H. *Macromolecules* **2010,** 43 (13), 5582−5588.

(60) Quirk, R. P.; Gomochak, D. L. *Rubber Chem. Technol.* **2003,** 76(4), 812−831.

(61) Tonhauser, C.; Obermeier, B.; Mangold, C.; Löwe, H.; Frey, H. *Chem. Commun.* **2011,** 47 (31), 8964−8966.

(62) Zhang, W.-B.; Sun, B.; Li, H.; Ren, X.; Janoski, J.; Sahoo, S.; Dabney, D. E.; Wesdemiotis, C.; Quirk, R. P.; Cheng, S. Z. D. *Macromolecules* **2009,** 42 (19), 7258−7262.

(63) Li, Z.; Kesselman, E.; Talmon, Y.; Hillmyer, M. A.; Lodge, T. P. *Science* **2004,** 306 (5693), 98−101.

(64) Higashihara, T.; Kitamura, M.; Haraguchi, N.; Sugiyama, K.; Hirao, A.; Ahn, J. H.; Lee, J. S. *Macromolecules* **2003,** 36 (18), 6730−6738.

(65) Bender, J. T.; Knauss, D. M. *Macromolecules* **2009,** 42 (7), 2411−2418.

(66) Dingels, C.; Schömer, M.; Frey, H. *Chem. unserer Zeit* **2011,** 45(5), 338−349.

(67) Quirk, R. P.; Ma, J. J. *J. Polym. Sci*., *Part A: Polym. Chem.* **1988,** 26 (8), 2031−2037.

(68) Furukawa, J.; Saegusa, T.; Tsuruta, T.; Kakogawa, G. *Macromol. Chem. Phys.* **1960,** 36 (1), 25−39.

(69) SECdata of PVFc polymer with PS standards are listed to enable the reproducibility of this works for other groups even if no PVFc standards are available.

(70) Deschenaux, R.; Even, M.; Guillon, D. *Chem. Commun.* **1998**, 5, 537−538.

(71) Mangold, C.; Wurm, F.; Obermeier, B.; Frey, H. *Macromol. Rapid Commun.* **2010,** 31 (3), 258−264.

(72) Mangold, C.; Dingels, C.; Obermeier, B.; Frey, H.; Wurm, F. *Macromolecules* **2011,** 44 (16), 6326−6334.

(73) Hofmann, A. M.; Wurm, F.; Hühn, E.; Nawroth, T.; Langguth, P.; Frey, H. *Biomacromolecules* **2010,** 11 (3), 568−574.

(74) Wilms, D.; Schömer, M.; Wurm, F.; Hermanns, M. I.; Kirkpatrick, C. J.; Frey, H. *Macromol. Rapid Commun.* **2010,** 31(20), 1811−1815.

(75) Pittman, C. U.; Lai, J. C.; Vanderpool, D. P.; Good, M.; Prado, R. *Macromolecules* **1970,** 3 (6), 746−754.

(76) Sunder, A.; Hanselmann, R.; Frey, H.; Mülhaupt, R. *Macromolecules* **1999,** 32 (13), 4240–4246.

(77) Hadjichristidis, N.; Pitsikalis, M.; Pispas, S.; Iatrou, H. *Chem. Rev.* **2001,** 101 (12), 3747–3792.

(78) Hadjichristidis, N. *J. Polym. Sci., Part A: Polym. Chem.* **1999,** 37(7), 857–871.

(79) Due to the difference in polymer architecture the dn/dc values were determined for both samples with 0,0802 for $PVFc_4$-BGE-PEO_{92} and 0,0778 for $PVFc_{11}$-$(PEO_{61})_2$

(80) Costa, L.; Gad, A. M.; Camino, G.; Cameron, G. G.; Qureshi, M. Y. *Macromolecules* **1992,** 25 (20), 5512–5518.

(81) Hoevetborn, T.; Hoelscher, M.; Keul, H.; Höcker, H. *Rev. Roum. Chim.* **2006,** 51, 781–793.

(82) Xiao, Z.-P.; Cai, Z.-H.; Liang, H.; Lu, J. *J. Mater. Chem.* **2010,** 20(38), 8375–8381.

(83) Power-Billard, K. N.; Spontak, R. J.; Manners, I. *Angew. Chem., Int. Ed.* **2004,** 43 (10), 1260–1264.

(84) Takeoka, Y.; Aoki, T.; Sanui, K.; Ogata, N.; Yokoyama, M.; Okano, T.; Sakurai, Y.; Watanabe, M. *J. Controlled Release* **1995,** 33(1), 79–87.

(85) Ma, Y.; Dong, W.-F.; Hempenius, M. A.; Möhwald, H.; Julius Vancso, G. *Nat. Mater.* **2006,** 5 (9), 724–729.

(86) Zhang, L.; Eisenberg, A. *Science* **1995,** 268 (5218), 1728–1731.

3.3: A Combined DPE/Epoxide Termination Strategy for Hydroxyl End-functional Poly(2-vinylpyridine) and Amphiphilic AB_2-Miktoarm Stars*

Adrian Natalello, Christoph Tonhauser, Elena Berger-Nicoletti and *Holger Frey*

Institute of Organic Chemistry, Organic and Macromolecular Chemistry, Duesbergweg 10-14 Johannes Gutenberg-University Mainz, 55099 Mainz, Germany

Published in *Macromolecules* **2011**, *44*, 9887-9890

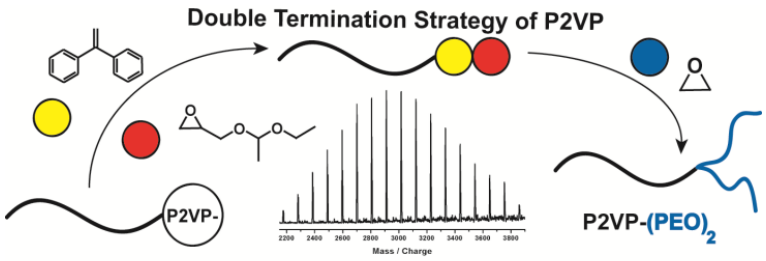

Keywords: poly(vinylpyridine), anionic polymerization, diphenylethylene, DPE, ethoxy ethyl glycidyl ether (EEGE), miktoarm star polymer

Abstract

End-functionalization of poly(2-vinylpyridine) (P2VP) obtained by living anionic polymerization via termination with an acetal-protected, functional epoxide is described. To avoid the branching side reaction at elevated temperature in the living polymerization of P2VP, a novel double termination strategy was developed. In the first termination step of the living P2VP with 1,1-diphenylethylene (DPE) the well-known branching reaction could be suppressed, and the desired hydroxyl chain-end was introduced by using ethoxy ethyl glycidyl ether (EEGE) as a second termination reagent. This “double” functionalization route leads to quantitative incorporation of EEGE at the chain terminus. Subsequent release of the protecting acetal by acidic hydrolysis leads to dihydroxyl end-functionalized P2VP (M_n=1500-

5700 g mol^{-1}, PDI = 1.12-1.09). This polymer was used as a macroinitiator to prepare a novel amphiphilic AB_2-miktoarm star polymer consisting of one P2VP and two poly(ethylene oxide) (PEO) chains. All polymers were characterized by size exclusion chromatography (SEC), NMR spectroscopy and MALDI-ToF MS, confirming full functionalization of the chain ends.

* results of joint work with Adrian Natalello in the content of a diploma thesis

Poly(vinylpyridine) (PVP) is a polymer with remarkable properties that plays an important role in complex polymer architectures, mainly due to its pH-responsive chain. There are numerous examples of block copolymers that contain at least one poly(2-vinylpyridine) (P2VP) block (diblock,[1] multiblock,[2] and miktoarm star polymers[3]). In a variety of elegant works the peculiar properties of PVP have been exploited, particularly with respect to its pH-sensitive[4,5] behavior, its interaction with transition metals salts,[6] and in the field of nanolithography.[7] Klingelhöfer et al.[8] have demonstrated the catalytic efficiency of colloidally dispersed palladium nanoparticles in block copolymer micelles of PS-*b*-P4VP and introduced the possibility of performing a Heck reaction in standard organic solvents with an increased catalyst stability compared to classical palladium complexes. On the basis of this work, P4VP- and P2VP-dispersed transition metals salts have been investigated, particularly with regard to their catalytic impact in coupling reactions such as Suzuki, Heck, and Stille.[9] Additionally, Ruokolainen et al. applied PS–P4VP block copolymers as temperature-sensitive electrical semiconductors by protonating the P4VP block quantitatively with methane-sulfonic acid (MSA), building up hydrogen bonds to pentadecylphenol. These materials form reversible, temperature-dependent microphaseseparation that controls ionic conductivity.[10] Although the living carbanionic polymerization represents a highly useful technique for the preparation of PVP with tailored chain length and narrow molecular weight distribution, there is a problematic issue: The carbanionic chain end of the living P2VP can attack the electron-poor pyridine ring of the backbone, leading to branched and cross-linked polymeric side products.[11] Characterization of this undesired process was achieved by Sigwalt and Tardi.[12] An established strategy to overcome the formation of high molecular weight side products is the addition of inorganic salts, such as lithium chloride to the reaction, followed by fast quenching.[13] In this case LiCl and the living P2VP are in equilibrium with the corresponding aggregates, which reduces the reactivity with simultaneous increase of the selectivity. However, this reaction route necessitates additional work-up and purification steps. Rapid termination of the living polymer with an appropriate compound to decrease the chain end reactivity could be an alternative strategy to suppress the side reactions. Commonly used termination reagents for PVP are chlorosilanes,[14] epoxides,[15] and diphenylethylene (DPE)[16] derivatives. In particular, DPE derivatives are prominent and have recently been employed to incorporate various functional groups at the polymer backbone[17]

or in the terminal position.[18] Furthermore, DPE derivatives can be used to build up unusual macromolecular architectures.[19] The significant advantage of DPE is the absence of self-propagation due to its sterical hindrance and the decrease in nucleophilicity of the carbanionic chain end. Although DPE is frequently used to moderate the reactivity of living carbanionic polymers, it is surprising to note that DPE has rarely been employed for end-capping reactions of P2VP. Müller and co-workers used DPE-terminated P2VP to polymerize tert-butyl methacrylate (tBMA), preparing two different linear terpolymers (PS-*b*-P2VP-*b*-PtBMA and PB-*b*-P2VP-*b*-PtBMA).[20,21]

Epoxides represent another class of valuable end-capping reagents for carbanionic polymerization.[15,22] On the one hand, they can provide a large variety of functional groups combined with a high reactivity toward nucleophilic attack due to the pronounced ring strain.[23,24] On the other hand, the termination allows for facile transformation of a carb-anionic chain end to an oxyanionic macroinitiator with a hydroxyl group.[25]

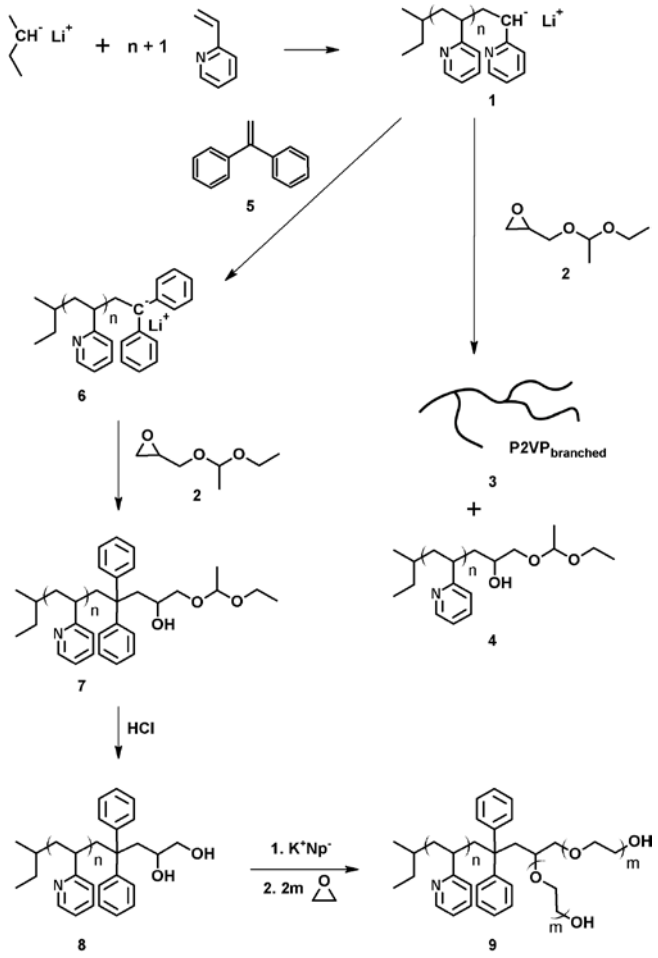

Scheme 1. Synthetic strategy for P2VP-EEGE and amphiphilic P2VP-$(PEO)_2$ miktoarm star.

In the current work a two-step termination strategy for the preparation of hydroxyl end-functional P2VP has been developed. P2VP was end-capped successively with DPE and ethoxy ethyl glycidyl ether (EEGE) to introduce hydroxyl termini after hydrolysis. After removal of the acetal protecting group by acidic hydrolysis, the resulting end-functional P2VP-$(OH)_2$ has been utilized as a macroinitiator for the polymerization of ethylene oxide (EO) to afford a novel AB_2 miktoarm star polymer P2VP−(PEO_2). An overview of the synthetic strategy is shown in Scheme 1. It is an unusual feature of this strategy that P2VP is used as the first block for the synthesis of miktoarm star structures.

All polymers described in this contribution have been synthesized by high-vacuum techniques at low temperatures (−78 °C) and in a polar solvent (THF) to obtain a highly reactive chain end for the desired end-capping procedure. For the direct end-capping reaction of living P2VP with EEGE, it is necessary to increase the temperature after the addition; otherwise, there is no incorporation of the epoxide (see Figures S4 and S5). As shown in Scheme 1 (top, right side), even at higher temperatures subsequent to the addition of EEGE to the living P2VP chains the reddish color remained for several hours, indicating the non-instantaneous termination with EEGE. In this period there is a competition between the desired epoxide termination and the attack of the P2VP carbanions on the electron-poor pyridine ring, resulting in the branched high molecular weight byproduct. Because of this competition, one obtains a bimodal, broad molecular-weight distribution (MWD) with a high PDI of 13.51 (no. 1, Table 1) in direct end-capping experiments, containing a main polymer mode at 2300 g mol^{-1} and a large amount of branched P2VP, which can be identified at high molecular weight in the SEC trace (Figure 1, left). Additionally the branching reaction was observed by ^{13}C NMR spectroscopy (Figure S2). Matrix-assisted laser desorption/ionization time-of-flight mass spectroscopy (MALDI-Tof MS) (Figure S3) of the low molecular weight, linear polymer confirmed complete functionalization with EEGE, indicating no undesired proton termination.

In contrast to this direct epoxide termination, we were able to prevent the undesired branching reaction by precapping the living P2VP with DPE and subsequent addition of EEGE. This “double termination” procedure has been studied for molecular weights in the range 1500−5700 g mol^{-1} and resulted in a single narrow distribution mode (PDI = 1.09−1.12, Table 1) for all polymer samples.

Table 1. Molecular characteristics of the polymers prepared.

no.	polymer[a]	M_n[a]	PDI[b]
1	P2VP-EEGE	5400	13.51
2	P2VP-DPE-EEGE	2100	1.12
3	P2VP-DPE-EEGE	3200	1.10
4	P2VP-DPE-EEGE	5700	1.09
5	P2VP-DPE-$EEGE_d$[c]	3200	1.11
6	P2VP-$(PEO)_2$	20600	1.13

[a]Molecular weight in g mol^{-1}, calculated from ^{1}H NMR, [b]MWD characterized by SEC in DMF (PS-standard), [c] polymer no. 3 after acidic hydrolysis leading to a dihydroxyl end-functional P2VP.

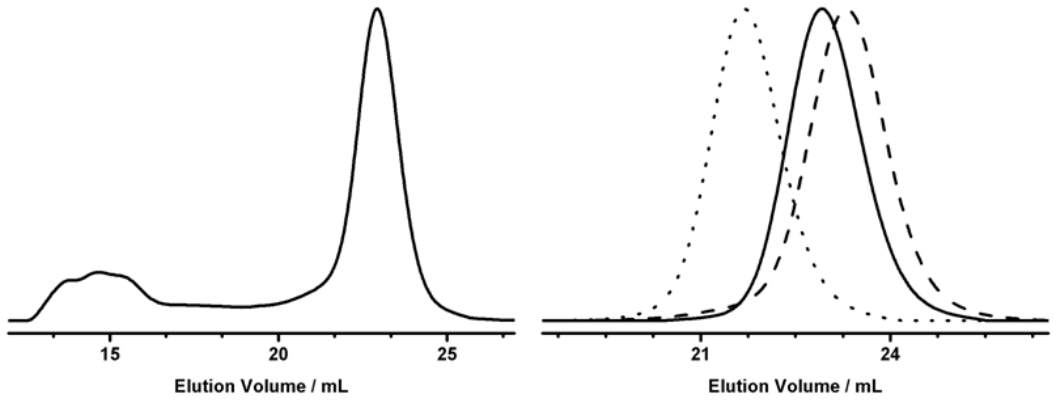

Figure 1. (left) SEC trace of P2VP-EEGE (no. 1) in case of direct EEGE termination. (right) Double termination resulting in P2VP-DPE-EEGE (nos. 2-4) (dotted line: no. 4; solid line: no. 3, dashed line: no. 2)

Conclusive evidence for quantitative termination of the double-terminated polymer samples (nos. 2–4, Table 1) was gained from MALDI-ToF MS. Each signal of the resulting spectra can be assigned to EEGE-terminated polymer chains (Figure S13). Both spectra of Figure 2 contain only one distribution mode for the desired polymer, which demonstrates that all chain ends are double-terminated. Subsequently, all acetal groups of the P2VP–DPE–EEGE were cleaved by treating the polymers with hydrochloric acid, which is confirmed by the calculated shift of the distribution by 72.11 Da (Figure 2).

In combination with the results of SEC characterization, it can be concluded that this procedure leads to quantitative end-functionalization of P2VP (**7**) without any side product. The potential of this strategy is emphasized, if one considers that the reaction mixture of the

DPE-capped P2VP (**6**) and the glycidyl ether capping reagent had to be warmed up to room temperature to obtain quantitative conversion. The key step of the presented work is thus DPE-capping of P2VP that allows for the reaction with an epoxide termination reagent and suppression of the branching side reaction, most probably due to the steric hindrance at the active chain end. We presume that the double termination strategy is general for a broad range of functionalized epoxides with various functionalities, such as multiple hydroxyl, amino, allyl, and nitroxy groups.[15]

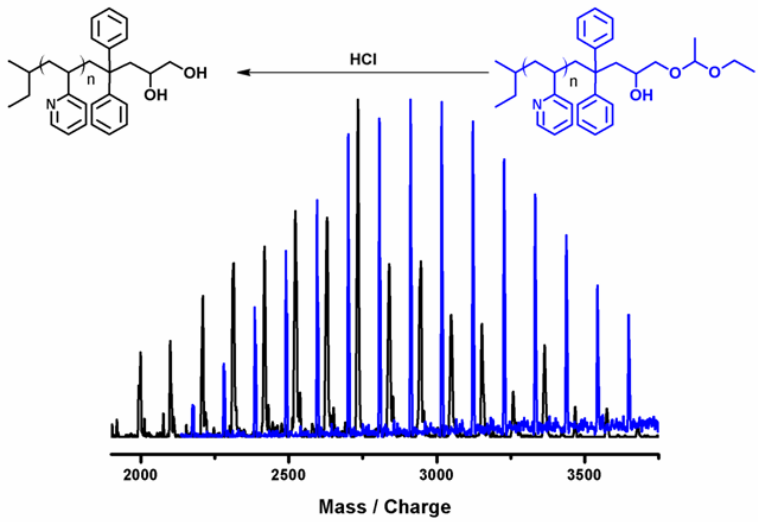

Figure 2. MALDI-ToF spectra of the cleavage of the protecting acetal by acidic hydrolysis (no. 3 → no. 5). Blue lines represent protected precursor compound.

In order to demonstrate a possible application for the synthesized P2VP–DPE–$EEGE_d$ (**8**), we employed the polymer as a macroinitiator for the anionic ring-opening polymerization of ethylene oxide (EO), resulting in an AB_2-type miktoarm star polymer. Miktoarm star polymers with AB_2 structure have e.g., been prepared by Glaied et al.[26,27] Seminal work on miktoarm star polymers has been carried out by Hadjichristidis and co-workers.[28,29] Linear AB-block copolymers containing PVP and PEO segments have also been described in several works that capitalize on the pH sensitivity to achieve reversible assembly and disassembly of polymer micelles in aqueous solution.[4,5,30,31] However, to the best of our knowledge, miktoarm stars consisting of PVP and PEO have not been described yet.

We have prepared an amphiphilic, pH-sensitive AB_2-miktoarm star polymer consisting of one P2VP and two PEO arms (P2VP–PEO_2, no. 6; cf. Scheme 1, bottom). The hydroxyl groups of the P2VP–DPE–$EEGE_d$ (no. 5, Table 1) were deprotonated by potassium naphthalide, and

subsequently polymerization of ethylene oxide has been carried out. Block copolymerization was monitored by SEC (see Figure 3; ^{1}H NMR: Figure S9), and the resulting materials have been analyzed by dynamic light scattering (DLS) at pH = 7 and pH = 1. Because of the PEO-*b*-P2VP structures, the micelles formed by the AB_2-miktoarm star polymer grow from 78.6 to 84.0 nm upon decreasing the pH value. This is a consequence of the protonation of the P2VP chain. Further, detailed studies on solution and bulk structures of the resulting amphiphilic AB_2-miktoarm stars with different chain length are in progress.

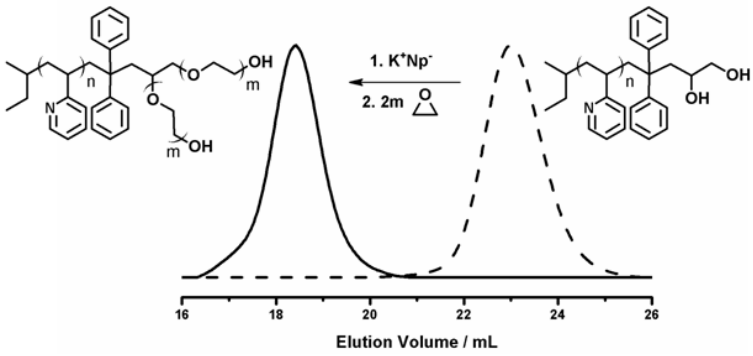

Figure 3. SEC curves of terminated precursor (P2VP-DPE-EEGE$_d$, right) and a miktoarm star polymer (P2VP-PEO$_2$, left) (no. 6) with two PEO chains.

In summary, well-defined hydroxyl end-functional P2VP with narrow molecular weight distribution has been synthesized by carbanionic polymerization. Quantitative end-capping was achieved by a novel double termination process by successively adding DPE and EEGE to the living polymer chains. The key step is the reaction of the living P2VP with DPE prior to epoxide termination, which prevents the coupling side reaction of the living P2VP chains. In addition, a novel AB_2 miktoarm star polymer P2VP–(PEO$_2$) has been synthesized. Further studies on the aggregation behavior as well as other functionalization sequences with other glycidyl ethers are in progress, aiming at other PVP-*b*-polyether miktoarm stars.

Acknowledgments

A.N. thanks the Stipendienstiftung Rheinland Pfalz for financial support. C.T. acknowledges the MPGC (Max Planck Graduate Center with Johannes Gutenberg-University) and the Excellence Initiative (DFG/GSC 266) for fellowships and financial support. We thank Svenja Winzen for the DLS measurements.

Supporting Information

Experimental Section

Reagents

All solvents and reagents were purchased from Acros Organics or Sigma Aldrich and used as received unless otherwise stated. Chloroform-d_1 was purchased from Deutero GmbH. Tetrahydrofuran (THF) was distilled from sodium/benzophenone under reduced pressure into a cooled reaction vessel (cryo-transfer). Vinyl pyridine, diphenyl-ethylene (DPE), and ethoxy ethyl glycidyl ether (EEGE) were dried over calcium hydride (CaH_2) and cryo-transferred prior to use. *Sec*-butyllithium (*sec*-BuLi, 1,3 M, Acros) was used as received and the concentration of the initiator was determined by the Gilman double titration method.[32] EEGE was synthesized as reported previously.[33]

Instrumentation

NMR spectra were recorded at 300 MHz or 400 MHz on a Bruker AC300 or Bruker AMX400 respectively and were referenced internally to residual proton signals of the deuterated solvent. For SEC measurements in DMF (containing 0.25 g/L of lithium bromide as an additive) an Agilent 1100 Series was used as an integrated instrument, including a PSS HEMA column (106/105/104 g/mol), a UV (275 nm) and a RI detector. All SEC diagrams show the RI detector signal, and the molecular weight refers to linear poly(styrene) (PS) standards provided by Polymer Standards Service (PSS). Dynamic light scattering (DLS) was measured on an ALV/CGS3 compact goniometer system with a He/Ne laser (632.8 nm), ALV/LSE-5004 correlator and ALV5000 software. Matrix-assisted laser desorption/ionization time-of-flight (MALDI-ToF) measurements were performed using a Shimadzu Axima CFR MALDI-ToF mass spectrometer, employing silver trifluoro-acetate as a cationizing agent and dithranol (1,8,9-trishydroxy-anthracene) as a matrix.

Synthesis of P2VP-EEGE (no. 1)

The P2VP-EEGE sample was synthesized by a sequential anionic living polymerization in 100 mL THF using 1.35 mL (1.76 mmol) *sec*-BuLi as initiator. The mixture of initiator in THF was cooled down to -78 °C using an acetone dry ice bath. Then 5.15 g (48.98 mmol) of 2VP was cryo-transferred to the vigorously stirred system and the typical reddish color was observed. After adding EEGE (0.50 g, 3.44 mmol, 2 eq.) to the reaction mixture via syringe, the mixture was allowed to warm up to room temperature. The color slowly changed from red to yellow over a period of several hours. After 24 h the reaction was terminated by methanol via syringe. The resulting polymer was precipitated in petroleum ether (yield = 90%). ^{1}H NMR (300 MHz, $CDCl_3$, δ in ppm): 8.50-7.99 (m, H3 of aromatic system of P2VP), 7.46-5.95 (m, H4-6 of aromatic system of P2VP), 4.57 (s, 1H, acetal group), 4.03-3.02 (m, 5H, CH_2 CH_3 EEGE), 2.70-0.72 (CH_3 EEGE, CH_2 CH initiator, P2VP backbone), 0.72-0.50 (m, 6H, Initiator)

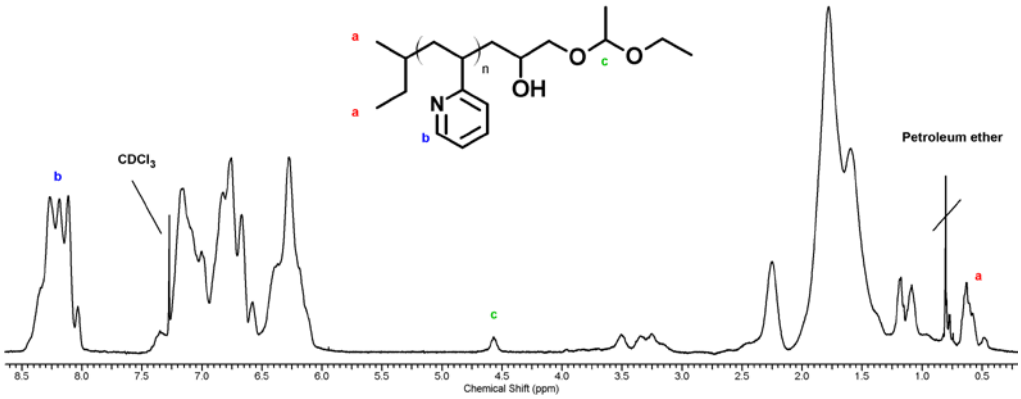

Figure S1. ^{1}H NMR (300 MHz, $CDCl_3$) spectrum of PS-EEGE (no. 1) (Table 1)

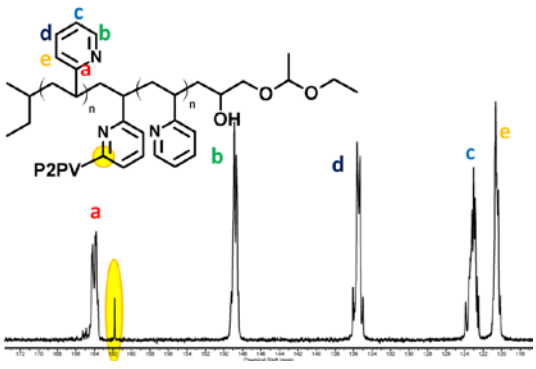

Figure S2. ^{13}C NMR (400 MHz, $CDCl_3$) spectrum of P2VP-EEGE (no. 1) shows (compared to linear P2VP) a signal at 162 ppm indicating the branching points.

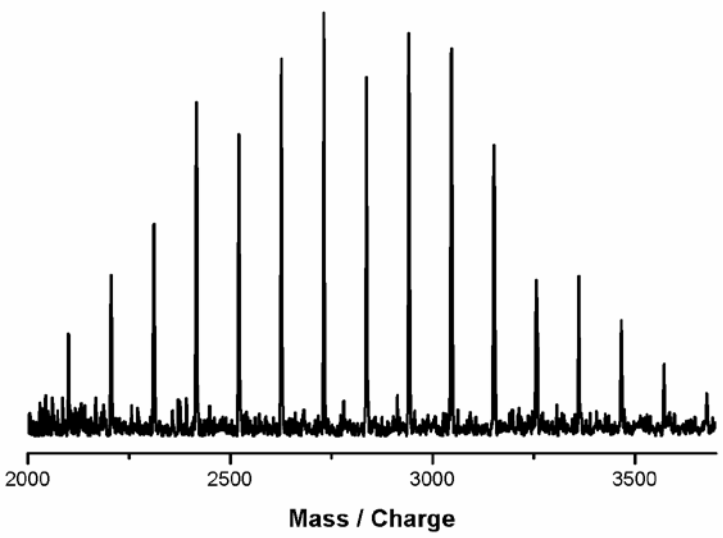

Figure S3. MALDI-ToF spectrum of P2VP-EEGE (no. 1)

Synthesis of P2VP-EEGE at -78 °C

The P2VP-EEGE sample was synthesized in close analogy to polymer no. 1. The anionic living polymerization was carried out in 60 mL THF under vacuum. Then 2.22 g (21.11 mmol) of 2VP were cryo-transferred to the vigorously stirred with 0.68 mL (0.88 mmol) *sec*-BuLi initiated THF solution (T = -78 °C), and the typical reddish color was observed. After adding EEGE (0.26 g, 1.77 mmol, 2 eq.) to the reaction mixture via syringe the color did not change over a period of 10 h. The reaction mixture was terminated by adding methanol via syringe and the color changed to colorless. The resulting polymer was precipitated in petroleum ether (yield = 91%). ^{1}H NMR (300 MHz, $CDCl_3$, δ in ppm): 8.55-7.97 (m, H3 of aromatic system of P2VP), 7.53-6.06 (m, H4-6 of aromatic system of P2VP), 2.67-0.74 (CH_2 CH initiator, P2VP backbone), 0.74-0.42 (m, 6H, Initiator)

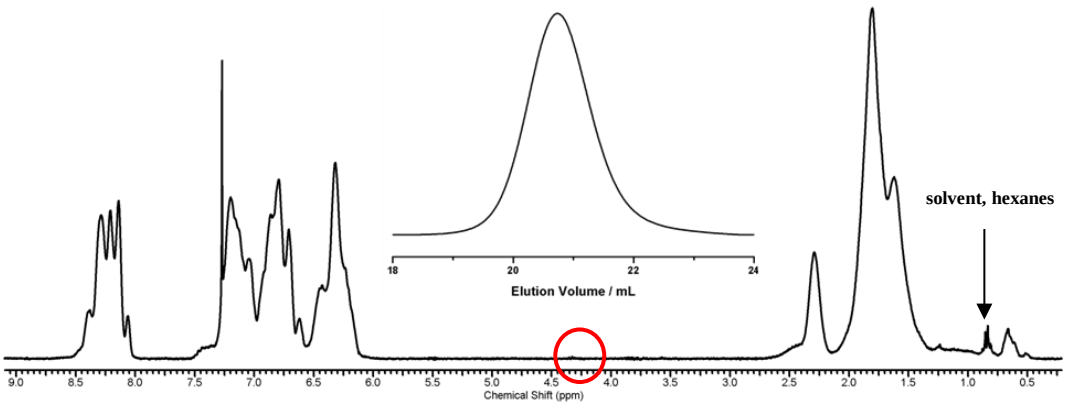

Figure S4. ^{1}H NMR (300 MHz, $CDCl_3$) spectrum of P2VP polymerized at -78 °C in the presence of EEGE (M_n = 7500 gmol^{-1}), SEC trace of P2VP (PDI = 1,09)

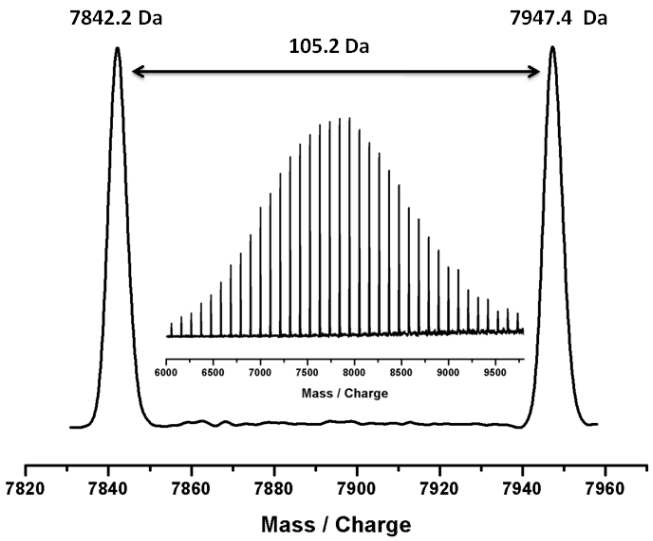

Figure S5. MALDI-ToF spectrum of P2VP polymerized at -78 °C in the presence of EEGE, the single distribution mode can be assigned to P2VP-H

Synthesis of P2VP-DPE-EEGE (no. 2-4)

The polymerization and termination of polymer no. 3 was carried out in analogy to the synthesis of P2VP-EEGE. After cryo-transferring 2.84 g (27.02 mmol) of 2VP to the initiator solution (0.87 mL (1.13 mmol) *sec*-BuLi dissolved in 60 mL THF), DPE (0.46 g, 2.55 mmol, 2.3 eq.) was added via syringe and stirred for 30 min before adding the corresponding amount of EEGE (0.33 g, 2.26 mmol, 2.0 eq.). The work-up was carried out as described

previously in the case of the P2VP-EEGE (yield: 90%; polymer no. 2 and no. 4 have been prepared by an analogous procedure). (polymer no. 3, 300 MHz, $CDCl_3$, δ in ppm): 8.51-7.98 (m, H3 of aromatic system of P2VP), 7.43-5.78 (m, H4-6 of aromatic system of P2VP, aromatic system of DPE), 4.40 (s, 1H, acetal group), 4.13-3.08 (m, 5H, CH_2 CH_3 EEGE), 3.04-0.73 (CH_3 EEGE, CH_2 CH initiator, P2VP backbone, CH_2 CH of DPE), 0.73-0.43 (m, 6H, initiator)

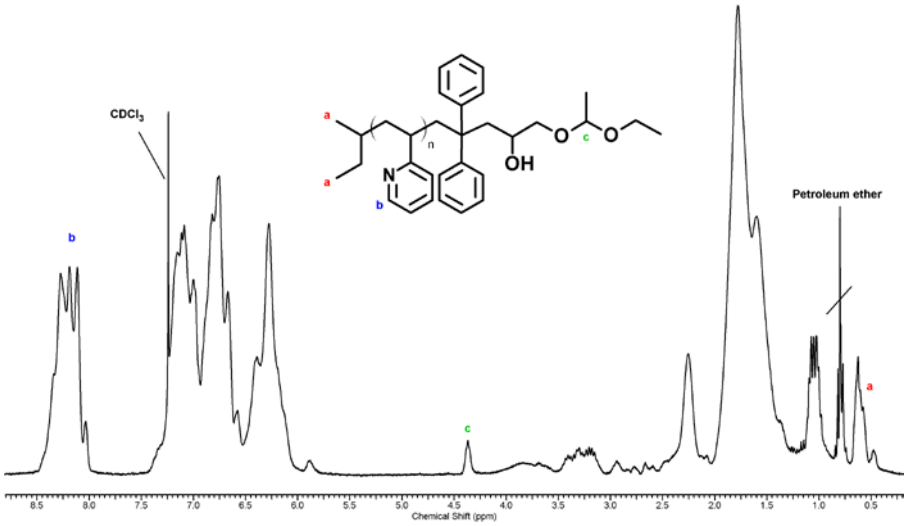

Figure S6. ^{1}H NMR (300 MHz, $CDCl_3$) spectrum of PS-DPE-EEGE (no. 3)

Synthesis of P2VP-DPE-EEGE$_d$ (no. 5)

For the deprotection of 1.6 g (0.5 mmol) P2VP-DPE-EEGE (no. 3) the polymer was dissolved in 75 mL acidified methanol (pH ≈ 1). Then the reaction mixture was stirred for 6 hours at 50 °C under argon atmosphere. After evaporating the solvent the polymer was dissolved in chloroform and neutralized with a saturated sodium hydrogen carbonate solution. The organic phase was concentrated by distillation under reduced pressure. The polymer was precipitated in petroleum ether (yield: 66%, lowered due to repeated precipitation steps). (300 MHz, CDCl3, δ in ppm): 8.54-7.97 (m, H3 of aromatic system of P2VP), 7.49-5.65 (m, H4-6 of aromatic system of P2VP, aromatic system of DPE), 4.05-0.73 (backbone), 0.73-0.44 (m, 6H, Initiator)

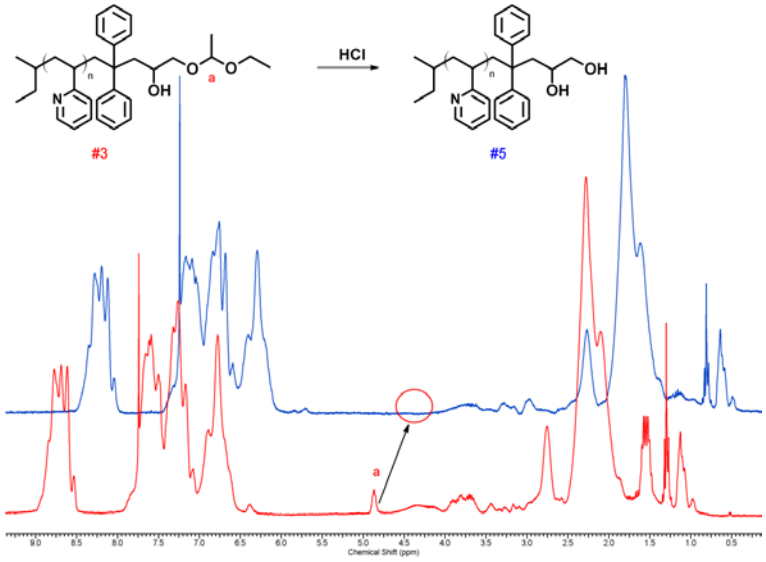

Figure S7. ^{1}H NMR (300 MHz, $CDCl_3$) spectrum of PS-DPE-EEGE (no. 3) and PS-DPE-$EEGE_d$ (no. 5)

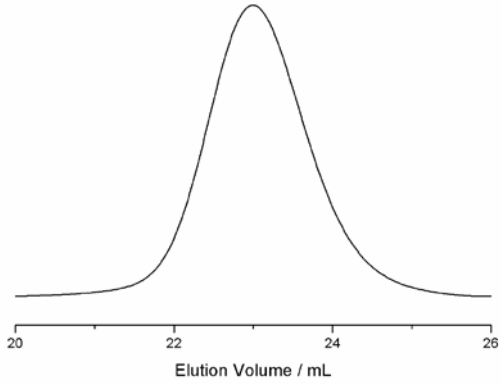

Figure S8. SEC trace of P2VP-DPE-$EEGE_d$ (no. 5)

Synthesis of P2VP-$(PEO)_2$ (no. 6)

150 mg (46.9 µmol) of P2VP-DPE-$EEGE_d$ (no. 5) were dissolved in 20 mL dry THF in a 50 mL Schlenk flask and titrated with potassium naphthalide (0.1 M) until a slight green color maintained under argon atmosphere. After evacuation of the reaction vessel the monomer ethylene oxide (EO, 1.41 g, 32.01 mmol) was cryo-transferred into a graduated ampoule and subsequently into the reaction flask at approximately -80 °C. The greenish color disappeared rapidly. The reaction mixture was heated up to 60 °C and stirred for 48 h. After evaporating the solvent the polymer was dissolved in chloroform and the pure polymer was obtained by

fractionating precipitation to remove small amounts of unreacted precursor in a solvent/ non-solvent mixture of chloroform/petroleum ether and dried in vacuum at room temperature. (300 MHz, $CDCl_3$, δ in ppm): 8.48-8.01 (m, H3 of aromatic system of P2VP), 7.40-5.89 (m, H4-6 of aromatic system of P2VP, aromatic system of DPE), 3.92-3.35 (m, PEO backbone), 3.03-0.74 (backbone), 0.74-0.45 (m, 6H, initiator).

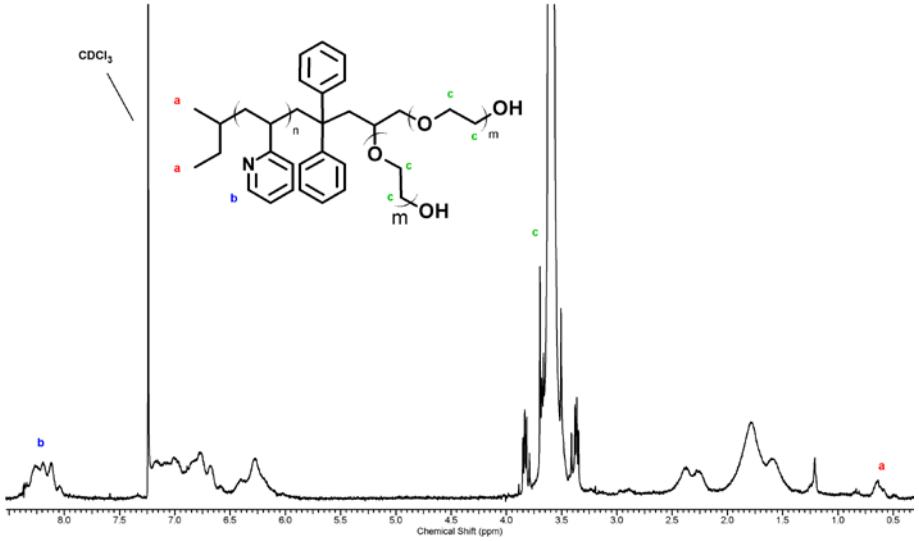

Figure S9. ^{1}H NMR (300 MHz, $CDCl_3$) spectrum of P2VP-$(PEO)_2$ (no. 6)

Additional Characterization Spectra:

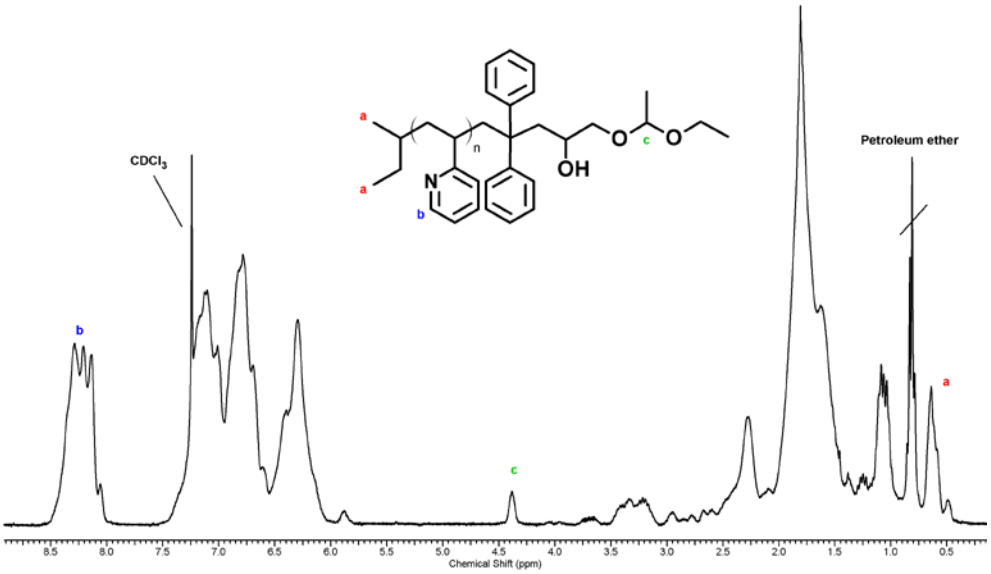

Figure S10. ^{1}H NMR (300 MHz, $CDCl_3$) spectrum of PS-DPE-EEGE (no. 2)

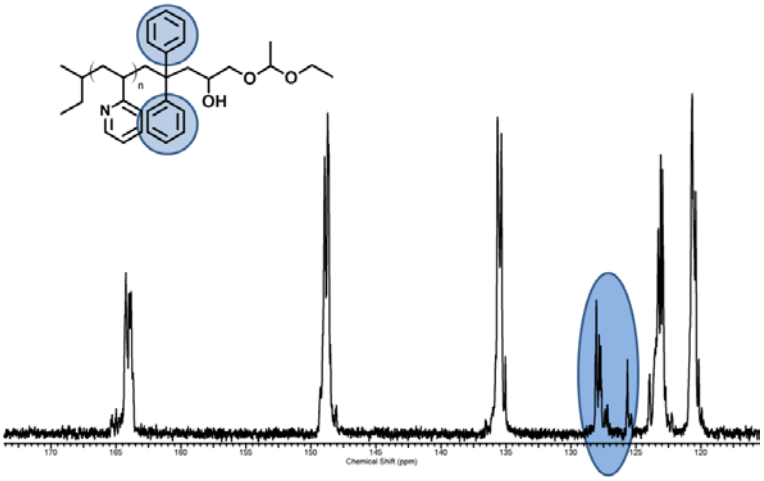

Figure S11. ^{13}C NMR (400 MHz, $CDCl_3$) spectrum of PS-DPE-EEGE (no. 3)

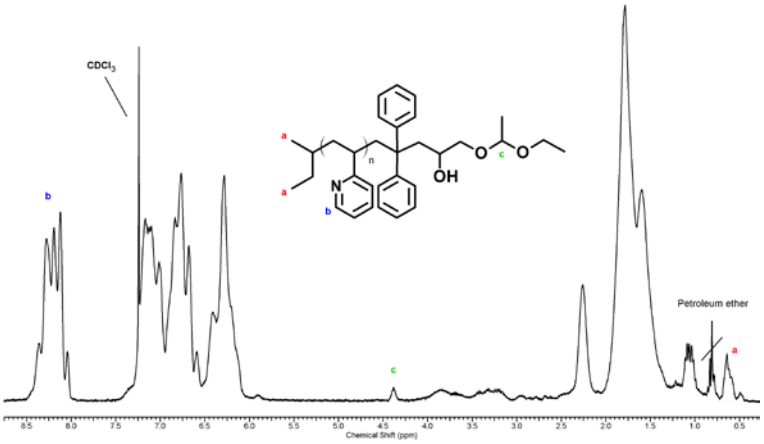

Figure S12. ^{1}H NMR (300 MHz, $CDCl_3$) spectrum of PS-DPE-EEGE (no. 4)

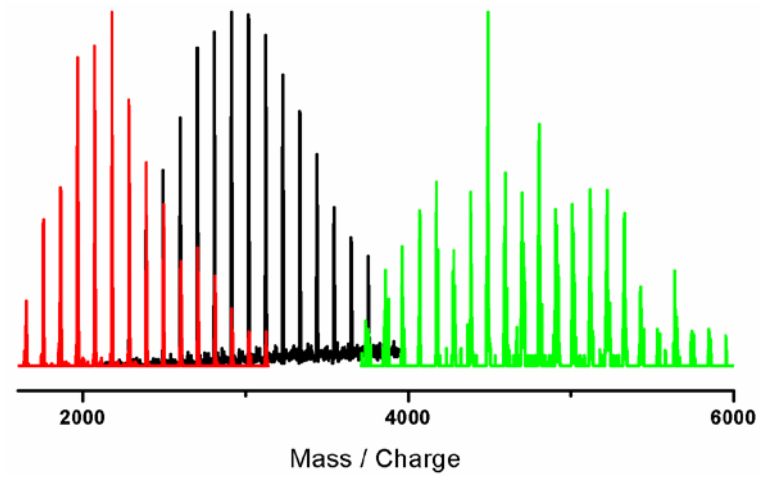

Figure S13. MALDI-ToF spectra of P2VP-EEGE (no. 2, no. 3 and no. 4)

References

(1) Kim, H.-C.; Park, S.-M.; Hinsberg, W. D. *Chem. Rev.* **2009**, *110*, 146−177.

(2) Takahashi, K.; Hasegawa, H.; Hashimoto, T.; Bellas, V.; Iatrou, H.; Hadjichristidis, N. *Macromolecules* **2002**, *35*, 4859−4861.

(3) Mavroudis, A.; Hadjichristidis, N. *Macromolecules* **2005**, *39*, 535−540.

(4) (a) Butsele, K. V.; Fustin, C. A.; Gohy, J. F.; Jérôme, R.; Jérôme, C. *Langmuir* **2008**, *25*, 107−111. (b) Borchert, U.; Lipprandt, U.; Bilang, M.; Kimpfler, A.; Rank, A.; Peschka-Süss, R.; Schubert, R.; Lindner, P.; Förster, S. *Langmuir* **2006,** *22,* 5843−5847.

(5) Martin, T. J.; Procházka, K.; Munk, P.; Webber, S. E. *Macromolecules* **1996**, *29*, 6071−6073.

(6) Tsutsumi, K.; Funaki, Y.; Hirokawa, Y.; Hashimoto, T. *Langmuir* **1999**, *15*, 5200−5203.

(7) Spatz, J. P.; Herzog, T.; Mößmer, S.; Ziemann, P.; Möller, M. *Adv. Mater.* **1999**, *11*, 149−153.

(8) Klingelhöfer, S.; Heitz, W.; Greiner, A.; Oestreich, S.; Förster, S.; Antonietti, M. *J. Am. Chem. Soc.* **1997**, *119*, 10116−10120.

(9) Pathak, S.; Greci, M. T.; Kwong, R. C.; Mercado, K.; Prakash, G. K. S.; Olah, G. A.; Thompson, M. E. *Chem. Mater.* **2000**, *12*, 1985−1989.

(10) Ruokolainen, J.; Mäkinen, R.; Torkkeli, M.; Mäkelä, T.; Serimaa, R.; ten Brinke, G.; Ikkala, O. *Science* **1998**, *280*, 557−560.

(11) Krasnoselskaya, I. G.; Erussalimsky, B. L. *Makromol. Chem., Rapid Commun.* **1985**, *6*, 191−195.

(12) Tardi, M.; Sigwalt, P. *Eur. Polym. J.* **1972**, *8*, 151−162.

(13) Quirk, R. P.; Corona-Galvan, S. *Macromolecules* **2001**, *34*, 1192−1197.

(14) Peters, M. A.; Belu, A. M.; Linton, R. W.; Dupray, L.; Meyer, T. J.; DeSimone, J. M. *J. Am. Chem. Soc.* **1995**, *117*, 3380−3388.

(15) Tonhauser, C.; Frey, H. *Macromol. Rapid Commun.* **2010**, *31*, 1938−1947.

(16) Quirk, R. P.; Yoo, T.; Lee, Y.; Kim, J.; Lee, B. In *Advances in Polymer Science*; Springer-Verlag: Berlin, 2000; Vol. 153, pp 67−162.

(17) Natalello, A.; Hall, J. N.; Eccles, E. A. L.; Kimani, S. M.; Hutchings, L. R. *Macromol. Rapid Commun.* **2011**, *32*, 233−237.

(18) Hutchings, L. R.; Sarih, N. M.; Thompson, R. L. *Polym. Chem.* **2011**, *2*, 851−861.

(19) Hirao, A.; Murano, K.; Oie, T.; Uematsu, M.; Goseki, R.; Matsuo, Y. *Polym. Chem.* **2011**, *2*, 1219−1233.

(20) Ludwigs, S.; Böker, A.; Abetz, V.; Müller, A. H. E.; Krausch, G. *Polymer* **2003**, *44*, 6815−6823.

(21) Schacher, F.; Walther, A.; Ruppel, M.; Drechsler, M.; Müller, A. H. E. *Macromolecules* **2009**, *42*, 3540−3548.

(22) Quirk, R. P.; Ma, J.-J. *J. Polym. Sci., Part A: Polym. Chem* **1988**, *26*, 2031−2037.

(23) Quirk, R. P.; Gomochak, D. L. *Rubber Chem. Technol.* **2003**, *76*, 812−831.

(24) Tonhauser, C.; Wilms, D.; Wurm, F.; Nicoletti, E. B.; Maskos, M.; Löwe, H.; Frey, H. *Macromolecules* **2010**, *43*, 5582−5588.

(25) Tonhauser, C.; Obermeier, B.; Mangold, C.; Löwe, H.; Frey, H. *Chem. Commun.* **2011**, *47*, 8964−8966.

(26) Glaied, O.; Delaite, C.; Dumas, P. *J. Polym. Sci., Part A: Polym. Chem.* **2007**, *45*, 4179−4183.

(27) Glaied, O.; Delaite, C.; Dumas, P. *J. Polym. Sci., Part A: Polym. Chem.* **2006**, *44*, 1796−1806.

(28) Hadjichristidis, N. *J. Polym. Sci., Part A: Polym. Chem.* **1999**, *37*, 857−871.

(29) Hadjichristidis, N.; Pispas, S.; Pitsikalis, M.; Iatrou, H.; Vlahos, C. *Adv. Polym. Sci.* **1999**, *142*, 71−127.

(30) Fragouli, P. G.; Iatrou, H.; Hadjichristidis, N. *Polymer* **2002**, *43*, 7141−7144.

(31) Yeh, C.-L.; Hou, T.; Chen, H.-L.; Yeh, L.-Y.; Chiu, F.-C.; Müller, A. J.; Hadjichristidis, N. *Macromolecules* **2011**, *44*, 440−443.

(32) H. Gilman and A. H. Haubein, *J. Am. Chem. Soc.*, **1944**, *66*, 1515-1516.

(33) Fitton, A. O.; Hill, J.; Jane, D. E.; Millar, R. *Synthesis* **1987**, *12*, 1140-1142.

Chapter 4: Stimuli-Responsive Polymer Films

4.1: Stimuli-Responsive Y-Shaped Polymer Brushes Based on Junction-Point Reactive Block Copolymers

Christoph Tonhauser,[1] *Ali A. Golriz,*[2] *Christian Moers,*[1] *Rebecca Klein,*[1] *Hans-Jürgen Butt**[2] and *Holger Frey**[1]

[1]Institute of Organic Chemistry, Organic and Macromolecular Chemistry Johannes Gutenberg-University (JGU), Duesbergweg 10-14, 55099 Mainz Germany

[2]Max-Planck-Institute for Polymer Research (MPI-P) Ackermannweg 10, 55128 Mainz Germany

Submitted for publication in *Advanced Materials* ***2012***

A general concept for the preparation of junction point-reactive, amphiphilic Y-shaped block copolymer brushes for ultrathin polymer films is demonstrated, combining anionic polymerization techniques. The polymer films (1-3 nm) exhibit reversible, stimuli-responsive wetting behavior upon application of different external stimuli (temperature and solvent). Contact angle measurements confirm the reversible hydrophobization with shifts up to 23°.

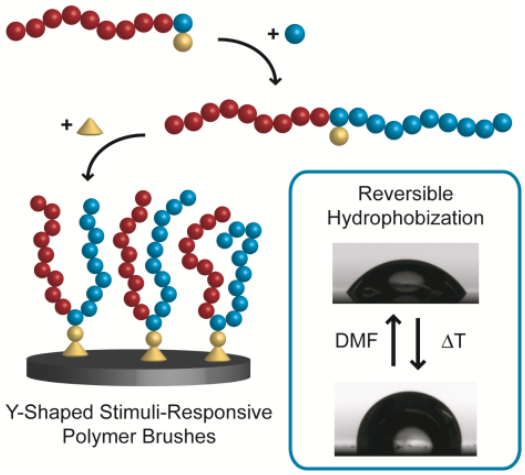

Keywords: Y-shaped polymer brushes, stimuli-responsive wetting, in-chain functionalized block copolymers, anionic polymerization, grafting-to method

Abstract

A general strategy for the synthesis of reversibly stimuli-responsive Y-shaped polymer brushes and their surface attachment is presented. The preparation of the respective junction point-reactive block copolymers (JPR-BC), the key materials of the strategy, relies on a combination of carbanionic and oxyanionic polymerization techniques. Allyl glycidyl ether (AGE) is utilized as an end-capping reagent for the anionic polymerization of poly-(styrene) (PS-(AGE)), achieving quantitative end-functionalization (MALDI-ToF MS). In the next step, PS-(AGE) is used as a macroinitiator for the anionic ring-opening polymerization of ethylene oxide to afford amphiphilic PS-(AGE)-PEO block copolymers with different block ratios in the range of 6 000 to 24 000 g mol^{-1}. The triethoxysilane anchor group (TEOS) for chemical grafting to silicon surfaces is introduced by hydrosilylation of PS-(AGE)-PEO leading to (PS-(TEOS)-PEO). All materials have been characterized by size exclusion chromatography (SEC), ^{1}H NMR spectroscopy and MALDI-ToF MS. After grafting the JPR-BC onto silicon surfaces under basic conditions, the Y-shaped polymer brush films were analyzed by X-ray reflectivity (XRR) and scanning force microscopy (SFM). The surface wetting shows reversible stimuli-responsive behavior when applying external stimuli (e.g., temperature and solvent), as observed via contact angle measurements. A contact angle shift of up to 23° from 61° to 84° and vice versa is observed after heating and *N,N*-dimethylformamide (DMF) treatment, respectively.

Introduction

Reversibly responsive, thin or ultrathin polymer films, often referred to as “smart surfaces”, can alter their properties upon application of external stimuli.[1, 2] One particular application field represents the engineering of nanostructured films mimicking cell membranes.[3, 4] Such materials offer application potential for sensors, textiles, construction materials and smart coatings due to a rapid change in surface energy and morphology.[5-7] The surface response can be triggered by various external stimuli such as light, temperature, electrical potential, mechanical force, magnetic field, pH change, or selective solvent treatment.[1, 8-12] A variety of different thin polymer films has been designed for this purpose. End-tethered polymers (e.g., (multiarm) block and homopolymers), layer-by-layer structures, cross-linked thin polymer films as well as hybrid systems with inorganic particles are established, complex structures to generate responsive surface coatings.[13-19]

Of particular interest are ultrathin polymer films capable of stimuli-responsive wetting, as they permit reversible switching in surface properties from hydrophilic to hydrophobic and thus offer potential applications in the field of self-cleaning[20], “smart” coatings[21, 22] and microfluidic devices[23]. With respect to polymers chemically bound to a surface, one can distinguish between homopolymer brushes[24] and mixed[25] or copolymer brushes[26]. Solvent treatment of copolymer or mixed polymer brushes induces a surface response that originates from phase segregation between the two incompatible polymer chains, depending on composition and morphology of the materials.[27]

In analogy to block copolymer brushes, mixed polymer brushes can be synthesized by grafting-from[28] and grafting-to[25] strategies. Minko et al. prepared a two-level structured self-adaptive surface consisting of (i) PTFE foils and (ii) poly(styrene–*co*-pentafluorostyrene) and poly(vinyl pyridine) polymer brushes, permitting to switch the wetting behavior from ultrahyrophobic to hydrophilic.[29] The morphologies of the mixed polymer brushes can be analyzed via SFM spectroscopy and the formation of ripple and dimple morphologies of the irreversibly attached polymer brushes can be controlled by treatment with non-selective or selective solvent, respectively.[30] These switching mechanisms pave the way to several applications, such as microfluidic “smart channels”, coated with stimuli-responsive polymer brushes.[31] Binary brushes of two oppositely charged polyelectrolytes (poly(vinyl pyridine)

and poly(acyrylic acid)) can be utilized in biosurface engineering to tune the pH-dependent protein adsorption behavior in aqueous solution.[32]

"Y-shaped" polymer brushes consisting of two incompatible polymer chains that are covalently linked with an in-chain anchor group to the surface represent a less studied area. The main advantage of these procedures is the homogenous distribution of both incompatible polymer chains over the complete surface, and suppression of segregation processes. In the few reported approaches these Y-shaped polymer brushes have been obtained by grafting-from[33] (attachment of a difunctional initiator to the substrate) or grafting-to[34] (grafting via junction-point functionalized block copolymers). Theoretical studies concerning the variation of morphology depending on the grafting density, molecular weight and composition were carried out by Zhulina and Balazs.[35] Tsukruk and coworkers used carboxy-terminated PS and poly(*tert*-butyl acrylate) attached to 3,5-dihyroxybenzoic acid, which was used as an AB_2 anchoring moiety. After grafting to silicon wafers, poly(*tert*-butyl acrylate) was hydrolyzed to poly(acrylic acid) chains with high incompatibility with PS, leading to structural surface reorganization.[36] Wang et al. utilized a hydrosilylation grafting-to process to link block copolymers to silicon surfaces via a Si-H junction point. To increase immiscibility of the two arms the poly(vinyl pyridine) chains were quaternized with methyl iodide and a contact angle shift of up to 23° was observed.[37]

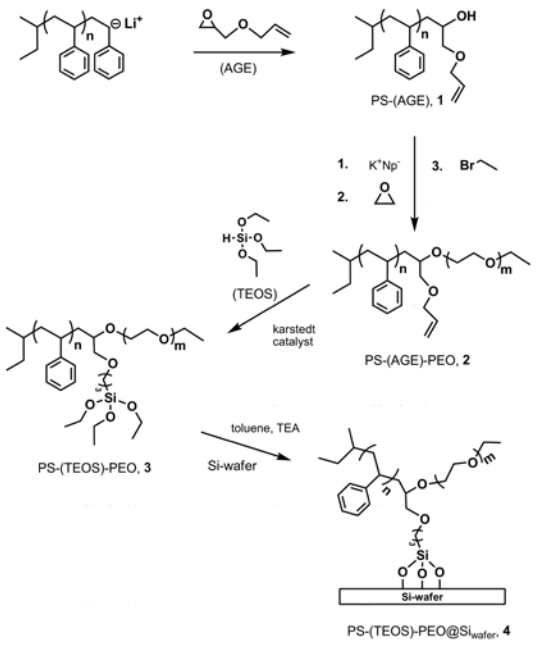

Scheme 1. Synthetic strategy to junction point reactive, amphiphilic Y-shaped polymer brushes (PS-(TEOS)-PEO@Si_{wafer}, **4**), TEA: triethylamine; K^+Np^-: potassium naphthalide.

In this contribution, we focus on reversibly switchable wettability[38] of polymer brushes by applying different external stimuli. We present a general concept that relies on prefabricated "junction point reactive" block copolymers (JPR-BC) with an in-chain functionality capable of covalent attachment to silicon surfaces. The novel concept relies on recent advances in the field of end[39] and in-chain[40] functionalization with epoxide derivatives in our group.[41-43]

Results and Discussion

The synthetic strategy developed for the preparation of junction-point reactive amphiphilic polymers and their attachment to silicon surfaces is shown in Scheme 1. In the first step, "living" PS[44] was end-capped with AGE (for experimental details see Supporting Information) to obtain precisely one hydroxyl group and one allyl functionality at the chain terminus (PS-(AGE), **1**). The hydroxyl group of the end-functionalized PS was then utilized to initiate the anionic ring-opening polymerization of ethylene oxide, [45] generating an amphiphilic block copolymer (PS-(AGE)-PEO, **2**) with exactly one allyl group at the junction point. To this end, the terminal hydroxyl group was deprotonated by potassium naphthalide titration to obtain a potassium alkoxide as initiating species. Prior to addition of the corresponding amount of ethylene oxide, the reaction mixture was cooled to -70 °C. The reaction was stirred at 60 °C for 24 h and then terminated with bromoethane to obtain PS-(AGE)-PEO (**2**) in high yields (94%). The resulting block copolymers were characterized by SEC, NMR spectroscopy and MALDI-ToF MS (Table 1, entries. 1-6).

In the final step of the synthesis, a triethoxysilyl group was introduced at the junction point by hydrosilylation, creating JPR-BCs (PS-(TEOS)-PEO, **3**). The reaction was carried out with Karstedt's catalyst in chlorobenzene at 60 °C for 3 days to obtain the TEOS-functionalized block copolymer (Table 1, entries 7-11). Block copolymers with molecular weights in the range of 6 000 to 23 000 g mol^{-1} and low polydispersities (PDI) have been synthesized (Table 1), and the block length of either PS or PEO was varied to realize different PEO/PS ratios (~1-6). In summary, the synthesis of a block copolymer with a junction point functionalization was obtained by a facile 3-step synthesis route, namely (i) end-functionalization, (ii) block copolymerization, and (iii) in-chain functionalization.

Table 1. Characterization data of PS-(AGE)-PEO and PS-(TEOS)-PEO block copolymers.

no.	formula[a]	M_n[a]	M_n[b]	PDI[b]
1	PS_{18}-(AGE)-PEO_{82}	5 600	6 000	1.17
2	PS_{27}-(AGE)-PEO_{123}	8 500	9 000	1.08
3	PS_{35}-(AGE)-PEO_{93}	8 000	11 000	1.09
4	PS_{27}-(AGE)-PEO_{261}	14 800	12 000	1.13
5	PS_{18}-(AGE)-PEO_{307}	15 900	14 500	1.06
6	PS_{41}-(AGE)-PEO_{302}	18 200	23 000	1.07
7	PS_{27}-(TEOS)-PEO_{123}	7 700	13 500	1.15
8	PS_{27}-(TEOS)-PEO_{123}	8 000	11 800	1.15
9	PS_{35}-(TEOS)-PEO_{145}	10 200	13 400	1.09
10	PS_{27}-(TEOS)-PEO_{261}	11 400	11 500	1.16
11	PS_{35}-(TEOS)-PEO_{277}	18 400	24 000	1.06

[a]Molecular weights in g mol^{-1} and degree of polymerization determined by ^{1}H NMR spectroscopy of PS-(AGE)-PEO samples [b]Molecular weight in g mol^{-1} and molecular weight distribution characterized by SEC ($CHCl_3$, PS standards).

Selected reactive block PS-(TEOS)-PEO copolymers have been attached to silicon surfaces (PS-(TEOS)-PEO@Si_{wafer}, **4**) via the tris(alkoxysilyl) group. The resulting films were studied regarding their structure and their stimuli-responsive behavior after tempering and treatment with solvent. Surface attachment was carried out in the following manner: After cleaning of the wafers by the RCA method[46], a solution of the block copolymer in toluene and triethylamine was stirred in the presence of the silicon wafers at room temperature over night. Residual, not attached block copolymer was extracted by dichloromethane to obtain PS-(TEOS)-PEO@Si_{wafer}. The silicon wafers with ultrathin polymer films were investigated by X-ray reflectivity and scanning force microscopy. The stimuli-responsiveness was determined by contact angle investigation subsequent to applying different external stimuli.

Several polymer samples were used for surface attachment (Table 2). The XRR curve demonstrates that ultrathin polymer films have been obtained. This can be deduced from the fringe distance (Figure 1, top). The plotted XRR data was simulated, using Paratt formalism implemented in the PARRATT32 software. Fitting of the data (red curves in Figure 1) yields additional information on the ultrathin polymer films, e.g., grafting density and roughness of the surfaces. For the investigated samples, depending on the concentration of the polymer in the solution employed for deposition, surface thicknesses in the range of 1.3-3.1 nm with grafting densities of 0.09-0.23 were obtained, which is in good

agreement with literature values.[34] For polymer concentrations of 1, 2 and 10 mM film thicknesses of 1.32, 1.71 and 3.09 nm were obtained, respectively.

Table 2. Characterization data: PS-(AGE)-PEO and PS-(TEOS)-PEO block copolymer films.

sample	c[a]	no.[b]	formula[c]	Thickness [nm]	Rough -ness	GD[d]	θ[e]	θ[f] (ΔT)	θ[g] (DMF)
I	10	7	PS_{27}-(TEOS)-PEO_{123}	1.3	0.2	0.09	62°	-	-
II	2	10	PS_{27}-(TEOS)-PEO_{261}	1.7	0.5	0.11	61°	84°	70°
III	1	10	PS_{27}-(TEOS)-PEO_{261}	3.1	1.0	0.23	69°	88°	68°
IV	1	4	PS_{27}-(AGE)-PEO_{261}	0.0	6.1	0.00	49°	-	-
V	1	-	PEO_{107}-(TEOS)[g]	1.1	0.4	0.17	42°	-	-

[a]Concentration of the toluene or DCM reaction mixture in mm [b]No. of block copolymer before the grafting-to process [c]Degree of polymerization determined by ^{1}H NMR spectroscopy [d]Grafting density in nm^2 [e]Contact angle measured after the grafting-to process [f]Contact angle after tempering [g]Contact angle after treatment with DMF under reflux.

In the first grafting experiment (sample I) precipitation of polymeric aggregates in the toluene solution was observed. Since the anchor group possesses three reactive sites, coupling reactions between the block copolymers are possible. These undesired coupling products limit the surface grafting process due to steric hindrance. However, decreasing the concentration of block copolymer suppresses theses coupling reactions and yields thicker films with increased grafting density, as can be seen for samples II and III in Table 2. The results of the XRR measurements confirm the successful preparation of polymer brushes.

One important issue was to clarify, whether the polymer is attached to the silicon surface by covalent bonds formed with the TEOS-functionality, or by mere non-covalent adsorption of the hydrophilic PEG-chains at the surface. To shed light on this issue, we carried out additional grafting experiments using the allyl-functional block copolymer PS-(AGE)-PEO instead of the reactive PS-(TEOS)-PEO. XRR results of PS-(TEOS)-PEO@Si_{wafer} (Figure 1 top) showed a fringe while on PS-(AGE)-PEO@Si_{wafer} (Figure 1 bottom) no fringe was detected. This confirms the successful attachment of the block copolymer via TEOS as an anchor group and supports the general concept for Y-shaped polymer brushes.

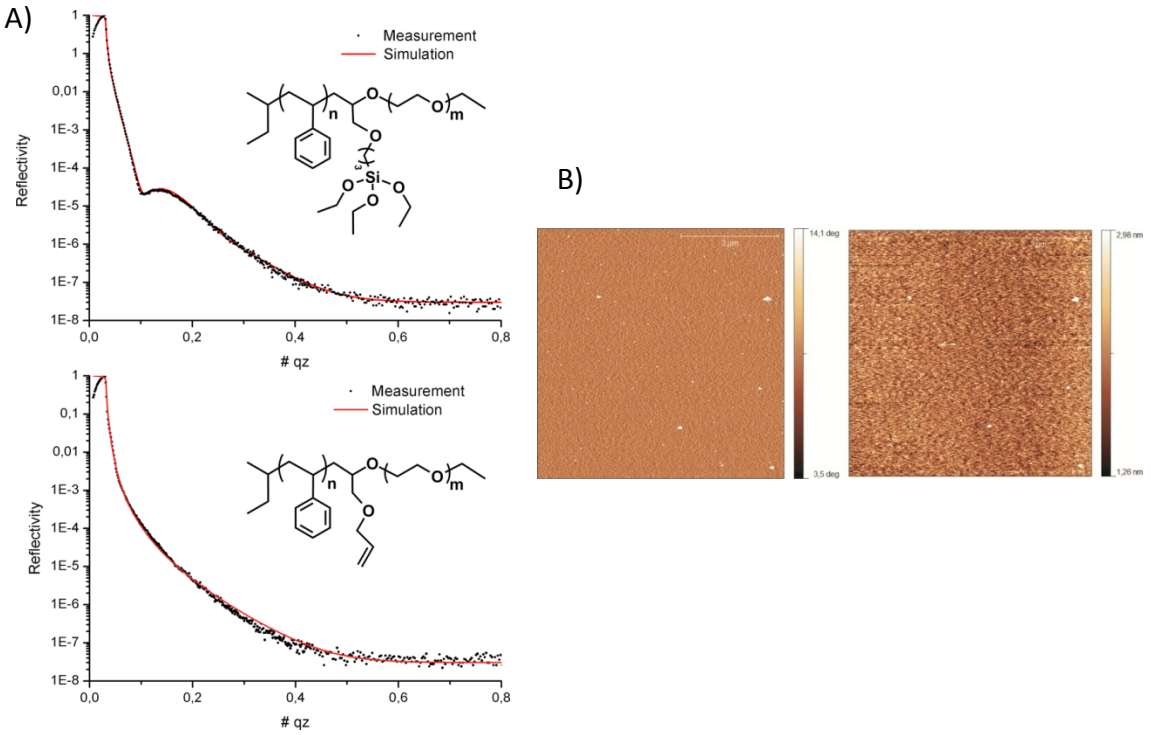

Figure 1. A) XRR analysis of silicon surfaces after grafting-to process with PS_{27}-(TEOS)-PEO_{261} (III) and PS_{27}-(AGE)-PEO_{261} (IV). A fringe could only be observed in the case of block copolymers functionalized with an appropriate anchor group (TEOS). B) SFM analysis of surface I with height image (left) and deflection image (right).

In addition, AFM images have been recorded. Smooth surfaces on the nanometer scale were observed (Figure 1). The evenly distributed hydrophilic and hydrophobic polymer chains result in a homogenous thin polymer film without any visible microphase segregation unlike conventional mixed brushes, which show distinct microphase-segregated surface morphologies with dimensions of up to hundreds of nanometers.[25] The confinement of dissimilar arms due to covalent attachment to the same grafting point represents a critical aspect in the suppression of the microscale phase segregation and determines the overall surface morphology.[34] The short length of the polymer chains in block copolymers deposited may additionally explain the absence of segregation.

To investigate the surface wetting properties of the amphiphilic Y-shaped brush films, the static contact angles at the liquid/vapor interface on the solid silicon surfaces were measured by adding a droplet of water (100 µL) on the thin polymer films. The measurements directly after the grafting-to process (DCM extraction) revealed contact angles between 60° and 70°. The contact angle of PS ($\theta = 92°$[37]) surfaces is 20-30° higher,

indicating a considerably more hydrophilic surface for the block copolymers. For comparison, PEO polymer brushes have also been prepared. First, monohydroxyl-functionalized PEO was converted to allyl-functionalized PEO (reagent: allyl bromide[47]). After hydrosilylation with TEOS the PEO chains can be attached to silicon surfaces in analogy to PS-(TEOS)-PEO. The contact angle of the homopolymer brushe was 42° (cf. Table 2, sample V). Thus, the Y-shaped polymer brushes in the initial state show an intermediate contact angle, indicating a mixed polymer surface consisting of PEO and PS chains.

To study the stimuli-responsive behavior of the tethered block copolymer films, the surfaces were treated with different solvents to either generate a collapse of the hydrophilic or hydrophobic segment. As non-polar solvents cyclohexane and chloroform were applied. As hydrophilic solvents methanol and water were used. In all cases the surfaces have been treated with the solvent under reflux. No significant change in contact angles was observed. One reason might be the inflexibility of the PS chains below its glass transition temperature (T_g) of 100 °C, which leads to a drastic decrease in the chain mobility of the block copolymer for hydrophilic solvents. Hydrophobic solvents should favor the exposure of PS and thus not change the contact angle much.

To increase the chain mobility, the samples were kept at 180 °C for several hours, which affords hydrophobization and contact angle shifts of approximately 20° (cf. sample II and III, Table 2). Figure 2 presents the contact angle images (top) and the proposed schematic illustration of the chain alignment. The PS chain flexibility is increased during the tempering process, and the PEO chains are enabled to segregate on the hydrophilic substrate. This results in a stratification of the polymer film with PS on the topmost layer and with a PEO layer segregated on the silicon surface as indicated by the water contact angles of 84-88°. A similar preference for PS over PEO towards the free surface was observed for PS-PEO diblock copolymers[48, 49]. This is caused by the lower surface tension of PS of 36 mN/m rather than 44 mN/m for PEO. A corresponding illustration is depicted in Figure 2 (bottom, right). Reversible switching of surface properties was realized by repeated solvent treatment. DMF turned out to be a suitable polar solvent, which may be related to its high boiling point of 153 °C above the T_g of PS. The samples were deposited in DMF under reflux and subsequent contact angle measurements showed a decreased contact angle of 68°, indicating a regression of the mixed polymer brushes at the topmost layer similar to the initial state. The

polar solvent is in competition with the hydrophilic silicon surfaces and partially detaches the PEO chains from the surface.

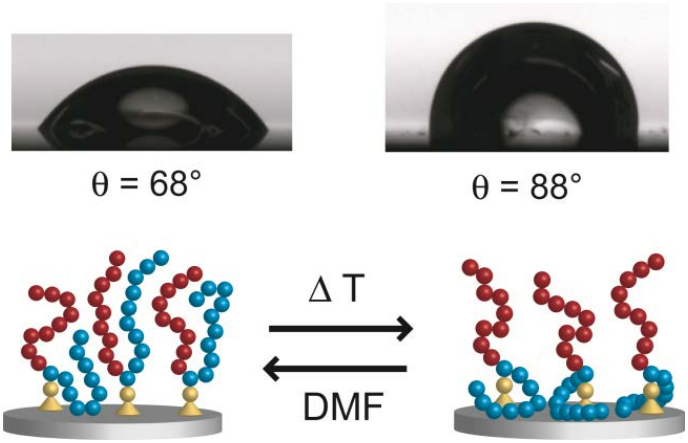

Figure 2. Sesile water drop of surface III (Table 2) after tempering and treatment with DMF under reflux. A contact angle change of 20° was observed. In the schematic PS is drawn in red, PEO in blue.

Heat and solvent treatment of the surfaces reveal the adaptive properties and the stimuli-responsive character of the Y-shaped block copolymer brushes, with observed contact angle shifts of up to 23°. The promising expansion to other Y-shaped polymer brushes with different oxy- or carbanionically polymerizable monomers is currently under investigation.

Conclusion

We have developed a synthetic sequence for junction point-reactive block copolymers (JPR-BCs) with a central tris(alkoxysilyl) functionality for surface attachment. The synthesis is based on anionic polymerization techniques and the use of allyl glycidyl ether (AGE) for functional end-capping of “living” poly(styrene) (PS). The end-capped polymer was utilized as macroinitiator for the anionic ring-opening polymerization of ethylene oxide to afford PS-(AGE)-PEO block copolymers with different block ratios in the range of 6 000 to 24 000 g mol^{-1}. A hydrosilylation reaction of the junction point with triethoxysilane (TEOS) was carried out to introduce the reactive tris(alkoxysilyl) group that can be grafted to silicon surfaces (PS-(TEOS)-PEO).

PS-(TEOS)-PEO was grafted chemically onto silicon surfaces to generate ultrathin, Y-shaped block copolymer brushes with dissimilar polymer chains. Films were 1-3 nm thick. Moreover, the covalent binding of the TEOS functionality could be confirmed by comparing with the

grafting process of the allyl-functionalized block copolymer. Reversible stimuli-responsive surface wetting behavior was observed by contact angle measurements. Upon keeping the samples at 180 °C, the water contact angle increases from 69° to 88°, and subsequent treatment with DMF under reflux offers switching of surface wetting properties back to the initial state with $\theta = 68°$. This reversible reorganization of the polymer brushes is promising for applications for surfaces with controlled release, self-cleaning and self-refreshing abilities.

Acknowledgement

C.T. and H.F. thank MPGC (Max Planck Graduate Center with Johannes Gutenberg-University) and the Excellence Initiative (DFG/GSC 266) for a fellowship and financial support. We thank Jens Emsermann and Jacky Thill for technical assistance. We are grateful to Janis Ochsmann for valuable discussions.

Supporting Information

Synthetic Strategy

The first step was the synthesis of end-functionalized poly(styrene) by end-capping with an epoxide derivative. As a suitable focal point allyl glycidyl ether (AGE) was selected since it possesses several advantages. Due to the highly strained 3-membered ring the epoxide is an efficient termination reagent[42]. In addition, a protection of the allyl functionality during the end-capping process in contrast to other multi-functional epoxides is not necessary and the functionality is capable of further reactions directly subsequent to the polymerization.[39, 40] Thus, styrene was initiated by *sec*-butyllithium (*sec*-BuLi) and the "living" PS chain was terminated with AGE generating a hydroxyl group and an allyl functionality at the terminal position (PS-(AGE)). As known from literature, the strong aggregation between the counterion lithium and the alkoxide, which is generated after termination of living PS with epoxide derivatives,[50] prevents further propagation of AGE and an immediate oxyanionic polymerization is not possible.[51]

A series of PS-(AGE) was synthesized and characterized by size exclusion chromatography (SEC), ^{1}H NMR spectroscopy and matrix-assisted laser desorption and ionization time-of-flight mass spectrometry (MALDI-ToF MS). The results of SEC and NMR analysis are summarized in Table S1.

Table S1. Characterization data of PS-(AGE).

no.	formula[a]	M_n[a]	M_n[b]	PDI[b]
S1	PS_{18}-(AGE)	1 900	1 700	1.15
S2	PS_{30}-(AGE)	3 700	3 100	1.11
S3	PS_{35}-(AGE)	3 600	3 600	1.09
S4	PS_{41}-(AGE)	4 500	4 300	1.08
S5	PS_{49}-(AGE)	5 200	5 100	1.08
S6	PS_{64}-(AGE)	6 500	6 700	1.08
S7	PS_{108}-(AGE)	13 000	11 200	1.07

[a]Molecular weight in g mol^{-1} and degree of polymerization determined by ^{1}H NMR spectroscopy [b]Molecular weight in g mol^{-1} and molecular-weight distribution characterized by SEC ($CHCl_3$, PS standards).

Well-defined polymers in a broad range of molecular weights (2 000 to 13 000 g mol^{-1}) were synthesized showing a narrow and monomodal molecular-weight distributions (MWDs). Corresponding SEC traces of the polymers are depicted in Figure S1.

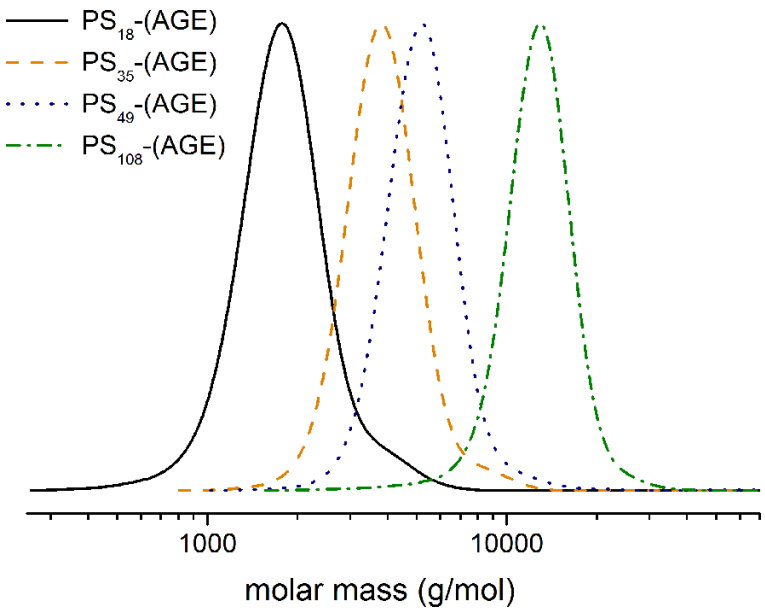

Figure S1. Molecular-weight distribution determined via SEC ($CHCl_3$, PS standards) of selected PS-(AGE) samples (no. S1, S3, S5, and S7, Table S1).

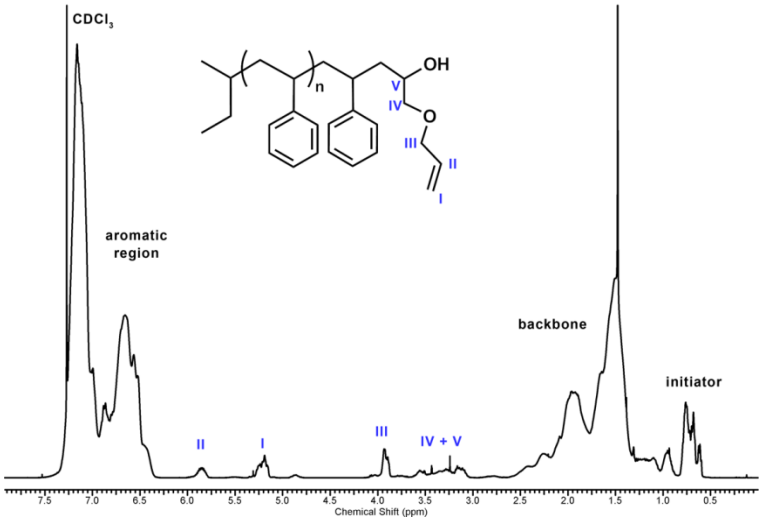

Figure S2. ^1H NMR spectra (400 MHz, $CDCl_3$) of PS_{18}-(AGE) (no. S1, Table S1).The characteristic signals of the AGE end group can be assigned (label I-V)

^1H NMR analysis was carried out to study the functionalization efficiency and the conversion. A spectrum of PS_{18}-(AGE) was recorded in $CDCl_3$ and is depicted in Figure S2. The respective

signals for the poly(styrene) backbone can be assigned and by referencing to the initiator signals (methyl groups of *sec*-BuLi) the molecular weight can be calculated. Furthermore, the signals of the terminal AGE group can be observed and separately integrated to determine the functionalization efficiency. The values of the methine proton (5.86 ppm, Signal II, Figure S2) were close to 1 in all cases, indicating a high degree of functionalization. However, with increasing molecular weight a precise end-group analysis is complicated due to the diminishing end-group signal intensity.

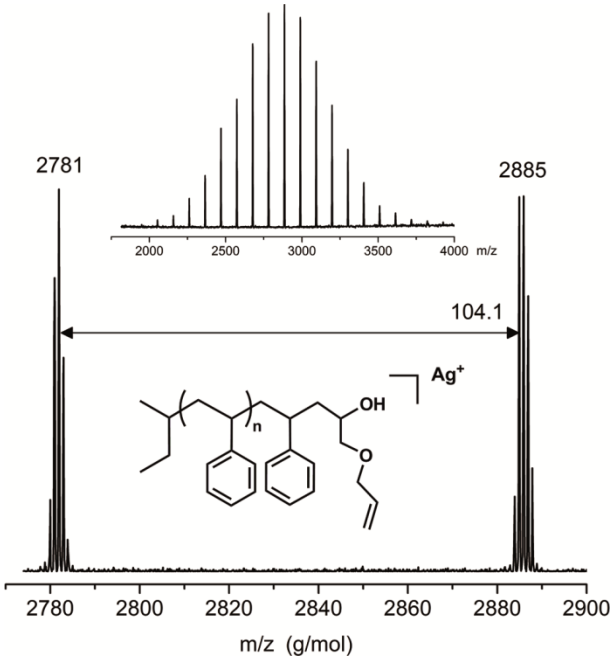

Figure S3. MALDI-ToF spectrum of PS_{35}-AGE (no. S3 Table S1), cationizing agent: silver trifluoroacetate, matrix: dithranol.

Thus, MALDI-ToF MS was used to investigate the functionalization efficiency. A corresponding spectrum of PS_{35}-(AGE) shows only one distribution mode which can unequivocally be assigned to the desired AGE-functionalized poly(styrene). The spectrum is shown in Figure S3 and two representative signals are enlarged. For instance, the mass peak at *m/z* 2781 corresponds to the 24-mer (PS_{24}-(AGE) + Ag^+) and fits to the calculated value (2780 g mol^{-1}). Moreover, one has to underline the absence of any non-functionalized PS signals (PS_{26}-H, 2874 g mol^{-1}), which additionally confirms the quantitative end-functionalization. The MALDI-ToF analysis of the other PS-(AGE) samples affords identical results.

The second step was the synthesis of amphiphilic block copolymers by utilizing PS-AGE as macroinitiator for the AROP of EO. The efficient block formation can be demonstrated by comparing the SEC traces of a block copolymer with the corresponding precursor. Figure S4 depicts these signals of homopolymer PS_{18}-(AGE) and the block copolymer PS_{18}-(AGE)-PEO_{307}, where a characteristic shift of molecular weight from 1 700 to 14 500 g mol^{-1} can be observed. Additional SEC results are depicted in Figure S5.

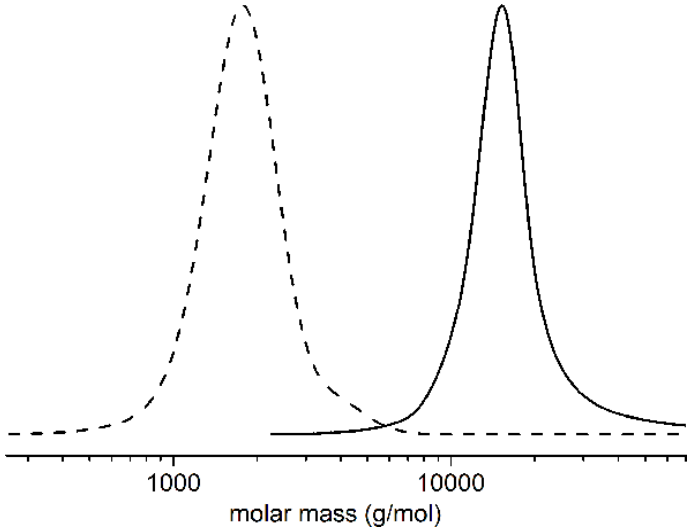

Figure S4. SEC traces of PS_{18}-(AGE) (no. S1, dashed line) and PS_{18}-(AGE)-PEO_{307} (no. 5, solid line) present the successful block formation after AROP of EO. SEC was carried out in $CHCl_3$. (RI signals. PS standards).

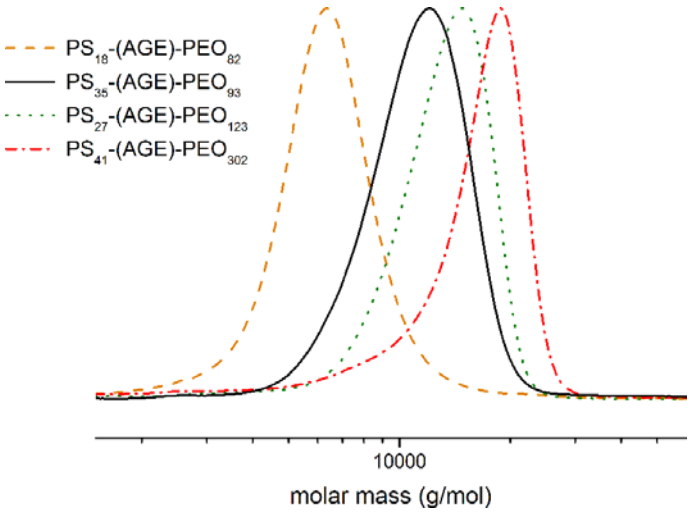

Figure S5. Molecular-weight distributions determined via SEC ($CHCl_3$, PS standards) of selected PS-(AGE)-PEO samples (no. 1, 3, 4, and 6, Table 1).

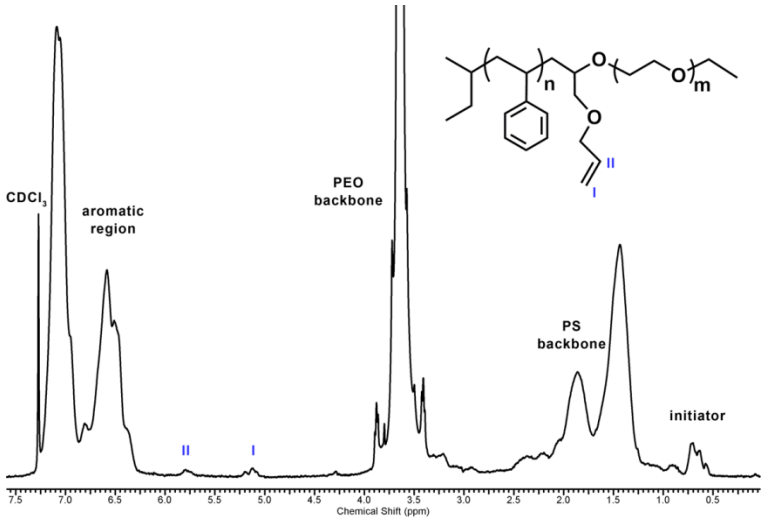

Figure S6. ^{1}H NMR spectra (400 MHz, $CDCl_3$) of PS-AGE_{18}-PEO (no. 2, Table 1). The characteristic signals of the allylic in-chain functionality can be assigned (label I-II)

Additionally, the amphiphilic materials were analyzed by ^{1}H NMR spectroscopy (Figure S6). The expected signals for the polymer chains (PS aromatic region, PS backbone, and PEO backbone) can be detected. The two signals of the allylic double bond can still be distinguished at 5.77 (methine, II) and 5.13 (methylene, I) ppm. Compared to PS-(AGE) it is more difficult to carry out a correct end-group analysis due to the increasing molecular weight, and thus decreasing end-group signal intensity. Therefore, analog to the PS-(AGE) characterization MALDI-ToF analysis was applied to confirm a complete in-chain functionalization. As expected beforehand, the full spectrum (Figure S7, left) shows a large amount of signals due to the possible linear combinations of the block copolymer. A magnification of the spectrum (Figure S7, right) confirms successful block formation due to the observation of molar mass intervals of both monomer units with 104.1 g mol^{-1} and 44 g mol^{-1} for styrene and EO, respectively. Moreover, the in-chain functionalization can be proved by considering the single peaks, which can be assigned to the desired allyl-functionalized block copolymer. For example, peak A (Figure S7) presents a molar mass of 3956 g mol^{-1} and can be assigned to PS_{22}-(AGE)-PEO_{33} block copolymer with potassium as counterion (calculated value: 3956 g mol^{-1}). Thus, similar to the homopolymer the quantitative implementation of the in-chain functionality could be confirmed.

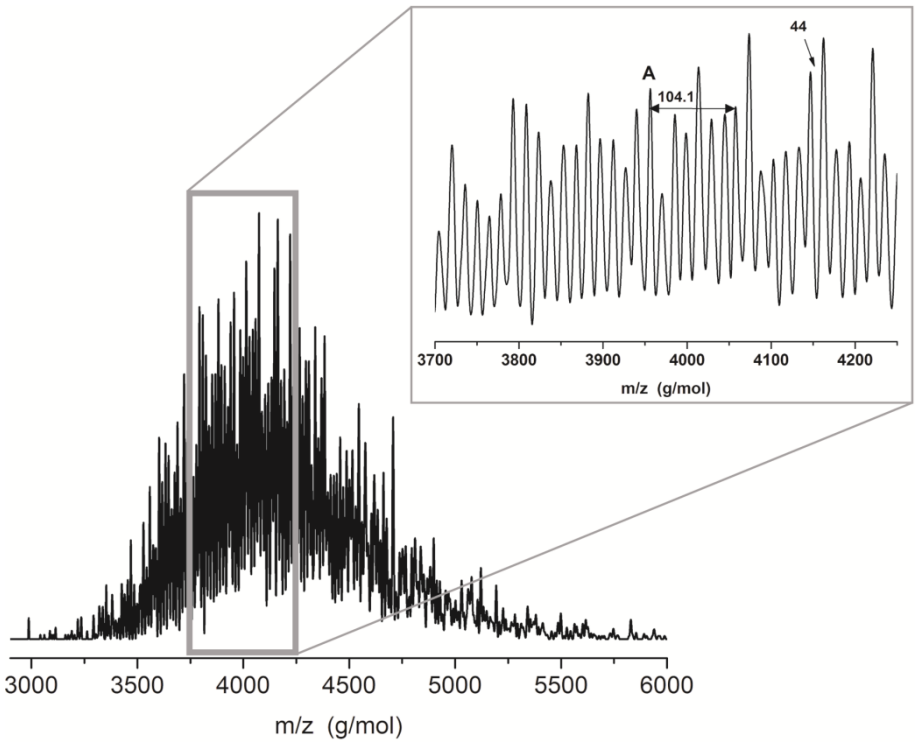

Figure S7. MALDI-ToF spectra of PS_{18}-(AGE)-PEO_{82} (no. 1, Table 1) present the complete spectrum (left) and a magnification (right). The magnification confirms, that all molar mass differences between the signals are linear combinations of 44 and 104.1 g mol^{-1} (molecular weight of EO and styrene, respectively), cationizing agent: potassium trifluoroacetate, matrix: dithranol.

In analogy to previous reports this synthetic strategy provides block copolymers with a single functionality between the two polymer blocks.[40, 41] After the successful introduction of hydroxyl and amine functionality, in this report we introduced for the first time an ally functionality, which is suitable for further reaction, e.g., with Si-H or S-H functionalized macro- or low molecular-weight molecules.

For the preparation of Y-shaped polymer brushes to silicon surfaces the in-chain reactive TEOS group offers a proper linking position and all grafting points will possesses exactly one hydrophilic and one hydrophobic polymer chain. Prior to the chemical grafting process an appropriate and reactive anchor group has to be introduced. Therefore a triethoxysilane functionality was attached to the allyl-functionalized block copolymer by hydrosilylation. The two incompatible polymer chains in proximity of the in-chain functionality most probably will retard the surface attachment.

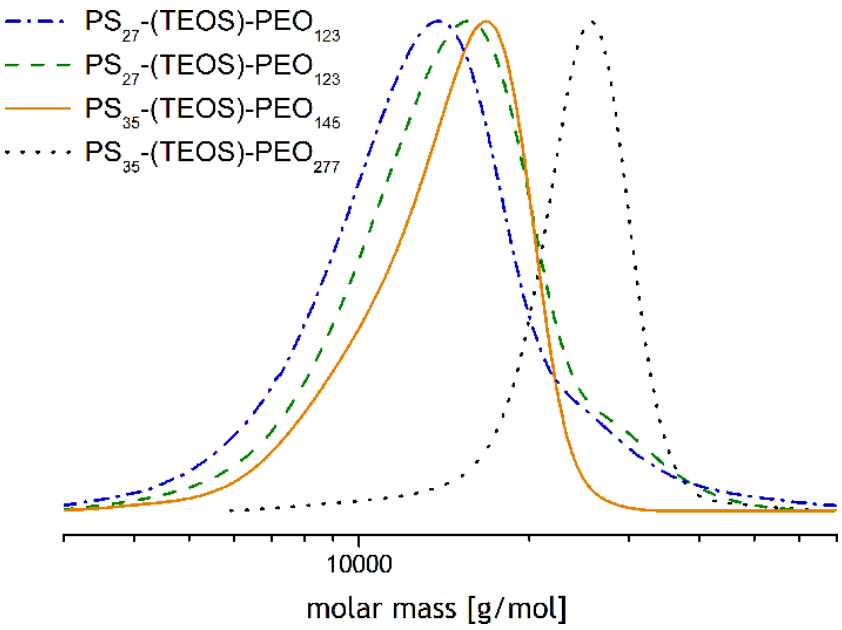

Figure S8. Molecular weight distribution determined via SEC ($CHCl_3$, PS standards) of selected PS-(TEOS)-PEO samples (no. 14-16 and 18, Table 2).

The PS-(TEOS)-PEO block copolymers were characterized by SEC and ^{1}H NMR spectroscopy and the respective results are listed in Table 1 (no. 7-11). SEC characterization shows similar traces with monomodal and narrow molecular-weight distribution (cf. Figure S8). ^{1}H NMR was used to monitor the progress of the reaction and after optimizing the reaction parameters a quantitative functionalization with TEOS was observed. Figure S9 presents the spectra of PS_{27}-(AGE)-PEO_{123} (no. 2, Table 1) and PS_{27}-(TEOS)-PEO_{123} (no. 7, Table 1) before and after hydrosilylation. There are no deviations between the two spectra concerning the signals of the polymer chains, but the disappearance of the double bond signals at 5.77 and 5.13 ppm confirms the completion of the reaction.

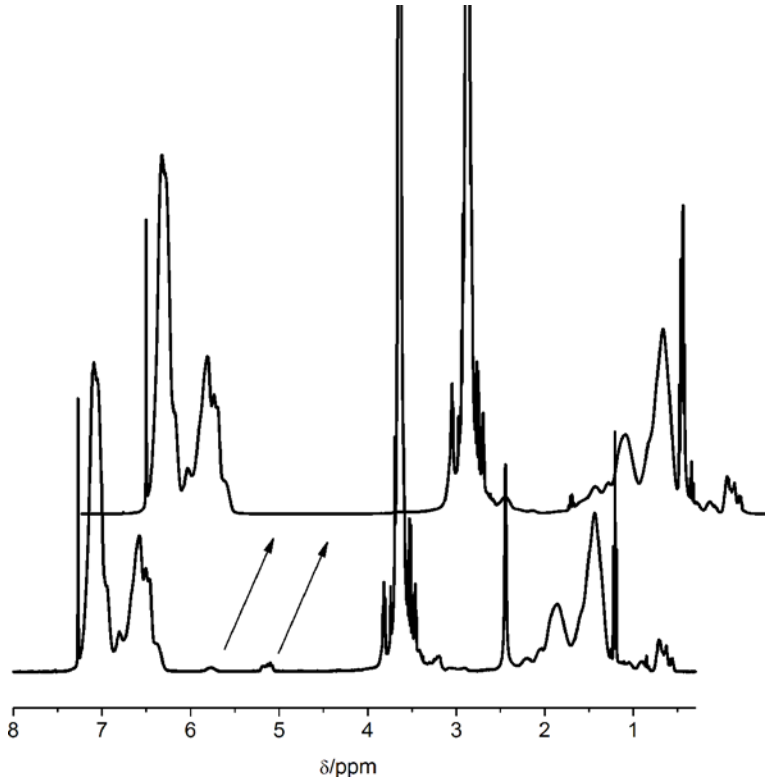

Figure S9. ^{1}H NMR spectra (400 MHz, $CDCl_3$) of PS_{27}-(AGE)-PEO_{123} (no. 9, bottom) and PS_{27}-(TEOS)-PEO_{123} (no. 14, top). The characteristic signals of the allylic double bond disappear after hydrosilylation with triethoxysilane and Karstedt's catalyst.

Experimental Section

Reagents. All solvents and reagents were purchased from Acros Organics, ABCR or Sigma Aldrich and used as received, unless otherwise stated. Chloroform-d_1 was purchased from Deutero GmbH. Tetrahydrofuran (THF) was distilled from sodium/benzophenone under reduced pressure (cryo-transfer). Styrene, bromoethane and allyl glycidyl ether (AGE) were dried over calcium hydride (CaH_2) and cryo-transferred prior to use. Cyclohexane was cryo-transferred from *n*-butyllithium/DPE. Silicon wafers were obtained from Si-Mat Silicon Materials,Germany. The polished silicium wafers with an (100) orientationwere cut into 1 × 1 cm^2 large substrates for sample preparation.

Instrumentation. ^{1}H NMR spectra were recorded at 400 MHz on a Bruker AMX 400, and are referenced internally to residual proton signals of the deuterated solvent. Size exclusion chromatography (SEC) measurements were carried out in $CHCl_3$ on an instrument consisting of a Waters 717 plus autosampler, a TSP Spectra Series P 100 pump, a set of three MZ SDV

columns (10^4/500/50 Å), RI- and UV-detectors (absorption wavelength: 254 nm or 500 nm). All SEC diagrams show the RI detector signal unless otherwise stated, and the molecular weight refer to linear poly(styrene) (PS) standards provided by Polymer Standards Service (PSS). Matrix-assisted laser desorption and ionization time-of-flight (MALDI-ToF) measurements were performed on a Shimadzu Axima CFR MALDI ToF mass spectrometer equipped with a nitrogen laser delivering 3 ns laser pulses at 337 nm.

End Functionalization. Vacuum-distilled styrene (5 g, 48 mmol) was dissolved in dry cyclohexane (30 mL) and cooled to 0 °C. The polymerization was initiated by adding the corresponding amount of *sec*-BuLi (1.3 M, 1.92 mL). After the red-colored reaction mixture was stirred for 20 h at 40 °C, AGE (2 eq., 5 mmol) was introduced via syringe and the dark red color disappeared immediately. The solution was stirred for additional 20 h and precipitated several times into MeOH to obtain PS-(AGE) (**1**). Yield: 90%. ^{1}H NMR (400 MHz, $CDCl_3$, δ in ppm): 7.50-6.31 (PS aromatic), 5.86 (m, 1H, C*H*=CH_2), 5.19 (m, 2H, CH=C*H*$_2$), 3.93 (m, 2H, C*H*$_2$-CH=CH_2), 3.66-3.02 (AGE, C*H*-C*H*$_2$), 2.6-0.85 (PS backbone), 0.79-0.50 (m, 6H, init C*H*$_3$).

Block Copolymerization. 1 g (0.35 mmol) of **1** was dissolved in dry THF and titrated with potassium naphthalide (0.1 m) until a slight green color maintained. Ethylene oxide (EO, 3 mL) was added and the greenish color disappeared rapidly. The reaction mixture was stirred for 24 h at 60 °C, the polymerization was terminated with bromoethane, concentrated and precipitated in cold diethyl ether and dried under vacuum to obtain PS-(AGE)-PEO (**2**) as a white powder. Yield: 94 %. ^{1}H NMR (400 MHz, $CDCl_3$, δ in ppm): 7.34-6.33 (PS aromatic), 5.79 (m, 1H, C*H*=CH_2), 5.10 (m, 2H, CH=C*H*$_2$), 3.86-3.33 (PEO backbone), 2.6-0.85 (PS backbone), 0.79-0.50 (m, 6H, init C*H*$_3$).

In-Chain Functionalization. 600 mg (0,07 mmol) of **2** was dissolved in chlorobenzene (3 mL), TEOS (130 μL, 14 eq.) as well as the Karstedt's catalyst (2 μL) was added and the reaction mixture was stirred for 72 h at 60 °C. Chlorobenzene was removed *in vacuo*. The polymer was precipitated from a concentrated chloroform solution in petroleum ether and dried *in vacuo* to obtain PS-(TEOS)-PEO (**3**). Yield: 94 %. ^{1}H NMR (400 MHz, $CDCl_3$, δ in ppm): 7.38-6.22 (PS aromatic), 4.96-3.32 (PEO backbone), 2.6-0.85 (PS backbone), 0.79-0.50 (m, 6H, init C*H*$_3$).

Generation of ultrathin polymer films (Surface Attachment). Silicon wafers were cleaned by the RCA method (H_2O_2, 35%; NH_4OH, 28%; Milli-Q water) at 90 °C for 30 minutes and subsequently washed twice with MilliQ water and once with ethanol and dried under air. 458 mg (0.05 mmol) of **3** was dissolved in 4 mL toluene and 50 µL triethylamine. The solution was reacted with the cleaned silicon wafers at room temperature under argon atmosphere for 24 h. To remove residual polymer material the wafers were extracted for 3 h with DCM.

X-ray Reflectivity. Measurements on wafers were conducted on a XRD 3003 TT, Seifert Ltd. GB diffraction system. Monochromatic and collimated X-rays were obtained from a Cu anode with a wavelength of λ = 0.154 nm. The obtained curves were fitted using PARRATT32. The starting values for scattering length densities used in the fit as well as the densities obtained by the fitted scattering length densities were calculated using the scattering length density calculator provided by NIST.[52]

Contact Angle Measurements. Contact angle measurements were conducted on a Krüss, DSA10-MK2. The static contact angle was measured in air under ambient conditions using Milli-Q water and reported values reflect the average of five measurements on each sample.

References

[1] I. Tokarev, M. Motornov, S. Minko, *J. Mater. Chem.* **2009**, *19*, 6932.

[2] S. Minko, *J. Macromol. Sci., Rev. Macromol. Chem.* **2006**, *46*, 397.

[3] F. Xia, L. Jiang, *Adv. Mater.* **2008**, *20*, 2842.

[4] M. Yoshida, R. Langer, A. Lendlein, J. Lahann, *J. Macromol. Sci., Rev. Macromol. Chem.* **2006**, *46*, 347.

[5] Z. Tang, Y. Wang, P. Podsiadlo, N. A. Kotov, *Adv. Mater.* **2006**, *18*, 3203.

[6] M. Motornov, S. Minko, K.-J. Eichhorn, M. Nitschke, F. Simon, M. Stamm, *Langmuir* **2003**, *19*, 8077.

[7] L. Ionov, S. Sapra, A. Synytska, A. L. Rogach, M. Stamm, S. Diez, *Adv. Mater.* **2006**, *18*, 1453.

[8] G. Chen, A. S. Hoffman, *Nature* **1995**, *374*, 49.

[9] E. S. Gil, S. M. Hudson, *Prog. Polym. Sci.* **2004**, *29*, 1173.

[10] I. Tokarev, S. Minko, *Soft Matter* **2009**, *5*, 511.

[11] T. Thurn-Albrecht, J. Schotter, G. A. Kästle, N. Emley, T. Shibauchi, L. Krusin-Elbaum, K. Guarini, C. T. Black, M. T. Tuominen, T. P. Russell, *Science* **2000**, *290*, 2126.

[12] D. Kessler, F. D. Jochum, J. Choi, K. Char, P. Theato, *ACS Appl. Mater. Interfaces* **2011**, *3*, 124.

[13] J. A. Hiller, M. F. Rubner, *Macromolecules* **2003**, *36*, 4078.

[14] Z. Zhu, S. A. Sukhishvili, *J. Mater. Chem.* **2012**, *22*, 7667.

[15] D. Zimnitsky, V. V. Shevchenko, V. V. Tsukruk, *Langmuir* **2008**, *24*, 5996.

[16] R. Toomey, D. Freidank, J. Rühe, *Macromolecules* **2004**, *37*, 882.

[17] R. Lupitskyy, Y. Roiter, C. Tsitsilianis, S. Minko, *Langmuir* **2005**, *21*, 8591.

[18] V. Kozlovskaya, E. Kharlampieva, B. P. Khanal, P. Manna, E. R. Zubarev, V. V. Tsukruk, *Chem. Mater.* **2008**, *20*, 7474.

[19] K.-S. Liao, H. Fu, A. Wan, J. D. Batteas, D. E. Bergbreiter, *Langmuir* **2008**, *25*, 26.

[20] J. A. Howarter, J. P. Youngblood, *Adv. Mater.* **2007**, *19*, 3838.

[21] B. Ghosh, M. W. Urban, *Science* **2009**, *323*, 1458.

[22] P. Uhlmann, L. Ionov, N. Houbenov, M. Nitschke, K. Grundke, M. Motornov, S. Minko, M. Stamm, *Prog. Org. Coat.* **2006**, *55*, 168.

[23] Z. Sui, J. B. Schlenoff, *Langmuir* **2003**, *19*, 7829.

[24] K. N. Plunkett, X. Zhu, J. S. Moore, D. E. Leckband, *Langmuir* **2006**, *22*, 4259.

[25] M. Lemieux, D. Usov, S. Minko, M. Stamm, H. Shulha, V. V. Tsukruk, *Macromolecules* **2003**, *36*, 7244.

[26] F. Xia, L. Feng, S. Wang, T. Sun, W. Song, W. Jiang, L. Jiang, *Adv. Mater.* **2006**, *18*, 432.

[27] M. D. Rowe, B. A. G. Hammer, S. G. Boyes, *Macromolecules* **2008**, *41*, 4147.

[28] P. Ye, H. Dong, M. Zhong, K. Matyjaszewski, *Macromolecules* **2011**, *44*, 2253.

[29] S. Minko, M. Müller, M. Motornov, M. Nitschke, K. Grundke, M. Stamm, *J. Am. Chem. Soc.* **2003**, *125*, 3896.

[30] S. Minko, I. Luzinov, V. Luchnikov, M. Müller, S. Patil, M. Stamm, *Macromolecules* **2003**, *36*, 7268.

[31] L. Ionov, N. Houbenov, A. Sidorenko, M. Stamm, S. Minko, *Adv. Funct. Mater.* **2006**, *16*, 1153.

[32] P. Uhlmann, N. Houbenov, N. Brenner, K. Grundke, S. Burkert, M. Stamm, *Langmuir* **2006**, *23*, 57.

[33] B. Zhao, R. T. Haasch, S. MacLaren, *J. Am. Chem. Soc.* **2004**, *126*, 6124.

[34] D. Julthongpiput, Y.-H. Lin, J. Teng, E. R. Zubarev, V. V. Tsukruk, *J. Am. Chem. Soc.* **2003**, *125*, 15912.

[35] E. Zhulina, A. C. Balazs, *Macromolecules* **1996**, *29*, 2667.

[36] D. Julthongpiput, Y.-H. Lin, J. Teng, E. R. Zubarev, V. V. Tsukruk, *Langmuir* **2003**, *19*, 7832.

[37] Y. Wang, J. X. Zheng, W. J. Brittain, S. Z. D. Cheng, *J. Polym. Sci., Part A: Polym. Chem.* **2006**, *44*, 5608.

[38] B. Xin, J. Hao, *Chem. Soc. Rev.* **2010**, *39*, 769.

[39] C. Tonhauser, D. Wilms, F. Wurm, E. Berger-Nicoletti, M. Maskos, H. Löwe, H. Frey, *Macromolecules* **2010**, *43*, 5582.

[40] C. Tonhauser, B. Obermeier, C. Mangold, H. Löwe, H. Frey, *Chem. Commun.* **2011**, *47*, 8964.

[41] C. Tonhauser, M. Mazurowski, M. Rehahn, M. Gallei, H. Frey, *Macromolecules* **2012**, *45*, 3409.

[42] C. Tonhauser, H. Frey, *Macromol. Rapid Commun.* **2010**, *31*, 1938.

[43] A. Natalello, C. Tonhauser, E. Berger-Nicoletti, H. Frey, *Macromolecules* **2011**.

[44] M. Szwarc, *Nature* **1956**, *178*, 1168.

[45] C. Dingels, M. Schömer, H. Frey, *Chem. unserer Zeit* **2011**, *45*, 338.

[46] G.-G. Bumbu, G. Kircher, M. Wolkenhauer, R. Berger, J. S. Gutmann, *Macromol. Chem. Phys.* **2004**, *205*, 1713.

[47] X.-S. Feng, D. Taton, E. L. Chaikof, Y. Gnanou, *J. Am. Chem. Soc.* **2005**, *127*, 10956.

[48] A. M. Botelho do Rego, O. Pellegrino, J. G. Martinho, J. Lopes da Silva, *Surf. Sci.* **2001**, *482-485, Part 2*, 1228.

[49] C. Neto, M. James, A. M. Telford, *Macromolecules* **2009**, *42*, 4801.

[50] R. P. Quirk, J. J. Ma, *J. Polym. Sci. Part A: Polym. Chem.* **1988**, *26*, 2031.

[51] J. Furukawa, T. Saegusa, T. Tsuruta, G. Kakogawa, *Macromol. Chem. Phys.* **1960**, *36*, 25.

[52] *http://www.ncnr.nist.gov/resources/sldcalc.html*.

Chapter 5: Viscoelastic Properties of Hyperbranched Polyethers

5.1: Entanglement Transition in Hyperbranched Polyether-Polyols

Christoph Tonhauser,[1] *Daniel Wilms,*[1] *Yasmin Korth,*[2] *Holger Frey**[1] and *Christian Friedrich**[2]

[1]Institute of Organic Chemistry, Organic and Macromolecular Chemistry, Duesbergweg 10-14, Johannes Gutenberg-University Mainz, 55099 Mainz, Germany

[2]Freiburg Materials Research Center (FMF), Albert-Ludwigs-University, Stefan-Meier-Straße 21, 79104 Freiburg, Germany

Published in Macromolecular Rapid Communications **2010**, *31*, 2127-2132

The viscoelastic properties of hyperbranched polyglycerol have been investigated with respect to molecular weight. The scaling relation between zero shear viscosity and molecular weight present an uncommon behavior since starting with a critical value (M_c^*) entanglement dynamics can be observed due to “star-like” interactions at high molecular weights.

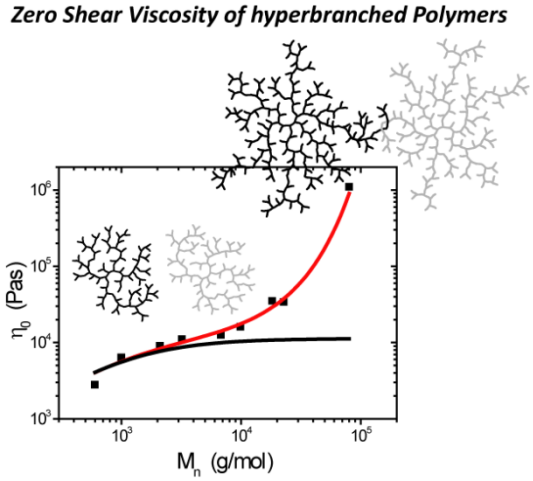

Keywords: entanglement; hyperbranched polymers; polyglycerol; rheology; viscosity

Abstract

Are hyperbranched polymers capable of forming entanglements? This is the central issue of this contribution. Hyperbranched polyglycerol (*hb*PG) samples with different molecular

weights (600–106 000 g mol^{-1}), narrow polydispersities (1.2–1.8) and high degrees of branching (≈ 0.6) were prepared by anionic ring-opening polymerization. The viscoelastic properties of these polymers with respect to molecular architecture and molar mass were investigated. At low molecular weights ‘‘classical’’ scaling behavior between zero shear viscosity and molecular weight can be observed, whereas between 3 000 and 10 000 g mol^{-1} a plateau-like area is found. The results indicate entanglement dynamics when exceeding a critical molar mass (M_c^* ≈ 20 000 g mol^{-1}) due to entangled hyperbranched polyglycerols.

Introduction

Hyperbranched polymers have attracted a steadily growing interest over the last decade, since they combine several unique properties with facile preparative access and economic viability.[1] Most synthetic approaches leading to hyperbranched polymers afford systems with very broad molecular weight distributions, in pronounced contrast to the monodisperse dendrimers,[2] which are typically prepared by multi-step processes. Despite the different synthetic prerequisites, perfectly branched dendrimers and hyperbranched macromolecules with their random distribution of branching points show common properties clearly different from their linear counterparts, such as noncrystallizability, high functionality and a specific solution viscosity behavior with increasing molecular weight (MW).[3]

The application of hyperbranched polymers requires a systematic understanding of the correlation between polymer structure (molecular weight, polydispersity, and degree of branching) and rheological properties. To this end, the synthesis protocol has to provide access to (i) controllable, hyperbranched polymerizations with respect to both molar mass and polydispersity in (ii) a broad range of molecular weights. About 10 years ago, our group reported the controlled anionic ring-opening multibranching polymerization of glycidol.[4] Molar masses remained limited to 6 000 g mol^{-1}, until more recent studies were carried out by Brooks et al.[5] as well as by our group,[6] employing an emulsion-type polymerization and a macroinitiator-based approach, respectively. All approaches allow obtaining highly functional hyperbranched polyethers with low polydispersities and high degrees of branching (DB) close to the theoretical limit of 0.67 for slow monomer addition. Most important, the molecular weight can be systematically varied from glycerol oligomers to polyglycerol macromolecules with M_n of several hundred kDa.[7] This structural variety of hyperbranched polyglycerol (hbPG) has motivated our interest for a systematic exploration of the viscoelastic behavior in dependence of both functionality and degree of polymerization.

The viscous behavior of linear polymers can be described by the power law:

$$\eta_0 = KM^{\alpha} \qquad (1)$$

This relationship between viscosity and molecular weight is characterized by two dependencies: $\alpha = 1$ (unentangled regime) and $\alpha = 3.4$ (entangled regime) for most linear polymers.[8] However, highly branched polymers exhibit uncommon rheological behavior (e.g., absence of entanglement or transition from open spherical to closed globular

structures), which is a direct consequence of the molecular architecture. At present, rheological studies for highly branched polymers give a non uniform picture. Most polymeric systems exhibit a change in high α-values (from 1 to 2) for low molecular weight samples, which correspond to open spherical structures. High molecular weights provide low α-values (from 0 to 1) representing closed globular structures.

Several groups have studied the solution and melt rheology of hyperbranched polymers dependent on concentration.[9] For instance, Nunez et al.[10] and Vukovic et al.[11] investigated solutions of hyperbranched polyesters prepared by polycondensation protocols and found Newtonian behavior, indicating the absence of entanglements. The linear dependence of melt viscosity on molecular weights (α = 0.5 - 2) confirmed the behavior of hyperbranched polymers as unentangled polymeric fractals for the hyperbranched polyesters studied.[12] In reports of Luciani et al.[13] and Hawker et al.[14] the power law exponent decreases asymptotically to 1 for high molecular weights of both structures, that is hyperbranched polymers and dendrimers. Moreover, simulation for hyperbranched polymers with nonequilibrium molecular dynamics (NEMD) demonstrated a single α-value of approximately 0.65 for both hyperbranched polymers and dendrimers and therefore the absence of entanglements, since the scaling relation does not split into two different regimes.[15]

However, within the scope of recent studies, some initial results suggesting entanglement in extremely high molecular weight hyperbranched polymers have been found. By considering a wide range of molecular weights, complex patterns of scaling relations between zero shear viscosity and molar mass have been observed.[5] While ‘‘power laws’’ hold with scaling exponents ≤ 2 for low molecular weights, branched polymers with very high molar masses are expected to exhibit a distinctly deviating, stronger behavior. In fact, the thermorheological behavior of functional linear and branched polymers (mostly with contribution by hydrogen bonding) has been affiliated with numerous anomalies and contradictions.[16] These range from violation of time-temperature superposition (TTS) for urazole-carrying linear polybutadienes to validation of TTS for hyperbranched polyglycerols[5], the polymers under investigation in this study.

In this paper we present a study on the thermorheological properties of hyperbranched polyglycerols (*hb*PGs) with systematically varied molecular weights in the range of 600 to 106 000 g mol^{-1} with a high, constant degree of branching and invariant low polydispersities.

Determination of a viscosity molar mass scaling relation, which allows tracking possible conformational transitions, is our primary interest.

Experimental Part

Synthesis of hyperbranched polyglycerols

The wide range of molecular weights (600–106 000 g mol^{-1}) was achieved by three different synthetic protocols. *hb*PG with low molecular weight ($M_n \leq 6\,000$ g mol^{-1}) was prepared according to the procedure established by Sunder et al.[4] *hb*PG with elevated molecular weights (6 000 g $mol^{-1} \leq M_n \leq 23{,}000$ g mol^{-1}) was prepared according to a recently published procedure[6] and *hb*PG with molecular weights (M_n = 80 000 and 106 000 g mol^{-1}) was prepared according to a method introduced by Kainthan et al.[5]

Instrumentation

^{1}H NMR spectra were recorded at 300 MHz on a Bruker AC and were referenced internally to residual proton signals of the deuterated solvent. ^{13}C NMR spectra were recorded at 100.15 MHz and referenced internally to solvent signals.

For SEC measurements in DMF (containing 1 g L^{-1} of lithium bromide as an additive), an Agilent 1100 series was used as an integrated instrument including a PSS HEMA column ($10^6/10^5/10^4$ g mol^{-1}) and a RI detector. Calibration was achieved with poly(styrene) standards provided by Polymer Standards Service (PSS). DSC curves were recorded on a Perkin Elmer DSC 7 and a Perkin Elmer Thermal Analysis Controler TAC 7/DX. Samples were dried at 80 °C for 24 h in vacuo directly before measurements. Rheological experiments were performed on a Paar Physica MCR-301 under nitrogen atmosphere, using plate-plate geometry. The linear viscoelastic behavior of the polymers was obtained by carrying out amplitude sweeps at a fixed frequency and deformation varied between a few % to 0.01% for highest and lowest temperatures, respectively. All subsequent analyses were based on frequency sweeps that were performed at temperatures between -25 °C and +50 °C (up to +150 °C for the high molecular weight samples). Frequencies were varied from 100 s^{-1} to 0.1 s^{-1}.

Results and Discussion

A series of hyperbranched PGs (Scheme 1) with molecular weights up to 23 000 g mol^{-1} as well as two polymer samples with very high molar mass (M_n = 80 000 and 106 000 g mol^{-1}) were obtained according to established literature procedures.[4–6] For all samples except for the two highest degrees of polymerization, molecular weights obtained from SEC measurements were compared to the values calculated from ^{1}H NMR spectra and found to be in good agreement (Table 1). All samples exhibited high degrees of branching (DB) as confirmed by ^{13}C NMR spectroscopy, close to the theoretical limit of 0.67. Glass transition temperatures were found to range between –12 °C and -28 °C. Table 1 summarizes the basic characterization data of the series of hyperbranched PG samples.

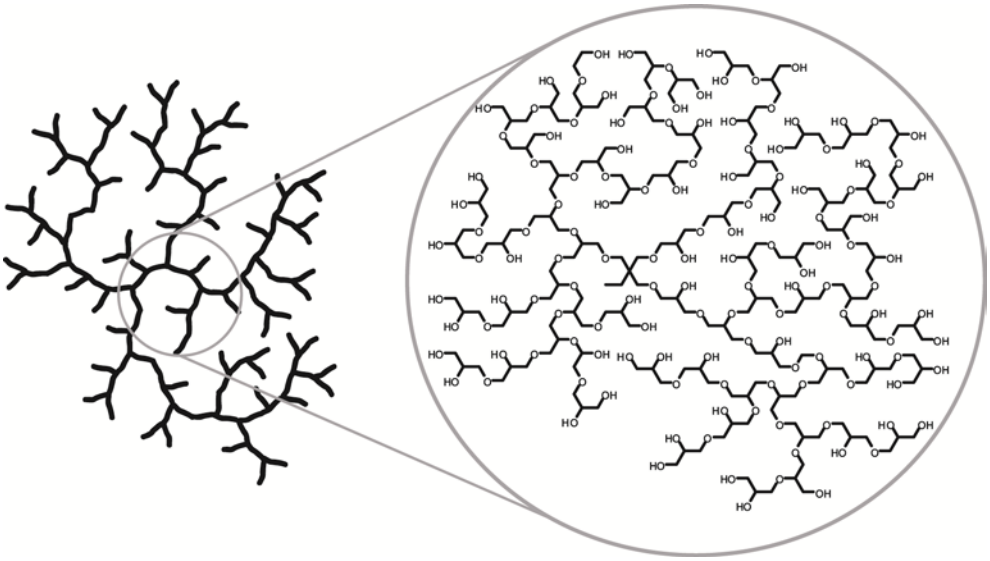

Scheme 1. Illustration of hyperbranched PG: schematic illustration (left) and chemical structure (right).

In the following the thermo-rheological properties and their relation to the molecular structure of *hb*PG will be discussed. Figure 1 shows the frequency sweep data obtained from PG-10000 at various temperatures, where the phase angle $\delta = \arctan G''/G'$ together with the storage modulus G' and the loss modulus G'' are plotted versus the complex modulus $|G^*| = (G'^2 + G''^2)^{1/2}$.[17]

Table 1. Basic characterization data of hyperbranched PGs prepared by anionic ring-opening polymerization for this study.

no.	$M_{n,calc}$ (g mol^{-1})	$M_{n,SEC}$ (g mol^{-1})[a]	$M_{n,NMR}$ (g mol^{-1})[b]	M_w/M_n[a]	DB[c]	T_g (°C)[d]
PG-600	500	600	700	1.41	0.52	-15.9
PG-1000	1 000	1 100	1 200	1.39	0.54	-17.1
PG-2000	2 000	2 100	2 500	1.31	0.56	-16.3
PG-3000	3 000	3 000	2 500	1.78	0.54	-17.3
PG-7000	7 000	6 800	6 300	1.87	0.59	-14.3
PG-10000	10 000	9 900	10 200	1.38	0.62	-20.8
PG-18000	18 000	18 200	19 400	1.43	0.63	-19.2
PG-23000	25 000	22 800	---[f]	1.77	0.61	-28.1
PG-80000[e]	8 000	80 500	---[f]	1.21	0.62	-18.7
PG-100000[e]	8 000	106 000	---[f]	1.19	0.62	-19.7

[a]Determined via SEC-RI in DMF using linear PS standards. [b]Calculated from ^{1}H NMR spectra by comparison of repeat unit signal intensity to core signal intensity. [c]Calculated from inverse gated ^{13}C NMR spectra. [d]Determined by DSC measurements. [e]The vast difference between theoretical and experimental molecular weight is a common observation when using dioxane as emulsifying agent. [f]A reliable calculation of the molar mass was not possible because of the relatively weak initiator signal.

These data indicate a transition from a viscous fluid in the terminal flow region (highest temperatures and lowest moduli; $G' \propto |G^*|^2 \propto \omega^2$, $G'' \propto |G^*|^1 \propto \omega^1$, $\delta \propto |G^*|^0 \propto \omega^0$) to a glassy solid ($G' \approx 10^9$ Pa, $\delta < 45°$) in a very narrow temperature range of 37 K. Moreover, the temperature dependence of δ-values shows 3 distinct regions. While TTS holds in the terminal regime and in the glassy zone, it is not fulfilled in an intermediate module range. This behavior is assumed to be a consequence of the dramatic influence imposed on the structural mobility and relaxation by hydrogen bonding, leading to the violation of TTS for these polymers. Also, segmental relaxation, which is usually prominent in a similar module range, cannot be excluded. The detailed investigation of structural reasons for this behavior is part of our future work. However, the absence of any crossover between G´ and G´´ just above the terminal zone indicates the lack of entanglements within this sample. As discussed, the crossover at higher frequencies marks the dynamic glass transition of the sample.

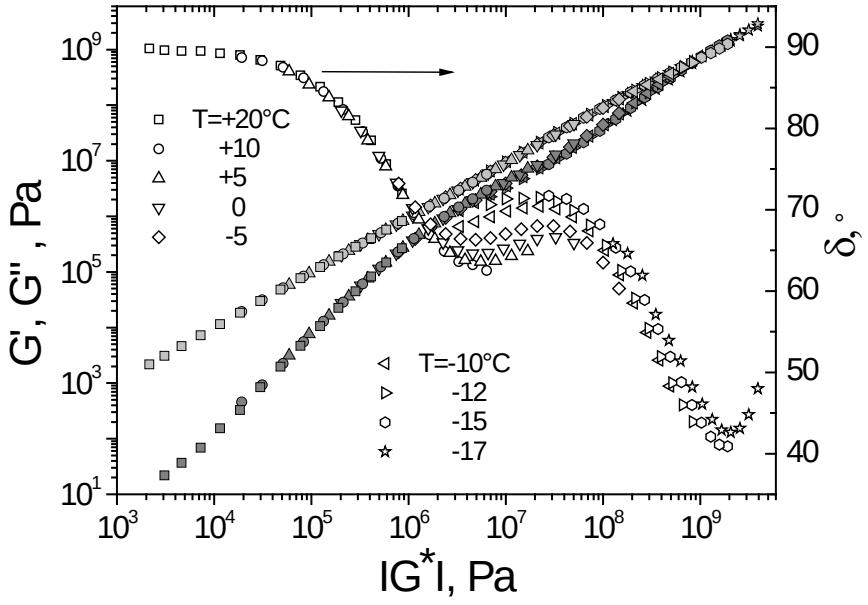

Figure 1. Frequency sweeps (PG-10000) at different temperatures. Storage modulus (G'), loss modulus (G'') and phase angle (δ) are plotted vs. the absolute value of the complex modulus (|G*|).

Further important structural information is gained from investigating the viscosity of the samples in dependence of molecular weight. In this context Figure 2a depicts the zero shear viscosity η_0 of *hb*PG samples with different molecular weights vs. temperature.

The zero shear viscosities were directly obtained from the existing plateau values of $\eta'(\omega) = G''(\omega)/\omega$ for the smallest frequencies or determined by a fitting procedure of the respective isotherms with an extrapolation to the plateau utilizing the Carreau-Jasuda equation. For measurements at even lower temperatures the distinct determination of $\eta_0(T)$ was almost impossible. Accordingly, the corresponding viscosity values of PG-100000 are missing in Figure 2a and b. Analyzing the frequency sweeps of this sample indicates a viscosity level of about 10^8 Pas at 20 °C and thus, Figure 2b contains an estimated value for the zero shear viscosity based on the data given in Figure 3b. However, all obtained $\eta_0(T)$ data follow the WLF (Williams-Landel-Ferry) equation in a consistent way. In general, the viscosity increases with decreasing temperature due to diminishing chain mobility and the strong influence of hydrogen bonding. The two samples with the highest molecular weight

(PG-80000 and PG-100000) have to be measured at higher temperatures (up to 150 °C) in order to obtain reliable data, indicating different structural influences in this molar mass regime.

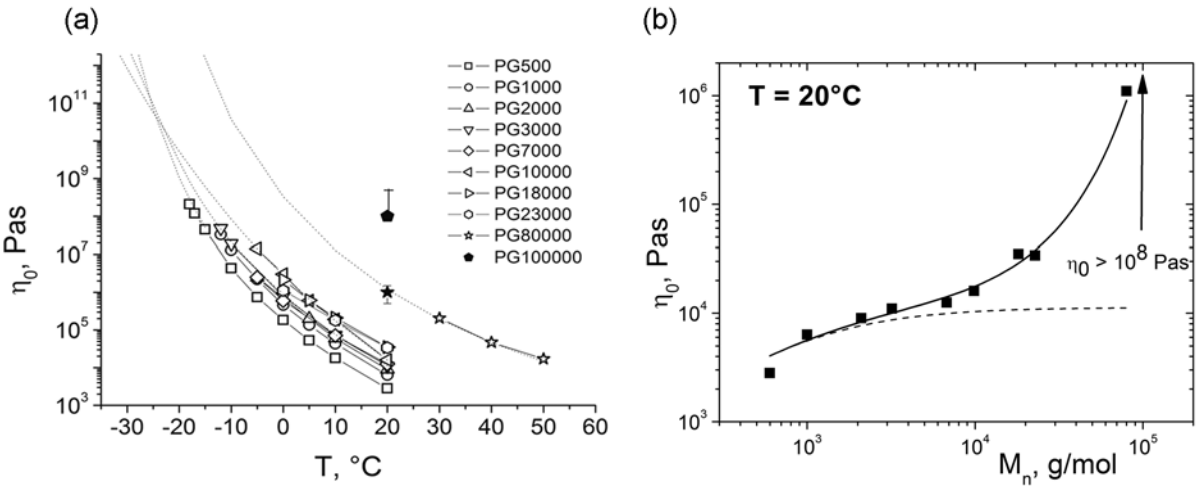

Figure 2. Temperature dependence of the zero shear viscosity η_0 of hyperbranched PG with different molecular weights (a), and zero shear viscosity at 20 °C vs. molecular weight (b).

Extrapolation of WLF behavior to a viscosity level of 10^{12} Pas (dotted lines in Figure 2a) marks the glass transition. The corresponding temperatures determined by rheological means range from -30 °C to -25 °C for lower molecular weights up to -15°C for the high molecular weight sample (PG-80000) and are in the same order of magnitude as the values given in Table 1. Plotting the zero shear viscosities given at 20 °C in Figure 2a together with the extrapolated value to this temperature of sample PG-80000 (extrapolation by help of WLF-parameters, see closed symbols) as well as the obtained value for PG-100000 permits to investigate the characteristic curve progression with varying molecular weight (Figure 2b). The curve shows first a linear increase and then a plateau like region, which is followed by a strong, exponential increase.

Previous studies on hyperbranched polyesters[12] (moderate DB) and dendrimers[14] in the low molecular weight regime report on a scaling that can be roughly expressed by eq. (1) with scaling exponents α = 0.5 - 2. While for low molecular weights, a similarly valid ‘‘power law’’ appears to be fulfilled, the relation becomes more complex once higher molecular weights are considered. These peculiar observations may result from two features: (i) a larger molecular weight range than it is usually considered and secondly (ii) the influence of

hydrogen bonding. After reaching a plateau-like area with fairly constant η_0 between 3 000 and 10 000 g mol^{-1}, the viscosity increases considerably above this region. The leveling, a known phenomenon[9a], can be explained by a constant density of the hyperbranched structures, which results in a ''dendrimer-like'' behavior (similar to hard spheres) and thus no increasing viscosity with higher molecular weight is observed. When a critical molecular weight of about 20 000 g mol^{-1} is reached the zero-shear viscosity shows exponential increase. This can be understood on the basis of entangled and interacting "star-like" polymers with a densely packed core region. Consequently, all data in Figure 2b can be described by the following empirical scaling behavior (black line in Figure 2b):

$$\eta_0 = K \cdot \frac{\left(\frac{M}{M_c}\right)^a}{1+\left(\frac{M}{M_c}\right)^a} \cdot \exp\left(\frac{M}{M_c^*}\right) \qquad (2)$$

with K = 10^4 Pas, M_c = 800 g mol^{-1}, a = 1 and M_c^* = 17 400 g mol^{-1}. Based on this equation the exponential increase of viscosity might appear at molecular weights exceeding the critical value of $M_c^* \approx$ 20 000 g mol^{-1}, which is in good agreement with the experimental data. However, this molecular weight underlines the significant deviation of the viscosity of higher molecular weight samples from the plateau region, which is represented by the "dendrimer part" (dashed line in Figure 2b, resulting from all except the exponential term) of the viscosity scaling in Equation (2).

Additional investigation of rheological features was carried out to support the idea of an entanglement transition in the high molecular weight regime of *hb*PG. Figure 3a shows the $\delta - |G^*|$ - isotherms measured at 0 °C for all samples listed in Table 1 together with the predictions of the Rouse model.[8] It is clearly visible that for the lowest molecular weights the behavior of all samples differs from the behavior of unentangled linear polymer chains. The appearing "bump" in the samples curve might be assigned to the hyperbranched structure of the macromolecules.[18] A detailed study of the potential influence of hydrogen bonding is one part of our future work. First results using modified *hb*PG with apolar substituted and thereby deactivated hydroxyl groups present a similar "bump" in the same region leading to the conclusion that the observed behavior can be attributed to the branching structure of the polymers and not solely to O-H interactions.

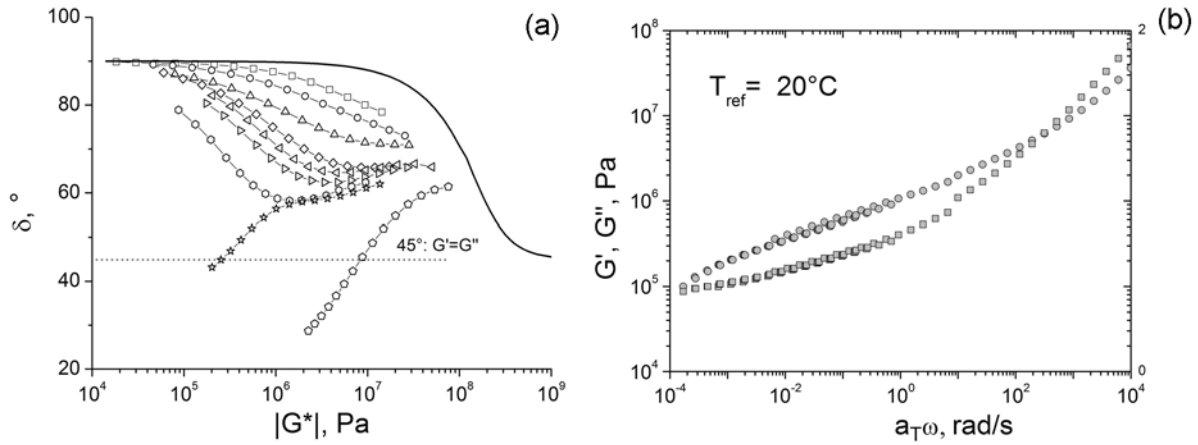

Figure 3. δ vs. |G*| plot for 0 °C-isotherms of all samples together with the Rouse behavior (black line, the symbols are defined in Figure 2a) (a) and master curve for G' (squares) and G'' (circles) of PG-100000 sample (b).

The δ-values of all *hb*PGs with molecular weights up to 23 000 g mol^{-1} exceed 45° in the whole module range up to the glass region. This property indicates missing entanglements for these polymers. In contrary, the isotherms of the high molecular weight samples (PG-80000 and PG-100000) intersect the δ = 45° line and mark a region on the |G*|-axis, in which G' > G'' holds. This behavior is an additional indication for the appearance of entanglements between the hyperbranched molecules.

In the case of the two samples with the highest molecular weights we were able to resolve the width of the specific region (G' > G'') by measuring the master curve in the module-frequency coordinates. In this way, true entanglement dynamics are visualized by the G´/G´´ crossover just above the terminal zone. This behavior is especially pronounced in the case of PG-100000 (see Figure 3b), where a distinct region with G´ >> G´´ can be observed over a broad frequency range.

Conclusion

A series of well-defined hyperbranched polyglycerols with molecular weights ranging from 600 to 106 000 g mol^{-1} has been prepared and characterized with respect to their thermo-rheological behavior. The terminal viscoelastic properties were found to obey the WLF behavior, while for intermediate frequencies the time-temperature superposition principle is

violated due to the pronounced influence of hydrogen bonding. We demonstrated that for *hb*PGs with high degree of branching and low molecular weights a scaling relation between zero shear viscosity and molecular weight, which is reminiscent for dendritic polymers, is obeyed, while a more complex, exponential behavior is observed for high molar masses. This is assumed to be a direct consequence of the increasing significance of entanglements between "star-like" structures once the size of the macromolecules exceeds a threshold value of about 20 000 g mol^{-1}. All results obtained support our idea of an entanglement transition for *hb*PGs at elevated molecular weights.

The thermo-rheological behavior of similar structures with varying functionalities as well as suppressing O-H interactions via end group modification is part of ongoing studies that aim at a more detailed insight in the influence of end group functionalities on the rheological properties of hyperbranched polymeric materials.

Acknowledgement

C.T. thanks the *Max Planck Graduate Center with Johannes Gutenberg-University (MPGC)* for fellowship and financial support. H.F. and D.W. acknowledge continuous financial support by the *Fonds der Chemischen Industrie.* D.W. and C.T. are grateful for further support by the *MAINZ Graduate School of Excellence*.

Supporting Information

Size Exclusion Chromatography

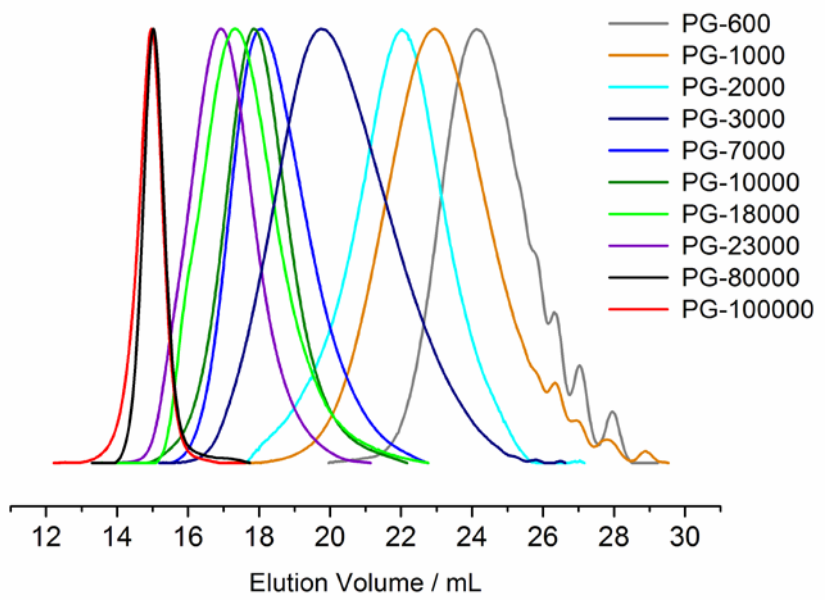

Figure S1. SEC traces of hyperbranched PGs.

NMR Spectroscopy

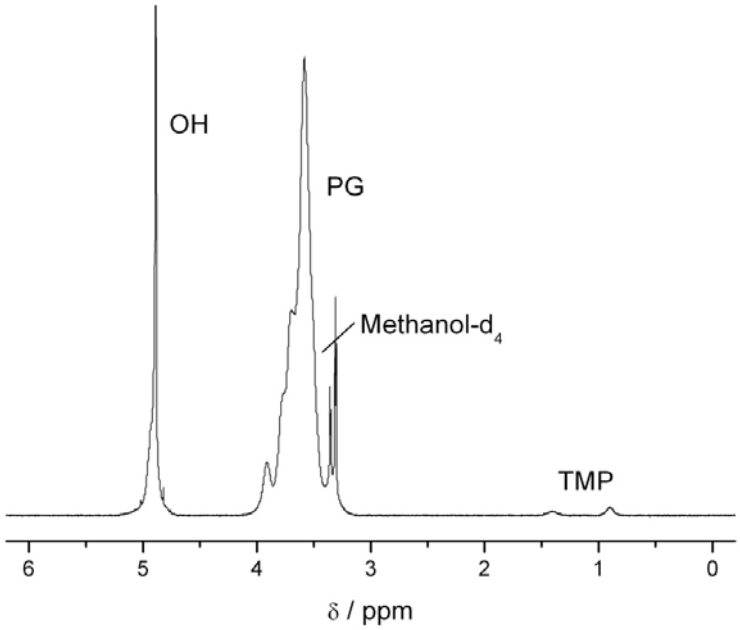

Figure S2. Exemplary ^{1}H NMR spectrum of hyperbranched PG. Molecular weights can be calculated by referencing to the proton signals of the TMP initiator core.

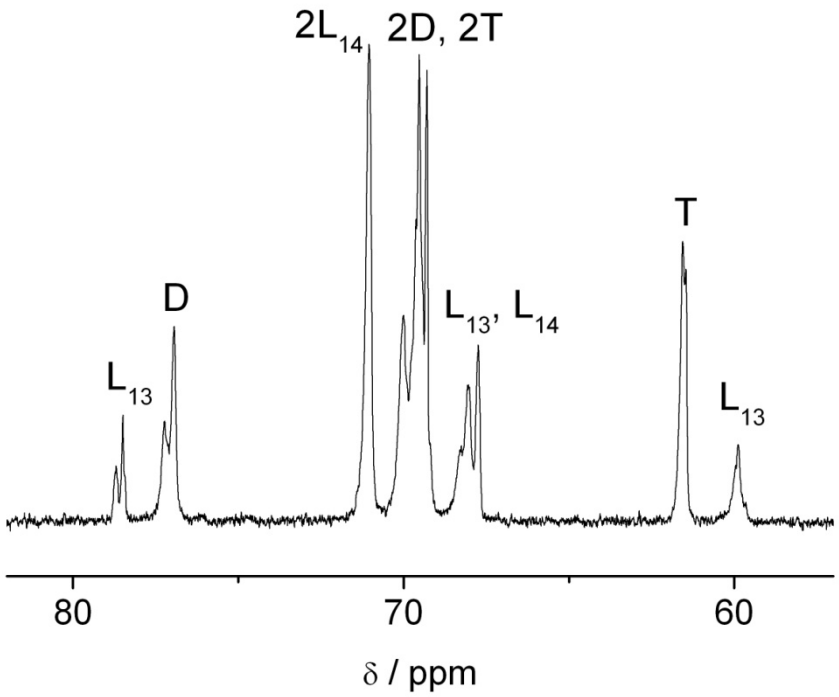

Figure S3. Exemplary inverse gated ^{13}C NMR spectrum of hyperbranched PG, depicting the different structural units.

Additional Exemplary Isotherms and van Gurp-Palmen Plots

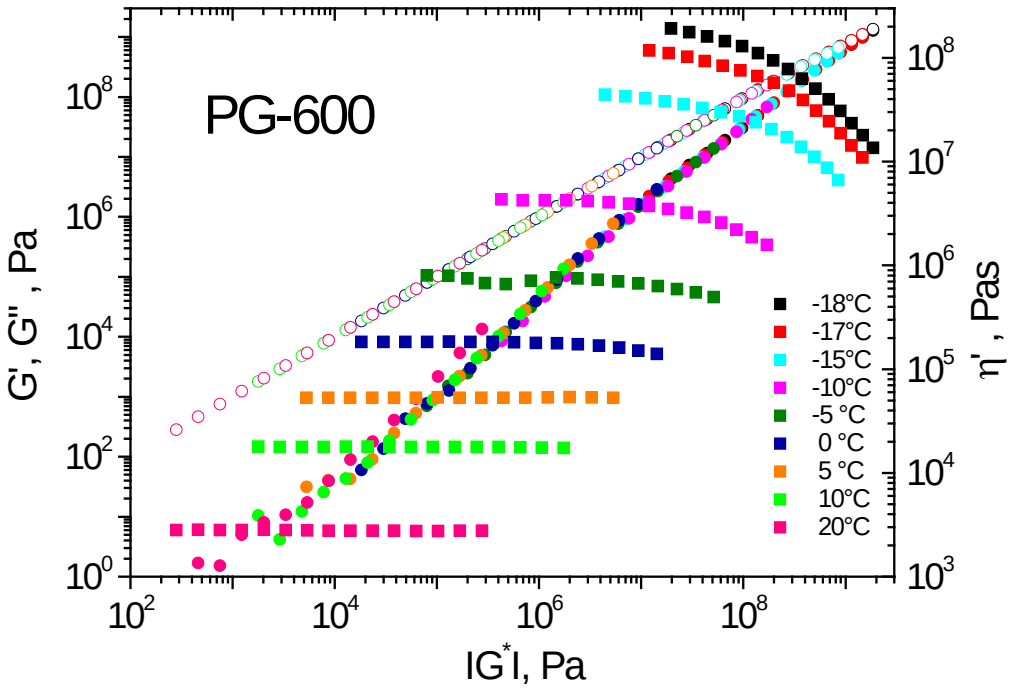

Figure S4. Isotherms for G' (filled circles), G'' (open circles) and viscosity (filled squares) (right) of PG-600.

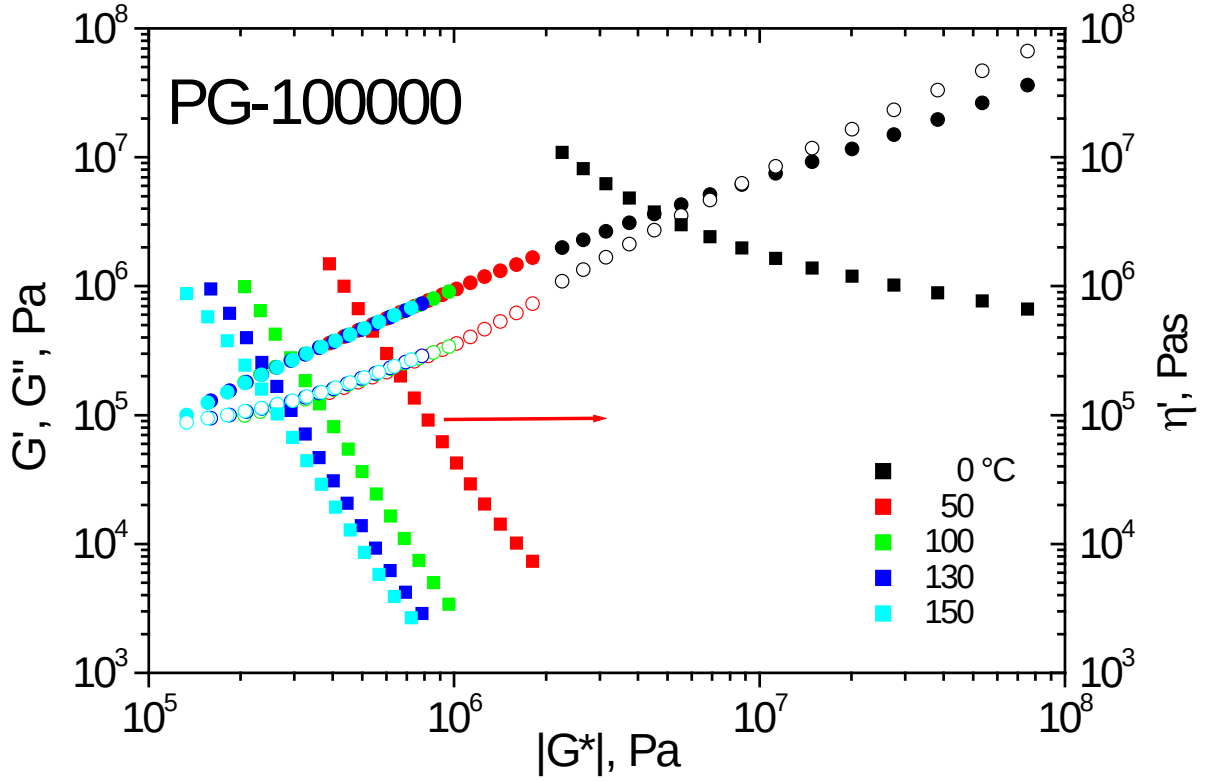

Figure S5. Isotherms for G'(filled circles), G'' (open circles) and viscosity (filled squares) (right) of PG-100000.

References

[1] [1a] D. Yan, C. Gao, *Prog. Polym. Sci.* **2004**, *29*, 183; [1b] B. I. Voit, *J. Polym. Sci., Part A: Polym. Chem.* **2000**, *38*, 2505; [1c] A. Sunder, J. Heinemann, H. Frey, *Chem. Eur. J.* **2000**, *6*, 2499.

[2] G. R. Newkome, C. N. Moorefield, F. Vögtle, *Dendrimers and Dendrons*; WILEY-VCH: Weinheim, Germany 2001.

[3] [3a] D. A. Tomalia, A. M. Naylor, W. A. Goddard III, *Angew. Chem. Int. Ed. Engl.* **1990**, *29*, 138. [3b] T. H. Mourey, S. R. Turner, M. Rubinstein, J. M. J. Fréchet, C. J. Hawker, K. L. Wooley, *Macromolecules* **1992**, *25*, 2401.

[4] A. Sunder, R. Hanselmann, H. Frey, R. Mülhaupt, *Macromolecules* **1999**, *32*, 4240.

[5] R. K. Kainthan, E. B. Muliawan, S. G. Hatzikiriakos, D. E. Brooks, *Macromolecules* **2006**, *39*, 7708.

[6] D. Wilms, F. Wurm, J. Nieberle, P. Böhm, U. Kemmer-Jonas, H. Frey, *Macromolecules* **2009**, *42*, 3230.

[7] [7a] D. Wilms, S.-E. Stiriba, H. Frey, *Acc. Chem. Res.* **2010**, *43*, 129. [7b] M. Calderón, M. A. Quadir, S. K. Sharma, R. Haag, *Adv. Mater.* **2010**, *22*, 190.

[8] M. Rubinstein, R.H. Colby, *Polymer Physics*, Oxford University Press, New York, 2003.

[9] [9a] A. Hult, M. Johansson, E. Malmström, "*Hyperbranched Polymers*" in Adv. Polym. Sci., Springer Verlag, Berlin, 1999, *143*; [9b] D. R. Daniels, T. C. B. McLeish, R. Kant, B. J. Crosby, R. N. Young, A. Pryke, J. Allgaier, D. J. Groves, R. J. Hawkins, *Rheol. Acta* **2001**, *40*, 403; [9c] P. F. W. Simon, A. H. E. Müller, T. Pakula, *Macromolecules* **2001**, *34*, 1677; [9d] K. Yamauchi, J. R. Lizotte, T. E. Long, *Macromolecules* **2003**, *36*, 1083; [9e] J. R. Dorgan, D. M. Knauss, H. A. Al-Muallem, T. Huang, D. Vlassopoulos, *Macromolecules* **2003**, *36*, 380; [9f] M. G. McKee, C. L. Elkins, T. E. Long, *Polymer* **2004**, *45*, 8705; [9g] M. G. McKee, C. L. Elkins, T. Park, T. E. Long, *Macromolecules* **2005**, *38*, 6015.

[10] C. M. Nunez, B.-S. Chiou, A. L. Andrady, S. A. Khan, *Macromolecules* **2000**, *33*, 1720.

[11] J. Vukovic, M. D. Lechner, S. Jovanovic, *Macromol. Chem. Phys.* **2007**, *208*, 2321.

[12] [12a] I. Sendijarevic, A. J. McHugh, *Macromolecules* **2000**, *33*, 590; [12b] D. M. A. Buzza, D. J. Groves, T. C. B. McLeish, D. Parker, A. J. Keeney, W. J. Feast, *Macromolecules* **2002**, *35*, 9605; [12c] H. Claesson, E. Malmström, M. Johansson, A. Hult, *Polymer* **2002**, *43*,

3511; [12d] J. Vukovic, S. Jovanovic, M. D. Lechner, V. Vodnik, *J. Appl. Polym. Sci.* **2009**, *112*, 2925.

[13] A. Luciani, C. J. G. Plummer, T. Nguyen, L. Garamszegi, J.-A. E. Manson, *J. Polym. Sci, Polym. Phys Ed.* **2004**, *42*, 1218.

[14] [14a] C. J. Hawker, P. J. Farrington, M. E. Mackay, K. L. Wooley, J. M. J. Fréchet, *J. Am. Chem. Soc.* **1995**, *117*, 4409; [14b] P. J. Farrington, C. J. Hawker, J. M. J. Fréchet, M. E. Mackay, *Macromolecules,* **1998**, *31*, 5043.

[15] T. C. Le, B. D. Todd, P. J. Daivis, A. Uhlherr, *J. Chem. Phys.* **2009**, *131*, 044902

[16] [16a] R. Stadler, L. De Lucca Freitas, *Colloid Polym. Sci.* **1986**, *264*, 773; [16b] R. Stadler, *Prog. Colloid Polym. Sci.* **1987**, *75*, 140; [16c] R. Stadler, L. De Lucca Freitas, *Macromolecules* **1989**, *22*, 714.

[17] S. Trinkle, C. Friedrich, *Rheol. Acta*, **2001**, *40*, 322.

[18] S. Trinkle, P. Walter, C. Friedrich, *Rheol. Acta*, **2002**, *41*, 103.

5.2: Effect of Hydrogen Bonds on Entanglement Behavior and Thermorheological Properties of Hyperbranched Polyglycerol Melts*

Carina Gillig,[1] *Christoph Tonhauser,*[2] *Christian Schubert,*[1] *Martina Schömer,*[2] *Daniel Wilms,*[2] *Holger Frey**[2] and *Christian Friedrich**[2]

[1]Freiburg Materials Research Center (FMF), Albert-Ludwigs-University, Stefan-Meier-Straße 21, 79104 Freiburg, Germany

[2]Institute of Organic Chemistry, Organic and Macromolecular Chemistry, Duesbergweg 10-14, Johannes Gutenberg-University Mainz, 55099 Mainz, Germany

To be submitted for publication in *Macromolecules* **2012**

Abstract

Two series of modified hyperbranched polyglycerols, methylated and trimethylsilylated, were synthesized in a broad molecular weight range (700 - 440 000 g mol^{-1}) and similar degree of branching (≈ 60%). Thermorheological properties of these polymers were determined and compared to their hydroxyl functionalized analogues. Glass transition temperature decreases of about 30 K when eliminating hydrogen bonds by modifying the hydroxyl groups. While viscoelastic spectra highlight break-down of time-temperature-superposition principle in frequency ranges, which can be attributed to segmental relaxation, terminal relaxation expressed by Newtonian viscosity scales with temperature by WLF-law. Zero-shear viscosities η_0, which are at individual levels for each type of functionalization, at the iso-free volume state (T_g +50 K) scale with molecular weight in the same way, which is known from polymers with star topology: a power law increase for lower in middle molecular weights is followed by a strong, exponential increase for highest molecular weights. Such behavior is attributed to the appearance of entanglements. Hydrogen bonds seem to favor entanglements in the sense that the entanglement molecular

weight is about 5/14 of the entanglement molecular weight of the modified samples. Furthermore, independent on functionality, a linear relation of the steady state compliance J_s^0 and molecular weight ($J_s^0 \sim M_n$) was obtained, also for the samples with highest molecular weights. Finally, we conclude that the dynamics of the presented hyperbranched polymers, synthesized by random branching originating from a trifunctional starter molecule, resemble to the dynamics known for star polymers.

*results of a collaboration with the group of Prof. Christian Friedrich (FMF, Freiburg, Germany

Introduction

The increasing amount of published papers on hyperbranched polymers indicates the increasing interest in this intriguing type of polymer. Hyperbranched (*hb*) polymers, postulated by Flory in the 1940s, possess a highly branched structure and a remarkable amount of functional groups.[1] Meanwhile, there are many different types of hyperbranched polymers, from polyester to polyether polyols, with all conceivable functionalities.[2-5] Although the preparation of hyperbranched polymers has been successfully and rapidly investigated over the last decades, the understanding of their dynamics and physical behavior in melt is still in its infancy. The influence of the numerous branches in these complex structures on the relaxation behavior is not fully resolved to-date. This could be due to a lack of knowledge on the precise macromolecular structure of *hb* polymers. The hyperbranched character of a polymer is defined by its degree of branching (DB), which can be calculated in different ways by combining the amount of dendritic (d), linear (l) and terminal (t) units.[6,7] While the definition of *Fréchet* (equation (1)) is not holding for low DB values, the definition of *Frey* (equation (2)) is valid in a broader range of DB. Depending on the applied definition of DB there can be a discrepancy of around 10%.

$$DB_{Fréchet} = \frac{d+t}{d+t+l} \quad (1) \qquad DB_{Frey} = \frac{2d}{2d+l} \quad (2)$$

However, the degree of branching represents only one parameter of the branched molecule and no local structure information are obtained. One can assume a statistical growth of the polymers structure but the actual sequence of linear, dendritic and terminal units can hardly be analyzed. As the structure is not consistent for polymers synthesized with different strategies, it is difficult to compare polymers of the hyperbranched regime with each other.

The individuality of various hyperbranched polymer structures impedes the creation of a universally applicable structure-to-property relationship. In literature several reports with different scaling theories on the zero shear viscosity (η_0) and molecular weight (M) relation are published. For instance, aliphatic *hb* polyesters up to a molecular weight of 8 000 g mol^{-1} showed a linear relation ($\eta_0 = KM$) as the Rouse model predicts for unentangled linear systems.[8] This is consistent with the idea of dendritic polymers unable to entangle due to the

high branch density and short fragments between two branching points.[2] Similar results were found for aromatic *hb* polyesters up to a molecular weight of 120 000 g mol^{-1}.[9] Dendritically branched poly(styrene)s on the other hand showed a scaling behavior of $\eta_0 = KM^{2.2\pm0.1}$ which is in between of the scaling of unentangled linear polymers and entangled linear systems ($\eta_0 = KM^{3.4}$).[10] Feast and coworker investigated the homologous series of branched poly(styrene)s and showed that the number of branching points was constant but the linear sequences between the branching points were varied in order to obtain different molecular weights. For the highest molecular weight samples around 200 000 g mol^{-1} an alleged transition to the entangled regime could be found. By integrating more linear units between two branching points entanglements could also be observed for aromatic polyesters.[11] The entanglement molecular weight in the case of the hyperbranched polyesters was found to be the same as for the linear analogous.

Recently, we published the viscoelastic investigation of a series of hyperbranched polyglycerols (OH-PG)[12,13] with a broad range of molecular weights and similar degrees of branching.[14] Transition to the entangled regime was observed for high molecular weights and an equation could be found to describe the η_0-M-relation (equation (3)). The entanglement molecular weight for these hydroxyl functionalized hyperbranched polyether-polyols was determined to 20 000 g mol^{-1}

$$\eta_0 = K \cdot \frac{\left(\frac{M}{M_c}\right)^a}{1+\left(\frac{M}{M_c}\right)^a} \cdot \exp\left(\frac{M}{M_c^*}\right). \qquad (3)$$

Here, we present the modification of a series of *hb*PGs in combination with the investigation of thermorheological properties. We synthesized two series of methylated and trimethylsilylated *hb*PGs. By modifying the hydroxyl groups and introducing sterically more demanding end groups we analyzed the changes in relaxation behavior and thermal properties as a function of interactions and free volume. Furthermore the origin of the entangled regime should be investigated in detail.

Experimental Part

Reagents. All solvents and reagents were purchased from Acros Organics or Sigma-Aldrich and used as received, unless otherwise stated. Glycidol (96%) was purified by vacuum

distillation over CaH_2 directly prior to use. Diethylene glycol dimethyl ether (diglyme) and dioxane were distilled over CaH_2 under reduced pressure and stored over molecular sieves. Chloroform-d_1 and DMSO-d_6 were purchased from Deutero GmbH.

Polymer Synthesis.

Synthesis of hyperbranched polyglycerols. hbPG was achieved by three different synthetic protocols. *hb*PG with low molecular weight ($M_n \leq 6\ 000$ g/mol) was prepared according to the procedure established by Sunder et al.[12] *hb*PG with elevated molecular weights (6 000 g/mol ≤ M_n ≤ 23 000 g/mol) was prepared according to a recently published procedure[13] and *hb*PG with molecular weights (M_n = 80 000 and 106 000 g/mol) was prepared according to a method introduced by Kainthan et al.[15]

Silylation of hyperbranched polyglycerol. To a stirred suspension of the respective hyper-branched PG (5 mmol OH groups) and iodine (0.05 mmol) in methylene chloride (20 mL), hexamethyldisilazane (4 mmol) was dropwise added over a period of 5 minutes. The suspension was stirred for 48 h. Upon silylation, the polymer suspension slowly turned into a solution. Subsequently, 2-3 g finely powdered $Na_2S_2O_3$ was added portionwise. After filtration over silica gel, the solvent was evaporated under reduced pressure. The pure silylated hyperbranched PGs were obtained by precipitation into methanol.

Methylation of hyperbranched polyglycerol. ME-PG was prepared as described previously.[16] To a solution of TBAB and NaOH in water, polyglycerol was added prior to the slow addition of methyl iodide under vigorous stirring. The isolated product after concentration appears as a pale yellow oil.

NMR. ^{1}H NMR spectra were recorded on a Bruker AC at 300 MHz. The degree of modification was determined via ^{1}H NMR by comparing the decreasing hydroxyl signal of the OH-PG starting material to the modified samples. ^{13}C NMR spectra were recorded at 100.15 MHz and were used to determine the degree of branching as already published.[7] Degrees of branching were determined for all OH-PGs to 52-63% and assigned to the modified polymers as the degree of branching is not changing by a polymer analogues reaction.

SEC. SEC measurements were done for OH-PGs in DMF or $CHCl_3$ using PS standards. SEC measurements of the differently modified samples are not comparable as they are not

soluble in the same solvent. Therefore the molecular weights of the modified samples were calculated on the basis of the degree of modification and the molecular weight of the OH-PG starting material.

IR. IR spectra were recorded on a Bruker Vektor 22 FT-IR in a wavelength range between 600-4000 nm. All spectra were measured with a resolution of 4 cm^{-1}. Room temperature measurements as well as temperature ranges up to 120 °C were done.

TGA. Thermo gravimetric measurements were done on a Netzsch STA 409 heating from 50-650 °C.All samples were measured under air atmosphere and with a heating rate of 10 K/min. The degradation temperature was determined by the onset of the mass loss curve.

DSC. DSC measurements were carried out in a Perkin-Elmer DSC7 and verified in a Perkin-Elmer Pyris1 instrument. The temperature range was chosen from -120 °C (DSC7) and -90 °C (Pyris1) respectively up to 50 °C using a heating rate of 10 K/min. The glass transition temperature (T_g) was determined by the maximum of the first derivative of the second heating rate.

Rheology. Rheological properties were measured on a Paar Physica MCR-301 under nitrogen with a 8 mm plate-plate geometry. Oscillatory measurements were carried out in a frequency range between 0.1-100 rad/s with deformations of 10% for the highest temperatures down to 0.01% at temperatures close to T_g. The temperature range was individually chosen for every sample, starting at 100 °C for the highest molecular weight sample down to -68 °C depending on the individual T_g of the samples.

Data Analysis

Time temperature superposition and glass transition temperature. The isotherms measured by rheometry were horizontally shifted to a mastercurve according to the time temperature superposition principle. The shift factors a_T were fitted by the WLF equation (4)

$$\log a_T = -\frac{c_1(T - T_0)}{c_2 + T - T_0} \tag{4}$$

T_0 is the individual reference temperature and c_1 and c_2 are the fitting parameters which were determined by the software IRIS Rheo Hub 2008.

The viscosity in the Newtonian regime, the zero shear viscosity η_0, was determined by extrapolation of $\eta^{|}$ to low frequencies

$$\eta_0(T_{ref}) = \lim_{\omega \to 0} \eta' = \lim_{\omega \to 0} \frac{G''}{\omega} \tag{5}$$

By extrapolation of η_0 to a value of 10^{12} Pas the rheological T_g can be calculated ($\eta_0(T_g) = 10^{12}$ Pas):

$$log a_T = log\left(\frac{\eta_0(T_{ref})}{\eta_0(T_g)}\right) = -\frac{c_1(T_g - T_{ref})}{c_2 + T_g - T_{ref}} \tag{6}$$

Entanglement molecular weight. For entangled polymers the plateau modulus G_N^0 can be determined which is equivalent to the storage modulus $G^{|}(\omega)$ at the minimum of the loss factor $\tan\delta(\omega)$. The entanglement molecular weight can be calculated according to equation (7).

$$G_e = \frac{5}{4} G_N^0 = \frac{\rho RT}{M_e} \tag{7}$$

Steady state compliance. The steady state compliance J_s^0 is a measure for the compliance in the terminal regime. It is defined as in equation (8):

$$J_S^0 = \left(\frac{1}{{\eta_0}^2}\right) \lim_{\omega \to 0} \left(\frac{G'(\omega)}{\omega^2}\right) = \frac{\tau_t}{\eta_0} \tag{8}$$

Fractional free volume. Ferry's theory of the iso-free volume also includes the understanding of the fractional free volume.[19] The iso-free volume increases linearly with temperature and is dependent of the distance to T_g respectively. f_G is the fractional free volume at T_g and B is a constant which is usually set to one. c_1 and c_2 are the fitting parameters obtained by the WLF equation.

$$f_g = \frac{B}{2.303 c_1^g} \tag{9}$$

$$c_1^g = \frac{c_1 c_2}{c_2 + T_g - T_0} \tag{10}$$

Results and Discussions

Synthesis. The synthesis of the trimethylsilyl (SY-PG) and methyl (ME-PG) *hb*PG was successfully accomplished by polymer analogous reactions of hyperbranched polyglycerols (OH-PG).[14] Two series of protected *hb*PG of molecular weights between 700 to 440 000 g mol^{-1} with a comparatively narrow polydispersity ($M_w/M_n \approx 1.3$) were obtained. All samples independent of modification were stable up to 200 °C or higher. All polymer were characterized by NMR spectroscopy and SEC. The corresponding details are summarized in Table 1. The polymer samples are named by their functionality followed by the corresponding molecular weight.

Table 1: Characterization data of trimethylsilyl (SY-PG) and methyl (ME-PG) modified polyglycerols.

Polymer	M_n *	M_w/M_n*	DB**	DM ***
SY-1 200	1 200	1.22	0.52	96
SY-1 900	1 900	1.20		95-100
SY-4 200	4 200	1.46	0.56	94
SY-16 000	16 000	1.35		99
SY-20 000	20 000	1.28	0.62	100
SY-36 000	36 000	1.18	0.63	100
SY-46 000	46 000	1.27	0.61	100
SY-175 000	175 000	1.14		94
SY-440 000	440 000	1.13		100
ME-700	700	1.83	0.49	100
ME-9 600	9 600	1.29	0.60	100
ME-11 200	11 200	1.33	0.62	100
ME-13 200	13 200	1.51	0.59	100
ME-26 800	26 800	1.29	0.58	100
ME-57 100	57 100	1.53	0.52	100
ME-251 000	251 000	1.14	0.47	100

*M_n in g mol^{-1} determined via SEC of OH-PG starting material in DMF with PS-standard in combination with the calculated values by the degree of modification of hydroxyl groups **DB (degree of branching): determined via inverse-gated ^{13}C NMR of OH-PG[12] ***DM (degree of modification) in %: determined via ^{1}H NMR in DMSO-d_6 or $CHCl_3$

All samples showed a degree of branching between 47 to 63% and a degree of modification between 94 to 100%. According to IR spectroscopy all samples were 100% modified due to

the absence of O-H stretching band at wave numbers of approximately 3500 cm^{-1} detected. Temperature dependent IR spectroscopy was done in order to verify hydrogen bonds in the unprotected samples. As known from literature, the O-H stretching band at 3500 cm^{-1} is shifted to higher frequencies when hydrogen bonds are weakened by increasing temperature.[17] In case of the OH-PG this effect was clearly observed as exemplary shown in Figure 1 (bottom), which is a clear evidence for existing hydrogen bonds. The modified PGs on the other hand showed no change in any absorbance band with increasing temperature (Figure 1, top) for a SY-PG sample. For ME-PG samples a similar behavior as for SY-PG was observed.

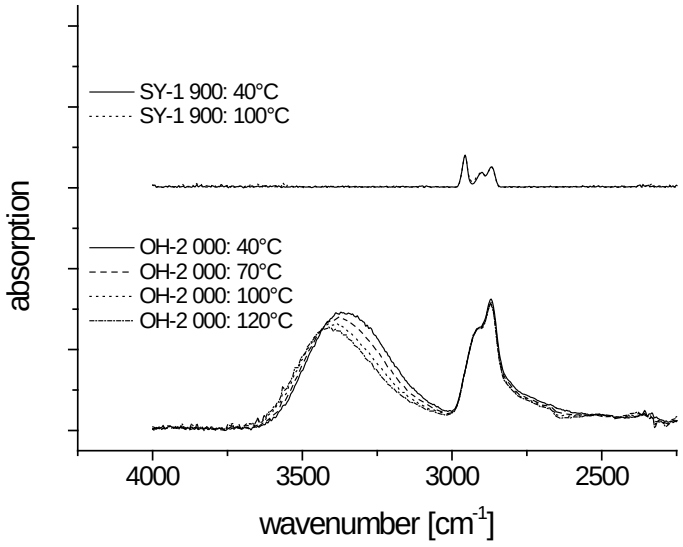

Figure 1: Proof of hydrogen bonds by temperature dependent IR spectroscopy of SY-1 900 and OH-2 000.

Glass transition temperature. Glass transition temperatures were determined with two different methods, via DSC measurements and by extrapolation of η_0 according to equation (6). In Figure 2 the rheological as well as the DSC-T_g are plotted for all investigated samples. The two different methods show good agreement even though the rheological T_g is in all cases determined slightly lower than the calorimetric T_g. The differences can be explained by the determination methods. The rheological T_g is determined while cooling whereas the DSC-T_g is determined while heating with differences in the applied heating rates respectively. Compared to the hydroxyl functionalized polyglycerols the glass transition temperatures of the protected polyglycerols are 30-40 K lower.[14] Partly modified

hyperbranched polyesters showed a similar reduction of T_g of about 60 K.[18] The lack of hydrogen bonds induces an increase of flexibility, which effects the dramatic decrease in T_g. The trimethylsilyl modified PGs have a slightly higher T_g than the methyl modified PGs which is due to the higher rigidity of the special more demanding trimethylsilyl groups. In addition an increased free volume can cause the effect, which will be discussed later in detail.

The glass transition temperature is known to be a function of molecular weight and the number of end groups n_e per molecule:[19]

$$T_g = T_{g\infty} - \frac{k' n_e}{M} \tag{11}$$

$$k' = \frac{\rho N_A v_f}{\alpha} \tag{12}$$

$T_{g\infty}$ is the glass transition temperature at infinite molecular weight, ρ the density, v_f the free volume per chain end and α the free-volume expansion coefficient. The number of end groups n_e is constantly 2 for linear polymers. In case of the anionic ring-opening multibranching polymerization of glycidol an AB_2 monomer the number of end groups increases linearly with increasing molecular weight. Each additional monomer unit induces one additional functional group which induces a constant value for n_e/M for high molecular weights when the molar mass of the initiator can be neglected.[20,21] Thus, T_g of high molar-mass samples reveal a plateau, representing $T_{g\infty}$.[22,23] By fitting the rheological T_gs according to equation (11) the glass transition temperatures at infinite molecular weight could be determined to 245 K for OH-PG, for SY-PG to 215 K and for ME-PG to 201 K. The rheological T_g for the highest molecular weight samples of OH-PG and SY-PG were not used for this calculation as the zero shear viscosities were determined by extrapolation to a plateau as already described in an earlier publication.[14] As indicated in Figure 2 the T_g of small molecular weights of the protected *hb*PG increases linearly with M_n due to the non-constant quotient n_e/M by considering the initiator molecular weight. In case of OH-PG the glass transition temperature is independent over the whole investigated molecular weight range since the hydrogen bonds dominate the T_g even in region of small molecular weights. These results are in good agreement to unprotected and protected hyperbranched polyesters.[24] It was also shown here that the degree of branching has a remarkable influence on glass

transition temperature – the higher the DB, the more chain ends and therefore increased segmental mobility was proven.

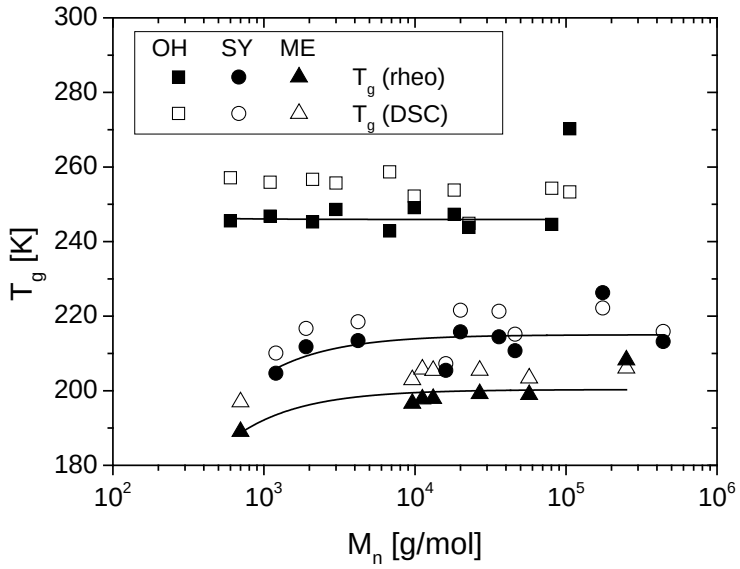

Figure 2: Comparison of rheological T_g and DSC-T_g as a function of molecular weight, fitted by equation (11).

Rheology. Rheological measurements were accomplished for all modified samples and compared to the already published series of OH-PGs.[14] In the Booij-Palmen-Plots of an entangled and unentangled sample of all three modifications are shown respectively. At values of G* around 10^6 Pa a breakdown of the time-temperature-superposition is observed, which is due to segmental relaxation and has already been mentioned for the OH-PG and dendritically branched poly(styrene)s.[10] Independent of molecular weight and functionalization, the segmental relaxation seems to be a result of the hyperbranched structure and not of the hydrogen bonds. A final proof for this assumption can be supplied when comparing linear PGs to the branched structures which will be part of our future work. Transition to the entangled regime ($\delta > 45°$ at $G^* \approx 10^5$-10^7 Pa and $G' > G''$) could be found for the highest molecular weight samples SY-175 000, SY-440 000, ME-251 000, OH-80 000 and OH-100 000 as exemplary shown in Figure 3.

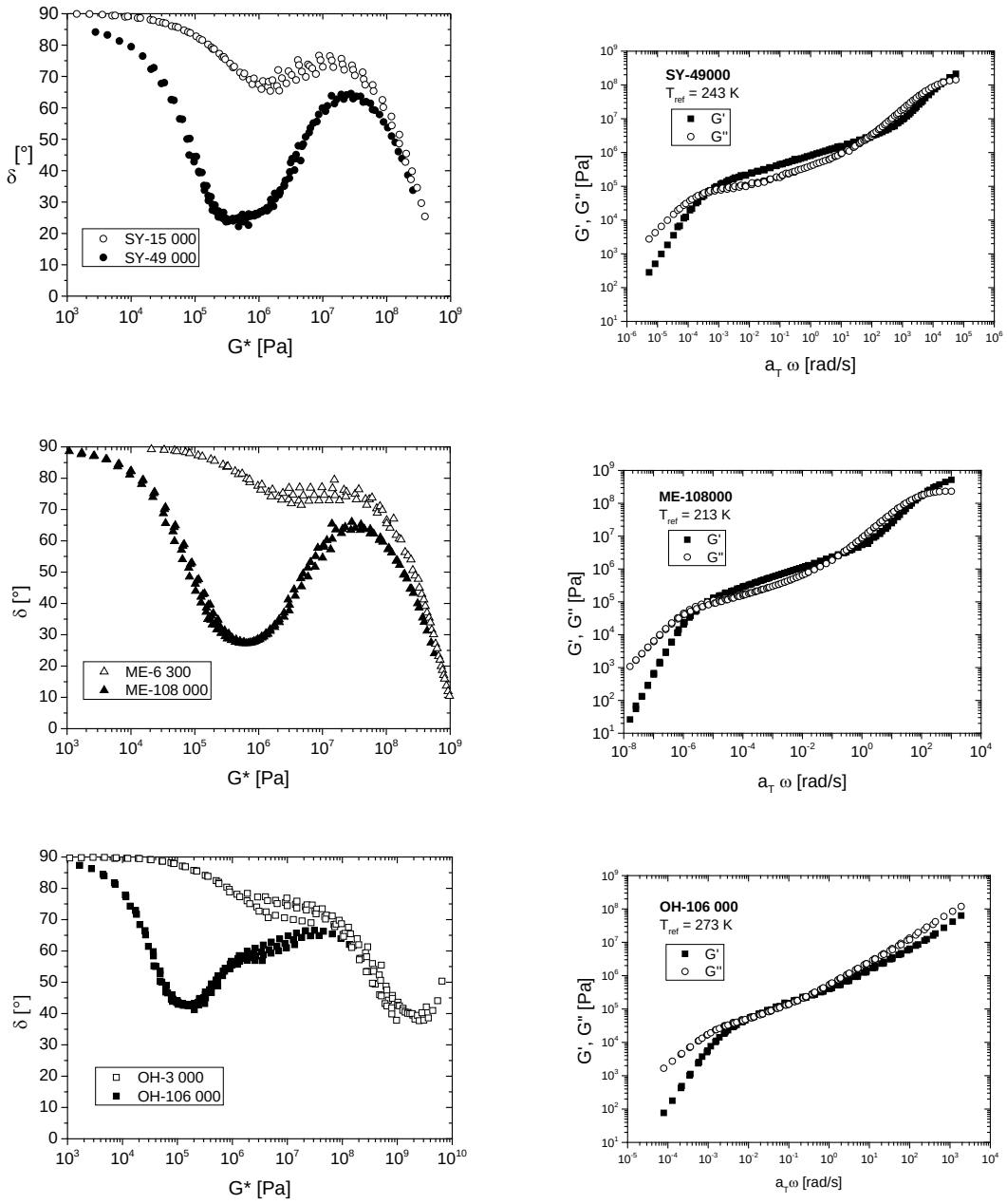

Figure 3: Booij-Palmen Plots of entangled and unentangled samples (left) and mastercurves (right, b_T=1) for SY-PG (top), ME-PG (middle) and OH-PG (bottom).

A list of thermorheological data for both series of modified polyglycerols is shown in Table 2.

Table 2: Thermorheological data for SY-PG and ME-PG determined by DSC and rheometry.

polymer	T_g (DSC)*	T_g (rheo)**	T_v-T_g(rheo)**	T_{ref} (Master)***	C_1	C_2****	$C_1 \cdot C_2$****
SY-1200	210,1	204,7	25,0	223	8,9	43,3	385,4
SY-1900	216,7	211,8	27,0	233	8,8	48,2	424,2
SY-4200	218,5	213,4	26,2	233	8,7	45,7	397,6
SY-16000	207,2	205,5	29,5	243	6,9	67,1	463,0
SY-20000	221,6	215,8	28,2	243	7,5	55,4	415,5
SY-36000	221,3	214,4	29,9	243	7,6	58,5	444,6
SY-46000	215,2	210,7	32,1	243	7,4	64,4	476,6
SY-175000	222,2	226,3	34,4	243	6,7	51,1	342,4
SY-440000	215,9	231,3	15,3	243	5,7	45,1	257,1
ME-700	196,9	189,1	26,7	213	7,9	50,8	401,3
ME-9600	202,9	196,6	24,9	213	8,2	41,4	339,5
ME-11200	205,8	197,8	26,1	213	8,8	41,5	365,2
ME-13200	205,4	197,9	28,9	213	9,3	44,3	412,0
ME-26800	205,5	199,2	28,3	213	9,3	42,3	393,4
ME-57100	203,4	199,0	29,7	213	9,5	44,0	418,0
ME-251000	206,1	208,3	40,5	213	9,9	45,5	450,5

*T_g(DSC) in K: determined via DSC **T_g(rheo) in K: calculated by equation (6) ***T_{ref}(Master) in K: reference temperature for the master curve ****c_2 in K: calculated by equation (4)

Fractional free volume. The fractional free volume at the glass transition temperature can be calculated by equation (9). In Figure 4 the fractional free volumes of all investigated samples are shown at a reference temperature $T_{ref}=T_g$(rheo). The highest molecular weight samples of each modification were omitted for the following analysis as they were extrapolated as described before.[14] All samples, independent of functionality and molecular weight, show with $f_g \approx 0.032$ a slightly higher fractional free volume than linear polymers which are known to have a fractional free volume of $f_g/B = 0.025 \pm 0.005$.[19] This is contrary to the results from Luciani et al. and Vukovic et al. who reported a lower value of fractional free volume for hb polyesters derivatives.[23,25] Similar to our results larger values as $f_g/B=0.025$, were found for dendritic polybenzylethers although the degrees of branching are not numerically mentioned.[26,27] An increased fractional free volume is equal to a less

compact shape which is equivalent to a higher flexibility of ether bonds compared to ester bonds.

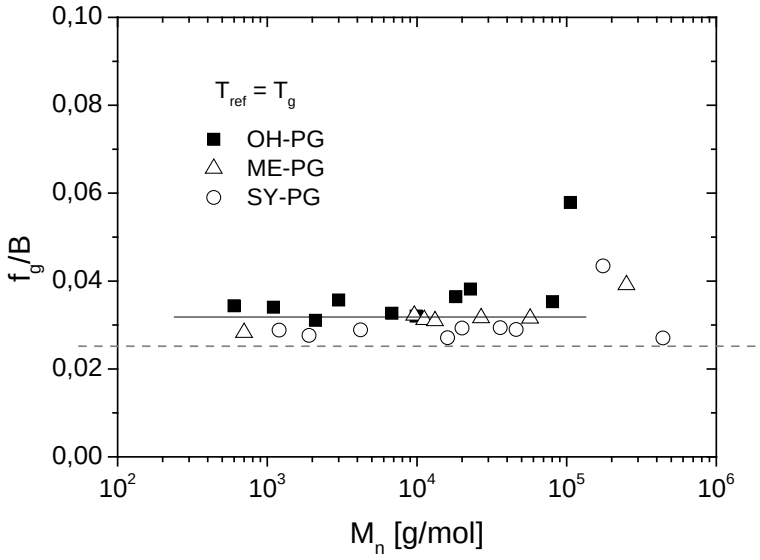

Figure 4: Molecular weight dependence of fractional free volume f_g for SY-PG, ME-PG and OH-PG at $T_{ref}=T_g$(rheo).

Zero-shear viscosity. The temperature dependence of the zero shear viscosities is shown in Figure 5. All viscosities can be fitted by the WLF equation (4). The viscosities of the entangled samples at high molecular weights are significantly higher compared to the unentangled samples if comparing at the same temperature.

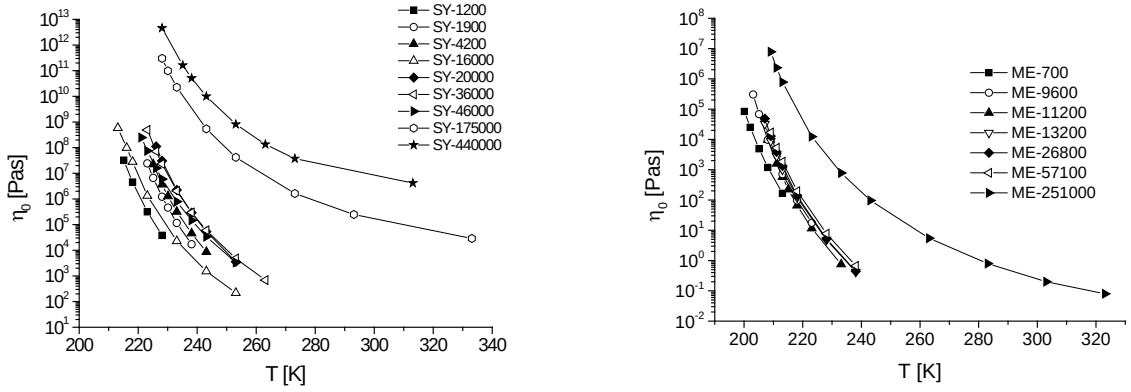

Figure 5: Temperature dependence of zero shear viscosities η_0 for SY- and ME-PGs fitted by WLF equation.

Due to the enormous differences in T_g a comparison of viscosities at the same reference temperature is not meaningful as the samples would be compared at different free volume states. As it was shown in Figure 4 the samples have similar fractional free volumes, independent of molecular weight and functionality. Taking into account that all samples have the same free volume expansion coefficient α all samples were shifted to an equal distance to the rheological T_g in order to compare the polymers at the iso-free-volume state: $T_{ref} = T_g+50K$. In Figure 6 the viscosities at the iso-free-volume state are plotted as a function of molecular weight for all samples. Both series of modified PGs have lower viscosities due to the lack of hydrogen bonds. This effect is consistent with the decrease of glass transition temperatures by protection of the hydroxyl groups as it was shown earlier. Contrary to the lower T_g of ME-PGs compared to SY-PGs, the viscosities at $T_{ref} = T_g+50$ K are higher for the methylated polyglycerols. The sterically demanding trimethylsilyl group creates a higher flexibility of the polymer and therefore a less viscous material at the iso-free-volume state is obtained.

As mentioned above a universally applicable η_0-M relation for hyperbranched polymers are not established to-date. In the earlier paper we postulated an equation (3) for the molecular weight dependency of the zero shear viscosities for the OH-PGs. This equation was found to be valid for OH-PGs at a reference temperature of 293 K which is almost 50 K above the individual T_g. Even though the postulated equation is valid for the OH-PGs at $T_{ref} = T_g+50K$, it cannot be applied to the modified PGs presented in this contribution. After switching of the hydrogen bonds the hyperbranched polymers seem to possess other dependencies on the η_0-M relation, e.g., stronger influence of entanglements on viscosity.

Taking a closer look on the chemical structure of the polyglycerol synthesized by using TMP as initiator it can be assumed that the polymer presents a branched three-arm star molecule. Under the assumption that all arms are equally growing, the molecular weight of one arm is equal to $M_a=M_n/3$. Reptation of star polymers is restricted to the fact that the arms cannot move individually since the arms are connected to a shared focal point (TMP initiator). Considering the three-arm star mobility a relation between zero shear viscosity η_0 and arm molecular weight M_a is known (equation 13).[28]

$$\eta_0 = K \cdot \left(\frac{M_a}{M_e}\right)^b \cdot exp\left(v' \frac{M_a}{M_e}\right) \qquad (13)$$

In Figure 6 the viscosities of all investigated polymers as a function of molecular weight are plotted and fitted to equation (13) taking into account that the molecular weight of one arm is one-third of the polymer molecular weight. The parameters b and v' were both set to 0.5 as it was reported in literature for star polymers.[29,30]

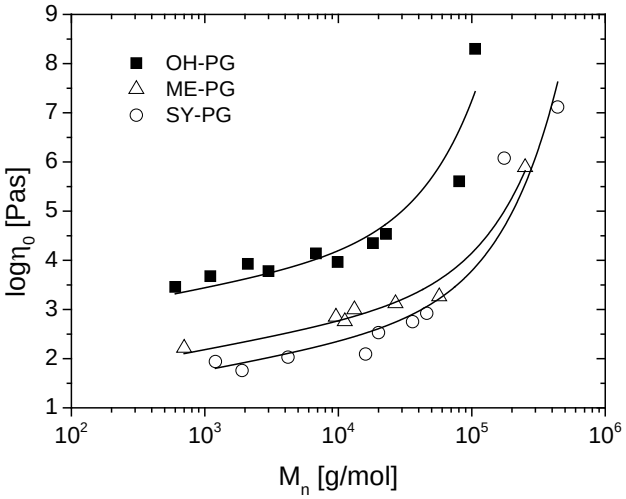

Figure 6: Molecular weight dependency of zero shear viscosities at $T_{ref}=T_g(rheo)+50$ K by fitting to equation (13) with b = 0.5 and v' = 0.5.

The zero shear viscosities of all *hb*PGs are in good agreement with the theory for star polymers. The first set of entanglement molecular weights (M_e) were obtained from equation (13) Furthermore, in order to proof this calculation, a second access to M_e were employed by using the plateau modulus G_N^0 in combination with equation (7). This procedure was done only for the highest molecular weight sample of each *hb*PG modification by assuming a density of 1 g ml^{-1}. The entanglement molecular weights of both determination methods are listed in Table 3. Both calculations provide good agreement within the error. The M_e of the protected polyglycerols (SY-PG and ME-PG) are about twice as high as the M_e of the OH-PG and are independent of the type of protection group. Interactions as hydrogen bonds seem to favor entanglements in the sense of lowering the entanglement molecular weight.

Table 3: Calculated entanglement molecular weights of all polymer modifications.

polymer	M_e [a]		M_e [b]	
OH-PG	2555	± 421	2565	± 342
ME-PG	7427	± 639	3605	± 995
SY-PG	7000	± 989	6651	± 666

[a] M_e in g mol^{-1}: calculated by equation (13) for star polymers with $M_a=M_n/3$, b=0.5 and v'=0.5. [b] M_e in g mol^{-1}: calculated by equation (7) with the plateau modulus for the highest molecular weight samples of each modification

Steady state compliance. The steady state compliance J_s^0 is defined as in equation (8). It can be determined by a plot of G'/G''^2 at $\lim(\omega\rightarrow 0)$ or by dividing the terminal relaxation time τ by η_0. Both methods have been applied and the resulting J_s^0 are plotted in Figure 7 for all analyzable polymers. Independent of the functionalities a linear relation of $J_s^0 \sim M_n$ was observed over the whole molecular-weight range. This behavior is unlike in linear polymers where the steady state compliance is known to be independent of molecular weight in the entangled regime.[19] Star polymers on the other hand show a relation $J_s^0 \sim M_n$ even at molecular weights of $M_a/M_e > 1$.[31-33] The investigated polymers clearly show a similar behavior as star polymers over the whole molecular weight range. This evidences an entanglement between the arms growing from the trifunctional initiator if the particular polymer arms exceed a certain chain length. At an elevated molecular weight the branches seem not to prevent polymer entanglements. Similar results were obtained for dendritically branched poly(styrene)s even though there was no trifunctional initiator used for the synthesis.[10] Also in arborescent polystyrene-graft-polyisoprene copolymers a linear increase of J_s^0 with the molecular weight was found even in the entangled regime.[34]

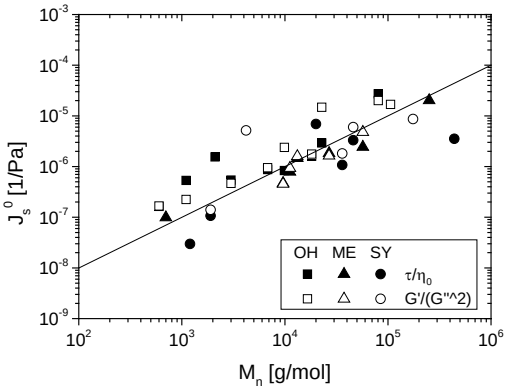

Figure 7: Steady state compliance J_s^0 determined by the plateau of $G'(\omega)/G''(\omega)^2$ and the terminal relaxation time τ/η_0 as a function of the molecular weight.

Conclusion

In this work we presented our studies on thermorheological properties of two series of differently modified hyperbranched polyglycerols compared to *hb*PGs. By polymer analogues reactions methyl and trimethylsilyl modfied *hb*PGs were synthesized in a broad range of molecular weight and similar degrees of branching. The effect of interactions on thermorheological properties and entanglements could be investigated.

Although the glass transition temperature is known to be a function of the number of end groups n_e and molecular weight M in case of hbPGs it is leveling off at high molecular weights due to a constant quotient of n_e/M. The methylated and trimethylsilylated PGs show a clear decrease of T_g with decreasing molecular weight which is attributed to the fact that the quotient n_e/M is not constant as the initiator influences the molecular weight. In case of *hb*PG the T_g is dominated by hydrogen bonds and independent over whole investigated molecular weight range. The lack of hydrogen bonds decreases the glass transition temperature of around 30 K.

Rheological measurements over a great temperature and frequency range showed independent of functionality a break-down of time-temperature-superposition principle. This behavior is due to segmental relaxation which is an effect of the highly branched structure and not the hydrogen bonds. The relaxation processes in the terminal flow region could be described by the WLF-equation. Zero shear viscosities were compared at the iso-free volume state (T_g+50K) and showed a scaling behavior with the molecular weight which is known for star shaped polymers. When the polymers are regarded as three arm star polymers due to the trifunctional starter molecule which was used for synthesis, the entanglement molecular weight can be calculated by assuming an arm molecular weight M_a of $M_a = 1/3\ M_n$. The obtained entanglement molecular weight of *hb*PG is about 5/14 of the entanglement molecular weight of the modified *hb*PGs. The steady state compliance J_s^0 scales for all functionalities with $J_s^0 \sim M_n$ over the whole investigated molecular weight range and is in good agreement for the scaling behavior of star polymers. In terms of relaxation behavior, the investigated samples of this paper can be regarded as three arm star polymers with hyperbranched arms in which the investigated properties are more dominated by the star shape than the hyperbranched structure.

References

1) Flory, P.J. *J. Am. Chem. Soc.* **1941**, *63*, 3083-3090.

2) Voit, B. I.; Lederer, A. *Chem. Rev* **2009**, *109*, 5924-5973.

3) Malmström, E.; Hult, A. *Polym. Rev.* **1997**, 37, 555-579.

4) Wilms, D.; Schömer, M.; Wurm, F.; Hermanns, M.I.; Kirkpatrick, C. J.; Frey, H. *Macromol. Rapid Commun.* **2010**, *31*, (20), 1811-1815.

5) Gottschalk, C.; Wolf, F.; Frey, H. *Macromol. Chem. Phys.* **2007**, *208*, (15), 1657-1665.

6) Hawker, C. J.; Lee, R.; Fréchet, J. M. J. *J Am. Chem. Soc*. **1991**, *113*, 4583-4588.

7) Hölter, D.; Burgath, A.; Frey, H. *Acta Polym*. **1997**, *48*, 30-35.

8) Sendijarevic, I.; McHugh, A. J. *Macromolecules* **2000**, *33*, 590-596.

9) Suneel; Buzza, D. M. A.; Groves, D. J.; McLeish, T. C. B.; Parker, D.; Keeney, A. J.; Feast, W. J. *Macromolecules* **2002**, *35*, 9605-9612.

10) Dorgan, J. R.; Knauss, D. M.; Al-Muallem, H. A.; Huang, T. *Macromolecules* **2003**, *36*, 380-388.

11) Kunamaneni, S.; Buzza, D. M. A.; Read, D. J.; Parker, D.; Kenwright, A. M.; Feast, W. J.; Larsen, A.L. *Macromolecules* **2006**, *39*, 6720-6736.

12) Sunder, A.; Hanselmann, R.; Frey, H.; Mulhaupt, R. *Macromolecules* **1999**, *32*, (13), 4240-4246.

13) Wilms, D.; Wurm, F.; Nieberle, J.; Böhm, P.; Kemmer-Jonas, U.; Frey, H. *Macromolecules 2009*, *42*, (9), 3230-3236.

14) Tonhauser, C.; Wilms, D.; Korth, Y.; Frey, H.; Friedrich, C. *Macromol. Rapid Commun.* **2010**, *31*, 2127-2132.

15) Kainthan, R. K.; Muliwan, E. B.; Hatzikiriakos, S. G.; Brooks, D. E. *Macromolecules* **2006**, *39*, (22), 7708-7717.

16) Haag, R.; Stumbé, J.-F.; Sunder, A.; Frey, H.; Hebel, A. *Macromolecules* **2000**, *33*, (22), 8158-8166.

17) Zagar, E.; Grdadolnik, J. *J. of Molecular Structure* **2003**, *658*, 143-152.

18) Foix, D.; Fernández-Francos, X.; Salla, J. M.; Serra, À.; Morancho, J. M.; Ramis, X. *Polym. Int.* **2011**, *60*, 389-397.

19) Ferry, J. D. *Viscoelastic Properties of Polymers*, Third Edition; John Wiley and Sons; New York, 1980.

20) Wooley,K.L.; Hawker, C.J.; Pochan, J. M.; Fréchet, J. M. J. *Macromolecules* **1993**, *26*, 1514-1519.

21) Gauthier, M.; Li, W.; Tichagwa, L. *Polymer* **1997**, *38*, 6363-6370.

22) Luciani, A.; Plummer,C. J. G.; Nguyen, T.;Garamszei, L.; Manson, J.-A. E. *J. Polym. Sci., Part B: Polym. Phys.* **2004**, *42*, 1218-1225.

23) Plummer, C. J. G.; Luciani, A.; Nguyen, T.-Q.; Garamszegi, L.; Rodlert, M.; Manson, J.-A. E. *Polym. Bull.* **2002**, *49*, 77-84.

24) Khalyavina, A.; Häußler, L.; Lederer, A. *Polymer* **2012**, *53*, 1049-1053.

25) Vukovic, J.; Jovanovic, S.; Lechner, M. D.; Vodnik, V. *J. Appl. Polym. Sci.* **2009**, *112*, 2925-2934.

26) Farrington, P.J.; Hawker, C.J.; Fréchet, J.M.J.; Mackay, M. E. *Macromolecules* **1998**, *31*, 5043-5050.

27) Sendijarevic, I.; McHugh, A. J. *Macromolecules* **2000**, *33*, 590-596.

28) Pearson, D. S.; Helfand, E. *Macromolecules* **1984**, *17*, 888-895.

29) Fetter, L. J.; Kiss, A. D.; Pearson, D. S.; Quack, G. F.; Vitus, F. J.*Macromolecules* **1993**, *26*, 647-654.

30) Roovers, J. *Polymer* **1985**, *26*, 1091-1095.

31) Graessley, W. W.; Roovers, J. *Macromolecules* **1979**, *12*, 959-965.

32) Fetters, L. J.; Kiss, A. D.; Pearson, D. S.; Quack, G. F.; Vitus, F. J. *Macromolecules* **1993**, *26*, 647-654.

33) Gell, C. B.; Graessley, W. W.; Efstratiadis, V.; Pitsikalis, M.; Hadjichristidis, N. *J. Polym. Sci., Part B: Polym. Phys.* **1997**, *35*, 1943-1954.

34) Teerstra, S. J.; Gauthier, M. *Macromolecules* **2007**, *40*, 1657-1666.

Appendix

A.1: Patents

Continuous Process for Preparing Quantitatively Terminally Functionalized Polymers Using Oxirane Derivatives as Termination Reagents

(19) Deutsches Patent- und Markenamt

(10) **DE 10 2010 021 388 A1** 2011.11.24

(12) **Offenlegungsschrift**

(21) Aktenzeichen: **10 2010 021 388.8**
(22) Anmeldetag: **25.05.2010**
(43) Offenlegungstag: **24.11.2011**

(51) Int Cl.: ***C08F 2/04*** (2006.01)
C08F 2/42 (2006.01)

(66) Innere Priorität:
10 2010 021 270.9 24.05.2010

(71) Anmelder:
[redacted]

(72) Erfinder:
[redacted]

(74) Vertreter:
[redacted]

Prüfungsantrag gemäß § 44 PatG ist gestellt.

Die folgenden Angaben sind den vom Anmelder eingereichten Unterlagen entnommen

(54) Bezeichnung: **Kontinuierliches Verfahren zur Herstellung quantitativ endfunktionalisierter Polymere unter der Verwendung von Oxiranderivaten als Terminierungsreagenzien**

Names on patent are deleted due to privacy protection. Namen auf dem Patent wurden aus datenschutzrechtlichen Gründen entfernt.

(57) Zusammenfassung: Ein Verfahren bietet eine zeitsparende und kostengünstige Methode zur kontinuierlichen Synthese endfunktioneller Polymere durch die Verwendung effizienter Terminierungsreagenzien aus der Gruppe umfassend Oxirane, schwefelhaltige Oxirananaloga und stickstoffhaltige Oxirananaloga. Das kontinuierliche Verfahren ermöglicht die Einführung unterschiedlicher funktioneller Gruppen. In relativ kurzer Zeit können die Eigenschaften der Polymere wie generelle chemische Zusammensetzung, Molekulargewicht, Polydispersität, chemische Zusammensetzung und Funktionalisierung des Kettenendes, sowie chemische Zusammensetzung der Endgruppen in einem weiten Bereich variiert werden. Die erfindungsgemäß erhaltenen Polymere eignen sich besonders als Dispersionsreagenz zur Vermischung oder Stabilisation von zwei Materialien unterschiedlichen Mischungsverhaltens. Als weitere Anwendung sind Beschichtungsmaterialien zum Einstellen von Oberflächeneigenschaften oder die Anpassung von rheologischen Eigenschaften von viskosen Materialien möglich.

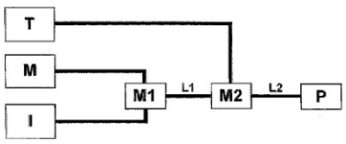

DE 10 2010 021 388 A1 2011.11.24

Beschreibung

[0001] Die vorliegende Erfindung betrifft eine Kombination aus Verfahren und Syntheseweg zur kontinuierlichen Herstellung von Polymeren mit mindestens einer funktionellen Gruppe in endständiger Position. Das Verfahren basiert auf der Mischung von mindestens zwei Reaktionspartnern (Monomer und Initiator), die nach beendeter Reaktion im weiteren Verlauf der kontinuierlichen Synthese mit mindestens einem Terminierungsreagenz vermischt werden. Die Polymerisation verläuft mit Vinylmonomeren und Oxiranderivaten als Terminierungsreagenzien.

[0002] Die kontinuierliche Synthese von Polymeren mit definierter Endgruppe gemäß der vorliegenden Erfindung eignet sich für die industrielle Herstellung. Die so dargestellten Polymere finden Anwendung als Dispersionsreagenz zur Vermischung oder Stabilisation von zwei Materialien mit unterschiedlichen Mischungsverhalten. Dies führt zu Verbundmaterialien mit neuartigen Eigenschaften. Als weitere Anwendung sind Beschichtungsmaterialien zum Einstellen von Oberflächeneigenschaften oder die Anpassung von rheologischen Eigenschaften von viskosen Materialien möglich.

[0003] Unter Verwendung der anionischen Polymerisation werden endfunktionelle Polymere üblicherweise durch die Zugabe eines elektrophilen Reagenz zur aktiven Polymerspezies erhalten. Dabei wird die luft- und sauerstofffreie Atmosphäre durch ein besonders hohes Vakuum oder durch die spezielle „Break-Seal"-Technik gemäß der von Hadjichristidis et al. „Anionic polymerization: High vacuum techniques" Journal of Polymer Science: Part A: Polymer Chemistry, 2000, 38, 3211–3234 vorgestellten Methode erhalten. Zwar liefert diese Vorgehensweise definierte Makromoleküle, jedoch ist ein hohes Maß an präparativen Aufwand notwendig.

[0004] Die Terminierung von anionischen Polymeren mit unterschiedlichen Terminierungsreagenzien ist eine übliche Methode zur Herstellung endfunktioneller Polymere. Die spezielle Terminierung mit Oxiranen wurde allerdings nur in begrenztem Umfang untersucht und verwendet. Zwar besitzen Epoxidderivate eine hohe Ringspannung und werden daher meist quantitativ an die Polymere addiert. Allerdings haben sich aufgrund der schwierigen anionischen Polymerisationsbedingungen erst wenige Forschungsgruppen mit dieser sehr effizienten Terminierungsmethode beschäftigt. Dabei konzentrierte man sich auf die detaillierte Charakterisierung weniger Oxirane. Dieses Prinzip auf ein allgemeines Terminierungsverfahren zu erweitern, bei der schnell und effizient eine Vielzahl von Materialien erhalten wird, zählt in der aktuellen Forschung nicht zu den umfassend untersuchten Gebieten.

[0005] Ende der 80er Jahre wurde Ethylenoxide (EO) als kleinster Vertreter der Oxirane gezielt zum lebenden Kettenende hinzugefügt, um ein quantitative hydroxyl-funktionelles Polystyrol zu erhalten. Grundlegende Untersuchungen über diese Terminierungsreaktion befinden sich in „Characterization of the functionalization reaction-product of poly(styryl)lithium with ethylene oxide" Journal of Polymer Science: Part A: Polymer Chemistry 1988, 26, 2031–2037 von Quirk et al. Dabei zeigten die Autoren mit unterschiedlichen Charakterisierungsmethoden, dass neben der vollständigen Terminierung eine mögliche Oligomerisierung des Epoxids ausgeschlossen werden kann.

[0006] In weiteren Untersuchungen konnten die höheren Homologen des EOs (Propylenoxide, 1,2-Epoxybutan, 1,2-Epoxybuten, Styroloxid, etc.) ebenfalls an das Kettenende addiert werden. Dabei wurde analog des Vorgehens bei EO verfahren und das lebende Polymer wurde mit dem entsprechenden Oxiran terminiert. Hierbei konnten unterschiedliche regioselektive Angriffe der aktiven Polymerspezies abhängig von Art und Größe der Seitengruppe festgestellt werden. Der Grad der Terminierung sowie die Regioselektivität der verschiedenen Oxirane wurden von Quirk und Mitarbeitern zusammenfassend in „Recent advances in anionic synthesis of chain-end functionalized elastomers using epoxides and related compounds" Rubber Chemistry and Technology, 2003, 76, 812–831 veröffentlicht. Die Anzahl der Terminierungen konnte zwar erweitert werden, jedoch blieb die erhaltene Funktionalität meist auf eine Hydroxylgruppe beschränkt und der präparative Aufwand konnte nicht reduziert werden.

[0007] US 3842059 beschreibt die Funktionalisierung von carbanionischen Polymeren mit verschiedenen Halogenhaltigenverbindungen. Darüber hinaus wird die Endfunktionalisierung von Polystyrol mit niedrigen Alkyloxiranen (Ethylenoxid und Propylenoxid) vorgestellt. Hierbei handelt es sich um eine herkömmliche Synthesevorschrift ohne die Verwendung eines kontinuierlichen Prozesses.

[0008] Zhibo et al., „Synthesis and characterization of triptych μ-ABC star triblock copolymers" Macromolecules, 2004, 37, 8933–8940, verwendeten dieses Funktionalisierungsprinzip zur Darstellung von Miktoarmsternpolymeren. Die Synthese beruht auf der Einführung von zwei Hydroxylgruppen in terminale Position. Diese

Polymere wurden daraufhin als Makroinitiatoren für weitere Polymerisationsschritte eingesetzt und physikalische und chemische Eigenschaften, Phasenverhalten und Morphologie der hergestellten Sternpolymere wurden intensiv untersucht.

[0009] Allerdings beschränken sich die bisherigen Untersuchungen auf die Einführung einer (bzw. zwei) Hydroxylgruppe(n) und es ist bisher nicht gelungen eine einfache, universelle und schnelle Methode zur Herstellung endfunktioneller Polymere aus der quantitativen Funktionalisierung zu entwickeln. Weiterhin eignen sich die aktuellen Forschungsergebnisse nicht für eine industrielle Anwendung, da sie einen oder mehrere der folgenden Nachteile aufweisen:

- Die Synthese ist präparativ sehr aufwendig und umfasst zahlreiche zeitintensive Einzelschritte.
- Die Aufarbeitung der Produkte ist meist sehr zeitintensive und benötigt mehrere Teilschritte bis man das aufgereinigte Produkt erhält.
- Die Verwendung der Materialien im Bereich von Oberflächenanbindung oder -beschichtung sowie als Dispersionsreagenz ist stark eingeschränkt, da bisher nur wenige unterschiedliche Funktionalitäten eingeführt wurden (Enol-, Hydroxy-, Siloxyendgruppen).
- Die Verwendung als Precursor für weitere Polymerisationen ist stark eingeschränkt aufgrund der bereits schwierigen Synthese der endfunktionellen Polymere.

[0010] Um die Wirtschaftlichkeit der Funktionalisierung von lebenden Polymeren zu erhöhen, wurde in der vorliegenden Erfindung ein neue Methode entwickelt, mit der in einem kontinuierlichen Verfahren endfunktionelle Polymere erhalten werden können.

[0011] Die Mikroreaktionstechnologie wurde in den letzten Jahrzehnten zuerst in der organischen Chemie eingesetzt, um Dauer und Reaktionsbedingungen einer chemischen Umsetzung schneller und genauer zu untersuchen und die Ausbeute oder Stereochemie mit geeigneter Wahl der Reaktionsbedingungen positiv zu beeinflussen. In den letzten Jahren wurden vermehrt verschiedene Polymerisationstechniken auf unterschiedliche Mikroreaktoren übertragen. Je nach Eigenschaften der Polymerisationsart konnten dadurch Vorteile wie z. B. verringerte Reaktionszeit, bessere Kontrolle und definiertere Polymere erhalten werden. Weiterführende Informationen über Polymerisationen im Mikroreaktor und Vorteile gegenüber den konventionellen Systemen sind in „Polymerisationen in mikrostrukturierten Reaktoren: Ein Überblick" Chemie Ingenieur Technik 2005, 77, 1693–1714 von Nessel et al. und „Microstructured reactors for polymer synthesis: A renaissance of continuous flow processes for tailor-made macromolecules?" Macromolecular Chemistry and Physics 2008, 209, 343–356 zu erhalten.

[0012] Chemische Reaktionen und im speziellen anionische Polymerisationen in mikrostrukturierten Reaktoren bieten einige Vorteile gegenüber der herkömmlichen Methode in Glasapparaturen:

- Mikroreaktoren besitzen aufgrund des kleinen Volumens einen deutlich besseren Stofftransport, wodurch Mischzeiten im Bereich von Millisekunden erreicht werden (konventionelle Systeme ≥ 10 s).
- In den Mikrokanälen sind meist laminare und hochsymmetrische Mehrphasenströmungen zu finden, die zwischen den Phasen eine hohe Ordnung aufweisen. Dabei spielen die Grenzflächen zwischen den unterschiedlichen Phasen eine wichtige Rolle. Sie betragen 5.000 bis 50.000 m^2m^{-3} und sind damit weitaus größer als in konventionellen Systemen (100 m^2m^{-3}). Dies führt zu extrem kurzen Diffusionszeiten und eine verbesserte Durchmischung der Reaktanden.
- Das Oberflächen-Volumen-Verhältnis eines mikrostrukturierten Reaktors entspricht dem 500fachen eines Glasreaktors. Dies ermöglicht einen optimalen Wärmeaustausch, der die Bildung von Aggregaten verhindert. Durch das Einstellen der Reaktionsparameter (Verweilschleife, Flussrate, etc.) kann eine chemische Reaktion bei isothermen Reaktionsbedingungen ermöglicht werden.
- Die Anzahl der Nebenreaktionen können durch die schnelle Durchmischung und die gute Wärmeabfuhr zurück gedrängt werden. Selektivität und Ausbeute können dadurch gesteigert werden.
- Reaktionen mit besonderem Energiebedarf (extrem endo- oder exotherme Reaktionen) können besser kontrolliert werden.
- Luft- und sauerstoffempfindliche Reaktionen können ohne großen zusätzlichen Aufwand problemlos durchgeführt werden.
- Die Reaktion findet auf einem sehr kleinen Volumen statt. Durch die Kontrolle von Druck, Temperatur, Verweilzeit und Fließgeschwindigkeit wird das Gefährdungspotential von stark exothermen, explosionsgefährlichen, toxischen und druckgesteigerten Reaktionen reduziert.
- Die kontinuierliche Synthese bietet ein wirtschaftlich interessantes Herstellungsverfahren. Obwohl es sich um einen kleinen Reaktionsraum handelt, können bei Großanlagen mehrere Reaktoren parallel geschaltet werden, um somit große Ansätze und geringere Lagerkosten zu erhalten.

[0013] Die anionische Polymerisation in polaren Lösungsmitteln eignet sich, aufgrund ihres stark exothermen Verhaltens, zur Übertragung auf ein Mikroreaktorsystem. Die Kühlung dieser stark exothermen Reaktion ist nicht nötig und man erhält sehr kurze Reaktionszeiten. Bezüglich der Polymereigenschaften konnten im Vergleich zur herkömmlichen Laborsynthese in Glasapparaturen ähnliche Ergebnisse erhalten werden. Die spezifische Terminierung mit Chlorosilanen wurde in den Arbeiten von Wilms et al. „Carbanions on tap – Living anionic polymerization in a microstructured reactor" Macromolecular Chemistry and Physics 2008, 209, 1106–1114 und Nagaki et al. "Microflow-system-controlled anionic polymerization of styrenes" Macromolecules 2008, 41, 6322–6330 untersucht.

[0014] DE 698 11 035 T2 beinhaltet verschiedene Verfahren zur anionischen Homo- und Blockcopolymerisation in einem Reaktor mit Mikrovermischung, bei dem zwei Strahlen J_a und J_b im Winkel von 90° frei aufeinander geführt werden. Wahlweise werden Initiatorlösungen oder lebende Polymere als Initiatoren für die Polymerisation von Methacrylaten eingesetzt. Es handelt sich hierbei allerdings um eine anionische Polymerisation im kontinuierlichen Fluss ohne Betrachtung einer gezielten Terminierung.

[0015] Die Aufgabe der vorliegenden Erfindung besteht darin, ein einfaches und wirtschaftliches Verfahren zu Herstellung von Polymeren mit unterschiedlicher Anzahl und Art von Funktionalitäten in endständiger Position zu entwickeln.

[0016] Diese Aufgabe wird gelöst durch ein Verfahren, umfassend die Schritte:

(a) Bereitstellen einer Lösung (LM) von Monomeren (M) aus der Gruppe umfassend vinylaromatische Monomere, Dienmonomere, Acrylmonomere, Methacrylmonomere, Maleimidmonomere; einer Lösung (LI) eines Initiators (I) aus der Gruppe umfassend Alkylmetallverbindungen und Arylmetallverbindungen aus linearen oder verzweigten Alkylketten oder substituierten oder unsubstituierten Arylresten mit einem Metall aus der Gruppe Li, Na, K, Cs, Mg, Ca, Ba; und einer Lösung (LT) eines oder mehrerer Terminierungsreagenzien (T) aus der Gruppe umfassend Oxirane, schwefelhaltige Oxirananaloga und stickstoffhaltige Oxirananaloga;
(b) optional Bereitstellen einer weiteren Lösung (LM') von Monomeren (M') aus der Gruppe umfassend vinylaromatische Monomere, Dienmonomere, Acrylmonomere, Methacrylmonomere, Maleimidmonomere;
(c) kontinuierliches Vermischen der Lösung (LM) mit der Lösung (LI) in einem molaren Verhältnis von Monomeren (M) zu Initiator (I) im Bereich von 6:1 bis 5000:1 in einem Mischungsreaktor M1, wobei aus den Monomeren (M) durch anionische Polymerisation kontinuierlich ein Polymer (P) gebildet wird;
(d) optional kontinuierliches Überführen des in Schritt (c) erhaltenen Gemisches (LM) + (LI) von dem Mischungsreaktor M1 in einen Mischungsreaktor M1' und kontinuierliches Vermischen mit der Lösung (LM'), wobei aus dem Polymer (P) und den Monomeren (M) und (M') ein Blockcopolymer (BCP) gebildet wird;
(e) kontinuierliches Überführen des in Schritt (c) oder (d) erhaltenen Gemisches (LM) + (LI) oder (LM) + (LI) + (LM') von dem Mischungsreaktor M1 oder M1' in einen Mischungsreaktor M2;
(f) kontinuierliches Vermischen des in Schritt (e) erhaltenen Gemisches (LM) + (LI) oder (LM) + (LI) + (LM') mit der Lösung (LT) in dem Mischungsreaktor M2 und Terminieren des Polymers (P) oder Blockcopolymers (BCP) mit einer oder zwei Endgruppen (E, E') des mindestens einen Terminierungsreagenz (T); und
(g) optional Umsetzen der in Schritt (f) erhaltenen makromolekularen Verbindung aus dem Polymer (P) oder Blockcopolymer (BCP) und einer oder zwei Endgruppen (E, E') mit einem weiteren Monomer, wie einem Lacton, Epoxid oder Siloxan oder einem funktionellen Reagenz, wie einer Carbonylverbindung.

[0017] Vorzugweise werden in den Schritt (a) bis (d) Monomere (M, M') verwendet, die in DE 698 11 035 T2 angegebenen sind. Es handelt sich bei den Monomeren (M, M') um vinylaromatische Monomere, Dienmonomere, Acrylmonomere, Methacrylmonomere und Maleimidmonomere.

[0018] Die Methacryl- und Acrylmonomere sind beispielsweise die Monomere, die den folgenden Formeln

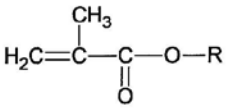

und

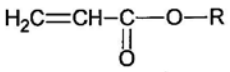

entsprechen, in denen R ausgewählt ist unter geradkettigem oder verzweigtem, primärem, sekundärem und tertiärem C_1-C_{18}-Alkyl, C_5-C_{18}-Cycloalkyl, (C_1-C_{18}-Alkoxy)-C_1-C_{18}-alkyl, (C_1-C_{18}-Alkylthio)-C_1-C_{18}-alkyl, Aryl und Arylalkyl, wobei diese Reste gegebenenfalls mit mindestens einem Halogenatom und/oder mindestens einer Hydroxygruppe nach dem Schutz dieser Hydroxygruppe substituiert sind, wobei die obigen Alkylgruppen geradkettig oder verzweigt sind; Glycidyl(meth)acrylat, Norbornyl(meth)acrylat, Isobornyl(meth)acrylat, den Mono-(C_1-C_{18}-alkyl)-(meth)-acrylamiden und Di-(C_1-C_{18}-alkyl)-(meth)acrylamiden.

[0019] Als Beispiele für erfindungsgemäß vorgesehene Methacrylate können angegeben werden: Methyl-, Ethyl-, 2,2,2-Trifluorethyl-, n-Propyl-, Isopropyl-, n-Butyl-, sec.-Butyl-, tert.-Butyl, n-Amyl-, i-Amyl-, n-Hexyl-, 2-Ethylhexyl-, Cyclohexyl-, Octyl-, i-Octyl-, Nonyl-, Decyl-, Lauryl-, Stearyl-, Phenyl-, Benzyl-, β-Hydroxyethyl-, Isobornyl-, Hydroxypropyl-, Hydroxybutylmethacrylat. Methylmethacrylat ist das bevorzugte Methacrylmonomer.

[0020] Als Beispiele für Acrylate der obigen Formel können angegeben werden: Methyl-, Ethyl-, n-Propyl, Isopropyl-, n-Butyl-, sec.-Butyl-, tert.-Butyl-, Hexyl-, 2-Ethylhexyl-, Isooctyl-, 3,3,5-Trimethylhexyl-, Nonyl-, Isodecyl-, Lauryl-, Octadecyl-, Cyclohexyl-, Phenyl-, Methoxymethyl-, Methoxyethyl-, Ethoxymethyl- und Ethoxyethylacrylat.

[0021] Der Ausdruck "Maleimid", wie er hier verwendet wird, bezeichnet ein unsubstituiertes Maleimidmonomer oder ein N-substituiertes Maleimidmonomer der Formel

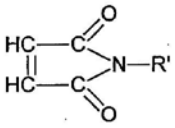

in der R' einen Alkyl-, Arylalkyl-, Aryl- oder Alkylarylrest bedeutet, der 1 bis 12 Kohlenstoffatome aufweist. Nicht einschränkende Beispiele hierfür sind: N-Ethylmaleimid, N-Isopropylmaleimid, N-n-Butylmaleimid, N-Isobutylmaleimid, N-tert.-Butylmaleimid, N-n-Octylmaleimid, N-Cyclohexylmaleimid, N-Benzylmaleimid und N-Phenylmaleimid. N-Cyclohexylmaleimid ist das bevorzugte Maleimid.

[0022] Unter vinylaromatischen Monomeren wird ein ethylenisch ungesättigtes aromatisches Monomer verstanden, wie Styrol, Vinyltoluol, α-Methylstyrol, 4-Methylstyrol, 3-Methylstyrol, 4-Methoxystyrol, 4-Ethylstyrol, 3,4-Dimethylstyrol, 3-tert.-Butylstyrol, 2,4-Dichlorstyrol, 2,6-Dichlorstyrol, 1-Vinylnaphthalin, 2-Vinylpyridin und 4-Vinylpyridin.

[0023] Unter Dienmonomer wird ein Dien verstanden, das unter den geradkettigen oder cyclischen, konjugierten oder nicht konjugierten Dienen ausgewählt wird, wie z. B. Butadien, Isopren, 1,3-Pentadien.

[0024] Eine besonders interessante Ausführungsform stellt die Polymerisation oder Copolymerisation auf anionischem Wege dar, bei der eines der Monomere ein Acryl- oder Methacrylmonomer, wie Methylmethacrylat, ist.

[0025] Vorzugweise wird in Schritt (c) ein mono- oder bifunktioneller Initiator verwendet, deren allgemeine Form in EP-A-749987 angegeben ist. Hierzu verwendet werden Alkyl- bzw. Arylmetallverbindungen mit verschiedenen Resten R (geradkettige oder verzweigte Alkylketten sowie substituierte oder unsubstituierte Arylreste) und ein Metall M aus der Reihe der Alkali- oder Erdalkalimetalle. Beispiele für monofunktionelle Initiatoren sind: sec.-Butyllithium, n-Butyllithium, Fluorenyllithium, α-Methylstyryllthium, 1,1-Diphenylhexyllithium (DPHLi), Diphenymethyllithium oder -natrium oder -kalium und 1,1-Diphenyl-3-methylpentyllithium. Beispiel für bifunktionelle Initiatoren sind 1,1,4,4-Tetraphenyl-1,4-dilithiumbutan, 1,1,4,4-Tetraphenyl-1,4-dinatriumbutan. Die Verwendung von bekannten Vorläufern kann auch als bifunktioneller Initiator verwendet werden. Als Beispiel sind zu nennen: Naphthalinlithium, Naphthalinnatrium, Naphthalinkalium und deren Homologe.

[0026] Als Initiator kann verwendet werden: ein monofunktioneller Initiator der allgemeinen Formel (I)

R^1-M (I),

in der bedeuten:
- M ein Alkalimetall oder Erdalkalimetall, und
- R^1
  - eine geradkettige oder verzweigte Alkylkette, die 2 bis 6 Kohlenstoffatome enthält, oder
  - einen Arylrest mit einem oder mehreren Ringen, der gegebenenfalls substituiert ist,
  - einen C2-C6-Alkenylrest, der mit Aryl oder Alkylaryl substituiert ist, oder

• einen geradkettigen oder verzweigten Alkylrest, der 1 bis 6 Kohlenstoffatome enthält, der mit mindestens einer Phenylgruppe substituiert ist, oder
• ein anionischer monofunktioneller Initiator der (Meth)acrylate, der unter den α-Lithiumisobutyraten und den Amiden ausgewählt wird, oder

ein bifunktioneller Initiator der Formel (II)

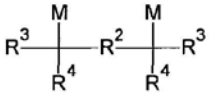

(II),

in der bedeuten:
– M ein Metall, das wie weiter oben definiert ist,
– R^2 einen zweiwertigen, aliphatischen, cycloaliphatischen, aromatischen organischen Rest oder einen zweiwertigen organischen Rest, der mindestens eine cycloaliphatische oder aromatische Gruppe aufweist, wobei R^2 Substituenten aufweisen kann, und
- R3 und R4 unabhängig voneinander einen einwertigen aliphatischen, cycloaliphatischen, aromatischen organischen Rest oder einen einwertigen organischen Rest, der mindestens eine cycloaliphatische oder aromatische Gruppe aufweist, wobei R3 und R4 Substituenten aufweisen können.

[0027] Als Lösungsmittel für die vorstehenden Monomere wird bevorzugt Tetrahydrofuran (THF) verwendet.

[0028] Vorzugsweise werden in den in den Schritten (c) bis (f) als Mikromischer ausgebildete Reaktionsmischer (M1, M1', M2) eingesetzt. Die Reaktionsmischer (M1, M1', M2) können als Mikromischer des Typs Schlitz Interdigital Mikromischer (SIMM), Raupenmischer, Rohrmikromischer, T-förmiger Mikromischer oder als Rohrreaktor ausgestaltet sein. Dabei können die inneren Abmessungen der Kanäle und der Verbindungsleitungen zwischen M, T, I, M1 und M2 (siehe Fig. 1) von 10 µm bis 10 cm vorzugsweise 20–100 µm im SIMM und Raupenmischer, sowie 100–1000 µm in Rohrreaktoren variieren.

[0029] In Schritt (f) wird die Konzentration des Terminierungsreagenzes T entsprechend der Initiatorkonzentration I aus Schritt (c) gewählt, so dass ein 1 bis 20-facher Überschuss vorzugsweise 1,5 bis 10-facher Überschuss von T zu I vorhanden ist.

[0030] Insbesondere wird in Schritt (f) mindestens ein Terminierungsreagenz (T) aus der Gruppe umfassend Ethoxyethylglycidylether (EEGE), 1,2-Isopropylidenglycerylglycidylether (IGG), 2-Phenyl-1,3-dioxanglycidylether (PDGE), Dibenzylaminaglycidylether (DBAG), Propylenoxid (1,2-Epoxypropan), 1,2-Epoxybutan (Ethyloxiran), Allylglycidylether (1-Allyloxy-2,3-epoxypropan), Benzylglycidylether (Benzyloxymethyloxiran), tert.-Butylglycidylether (tert.-Butoxymethyloxiran), Styroloxid (2-Phenyloxiran), Fluoroalkyloxirane, Fluoroalkylglycidylether, Aziridin (Ethylenimin) und Thiiran (Ethylensulfid) eingesetzt. Hierbei liegt das molare Verhältnis von Terminierungsreagenz (T) zu Initiator (I) vorzugsweise im Bereich von 1:1 bis 20:1, insbesondere von 1:1 bis 5:1.

[0031] Als Lösungsmittel für die vorstehenden Oxirane wird bevorzugt Tetrahydrofuran (THF) verwendet.

[0032] Weitere erfindungsgemäße Ausführungsformen des Verfahrens zeichnen sich dadurch aus, dass:
– der in Schritt (f) eingesetzte Mischungsreaktor M2 den gleichen Aufbau wie der in Schritt (c) verwandte Mischungsreaktor M1 aufweist;
– die in den Schritten (c) bis (f) verwendeten Mischungsreaktoren M1, M1' und M2 als Mikromischer ausgebildet sind und eine Mischkammer mit einer Einlassstufe und einem Auslass aufweisen, wobei die Einlassstufe derart ausgestaltet ist, dass in Schritt (c) die Lösungen (LM) und (LI), sowie gegebenenfalls in Schritt (d) das Gemisch (LM) + (LI) und die Lösung (LM'), respektive in Schritt (f) das Gemisch (LM) + (LI) oder (LM) + (LI) + (LM') und die Lösung (LT) in Form von zwei oder mehreren, jeweils zueinander benachbarten Strömungslamellen in die Mischkammer der Mischungsreaktoren M1, M1' und M2 treten, wobei jede der Strömungslamellen eine Dicke von 20 bis 1000 µm, vorzugsweise 20 bis 100 µm aufweist;
– die den Mischungsreaktoren M1, M1' und M2 zugeführten Volumenströme (ml/sec) der Lösungen (LM), (LI), (LM') und (LT) derart bemessen werden, dass für die in den Mischkammern der Mischungsreaktoren M1, M1' und M2 fließenden Strömungen die Reynoldszahl Re größer als 2300, vorzugsweise größer als 3000 ist;
– in Schritt (c) eine Monomerkonzentrationen M von 0,01–95% eingesetzt wird;
– in Schritt (c) eine Initiatorkonzentrationen I von 0,01–95% verwandt wird;

– in Schritt (c) das Molekulargewicht des gebildeten Polymers P über das molare Verhältnis von Initiator I zu Monomer M eingestellt wird, wobei das molare Verhältnis von I zu M über die Konzentration der Lösungen LI und LM und/oder über die Flussraten, d. h. die dem Mischungsreaktor M1 zugeführten Volumenströme (ml/sec) von LI und LM bestimmt wird;
– in Schritt (f) das molare Verhältnis von Terminierungsreagenz T zu Initiator I über die Konzentration der Lösungen LT und LI und/oder über die Flussraten, d. h. die dem Mischungsreaktor M2 bzw. M1 zugeführten Volumenströme (ml/sec) von LT und LI bestimmt wird;
– das Verfahren in luft- und sauerstofffreier Atmosphäre durch einen gegen die Umwelt geschlossenen mikrostrukturierten Reaktor erreicht wird;
– innere Oberflächen der Mischungsreaktoren M1, M1', M2 aus einem resistenten Material, wie Edelstahl, Titan und dergl. bestehen, so dass eine Reaktion mit den aggressiven aktiven Polymerketten unterbleibt;
– das Verfahren bei einer Temperatur von –80 bis 200°C vorzugsweise von 20 bis 40°C ausgeführt wird;
– das Verfahren in einer Stickstoff- und Sauerstoff-freien Atmosphäre oder unter Vakuum geführt wird;
– das Verfahren in einer Niederdruckatmosphäre von 0,0001 bis 0,95 bar ausgeführt wird;
– das Verfahren in einer Hochdruckatmosphäre von 1,1 bis 40 bar ausgeführt wird;
– das Verfahren bei Normaldruckatmosphäre bei 1 bar ausgeführt wird;
– in Schritt (f) ein schwefelhaltiges Oxirananalogon als Terminierungsreagenz eingesetzt wird;
– in Schritt (f) ein stickstoffhaltiges Oxirananalogon als Terminierungsreagenz eingesetzt wird;
– in Schritt (f) dem Mischungsreaktor M2 Wasser oder ein Alkohol zugeführt wird, um Oxide von Li, Na, K, Cs, Mg, Ca oder Ba zu protonieren; und
– die in Schritt (f) erhaltene Verbindung mit einem weiteren Reagenz (Monomer, funktionalisierendes Reagenz) umgesetzt wird, wobei das Reagenz mit der eingeführten Funktionalität oder der entstandenen OH-Gruppe der besagten Verbindung reagiert.

[0033] Das erfindungsgemäße Verfahren ermöglicht die Herstellung von hoch definierten endfunktionalisierten Polymeren, wobei durch die Veränderung der Funktionalität, die Eigenschaften der erhaltenen Polymere bezogen auf Oberflächenbeschichtung, Dispersion und Verwendung als Vorstufe zu komplexeren makromolekularen Architekturen, eingestellt und an die spezifischen Anwendungen angepasst werden kann.

[0034] Insbesondere wurde gefunden, dass durch den Einbau von hydrophoben bzw. hydrophilen Funktionalitäten die Oberflächeneigenschaften gezielt verändert werden können. Dazu wurden geschützte und ungeschützte Oxirane mit speziellen Funktionalitäten eingesetzt.

[0035] Vorzugsweise ermöglicht die Erfindung ein kontinuierliches Verfahren zur Herstellung von quantitativ funktionalisiertem Polystyrol unter der Verwendung von speziellen Glycidylethern. Das Verfahren in einer vorteilhaften Ausführungsform umfasst mindestens die folgenden Schritte:
(1) Bereitstellen einer Styrollösung;
(2) Bereitstellen einer Initatorlösung (sec.-Butyllithium);
(3) Bereitstellen einer Terminierungslösung (EEGE/IGG/PDGE);
(4) Anschluss der in (1), (2) und (3) genannten Lösungen an verschiedene Mischungsreaktoren. Die Lösungen aus (1) und (2) werden im Mischungsreaktor M1 vermischt und Reaktionslösung aus M1 wird mit der Lösung aus (3) im Mischungsreaktor M2 vermischt;
(5) Auffangen des Produkts;
(6) Isolation des Produkts;

[0036] Eine weitere Möglichkeit der Erfindung besteht darin, hetero- und homo-α,ω-funktionelle Polymere herzustellen. Dies kann durch verschiedene Strategien erreicht werden:
– Durch den Einsatz eines bifunktionellen Initiators können homotelechele Polymere erhalten werden.
– Durch den Einsatz von funktionellen Initiatoren, die gegen die anionischen Bedingungen geschützt oder stabil sind, können hetero-α,ω-funktionelle Polymere erhalten werden.

[0037] Eine weitere Aufgabe der Erfindung besteht darin eine funktionalisierte polymere Verbindung zu schaffen.

[0038] Diese Aufgabe wird gelöst durch eine makromolekulare Verbindung, umfassend ein an einem Ende oder an zwei Enden mit einer oder zwei Endgruppen (E, E') terminiertes Polymer (P) oder Blockcopolymer (BCP), wobei

– das Polymer (P) oder Blockcopolymer (BCP) aus einem Monomeren (M) oder aus zwei Monomeren (M, M') aus der Gruppe umfassend vinylaromatische Monomere, Dienmonomere, Acrylmonomere, Methacrylmonomere und Maleimidmonomere gebildet ist; und
– die Endgruppen (E, E') abgeleitet sind aus einem oder zwei Terminierungsreagenzien (T, T') aus der Gruppe umfassend Oxirane, schwefelhaltige Oxirananaloga und stickstoffhaltige Oxirananaloga.

[0039] Weitere Ausführungsformen der makromolekularen Verbindung sind dadurch gekennzeichnet, dass:
– die Terminierungsreagenzien (T, T') gewählt sind aus der Gruppe umfassend Ethoxyethylglycidylether (EEGE), 1,2-Isopropylidenglycerylglycidylether (IGG), 2-Phenyl-1,3-dioxanglycidylether (PDGE), Dibenzylaminoglycidylether (DBAG), Allylglycidylether (1-Allyloxy-2,3-epoxypropan), Benzylglycidylether (Benzyloxymethyloxiran), tert.-Butylglycidylether (tert.Butoxymethyloxiran), Styroloxid (2-Phenyloxiran), Fluoroalkyloxirane, Fluoroalkylglycidylether, Aziridin (Ethylenimin) und Thiiran (Ethylensulfid);
– sie weitere Monomere, insbesondere Lactone, Epoxide oder Siloxane oder funktionelle Gruppen, insbesondere aus Carbonylverbindungen abgeleitete Gruppen, umfasst;
– sie in terminaler Position 1 bis 1000, vorzugsweise 1 bis 20, und insbesondere 1 bis 5 funktionelle Gruppen aufweist;
– sie ein Molekulargewicht von 400 bis 100000 g/mol, vorzugsweise von 100 bis 20000 g/mol, und insbesondere 1000 bis 10000 g/mol aufweist;
– sie eine monomodale Molmassenverteilung mit einer Polydispersität $\overline{M}_w/\overline{M}_n$ von 1,01 bis 50, vorzugsweise von 1,01 bis 2 und insbesondere von 1,05 bis 1,3 aufweist;
– und sie durch ein Verfahren nach den Ansprüchen 1 bis 10 erhältlich ist.

[0040] Bei den erfindungsgemäßen Verbindungen handelt es sich insbesondere um makromolekulare, lineare, endfunktionelle Polystyrole, die mit verschiedenen Glycidylethern terminiert werden und verschiedene Endgruppen einführen.

[0041] Die Erfindung stellt Polymere vorzugsweise Polystyrole zur Verfügung, deren Eigenschaften wie generelle chemische Zusammensetzung, Molekulargewicht, Polydispersität, chemische Zusammensetzung und Funktionalisierung des Kettenendes und chemische Zusammensetzung der Endgruppen in einem weiten Bereich gezielt anpassbar sind.

[0042] Die erfindungsgemäßen endfunktionellen Polystyrole sind vorzugsweise nach einem Verfahren gemäß den Ansprüchen 1 bis 11 hergestellt.

[0043] Die Erfindung wird nachfolgend anhand von Zeichnungen und Beispielen näher erläutert. Es zeigen:

[0044] Fig. 1 ein Fließschema für eine Vorrichtung zur Durchführung chemischer Reaktionen nach dem erfindungsgemäßen Verfahren;

[0045] Fig. 2 Beispiele von Oxiranen, die zur Herstellung der erfindungsgemäßen Verbindungen verwendet werden;

[0046] Fig. 3 die Struktur endfunktioneller Polystyrole terminiert mit jeweils einem der Oxiranen EEGE, IGG oder PDGE (inklusive Abspaltung der acetalischen/ketalischen Schutzgruppen);

[0047] **Fig.** 4 GPC-Kurven von PS-EEGE, PS-IGG und PS-PDGE mit unterschiedlichen Molekulargewichten;

[0048] **Fig.** 5 ^{1}H-NMR-Spektren der erfindungsgemäß hergestellten PS-IGG und PS-PDGE;

[0049] **Fig.** 6 MALDI-ToF-Spektren der erfindungsgemäßen Verbindungen (PS-EEGE, PS-IGG, PS-PDGE);

[0050] Fig. 1 zeigt das Fließschema des erfindungsgemäßen Verfahrens zur kontinuierlichen Synthese endfunktioneller Polymere. Es ist der schematische Aufbau, bestehend aus den Vorlagebehältern für die Reaktionspartner, die über Leitungen mit den entsprechenden Mischungsreaktoren verbunden sind, gezeigt. In Ausgestaltung des Verfahrens wird das eine Edukt aus Monomer und Lösungsmittel (M) sowie das zweite Edukt aus Initiator und Lösungsmittel (I) in den Mischungsreaktor M1 geleitet. Das dritte Edukt aus Terminierungsreagenz und Lösungsmittel (T) wird in den Mischungsreaktor (M2) geleitet. In Ausführung des Verfahrens wird das Edukt aus Monomer-Lösungsmittel und das Edukt aus Initiator-Lösungsmittel in einem Mischungsverhältnis 1:1 bis 100:1 insbesondere von 1:1 bis 1:5 in den Mikromischer eingespeist. Der molare Anteil von T be-

zogen auf I beträgt mindestens 1–20 Äquivalente insbesondere 1–5 Äquivalente. Der Probenaustragsbehälter (P) für die Lösung der endfunktionellen Polymere steht in Verbindung mit M2.

[0051] Unmittelbar nach dem Vermischen von M und I startet die anionsiche Polymerisation und die aktive Polymerlösung wird über eine Leitung von M1 zu M2 geführt, wobei die Länge der Leitung so gewählt ist, dass die Polymerisation bis zu M2 vollständig abgelaufen ist (beispielsweise 30 cm). M2 wird daraufhin verwendet um die Polymerlösung mit T zu vermischen und dadurch eine kontinuierliche Funktionalisierung der Polymere zu erhalten.. Die terminierte Polymerlösung wird daraufhin von M2 zu P geleitet und die Proben können entnommen werden.

[0052] M1 und M2 stellen Mischungsreaktoren der Gruppe umfassend Schlitz Interdigital Mikromischer (SIMM), Raupenmischer, Mikrorohrreaktoren, T-förmiger Mikromischer oder Rohrreaktor dar. Insbesondere werden zur besseren Vermischung der Edukte Mikroreaktoren eingesetzt. Die Eduktströme werden dabei über sehr kleine Mikrokanäle zusammengeführt. In den Mikrokanälen sind meist laminare und hochsymmetrische Mehrphasenströmungen zu finden, die zwischen den Phasen eine hohe Ordnung aufweisen. Dies führt zu extrem kurzen Diffusionszeiten und eine verbesserte Durchmischung der Reaktanden. Man würde konstruktionsbedingt in den extrem kleinen Mikrokanälen eine erhöhte Wahrscheinlichkeit der Belagsbildung und somit eine erhöhte Wahrscheinlichkeit zur Verstopfung des Mischungssystem erwarten. Jedoch ist es möglich durch die effiziente Vermischung die Bildung von Aggregaten und Nebenprodukten zu vermeiden. Wahlweise können für die hier verwendeten Mischungsreaktoren erfindungsgemäß andere Mischergeometrien sowie Mischerarten eingesetzt werden.

[0053] Die Polymerisation wird durch die Umsetzung einer der oben genannten Initiatoren mit einem der zuvor erwähnten Monomere ausgeführt. In diesem kontinuierlichen Prozess wird eine Terminierung direkt im Reaktor durchgeführt. Dazu werden Terminierungsreagenzien gewählt aus der Gruppe umfassend substituierte und nicht-substituierte Oxirane (Fig. 2x) und schwefel- oder stickstoffhaltige Oxirananaloga. Vorzugsweise werden Glycidylether im Speziellen EEGE, IGG oder PDGE verwendet. Fig. 2 zeigt Beispiele von Oxiranen, die erfindungsgemäß eingesetzt werden, wobei die Buchstaben (a) bis (n) die folgenden Oxirane bezeichnen:

(a) Ethoxyethylglycidylether (EEGE),
(b) 1,2-Isopropylidenglycerylglycidylether (IGG),
(c) 2-Phenyl-1,3-dioxan-glycidylether (PDGE),
(d) Allylglycidylether (1-Allyloxy-2,3-Epoxypropan),
(e) Benzylglycidylether (Benzyloxymethyloxiran),
(f) tert-Butylglycidylether (tert-Butoxymethyloxiran),
(g) Dibenzylaminoglycidylether (DBAG),
(h) Alkylepoxid (R = verzweigt oder unverzweigter Alkylrest),
(i) Propylenoxid (1,2-Epoxypropan),
(j) 1,2-Epoxybutan (Ethyloxiran),
(k) Epoxybuten (3,4-Epoxy-but-1-en),
(l) Styroloxid (2-Phenyloxiran),
(m) Fluoroalkyloxirane (n = 1–100 vorzugsweise 1–20),
(n) Fluoroalkylglycidylether (n = 1–100 vorzugsweise 1–20).

[0054] Neben den vorstehenden substituierten Oxiranen kommen schwefel- oder stickstoffhaltige Oxirananaloga wie Aziridin (Ethylenimin) und Thiiran (Ethylensulfid) in Betracht. (Fig. 2, Ziffern (o) und (p)).

[0055] In Fig. 3 sind die Herstellung sowie die vollständigen Strukturen der erfindungsgemäßen kontinuierlich dargestellten endfunktionellen Polystyrole gezeigt. Die Polymerkette wird initiiert durch z. B. sec.-Butyllithium und wird mit einem der vorgestellten Oxiranderivaten terminiert. Als Terminierungsreagenzien werden hier im spezielen die drei Glycidylether Ethoxyethylglycidylether (FEGE), 1,2-Isopropylidenglycerylglycidylether (IGG) und 2-Phenyl-1,3-dioxan-glycidylether dargestellt. Nach der quantitativen Funktionalisierung im Mikroreaktor konnte in einem zweiten Schritt eine quantitative Abspaltung der Schutzgruppen erreicht werden. Durch einen geringen Zeit- und Arbeitsaufwand kann in sehr viel kürzerer Zeit verglichen mit herkömmlichen Laborsystemen ein breiter Molekulargewichtsbereich, sowie unterschiedlich funktionalisierte Polymere schnell verfügbar gemacht werden. Dadurch ist es möglich Bibliotheken von Polymeren herzustellen und chemische sowie physikalische Eigenschaften dieser interessanten Materialien einzustellen.

[0056] Nach der erfolgreichen Terminierung entstehen aus den zuvor gespannten Epoxidringen die Lithiumalkoxide, die aufgrund der starken Aggregation zwischen Sauerstoff und Lithium keine weitere Propagation des Oxiranderivats zulässt. Durch die Zugabe von geeigneten Katalysatoren kann allerdings das Lithiumion

chelatisiert werden, um weitere Reaktionen unter gewissen Umständen zu ermöglichen und dadurch Funktionalitäten einzuführen oder Blockcopolymere mit Funktionalitäten an der Grenzfläche herzustellen.

[0057] Der geringe Arbeitsaufwand sowie die Verwendung von neuartigen Oxiranderivaten (Fig. 2a–n) zeigen, dass die vorgestellte Erfindung durch die kontinuierliche Reaktionsführung in sehr kurzer Zeit Produkt liefert darüber hinaus auch die Synthese neuer Materialien ermöglicht.

[0058] Einer der großen Vorteile des erfindungsgemäßen Verfahrens ist die Veränderung des Molekulargewichts während der kontinuierlichen Reaktion. Die Veränderung der Flussratenverhältnisse zwischen Monomer und Initiator resultiert in einem neuen Molekulargewicht. Dadurch können die funktionellen Polymere mit geringem Arbeitsaufwand in einem großen Molekulargewichtsbereich hergestellt werden. Die Polymerisation wird kontinuierlich vom zugeführten Terminierungsreagenz beendet und durch die Zugabe von wenig Alkohol oder Wasser wird das Lithiumoxid in die OH-Gruppe überführt. Restliches Terminierungsreagenz kann problemlos durch mehrfaches Fällen in MeOH entfernt werden.

[0059] Die Größe der erfindungsgemäß hergestellten Polymere wird mittels Gelpermeationschromatographie (GPC) analysiert. Die Polymere weisen eine monomodale Verteilung mit niedriger Polydispersität auf. Dies wurde aufgrund der Charakteristika anionischer Polymerisationen erwartet. **Fig.** 4 zeigt die GPC-Kurven von verschiedenen erfindungsgemäß hergestellten Polymeren bei denen drei unterschiedliche Terminierungsreagenzien eingesetzt wurden. Bei jedem der drei Glycidylether (EEGE, IGG, PDGE) wurden die Flussratenverhältnisse variiert wodurch ein breiter Bereich von Molekulargewichten erschlossen werden konnte.

[0060] Die Molekulargewichte der erhaltenen Polystyrole liegen bevorzugt in einem Bereich zwischen 1.000 und 10.000 g/mol. Die Streuung der Molekulargewichte (Polydispersität, M_w/M_n) ist gering und liegt in einem Bereich von 1,01 bis 1,4. Die zugehörigen Werte der einzelnen GPC-Kurven befinden sich in Tabelle 1. In dieser Tabelle ist die Reaktionstemperatur, das Molekulargewicht und der Polydispersität angegeben. Weiterhin ist auch die Verweilzeit der anionschen aktiven Polymerkette im Reaktor angegeben. Es handelt sich dabei um die Verweilzeit zwischen dem Start der Polymerisation in M1 und der Terminierung der Polymerisation in M2. Die Zeiten betragen 5–15 Sekunden und zeigen, dass eine kurze Reaktionszeit zu definierten endfunktionellen Polymeren führen kann.

Tabelle 1

Probe	T /°C	Verweilzeit /s	Molekulargewicht (GPC) g/mol	Polydispersität M_n/M_w
PS-EEGE-1	25	12	1.800	1,14
PS-EEGE-2	40	12	1.900	1,15
PS-EEGE-3	40	10	3.000	1,14
PS-EEGE-4	25	5	3.900	1,13
PS-EEGE-5	40	8	4.500	1,26
PS-EEGE-6	50	8	6.400	1,18
PS-EEGE-7	50	10	17.000	1,30
PS-IGG-1	25	6	1.900	1,22
PS-IGG-2	60	12	2.300	1,18
PS-IGG-3	25	12	2.900	1,28
PS-IGG-4	25	8	4.100	1,29
PS-IGG-5	25	10	5.000	1,21
PS-IGG-6	60	8	5.300	1,23
PS-IGG-7	25	8	7.700	1,22

PS-PDGE-1	25	12	3.600	1,26
PS-PDGE-2	25	12	4.100	1,36
PS-PDGE-3	25	8	8.800	1,24

[0061] Die Struktur der erhaltenen Polymere wird mittels Protonen-Kernspinresonanz-Spektroskopie (^{1}H-NMR) analysiert. Im Fall von Polystyrol terminiert mit EEGE, IGG oder PDGE können mittels ^{1}H-NMR-Spektroskopie die Wasserstoffatome nach ihrer unterschiedlichen chemischen Umgebung untersucht werden. Die quantitative Auswertung der ^{1}H-NMR-Spektren gestattet es, die relative Anzahl verschiedener Wasserstoff enthaltender Gruppen zu ermitteln. Hierzu werden die Intensitäten bzw. Flächen der bei charakteristischen Frequenzen (bzw. Frequenzverschiebungen) auftretenden Resonanzlinien (bzw. Resonanzpeaks) integriert und miteinander verglichen. Anhand der Peakintensitäten der ^{1}H-NMR-Spektren können verschiedene Verhältnisse sowie das Molekulargewicht bestimmt werden.

[0062] Im aromatischen Bereich sind die Signale der Phenylprotonen gut zu erkennen. Setzt man ihre Intensität mit den Initiatorsignalen ins Verhältnis erhält man das Molekulargewicht. Nach der Anbindung der Glycidylether verschieben sich die Endgruppenprotonen (z. B. acetalisches Proton) und eine eindeutige Zuordnung von Polymerendgruppe und überschüssigem Terminierungsreagenz ist möglich. Im Fall des PS-PDGE ist bei einer vollständigen Terminierung die relative Intensität des acetalischen Protons 1. Bei Werte zwischen 0,95 und 1 kann im Rahmen des Fehlers auf einen hohen Grad der Terminierung geschlossen werden. Die anschließende Abspaltung der Acetal- oder Ketalschutzgruppe kann mit Hilfe der ^{1}H-NMR Spektroskopie nachgewiesen werden, da die entsprechenden Signale der Endgruppe nach erfolgreicher Entfernung der Schutzgruppe nicht mehr auftreten. **Fig.** 5 zeigt die entsprechenden ^{1}H-NMR Spektren von PS-IGG und PS-PDGE nach und vor dem Abspaltungsprozess. Es ist deutlich zuerkennen, dass die die Signale der abgespaltenen Gruppen nicht mehr vorhanden sind.

[0063] Die „Matrix Assisted Laser Desorption Ionisation – Time of Flight"-Massenspektrometrie (MALDI-ToF-MS) ist heutzutage eine Standardmethode in der Polymeranalytik zur Bestimmung von absoluten Molekulargewichten. Dabei wird das Polymer mit einem Laser ionisiert und im elektrischen Feld beschleunigt. Die Trennung erfolgt nach dem Verhältnis von Masse zu Ladung, wobei die unterschiedlichen Flugzeiten der Polymere detektiert werden. Polymere mit einem Molekulargewicht im Bereich zwischen 1.000–20.000 g/mol können mit einem Fehler von ±0,01% nachgewiesen werden. MALDI-ToF-MS ist bislang die Methode der Wahl, um die Endgruppen eines Polymers zu bestimmen und damit die vollständige Initiierung oder Terminierung eines Polymers zweifelsfrei nachzuweisen bzw. um Informationen über eventuelle Nebenreaktionen zu erhalten. Dies ist durch die Signale aller einzelnen Molekülspezies möglich, die durch Einbettung in einen hohen Überschuss der Matrix fragmentierungsarm mit Hilfe von Laserbeschuss verdampft und ionisiert werden, wodurch im Idealfall vollständige Moleküle anstelle einzelner Fragmente detektiert werden. Für ein qualitativ hochwertiges Massenspektrum müssen die äußeren Bedingungen, wie z. B. Art der Matrix und Konzentrationszusammensetzung richtig gewählt werden. Für das System Polystyrol verwendet man üblicherweise Dithranol (1,8,9-Trihydroxyanthracen) als Matrix und Silberfluoracetat als Ionisierungsreagenz.

[0064] Die MALDI-ToF-Spektren von den 3 erfindungsgemäß hergestellten Polymeren befinden sich in **Fig.** 6. Die Abstände der einzelnen Signale entsprechen in allen Spektren der Wiederholungseinheit Styrol mit 104,15 g/mol. Unter der Annahme einer vollständigen Terminierung sollte sich die Masse einer detektierten Kette aus Masse des Initiators, der Endgruppe, der Wiederholungseinheit und des zugegebenen Kations zusammensetzen. In allen drei Fällen stimmen die theoretisch errechneten Werte mit den gemessenen Signalen überein. Es werden neben dieser Verteilung keine anderen Unterverteilungen in den Spektren beobachtet, was eine quantitative Funktionalisierung des Polymers beweist.

[0065] Durch den Beweis der quantitativen Terminierung ist neben den zuvor aufgelisteten Vorteilen des kontinuierlichen Verfahrens die Abwesenheit von Nebenprodukten ein weiterer wichtiger Punkt. Im Vergleich zur herkömmlichen Laborsynthese müssen keine aufwendigen Aufreinigungsschritte zur Entfernung von Nebenprodukten an die Reaktion angeschlossen werden. Dadurch wird weiterhin die Gesamtreaktionszeit verkürzt und der Arbeitsaufwand verringert.

[0066] Im Folgenden werden beispielhafte Syntheseverfahren zur Herstellung der erfindungsgemäßen Verbindungen wiedergegeben.

Beispiel 1

Herstellung von PS-EEGE (Funktionalisierung von Styrol mit Ethoxyethylglycidylether)

[0067] Reaktionsgefäße I–III aus Glas mit zwei Stutzen, Septum und drei Teflonhähnen werden an eine Vakuumpumpe angeschlossen und evakuiert. Nacheinander werden 13 g (124 mmol) Styrol (getrocknet über CaH_2) und 100 mL frisch destilliertes Tetrahydrofuran (THF) unter statischem Vakuum in Reaktionsgefäß I überführt. Reaktionsgefäß II wird ebenfalls unter statischem Vakuum mit 2 g (13,6 mmol) EEGE und 100 mL THF befüllt. 100 mL trockenes Hexan werden mittels einer Kanüle in das evakuierte Reaktionsgefäß III transferiert und 3,8 mL einer 1,3 m sec.-Butyllithium Lösung werden mit einer Spritze über das Septum dazugegeben. Die drei Reaktionsgefäße werden anschließend mit PTFE-Schläuchen an drei HPLC-Pumpen angeschlossen und entsprechend Fig. 1 mit M1 und M2 verbunden. M1 (hier: Schlitz Interdigtal Micromischer) wird in ein Wasserbad (Raumtemperatur) getaucht. Um restliche Verunreinigungen im gesamten Reaktor zu eliminieren werden zuerst Pumpe 1 und 2 mit den Lösungen I und M aktiviert. Nach kurzer Zeit entsteht am Auslass des Reaktors die charakteristisch rot-orangefarbene Lösung aktiver anionischer Polymerketten. Schließlich wird die EEGE-Lösung mittels M2 (hier T-förmiger Mikromischer) zur aktiven Polymerlösung dazu gegeben. Die austretende entfärbte Lösung wird bei unterschiedlichen Flussratenverhältnissen in unterschiedlichen Kolben aufgefangen. Sämtliche Lösungsmittel werden unter Niederdruck entfernt und das Produkt in minimalen Mengen Dichlormethan (DCM) gelöst und in Methanol (MeOH) gefällt. Durch mehrfaches Fällen in MeOH kann überschüssiges EEGE vom Produkt abgetrennt werden. Die Trocknung unter Vakuum bei Raumtemperatur über 24 h führt zu einem farblosen Feststoff. Die Charakterisierung mittels ^{1}H-NMR Spektroskopie, GPC und MALDI-ToF-MS bestätigt eine quantitative Polymerisation und Endfunktionalisierung des Polystyrols.

Herstellung von bishydroxyl-funktionellem Polystyrol [PS-$(EEGE)_d$]durch saure Hydrolyse

[0068] 400 mg des zuvor erhaltenen PS-EEGE werden in 30 mL THF mit 3 mL 1 N HCl zusammengeben und für 8 Stunden unter Rückfluss erhitzt. Das Produkt wird in Chloroform aufgenommen und mit $NaHCO_3$ und H_2O neutralisiert. Sämtliche Lösungsmittel werden unter Niederdruck entfernt und das Produkt in 1 mL DCM gelöst. Nach Fällung in MeOH und Trocknung unter Vakuum bei einer Raumtemperatur über einen Zeitraum von 24 h wird ein farbloses Produkt in einer Ausbeute von 80 bis 90% erhalten.

Beispiel 2

Herstellung von PS-IGG (Funktionalisierung von Styrol mit 1,2-Isopropylidenglycerylglycidylether)

[0069] Reaktionsgefäße I–III aus Glas mit zwei Stutzen, Septum und drei Teflonhähnen werden an eine Vakuumpumpe angeschlossen und evakuiert. Nacheinander werden 17,9 g (172 mmol) Styrol (getrocknet über CaH_2) und 100 mL frisch destilliertes THF unter statischem Vakuum in Reaktionsgefäß I überführt. Reaktionsgefäß II wird ebenfalls unter statischem Vakuum mit 2,5 g (13,3 mmol) IGG und 100 mL THF befüllt. 100 mL trockenes Hexan werden mittels einer Kanüle in das evakuierte Reaktionsgefäß III transferiert und 3,8 mL einer 1,3 M sec.-Butyllithium Lösung werden mit einer Spritze über das Septum dazugegeben. Die drei Reaktionsgefäße werden anschließend mit PTFE-Schläuchen an drei HPLC-Pumpen angeschlossen und entsprechend Fig. 1 mit M1 und M2 verbunden. M1 (hier: Schlitz Interdigtal Micromischer) wird in ein Wasserbad (Raumtemperatur) getaucht. Um restliche Verunreinigungen im gesamten Reaktor zu eliminieren werden zuerst Pumpe 1 und 2 mit den Lösungen I und M aktiviert. Nach kurzer Zeit entsteht am Auslass des Reaktors die charakteristisch rot-orangefarbene Lösung aktiver anionischer Polymerketten. Schließlich wird die IGG-Lösung mittels M2 (hier T-förmiger Mikromischer) zur aktiven Polymerlösung dazu gegeben. Die austretende entfärbte Lösung wird bei unterschiedlichen Flussratenverhältnissen in unterschiedlichen Kolben aufgefangen. Sämtliche Lösungsmittel werden unter Niederdruck entfernt und das Produkt in minimalen Mengen DCM gelöst und in MeOH gefällt. Durch mehrfaches Fällen in MeOH kann überschüssiges IGG vom Produkt abgetrennt werden. Die Trocknung unter Vakuum bei Raumtemperatur über 24 h führt zu einem farblosen Feststoff Die Charakterisierung mittels ^{1}H-NMR Spektroskopie, GPC und MALDI-ToF-MS bestätigt eine quantitative Polymerisation und Endfunktionalisierung des Polystyrols.

Herstellung von trishydroxyl-funktionellem Polystyrol [PS-$(IGG)_d$]durch saure Hydrolyse

[0070] 400 mg des zuvor erhaltenen PS-IGG werden in 30 mL THF mit 3 mL 1N HCl zusammengeben und für 8 Stunden unter Rückfluss erhitzt. Das Produkt wird in Chloroform aufgenommen und mit $NaHCO_3$ und H_2O neutralisiert. Sämtliche Lösungsmittel werden unter Niederdruck entfernt und das Produkt in 1 mL DCM gelöst.

Nach Fällung in MeOH und Trocknung unter Vakuum bei einer Raumtemperatur über einen Zeitraum von 24 h wird ein farbloser Feststoff in einer Ausbeute von 80 bis 90% erhalten.

Beispiel 3

Herstellung von PS-PDGE (Funktionalisierung von Styrol mit 2-Phenyl-1,3-dioxanglycidylether)

[0071] Reaktionsgefäße I–III aus Glas mit zwei Stutzen, Septum und drei Teflonhähnen werden an eine Vakuumpumpe angeschlossen und evakuiert. Nacheinander werden 24,3 g (233 mmol) Styrol (getrocknet über CaH_2) und 100 mL frisch destilliertes THF unter statischem Vakuum in Reaktionsgefäß I überführt. 2 g (8,5 mmol) von PDGE werden in Reaktionsgefäß II vorgelegt und 50 mL THF werden unter statischen Vakuum in das Reaktionsgefäß 2 überführt. 100 mL trockenes Hexan werden mittels einer Kanüle in das evakuierte Reaktionsgefäß III transferiert und 3,8 mL einer 1,3 M sec.-Butyllithium Lösung werden mit einer Spritze über das Septum dazugegeben. Die drei Reaktionsgefäße werden anschließend mit PTFE-Schläuchen an drei HPLC-Pumpen angeschlossen und entsprechend Fig. 1 mit M1 und M2 verbunden. M1 (hier: Schlitz Interdigtal Micromischer) wird in ein Wasserbad (Raumtemperatur) getaucht. Um restliche Verunreinigungen im gesamten Reaktor zu eliminieren werden zuerst Pumpe 1 und 2 mit den Lösungen I und M aktiviert. Nach kurzer Zeit entsteht am Auslass des Reaktors die charakteristisch rot-orangefarbene Lösung aktiver anionischer Polymerketten. Schließlich wird die PDGE-Lösung mittels M2 (hier T-förmiger Mikromischer) zur aktiven Polymerlösung dazu gegeben. Die austretende entfärbte Lösung wird bei unterschiedlichen Flussratenverhältnissen in unterschiedlichen Kolben aufgefangen. Sämtliche Lösungsmittel werden unter Niederdruck entfernt und das Produkt in minimalen Mengen DCM gelöst und in MeOH gefällt. Durch mehrfaches Fällen in MeOH kann überschüssiges PDGE vom Produkt abgetrennt werden. Die Trocknung unter Vakuum bei Raumtemperatur über 24 h fährt zu einem farblosen Feststoff. Die Charakterisierung mittels ^{1}H-NMR Spektroskopie, GPC und MALDI-ToF-MS bestätigt eine quantitative Polymerisation und Endfunktionalisierung des Polystyrols.

Herstellung von trishydroxyl-funktionellem Polystyrol [PS-$(PDGE)_d$]durch saure Hydrolyse

[0072] 400 mg des zuvor erhaltenen PS-PDGE werden in 30 mL THF und 3 mL 1N HCl zusammengeben und für 8 Stunden unter Rückfluss erhitzt. Das Produkt wird in Chloroform aufgenommen und mit $NaHCO_3$ und H_2O neutralisiert. Sämtliche Lösungsmittel werden unter Niederdruck entfernt und das Produkt in 1 mL DCM gelöst. Nach Fällung in MeOH und Trocknung unter Vakuum bei einer Raumtemperatur über einen Zeitraum von 24 h wird ein farbloser Feststoff in einer Ausbeute von 80 bis 90% erhalten.

ZITATE ENTHALTEN IN DER BESCHREIBUNG

Diese Liste der vom Anmelder aufgeführten Dokumente wurde automatisiert erzeugt und ist ausschließlich zur besseren Information des Lesers aufgenommen. Die Liste ist nicht Bestandteil der deutschen Patent- bzw. Gebrauchsmusteranmeldung. Das DPMA übernimmt keinerlei Haftung für etwaige Fehler oder Auslassungen.

Zitierte Patentliteratur

- US 3842059 [0007]
- DE 69811035 T2 [0014, 0017]
- EP 749987 A [0025]

Zitierte Nicht-Patentliteratur

- Hadjichristidis et al. „Anionic polymerization: High vacuum techniques" Journal of Polymer Science: Part A: Polymer Chemistry, 2000, 38, 3211–3234 [0003]
- „Characterization of the functionalization reaction-product of poly(styryl)lithium with ethylene oxide" Journal of Polymer Science: Part A: Polymer Chemistry 1988, 26, 2031–2037 von Quirk et al. [0005]
- „Recent advances in anionic synthesis of chain-end functionalized elastomers using epoxides and related compounds" Rubber Chemistry and Technology, 2003, 76, 812–831 [0006]
- Zhibo et al., „Synthesis and characterization of triptych μ-ABC star triblock copolymers" Macromolecules, 2004, 37, 8933–8940 [0008]
- „Polymerisationen in mikrostrukturierten Reaktoren: Ein Überblick" Chemie Ingenieur Technik 2005, 77, 1693–1714 von Nessel et al. [0011]
- „Microstructured reactors for polymer synthesis: A renaissance of continuous flow processes for tailor-made macromolecules?" Macromolecular Chemistry and Physics 2008, 209, 343–356 [0011]
- Wilms et al. „Carbanions on tap – Living anionic polymerization in a microstructured reactor" Macromolecular Chemistry and Physics 2008, 209, 1106–1114 [0013]
- Nagaki et al. "Microflow-system-controlled anionic polymerization of styrenes" Macromolecules 2008, 41, 6322–6330 [0013]

DE 10 2010 021 388 A1 2011.11.24

Patentansprüche

1. Verfahren zur Herstellung von endfunktionalisierten makromolekularen Verbindungen, umfassend die Schritte:
(a) Bereitstellen einer Lösung (LM) von Monomeren (M) aus der Gruppe umfassend vinylaromatische Monomere, Dienmonomere, Acrylmonomere, Methacrylmonomere, Maleimidmonomere; einer Lösung (LI) eines Initiators (I) aus der Gruppe umfassend Alkylmetallverbindungen und Arylmetallverbindungen aus linearen oder verzweigten Alkylketten oder substituierten oder unsubstituierten Arylresten mit einem Metall aus der Gruppe Li, Na, K, Cs, Mg, Ca, Ba; und einer Lösung (LT) eines oder mehrerer Terminierungsreagenzien (T) aus der Gruppe umfassend Oxirane, schwefelhaltige Oxirananaloga und stickstoffhaltige Oxirananaloga;
(b) optional Bereitstellen einer weiteren Lösung (LM') von Monomeren (M') aus der Gruppe umfassend vinylaromatische Monomere, Dienmonomere, Acrylmonomere, Methacrylmonomere, Maleimidmonomere;
(c) kontinuierliches Vermischen der Lösung (LM) mit der Lösung (LI) in einem molaren Verhältnis von Monomeren (M) zu Initiator (I) im Bereich von 6:1 bis 5000:1 in einem Mischungsreaktor M1, wobei aus den Monomeren (M) durch anionische Polymerisation kontinuierlich ein Polymer (P) gebildet wird;
(d) optional kontinuierliches Überführen des in Schritt (c) erhaltenen Gemisches (LM) + (LI) von dem Mischungsreaktor M1 in einen Mischungsreaktor M1' und kontinuierliches Vermischen mit der Lösung (LM'), wobei aus dem Polymer (P) und den Monomeren (M) und (M') ein Blockcopolymer (BCP) gebildet wird;
(e) kontinuierliches Überführen des in Schritt (c) oder (d) erhaltenen Gemisches (LM) + (LI) oder (LM) + (LI) + (LM') von dem Mischungsreaktor M1 oder M1' in einen Mischungsreaktor M2;
(f) kontinuierliches Vermischen des in Schritt (e) erhaltenen Gemisches (LM) + (LI) oder (LM) + (LI) + (LM') mit der Lösung (LT) in dem Mischungsreaktor M2 und Terminieren des Polymers (P) oder Blockcopolymers (BCP) mit einer oder zwei Endgruppen (E, E') des mindestens einen Terminierungsreagenz (T); und
(g) optional Umsetzen der in Schritt (f) erhaltenen makromolekularen Verbindung aus dem Polymer (P) oder Blockcopolymer (BCP) und einer oder zwei Endgruppen (E, E') mit einem weiteren Monomer, wie einem Lacton, Epoxid oder Siloxan oder einem funktionellen Reagenz, wie einer Carbonylverbindung.

2. Verfahren nach Anspruch 1, dadurch gekennzeichnet, dass in Schritt (c) ein bifunktioneller Initiator (I) verwendet und beide Polymerkettendenden funktionalisiert werden, um homo-α,ω-funktionelle Polymere herzustellen.

3. Verfahren nach Anspruch 1, dadurch gekennzeichnet, dass in Schritt (c) ein funktioneller Initiator (I), der gegen die anionischen Bedingungen geschützt oder stabil ist, verwendet wird, um hetero-α,ω-funktionelle Polymere herzustellen.

4. Verfahren nach einem der Ansprüche 1, 2 oder 3, dadurch gekennzeichnet, dass in Schritt (f) dem Mischungsreaktor M2 Wasser oder ein Alkohol zugeführt wird, um Oxide von Li, Na, K, Cs, Mg, Ca oder Ba zu protonieren.

5. Verfahren nach einem oder mehreren der Ansprüche 1 bis 4, dadurch gekennzeichnet, dass als Monomer (M) ein vinylaromatisches Monomer und als Initiator (I) eine Alkylmetallverbindung verwendet wird.

6. Verfahren nach einem der Ansprüche 1 bis 5, dadurch gekennzeichnet, dass das mindestens eine Terminierungsreagenz (T) gewählt ist aus der Gruppe umfassend Ethoxyethylglycidylether (EEGE), 1,2-Isopropylidenglycerylglycidylether (IGG), 2-Phenyl-1,3-dioxanglycidylether (PDGE), Dibenzylaminaglycidylether (DBAG), Propylenoxid (1,2-Epoxypropan), 1,2-Epoxybutan (Ethyloxiran), Allylglycidylether (1-Allyloxy-2,3-epoxypropan), Benzylglycidylether (Benzyloxymethyloxiran), tert.-Butylglycidylether (tert.-Butoxymethyloxiran), Styroloxid (2-Phenyloxiran), Fluoroalkyloxirane, Fluoroalkylglycidylether, Aziridin (Ethylenimin) und Thiiran (Ethylensulfid) eingesetzt wird, wobei des molare Verhältnis von Terminierungsreagenz (T) zu Initiator (I) von 1:1 bis 20:1, vorzugsweise von 1:1 bis 5:1 beträgt.

7. Verfahren nach einem oder mehreren der Ansprüche 1 bis 6, dadurch gekennzeichnet, dass die in den Schritten (c) bis (f) verwendeten Mischungsreaktoren M1, M1' und M2 als Mikromischer ausgebildet sind und eine Mischkammer mit einer Einlassstufe und einem Auslass aufweisen, wobei die Einlassstufe derart ausgestaltet ist, dass in Schritt (c) die Lösungen (LM) und (LI), sowie gegebenenfalls in Schritt (d) das Gemisch (LM) + (LI) und die Lösung (LM'), respektive in Schritt (f) das Gemisch (LM) + (LI) oder (LM) + (LI) + (LM') und die Lösung (LT) in Form von zwei oder mehreren, jeweils zueinander benachbarten Strömungslamellen in die Mischkammer der Mischungsreaktoren M1, M1' und M2 treten, wobei jede der Strömungslamellen eine Dicke von 20 bis 1000 µm, vorzugsweise 20 bis 100 µm aufweist.

8. Verfahren nach Anspruch 7, dadurch gekennzeichnet, dass die den Mischungsreaktoren M1, M1' und M2 zugeführten Volumenströme (ml/sec) der Lösungen (LM), (LI), (LM') und (LT) derart bemessen werden, dass für die in den Mischkammern der Mischungsreaktoren M1, M1' und M2 fließenden Strömungen die Reynoldszahl Re größer als 2300, vorzugsweise größer als 3000 ist.

9. Verfahren nach einem oder mehreren der Ansprüche 1 bis 8, dadurch gekennzeichnet, dass es in einer Stickstoff- und Sauerstoff-freien Atmosphäre oder unter Vakuum geführt wird.

10. Verfahren nach einem oder mehreren der Ansprüche 1 bis 9, dadurch gekennzeichnet, dass es bei einer Temperatur von –80 bis 200°C, vorzugsweise 20 bis 40°C geführt wird.

11. Makromolekulare Verbindung, umfassend ein an einem Ende oder an zwei Enden mit einer oder zwei Endgruppen (E, E') terminiertes Polymer (P) oder Blockcopolymer (BCP), wobei
– das Polymer (P) oder Blockcopolymer (BCP) aus einem Monomeren (M) oder aus zwei Monomeren (M, M') aus der Gruppe umfassend vinylaromatische Monomere, Dienmonomere, Acrylmonomere, Methacrylmonomere und Maleimidmonomere gebildet ist; und
– die Endgruppen (E, E') abgeleitet sind aus einem oder zwei Terminierungsreagenzien (T, T') aus der Gruppe umfassend Oxirane, schwefelhaltige Oxirananaloga und stickstoffhaltige Oxirananaloga.

12. Makromolekulare Verbindung nach Anspruch 11, dadurch gekennzeichnet, dass die Terminierungsreagenzien (T, T') gewählt sind aus der Gruppe umfassend Ethoxyethylglycidylether (EEGE), 1,2-Isopropylidenglycerylglycidylether (IGG), 2-Phenyl-1,3-dioxanglycidylether (PDGE), Dibenzylaminoglycidylether (DBAG), Allylglycidylether (1-Allyloxy-2,3-epoxypropan), Benzylglycidylether (Benzyloxymethyloxiran), tert.-Butylglycidylether (tert.Butoxymethyloxiran), Styroloxid (2-Phenyloxiran), Fluoroalkyloxirane, Fluoroalkylglycidylether, Aziridin (Ethylenimin) und Thiiran (Ethylensulfid).

13. Makromolekulare Verbindung nach Anspruch 11 oder 12, dadurch gekennzeichnet, dass sie weitere Monomere, insbesondere Lactone, Epoxide oder Siloxane oder funktionelle Gruppen, insbesondere aus Carbonylverbindungen abgeleitete Gruppen, umfasst.

14. Makromolekulare Verbindung nach einem oder mehreren der Ansprüche 11 bis 13, dadurch gekennzeichnet, dass sie in terminaler Position 1 bis 1000, vorzugsweise 1 bis 20, und insbesondere 1 bis 5 funktionelle Gruppen aufweist.

15. Makromolekulare Verbindung nach einem oder mehreren der Ansprüche 11 bis 14, dadurch gekennzeichnet, dass sie ein Molekulargewicht von 400 bis 100000 g/mol, vorzugsweise von 100 bis 20000 g/mol aufweist.

16. Makromolekulare Verbindung nach einem oder mehreren der Ansprüche 11 bis 15, dadurch gekennzeichnet, dass sie eine monomodale Molmassenverteilung mit einer Polydispersität $\overline{M}_w/\overline{M}_n$ von 1,01 bis 50, vorzugsweise von 1,01 bis 2 und insbesondere von 1,05 bis 1,3 aufweist.

17. Makromolekulare Verbindung nach einem oder mehreren der Ansprüche 11 bis 16, dadurch gekennzeichnet, dass sie durch ein Verfahren nach den Ansprüchen 1 bis 10 erhältlich ist.

Es folgen 9 Blatt Zeichnungen

Anhängende Zeichnungen

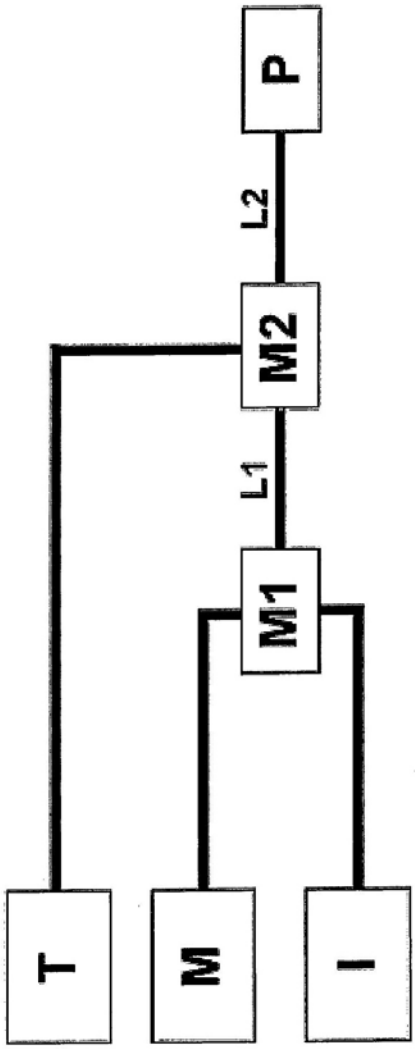

Fig. 1: Fließschema des erfindungsgemäßen Verfahren zur Herstellung von funktionellen Polymeren mit unterschiedlichen Mischungsreaktoren (M1 und M2).

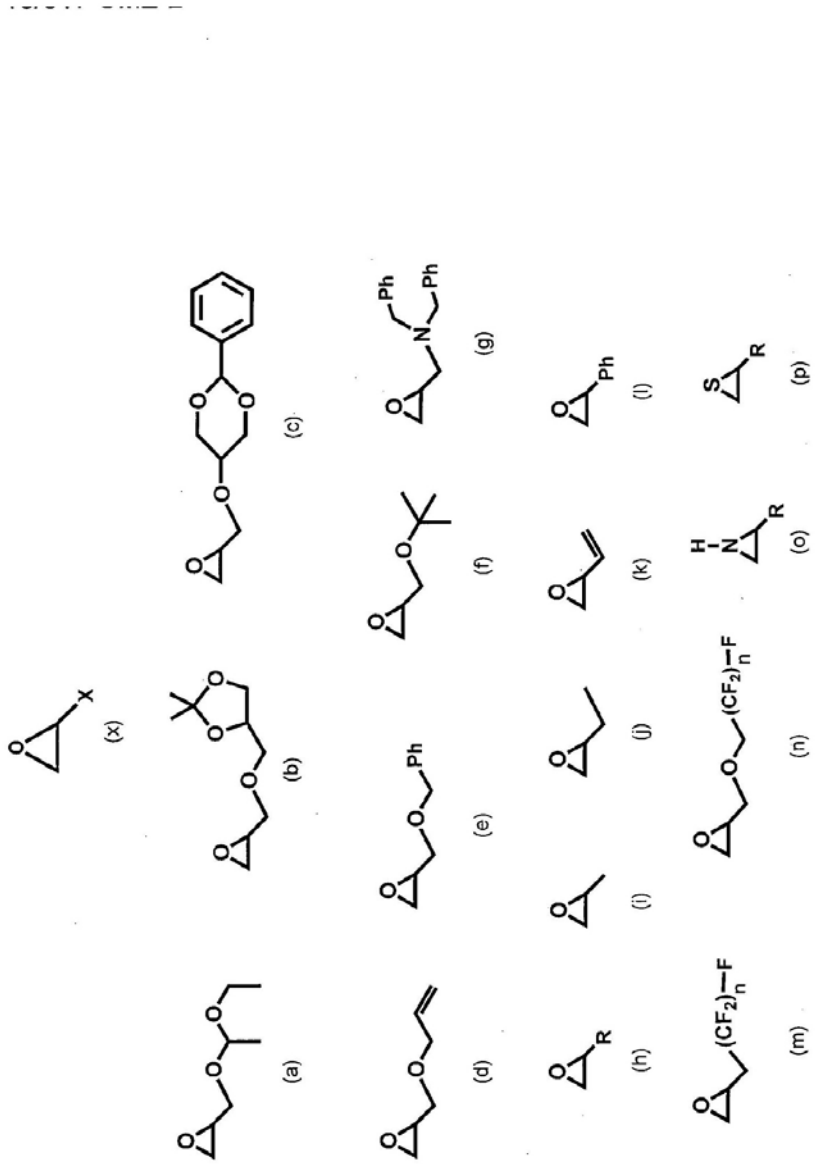

Fig. 2: Beispiele von Oxiranen und deren N bzw. S Analoga, die zur Herstellung der erfindungsgemäßen Verbindungen verwendet werden.

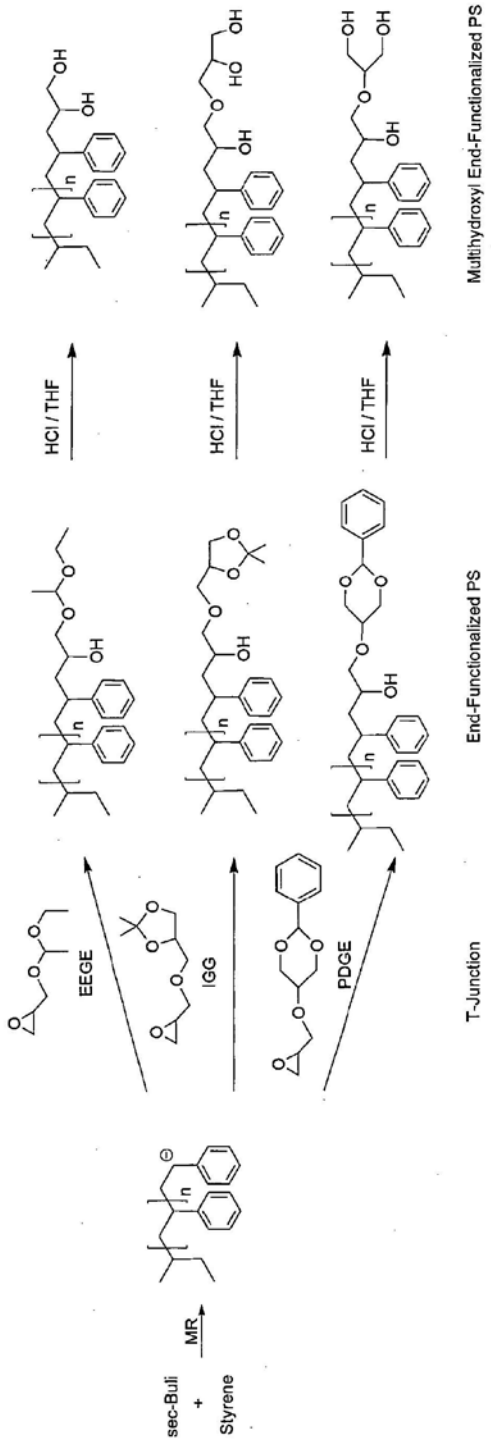

Fig. 3: Synthesestrategie zur Herstellung von multihydroxyl funktionellem Polystyrolen

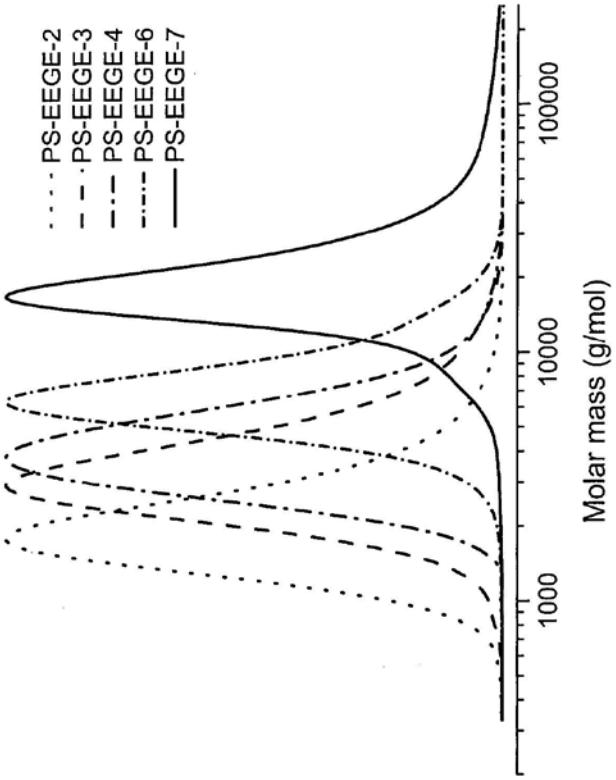

Fig. 4a) Ausgewählte GPC-Kurven von PS-EEGE

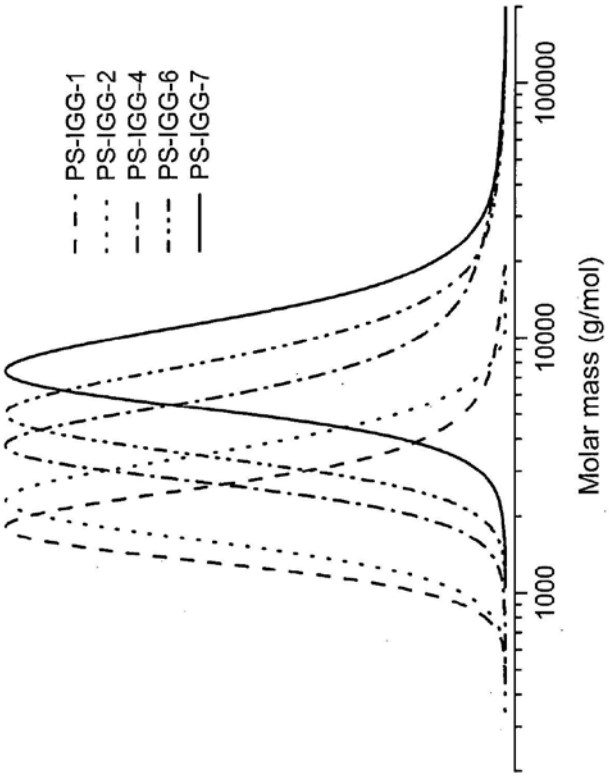

Fig. 5b) Ausgewählte GPC-Kurven von PS-IGG

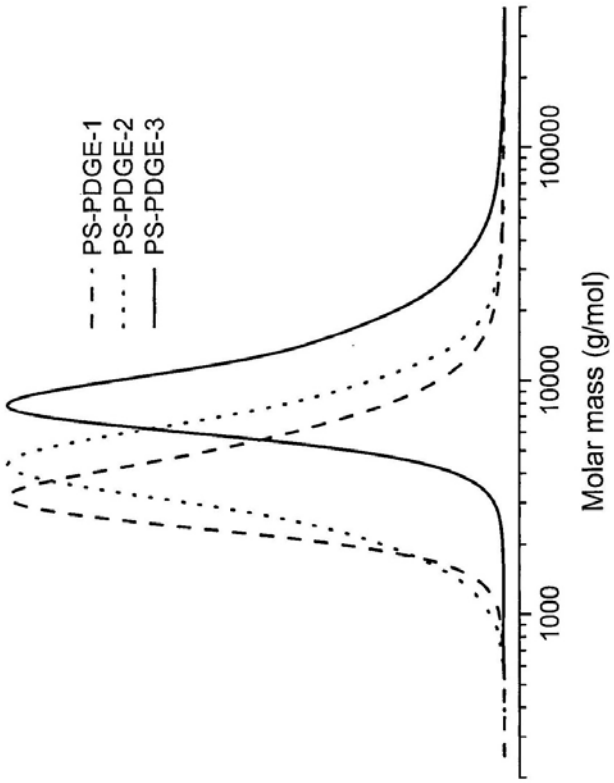

Fig. 6c) Ausgewählte GPC-Kurven von PS-PDGE

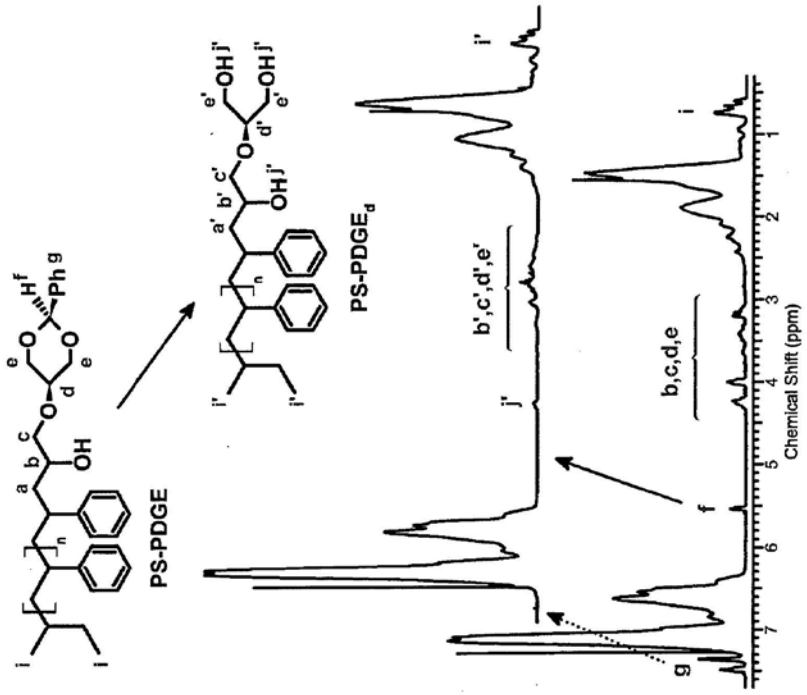

Fig. 7a) ^{1}H-NMR-Spektrum von PS-PDGE und PS-(PDGE)$_d$ in $CDCl_3$ (400MHz)

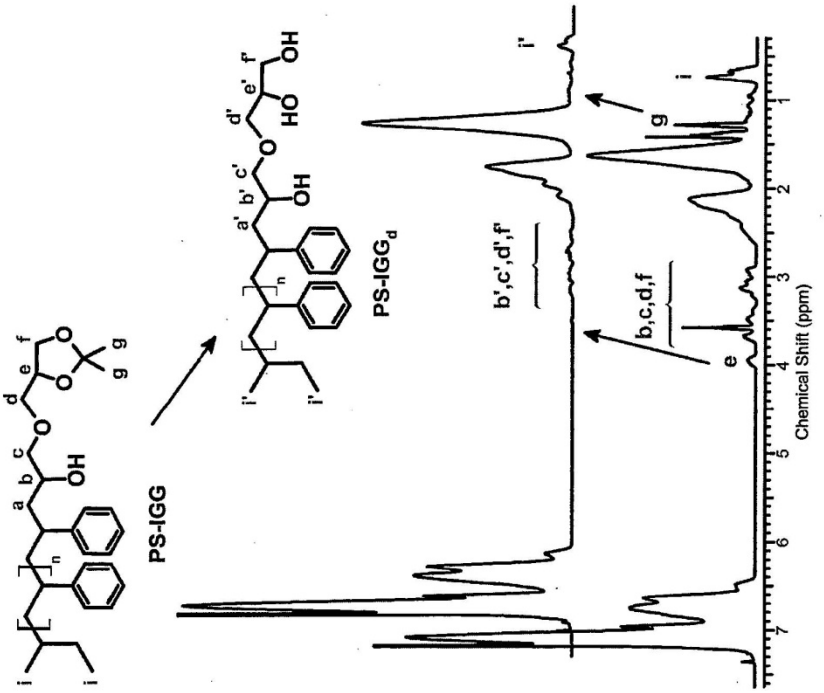

Fig. 8b) ^{1}H-NMR-Spektrum von PS-IGG und PS-(IGG)$_d$ in $CDCl_3$ (400MHz)

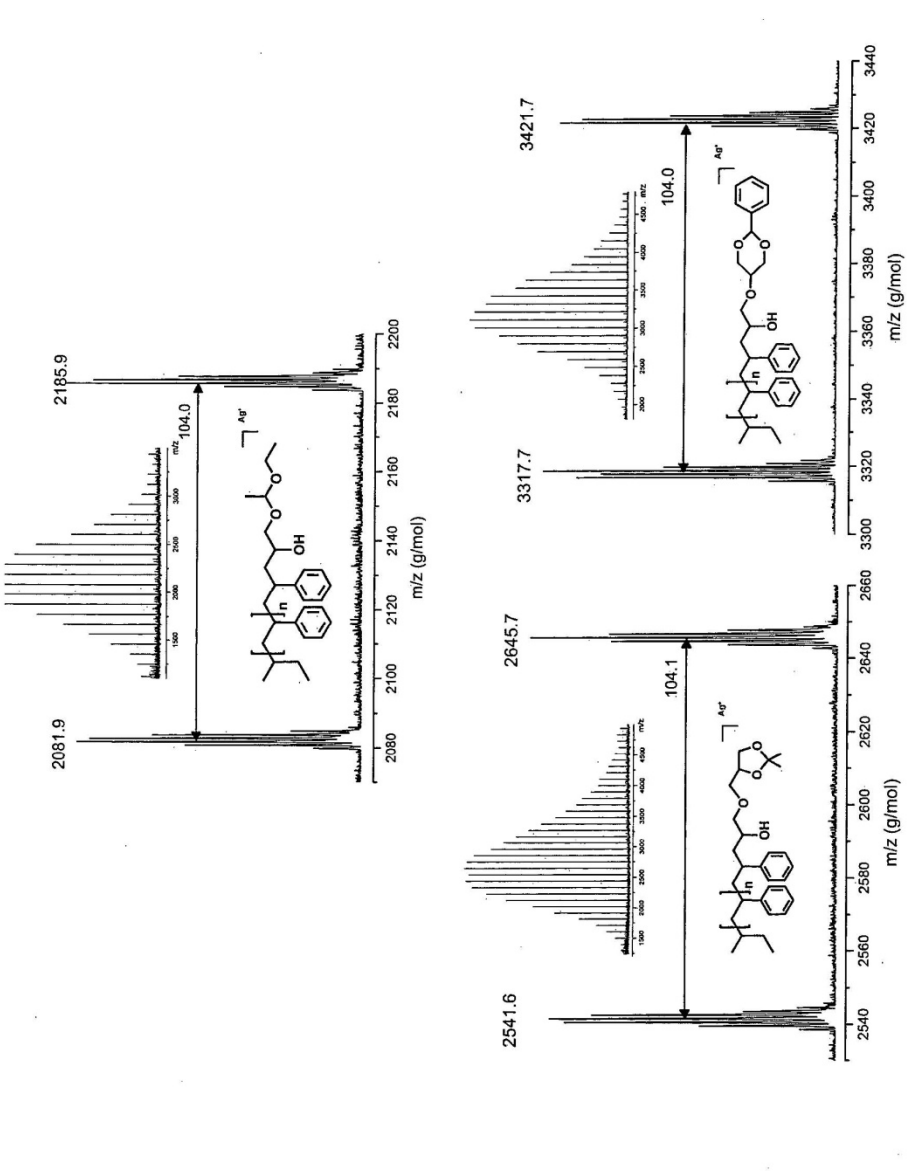

Fig. 9: MALDI-ToF-Spektren der erfindungsgemäßen Verbindungen (PS-EEGE, PS-IGG, PS-PDGE)

A.2: List of Publications

PATENT

„Continuous Process for Preparing Quantitatively Terminally Functionalized Polymers Using Oxirane Derivatives as Termination Reagents“
C. Tonhauser and Co-Autoren (Names of co-authors are deleted due to privacy protection. Namen der Co-Autoren wurden aus datenschutzrechtlichen Gründen entfernt.)
WO 2011147545, DE102010021388

PUBLICATIONS

First-Author

“Micro Reaction Technology: Recent Advances in Polymer Synthesis”
C. Tonhauser, A. Natalello, H. Löwe, H. Frey **2012** (*to be submitted*)

„Y-shaped Polymer Brushes with Stimuli-responsive Wetting Behavior via Grafting-to Technique“
C. Tonhauser, A. Golriz, H.-J. Butt, H. Frey **2012** *(submitted)*

„Water-soluble Poly(vinylferrocene)-*b*-Poly(ethylene oxide) Diblock and Miktoarm Star Polymers“
C. Tonhauser, M. Mazurowski, M. Rehahn, M. Gallei, H. Frey
Macromolecules **2012**, *45*, 3409-3418

„Amphiphilic Block Copolymers with an In-chain Allyl Functionality at the Block Junction by Anionic Polymerization Strategies“
C. Tonhauser, R. Klein, J. Emsermann, H. Frey
PMSE-Preprint **2012** *(accepted)*

„Introducing an Amine Functionality at the Block Junction of Amphiphilic Block Copolymers by Anionic Polymerization Strategies“
C. Tonhauser, B. Obermeier, C. Mangold, H. Löwe, H. Frey
Chemical Communications **2011**, *47*, 8964–8966

„Entanglement Transition in Hyperbranched Polyether-Polyols“
C. Tonhauser, D. Wilms, Y. Korth, H. Frey, C. Friedrich
Macromolecular Rapid Communications **2010**, *31*, 2127–2132

„A Road Less Traveled to Functional Polymers: Epoxide Termination in Living Carbanionic Polymer Synthesis“ *(Review)*
C. Tonhauser, H. Frey
Macromolecular Rapid Communications **2010**, *31*, 1938–1947

„Multihydroxyl-Functional Polystyrenes in Continuous Flow“
C. Tonhauser, D. Wilms, F. Wurm, E. Berger-Nicoletti, M. Maskos, H. Löwe, H. Frey
Macromolecules **2010**, *43*, 5582–5588

Co-Author

„Effect of Hydrogen Bonds on Entanglement Behavior and Thermorheological Properties of Hyperbranched Polyglycerol Melts“
C. Gillig, C. Tonhauser, C. Schubert, M. Schömer, D. Wilms, H. Frey. C. Friedrich
2012 (to be submitted)

„A Combined DPE/Epoxide Termination Strategy for Hydroxyl End-functional Poly(2-vinylpyridine) and Amphiphilic AB_2-Miktoarm Stars“
A. Natalello, C. Tonhauser, E. Berger-Nicoletti, H. Frey
Macromolecules **2011**, *44*, 9887–9890